STATISTICAL METHODS FOR ESTIMATING TEPHRA SOURCE AND DISPERSAL

A thesis presented in partial fulfilment of the requirements for the degree of

Doctor of Philosophy

in

Statistics

at Massey University, Palmerston North,

New Zealand.

Emily Kawabata

2016

Abstract

Tephra refers to any pyroclastic fragments ejected from a volcanic vent and its dispersal is one of the major hazards with explosive eruptions. The attenuation of tephra fall thickness is most commonly estimated after contouring field measurements into smooth isopachs. I explicitly describe the variability in thickness by using a semiempirical tephra attenuation relation as a link function. This opens the way to fitting models to actual tephra observations through maximum likelihood estimation (MLE). The method is illustrated using data published from the 1973 Heimaey eruption in Iceland.

Complex eruptions commonly produce several phases of tephra fall from multiple vents. When attempting to precisely reconstruct past eruptions from the geological record alone, separate phases are often indistinguishable. Augmented by a mixture framework, the MLE attenuation model was able to identify the sources and directions of tephra deposition for the 1977 Ukinrek Maars eruption in Alaska, US, from only the tephra thickness data. It was then applied to the unobserved 1256 AD Al-Madinah eruption in Saudi Arabia.

The estimation of the spatio-temporal hazard from a monogenetic volcanic field is critically dependent on a reconstruction of past events. The Auckland Volcanic Field (AVF) has produced about 50 volcanoes in the last 250,000 years. Although inconsistent, age data for many of these volcanoes exist from various dating methods with various reliabilities. The age order of some pairs is also known due to the overlaying of lavas

(stratigraphy). A discussion is provided on how informative priors are obtained via expert elicitation, on both the individual volcano ages, and the reliabilities of the dating methods. A possible Bayesian model for reconciling the available inconsistent volcano age data to estimate the true eruption ages is also discussed.

To improve these eruption age estimates, some of the volcanoes can be correlated with the better dated tephra layers recovered from five maars in the field. The likelihood of any combination of volcano and tephra, incorporating the spatial variability based on the attenuation model and temporal components, is evaluated and is maximised numerically using linear programming. This statistical matching provides an improvement in the volcano age-order model and age estimates of the volcanoes in the AVF.

Acknowledgements

I would like to thank Professor Mark Bebbington, Professor Shane Cronin, and Dr Ting Wang for their guidance and showing me the joy of doing research.

I would like to thank Professor Stephen Marsland, Associate Professor Geoff Jones, Dr Christopher Tuffley, Dr Jonathan Marshall, Professor Martin Hazelton, and Dr Jonathan Godfrey for their time and support.

I would like to thank Dr Rebecca Green and Dr Kate Richards for their friendships and company.

Publications arising from this thesis

- **Kawabata, E., Bebbington, M., Cronin, S., and Wang, T.** (**2013**). *Modelling thickness variability in tephra deposition. Bulletin of Volcanology*, 75(8): 1–14.

- **Kawabata, E., Cronin, S., Bebbington, M., Moufti, M., El-Masry, N., and Wang, T.** (**2015**). *Identifying multiple eruption phases from a compound tephra blanket: an example of the AD1256 Al-Madinah eruption, Saudi Arabia. Bulletin of Volcanology*, 77(1): 6.

- **Kawabata, E., Bebbington, M., Cronin, S., and Wang, T.** (**under review**). *Optimal likelihood-based matching of volcanic sources and deposits in the Auckland Volcanic Field. Journal of Volcanology and Geothermal Research.*

Contents

List of Figures

List of Tables

Chapter 1

Introduction

1.1 Motivation

The estimation of hazards arising from volcanic eruptions is a research topic of great interest to New Zealand, given the number and location of active and dormant volcanoes. Recent targeting of long-continuous records of volcanism, and new dating and geostatistical studies have resulted in the acquisition of greater quantities of more precise data about eruption occurrences and properties. This has opened the door to improvements in statistical hazard models.

In New Zealand, one of the largest sources of volcanic risk comes from the Auckland Volcanic Field (AVF) (Figure 1.1), on which the city of Auckland is built. In such a volcanic field, the dual focus of interest is both the timing and location of the next event. It is often assumed that each event is initiated from a new volcano within the field, but there is some evidence of multiple phases of activity from certain volcanoes in the volcanic fields in Auckland and Jeju, South Korea. Apart from the definition of ‘volcanoes’ and ‘phases’ the main statistical problems include: That the age data are both incomplete and imprecise, including estimated errors, and in places contradictory. While the errors can be treated within a Monte Carlo simulation framework

Figure 1.1: The Auckland region (inset), obtained from `http://transportblog.co.nz/tag/population-growth/`, is highly populated and its geography presents significant challenges for evacuation planning.

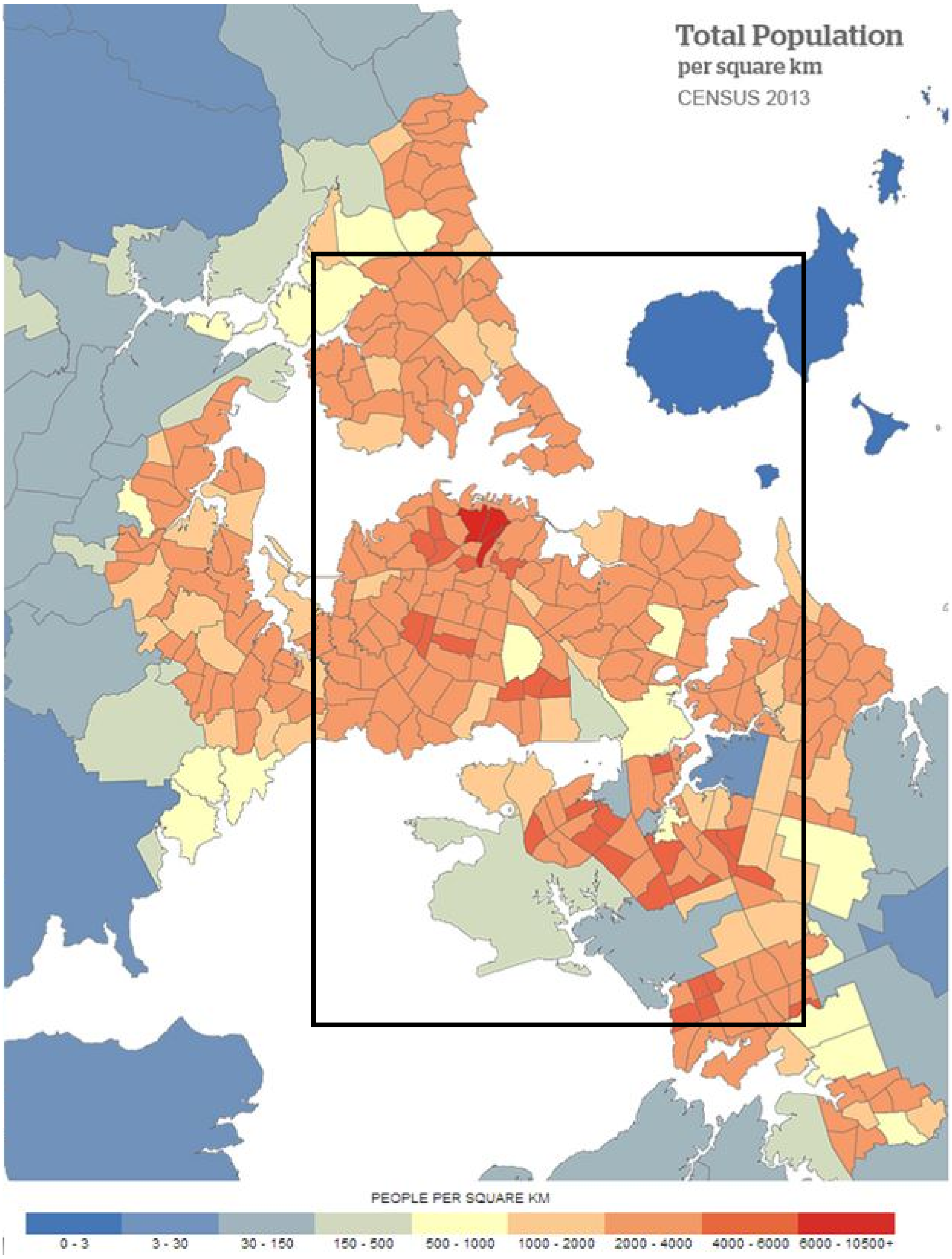

(Bebbington and Cronin, 2011), the computational complexity becomes an issue when a given volcano may have eruption dates differing by hundreds of thousands of years. Moreover, transparency and understanding of what the model is doing is lost.

There has been little investigation of true, integrated, spatio-temporal models for volcanic fields (Connor and Hill, 1995; Magill et al., 2005): Generally the temporal and spatial terms have been treated independently (e.g., Bebbington and Cronin (2011)). The overall aim of the research is to develop statistical methods that will allow the construction of hazard forecasting models which include spatio-temporal behaviour, particularly in volcanic fields. This thesis seeks to develop methods that will allow robust forecasts to be made of the likelihood of a volcanic eruption at a given point in time and space. These detailed hazard estimates will provide emergency managers, planners, and insurers with more accurate information with which to make informed decisions. This will help inform the sustainable development of urban areas built on volcanic fields, such as Auckland.

As part of the process, tephra attenuation estimation is also discussed. Tephra, collectively refers to rocks and ash, is found at considerable distances from the source and tephra attenuation models tephra thickness as a function of its location relative to the source. Tephra fallout is one of the major hazards, and one of the major sources of data, from explosive eruptions. Apart from the hazard to aviation from fine particles suspended in the upper atmosphere (Miller and Casadevall, 2000), tephra hazards are associated with its deposited depth, loading, grain size, and electromagnetic and chemical properties. Tephra fall may cause respiratory illness, damage to buildings, and storm-water infrastructure, render roads impassable, disable electrical distribution networks, contaminate water supplies, destroy crops, kill livestock, and drastically change landscape stability and flood vulnerability (Baxter et al., 1981; Heiken et al., 1998; Cronin et al., 1998; Stewart et al., 2006).

Tephra falls may blanket many tens to thousands of square kilometres with deposit geometry typically established by spot analysis of thickness (or mass) and other properties at individual sites. Rapid local redeposition of tephra via fluvial and aeolian processes is common and, along with compaction, means that considerable measurement error can be introduced, increasing with time from deposition. When attempting to precisely reconstruct past eruptions from the geological record, separate phases from a composite tephra blanket are often indistinguishable due to a lack of obvious distinct physical or chemical characteristics. Instead a mixture of attenuation models can be used for identifying the most likely combination of multiple components from complex tephra-producing eruptions.

The theme of this thesis is statistically describing the tephra fallout by explicitly accounting for the variability in thickness. This description, together with the existing age data, will be used to improve our understanding of spatio-temporal hazards, particularly in volcanic fields.

1.2 Overview

Chapter 2 provides an overview of the volcanological terms used in the rest of the thesis and discusses the existing statistical models developed for fitting tephra thickness data.

Chapter 3 develops an improved *statistical* tephra attenuation model, using the ideas of Rhoades et al. (2002) and Gonzlalez-Mellado and De la Cruz-Reyna (2010) as starting points. The attenuation of tephra fall thickness is most commonly estimated after contouring isolated and often irregular field measurements into smooth isopachs, with varying degrees of subjectivity introduced in the process. Here, the variability of thickness is explicitly accounted with an error distribution. This opens the way to fitting models to actual tephra observations through maximum likelihood estimation (MLE), rather than using weighted least-squares estimation on the isopachs. The method is illustrated for small-scale basaltic explosive eruptions using a simple, but typical, data set of the actual tephra thickness data published from the 1973 Heimaey eruption in

Iceland.

Chapter 4 extends the attenuation model to allow for the incorporation of multiple lobes and/or vents as commonly occurs in complex eruption episodes. When attempting to precisely reconstruct past eruptions from the geological record, separate phases in a composite tephra blanket are often indistinguishable due to a lack of obvious distinct physical or chemical characteristics. Augmented by a mixture framework allowing for the incorporation of multiple lobes and/or vents, the MLE attenuation model was able to identify the most likely combination of sources and directions of tephra deposition for the 1977 Ukinrek Maars eruption in Alaska, USA, from only the tephra thickness data, validating the model. The model was then applied to the unobserved 1256 AD Al-Madinah fissure eruption in Saudi Arabia. This required a modification in the error distribution to account for weathering, wind-remobilisation, and settling. In addition to the identified number of phases from the model, physical data such as grain size distribution and geochemical data of the tephra samples provides a template for more realistic hazard scenarios and event reconstructions from the geological record.

Chapter 5 provides an overview of the AVF. Monogenetic volcanic fields are areas of a few hundred to a few thousand square kilometres, where each eruption forms a new volcano. Due to their fertile soils and generally low eruption rates, such fields are often heavily populated, thus hazard estimates are important for land-use and evacuation planning. While spatial data on which to base such estimates are readily available, migration of activity over time is a very real possibility. In order that the hazard estimates reflect future, rather than past, behaviour, it is vital to assemble as much reliable age data as possible on past eruptions. Many eruptions cannot be directly dated at all, or differing methods return inconsistent ages. Some of these ages can be constrained by the stratigraphy of overlaying lavas. The available data can be used to increase our understanding of tephra and spatio-temporal hazards in the AVF, including reconciling the inconsistent age data and correlating the eruption ages and the dated deposits to improve the ages of the eruptions.

Chapter 6 discusses a possible way of reconciling the available inconsistent volcano age data to estimate the true eruption ages in a Bayesian framework. Informative priors are obtained, via expert elicitation, on both the individual volcano ages and the reliabilities of the dating methods used to date the samples. The dated ages are used as data, weighted appropriately by the reliability of their dating methods. Although this idea looks promising, there was insufficient data to generate reliable results.

Chapter 7 examines the problem of matching the dated deposits found in five swamps within the AVF to the volcanoes that produced them. The eruption volumes and dominating wind directions for these volcanoes are also estimable. The simplest issue is separation in time, which is handled by simulating prior volcano age sequences from direct dates where known, thinned via ordering constraints between the volcanoes. The subproblem of varying deposition thicknesses (which may be zero) at five locations of known distance and azimuth is quantified using the statistical attenuation model for the volcanic ash thickness developed in Chapter 3. These elements are combined with other constraints, from widespread fingerprinted ash layers that separate eruptions and time-censoring of the records, into a likelihood that was optimised via linear programming. A second linear program was used to optimise over the Monte Carlo simulated set of prior age profiles to determine the best overall match and consequent volcano age assignments.

Chapter 8 summarises the conclusions of this thesis and provides four suggestions for possible future research. Firstly, a discussion is provided on the possibility of extending the Bayesian age model (Chapter 6) to treat the matching process (Chapter 7) as an iteration in its model. However, careful thought is required on how to combine the two models. Priors from the expert elicitation and the pseudo prior ages produced from the matching procedure from the previous iteration are currently both considered as priors in their models and now need to be combined. However there is no obvious way of weighting or iterating these. Secondly, a discussion is provided on the possibility of incorporating grain size information into the tephra attenuation model which was used to identify phases of a complex eruption. The aim of the new model would be to extract statistical estimates of important eruption parameters such as column height. Thirdly, the possibility of building a stochastic model for estimating the number of phases of the next eruption in a volcanic field is proposed. However, in reality, there are not yet enough studied eruptions from which to simulate a possible future eruption. Lastly, a dynamic model is suggested to account for the changes in wind directions over time during an eruption. A spatial hazard model may be constructed for each phase which can be identified by an appropriate time series model for the wind directions.

Chapter 2

Literature Review

2.1 Volcanological background

This section provides an overview of the volcanological terminology used in the rest of the thesis.

2.1.1 Volcanic eruptions

Volcanic eruptions involve the ejection of magma (molten rock) at the Earth's surface. They occur through a vent, which is an opening on the ground formed during an eruption. A fissure is a linear alignment of vents and is common in many volcanic areas (Sigurdsson et al., 1999). Since volcanic eruptions occur at irregular intervals, Siebert et al. (2010) defines an eruptive event to be an activity that is separated by at least three months of quiescence since the previous activity. An event can have one or multiple source vents and one or multiple stages (or phases). Jenkins et al. (2007) defines a stage to be a period of activity with a distinctive style such as wind direction. Eruptions may vary considerably, for example, the 1973 Heimaey eruption (Self et al., 1974) had one vent and one phase, whereas the 1977 Ukinrek Maars eruption (Kienle et al., 1980; Self et al., 1980), and the 1256 AD Al-Madinah eruption (Camp et al.,

1987) are examples of multi-source and multi-phase eruptions.

In a polygenetic volcano system, typically a stable reservoir hosts magma from which batches periodically ascend to the surface up a stable conduit system (Walker, 1993). On the other hand, in a monogenetic volcano system, infrequent bursts of magma ascend from separate magma batches, generally with each new eruption occurring at a separate location at the surface (Walker, 1993). Such monogenetic systems, also known as continental or distributed volcanic fields are common throughout the world in stable crustal locations, typically hundreds of kilometres from active tectonic margins, such as Harrat Rahat in Saudi Arabia (El Difrawy et al., 2013), Jeju Island in South Korea (Brenna et al., 2012) and Auckland in New Zealand (Kermode et al., 1992; Allen and Smith, 1994; Kereszturi et al., 2013). Hence, in a monogenetic volcanic field, the focus of statistical modelling is on forecasting both the timing and location of the next eruption. In this thesis, modelling such eruptions from monogenetic volcanic fields is the main focus.

Volcanic activity can be either explosive, producing high columns of ash, pyroclastic flows, and plumes (mixtures of volcanic particles, gases, and air) (Sigurdsson et al., 1999) or effusive (non-explosive), expelling lava flows (Sigurdsson et al., 1999), depending on the magmatic flux, magma composition, gas content, and coupling vs. decoupling of gas with the rising magma. Various types of mainly basalt-composition eruption in monogenetic fields are typically classified into behaviours from Hawaiian to more explosive Strombolian styles (Siebert et al., 2010).

Monogenetic eruptions tend to be small in volume (Walker, 1993), producing vents surrounded by spatter ramparts, lava flows, and most commonly cinder or scoria cones (Wentworth and Macdonald, 1953; Walker, 1993).

Where rising magmas encounter ground water or surface water at sufficient pressure and in optimal magma-water ratios (usually around 1:3), violent phretomagmatic explosions occur (Sigurdsson et al., 1999). These produce deep and steep-sided craters known as maars (Figure 2.1), and surrounding tuff rings (Lorenz, 1985; Walker, 1993). Maars are

Figure 2.1: An example of a maar: Ukinrek Maars in Alaska, US, obtained from http://volcano.si.edu/.

excavated into the substrate (Lorenz, 1986; Vespermann and Schmincke, 2000) while shallow craters and tuff rings commonly result from magma interacting with shallow water (Vespermann and Schmincke, 2000) and sit above the pre-eruption substrate (Lorenz, 1986). Many monogenetic volcanoes located near the coast form tuff rings or maars (Walker, 1993).

2.1.2 Tephra

The term tephra comes from a Greek word for ash $\tau\epsilon\phi\rho\alpha$ (Gornitz, 2008) and was generically defined by Thórarinsson (1954) as any pyroclastic fragments (pumice, ash, and rock fragments) ejected from a volcanic vent (Wentworth and Williams, 1932; Sigurdsson et al., 1999) regardless of size, shape, or composition (Biass et al., 2014).

Typically tephra is dispersed long distances from volcanoes because it is ejected into the air in vertical eruption columns driven by gas thrust and buoyancy. However the distance from the volcano can vary, depending on the height of the eruption column, the particle size of the fragments, and the strength of the wind. In very large eruptions it is not uncommon for fine-grained (e.g., < 0.25mm diameter) tephra to be dispersed distally, hundreds to thousands of kilometres, from the source volcano (Froese et al., 2008; Folch, 2012). In small scale basaltic eruptions, however, tephras are normally dispersed only a few tens of kilometres in most instances. During a phreatomagmatic eruption, explosions produce laterally-directed currents, known as base surges, which extend a few kilometres from the source, also dispersing tephra (Einsele, 2000). These are the main component making up tephra and tuff rings surrounding maars or craters. Following Cas and Wright (1987), 'bombs' are referred only for volcanic pyroclasts with an intermediate axis dimension greater than 64mm and ballistic refers to particles that are larger than 32mm (Mannen, 2006).

Tephra is typically classified according to its grain size and emplacement mechanism (i.e., either as fall or base surge in the basaltic examples described in this thesis).

2.1.3 Grain size

Determining the grain size of tephra deposits requires collecting samples from the field, drying, and sieving by hand in a laboratory. The diameter is typically reported in the Krumbein phi (ϕ) scale (Krumbein, 1934). The grain size distribution (Table 2.1) describes the proportion of the grain size of the particles that are present in the sample,

$$\phi = -\log_2(D/D_0),$$

where ϕ is the Krumbein phi scale, D is the diameter of the particle and D_0 is a reference diameter, equal to 1mm.

Table 2.1: ϕ scale conversion for the grain size distribution.

ϕ scale	Diameter (D/D_0)
$-8 <$	256mm $<$
-6 to -8	64 to 256mm
-5 to -6	32 to 64mm
-4 to -5	16 to 32mm
-3 to -4	8 to 16mm
-2 to -3	4 to 8mm
-1 to -2	2 to 4mm
0 to -1	1 to 2mm
1 to 0	0.5 to 1mm
2 to 1	0.25 to 0.5mm
3 to 2	125 to 250µm
4 to 3	62.5 to 125µm
8 to 4	4 to 62.5µm
10 to 8	1 to 4µm
20 to 10	1 to 1,000nm

2.2 Tephra spatial hazard models

The dispersal of tephra is one of the major hazards associated with explosive eruptions. Even a small amount of it affects lives, livestock, infrastructure, and transport, and causes air and water pollution. (Baxter et al., 1981; Heiken et al., 1998; Cronin et al., 1998; Stewart et al., 2006). Hence it is important to be able to estimate how much tephra may fall at a given location, given an eruption.

Broadly there are two approaches to modelling the tephra dispersal: numerical and empirical. The eruptive volume, which can be estimated from these models, is very important for hazard forecasting (Marzocchi and Bebbington, 2012).

2.2.1 Isopachs

Tephra dispersal is commonly displayed visually as smoothed out isopachs (contours of equal thickness) on a map. Figure 2.2 shows an example of an isopach map. The contours of equal tephra thicknesses are drawn based on the spot tephra measurements.

Figure 2.2: An isopach map of the tephra deposits from the Fogo A Plinian deposit, Sao Miguel (Azores) (Bursik et al., 1992). The red star indicates the vent.

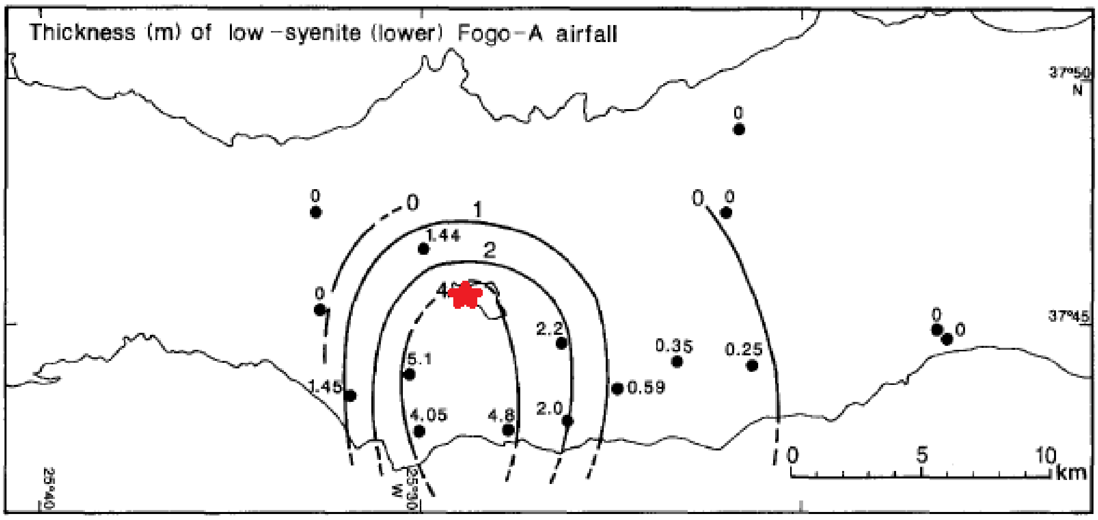

It shows a tephra lobe that is predominantly distributed to the south of the vent or source (indicated by the star). The 4m contour shows that there is almost no region observing more than 4m of tephra on the northern side of the vent, while a large region observed 4m or more on the southern side of the vent. This indicates that the wind was blowing to the south at the time of the eruption.

The isopach map can be used to differentiate the different wind directions during an eruption. They usually correspond to individual phases but not all different phases of an eruption are distinguishable from an isopach map alone, particularly if there was little variation in wind direction. A statistical method is required to estimate the number of phases and their directions.

Isopachs are the basis, along with grain size distribution, for the most widely applied empirical methods (which will be discussed in Section 2.2.3) used for estimation of volcanic eruption properties and hazard (i.e., total erupted volume, eruption column height, and mass ejection rate (Carey and Sparks, 1986; Sparks, 1986; Pyle, 1989; Fierstein and Nathenson, 1992; Bonadonna et al., 1998; Sparks et al., 1997; Pyle, 2000; Sulpizio, 2005)). All these methods involve application of a mathematical function representing tephra attenuation in terms of the square root of isopach area, indexed by a small number of parameters, which is fitted to the data using a least squares approach.

Traditionally isopachs are drawn by interpolating observed tephra measurements by hand (e.g., Figure 2.2) but increasingly these are carried out by GIS interpolation methods. When drawn by hand there is more flexibility in the shape (smoothness).

Any error that is introduced while producing isopach maps will be imposed on any estimates that arise from them, such as volume estimates (Bonadonna et al., 2015). Klawonn et al. (2014) analysed the hand drawn isopachs of the tephra fallout from the 1959 Kilauea Iki eruption from 101 volcanologists world wide and reported consistency in the volume estimates with different sampling densities. However, Burden et al. (2013) claimed there can be up to 40% of error produced during the process of producing isopach maps. This error can be avoided if the actual measurements are used (Burden et al., 2013; Engwell et al., 2013).

By smoothing the data first, the isopach maps avoid the question of sampling error. The actual thickness observed at any given point differs from an 'ideal' thickness due to small random effects of wind strength and direction, but primarily due to local redistribution of fallen tephra by wind, rain, and slope processes (especially in highly irregular topography) (Engwell et al., 2013). This sampling error is termed aleatory uncertainty by Marzocchi et al. (2004) and Marzocchi and Bebbington (2012). It describes the inherent variability of the observations. Rhoades et al. (2002) and Burden et al. (2013) fitted attenuation functions to the actual measurements using least squares on the log scale. Hence, the variability in the deposited thickness at a given point is assumed to be lognormally distributed. It is not known whether this is the most accurate representation of variability in tephra deposition. Obviously, the distribution must be limited to non-negative values, but this leaves open many questions regarding its skewness and tail characteristics. For example, the lognormal distribution has a thick tail, implying that unrealistically large amounts of over-thickening can occur, especially at long distances from the volcano.

2.2.2 Numerical models

Based on the two-dimensional differential equation for diffusion in uniform wind (Suzuki, 1983), numerical models such as HAZMAP (Armienti et al., 1988; Macedonio et al., 1988; Barberi et al., 1990; Macedonio et al., 2005), ASHFALL (Hurst and Turner, 1999), and Tephra2 (Connor et al., 2001; Bonadonna and Houghton, 2005; Costa et al., 2006; Johnston et al., 2012) simulate the movement of individual tephra particles which are advected by wind and diffused by turbulence until they are dispersed on the ground at each discretised vertical point, assuming flat topography. This is computed from an analytical solution to

$$\frac{\mathrm{d}C_j}{\mathrm{d}t} + \nabla \cdot (C_j \mathbf{u}) = \nabla^2 (C_j \mathbf{K}) + S, \tag{2.1}$$

where C_j is the mass concentration of particles (kg/m^3) in a grain size category j, t is time (s), $\mathbf{u}$ is velocity (m/s), $\mathbf{K}$ is the diffusion coefficient (m^2/s) at (x, y, z), and S is the mass concentration of particles brought into the domain per unit of time, referred to as the source term (Bursik, 1998; Bonadonna, 2006). Note that this is a mass conservation equation from fluid mechanics. Numerically solving Equation 2.1 yields a three-dimensional model which relaxes the assumption. Examples of such models are FALL3D (Costa et al., 2006; Folch et al., 2009) and VOL-CALPUFF (Barsotti et al., 2008).

The input parameters in the models are the eruption data such as vent location, eruption mass, plume height, grain size; particle data such as diffusion coefficient (a diffusivity constant to indicate how much particles move horizontally during their fall, measured in m^2/s), particle densities, total grain size distribution of sediment, etc.; and meterological data such as wind speed and direction at different altitude bands over time. Their output will be thickness of tephra at each grid location. These numerical models can be used for hazard forecasting as part of a Monte Carlo procedure along with probabilistic models of eruption size and meteorological conditions (Hurst and Smith, 2004; Bonadonna and Houghton, 2005; Costa et al., 2009). They determine the probability of a particular thickness of tephra or mass loading per unit area (density multiplied by thickness) being deposited at a given location.

While these models can be used for hazard forecasting, the inverse problem is less amenable due to difficulty in finding the optimal fit (Connor and Connor, 2006). Approaches to inverting the observed tephra dispersal to estimate the eruptive parameters usually use a specified wind profile (e.g., Scollo et al. 2007, 2008; Kratzmann et al. 2010), neglect wind (e.g., Volentik et al. 2010), or apply an exogenously specified average (e.g., Pfeiffer et al. 2005; Johnston et al. 2012), and often fix other parameters as well. The parameters being inverted for are either specified in an experimental design, optimised in a 'one-at-a-time' (Johnston et al., 2012), or downhill simplex scheme (Connor and Connor, 2006). There is no objective measure of 'best fit'; typically some form of weighted least-squares error (Costa et al., 2009) is minimised. The results are that the solutions are possibly non-optimum, not least due to leaving wind out of the design, and can be non-unique (Pfeiffer et al., 2005; Scollo et al., 2007; Kratzmann et al., 2010; Bonasia et al., 2010; Volentik et al., 2010; Johnston et al., 2012) particularly for relatively sparse deposit data, due to the dependencies among the parameters involved.

2.2.3 Empirical models

An empirical tephra attenuation model is an alternative to the numerical approach. One of the biggest differences between the numerical approach and this empirical approach is that the numerical approach requires a large range of topological, eruption and meteorological data, such as grain size data and wind speed and direction data, to estimate the tephra loading on the ground. However, the empirical approach contains such information as parameters in the model and uses the tephra spot measurement data to estimate them. Therefore the input data required in this model is the thickness measurements and their locations in relation to the source. Such data are easily obtained from observation, even many hundreds of years after the eruption.

Another difference is that in the forward problem, unlike the numerical approach, the empirical approach does not require simulating many physical numerical models, meaning it is computationally easier.

The expected tephra thickness at a location in relation to the source can be modelled using the spot tephra thickness measurements. In general tephra thickness decreases with distance from the source. But the dispersal is often affected by wind hence the dispersal is often not symmetric.

Pyle (1989) and Legros (2000) suggested that tephra thickness T (cm) is exponentially related to the square root of isopach area $\sqrt{A}$ from past research,

$$T(A) = \gamma \exp(-\delta\sqrt{A}) \tag{2.2}$$

where δ and γ are parameters to be estimated.

However the relationship between $\log T$ and $\sqrt{A}$ is not a straight line when plotted on a semi-log plot. In fact it does not have a constant slope for all $\sqrt{A}$ values. Pyle (1989) and Bonadonna and Houghton (2005) found a solution by splitting the data into multiple segments for different distance ranges and fitting an exponential line for each. The choice of both number and position of segments need to be determined (Bonadonna and Costa, 2012).

As an alternative Bonadonna and Houghton (2005) fitted a power law model,

$$T(A) = \gamma\sqrt{A}^{-\alpha}. \tag{2.3}$$

This model allows more flexibility in capturing the thinning of the deposits but the power law is not integrable at zero and infinity (Bonadonna and Houghton, 2005;

Bonadonna and Costa, 2012). To get around this Bonadonna and Costa (2012) proposed a Weibull distribution model by generalising the exponential model with an extra parameter n:

$$T(A) = \gamma(\delta\sqrt{A})^{n-2} \exp\left[-(\delta\sqrt{A})^{n}\right], \tag{2.4}$$

where δ allows some flexibility in the decay rate which the exponential model fails to do. Note that for $n = 1$, the volume V as a function of $\sqrt{A}$ follows an exponential distribution.

2.2.4 Semiempirical models

For modelling tephra fall attenuation from single eruptions, a compromise between the simple tephra attenuation models and the numerical simulations is provided by the class of 'semiempirical models'.

Rhoades et al. (2002) and Gonzlalez-Mellado and De la Cruz-Reyna (2010) incorporated wind effect to allow a tephra dispersal in a quasi-elliptic shape. Given the eruptive volume V (km^3) and tephra thickness T (cm) at a distance from the vent r (km) in direction θ relative to the wind direction, the direction attenuation relation model (Rhoades et al., 2002) is given by

$$T(V, r, \theta) = kV^{(c+1)/3} \exp\left[\sum_{i=1}^{n} \alpha_i \sin(i\theta) + \beta_i \cos(i\theta)\right](r + dV^{1/3})^{-c}, \tag{2.5}$$

where attenuation parameters $k, c,$ and d and directional parameters α_i and β_i are parameters to be estimated. Each of the α_i and β_i parameters takes non-zero values only if they are significant. The term $dV^{1/3}$ is added to r to ensure a finite thickness at the source, i.e., $r = 0$. The terms involving θ allow for a perturbed elliptic shape determined by wind.

Gonzlalez-Mellado and De la Cruz-Reyna (2010) proposed an alternative model involving a wind-based radial dependence term θ and a power law decay with distance

r:

$$T(r, \theta) = \gamma \exp\left[-\beta U r(1 - \cos\theta)\right] r^{-\alpha}, \tag{2.6}$$

where γ is the expected thickness at 1km from the vent along the dispersal axis (wind direction), β is inversely related to the diffusion coefficient (larger diffusion coefficients indicate faster diffusion), and U is wind speed (km/h). The dispersal axis is the wind direction. Gonzlalez-Mellado and De la Cruz-Reyna (2010) linked α to eruption column height, which is the height of volcanic ash emitted into the air during an explosive eruption (Johnson and Threlfall, 1937).

The models of Gonzlalez-Mellado and De la Cruz-Reyna (2010) and Rhoades et al. (2002) have similar parameterisations; the expected thickness is the product of a constant $kV^{(c+1)/3}$ or γ, a nonlinear wind term $\exp\left[\sum_{i=1}^{n} \alpha_i \sin(i\theta) + \beta_i \cos(i\theta)\right]$ or $\exp\left[-\beta U r(1 - \cos\theta)\right]$, and a power law decay with distance $(r + dV^{1/3})^{-c}$ or $r^{-\alpha}$, respectively.

Figure 2.3 shows the fitted thickness obtained using least squares on the log scale from the two models (Equations 2.5 and 2.6) on the 1973 Heimaey eruption data (Self et al., 1974) (Figure 3.1). The scoria volume of 0.04km^3 (Self et al., 1974) is used for volume V in Equation 2.5 and only one wind parameter (α_1) was found significant.

Using the same Heimaey data the fitted thicknesses from the two models are plotted against their observed thicknesses in Figure 2.4. Again they show very similar fitted dispersals due to the similarity in the parameterisations. However Figure 2.4(i) shows that there is an unusually large residual (at top right) in the Rhoades et al. (2002) model.

Without wind ($U = 0$), Equation 2.6 reduces to radial symmetry of the tephra dispersal around the vent. The resultant power law model (Gonzlalez-Mellado and De la Cruz-Reyna, 2010; Engwell et al., 2013) is equivalent to Equation 2.3,

$$T(r) = \gamma r^{-\alpha}, \tag{2.7}$$

Figure 2.3: Contours of fitted thicknesses on the Heimaey data (Self et al., 1974). The observed thicknesses (cm) are shown. The vent is indicated by the origin.

(i) Directional attenuation relation (Rhoades et al., 2002) (Equation 2.5)

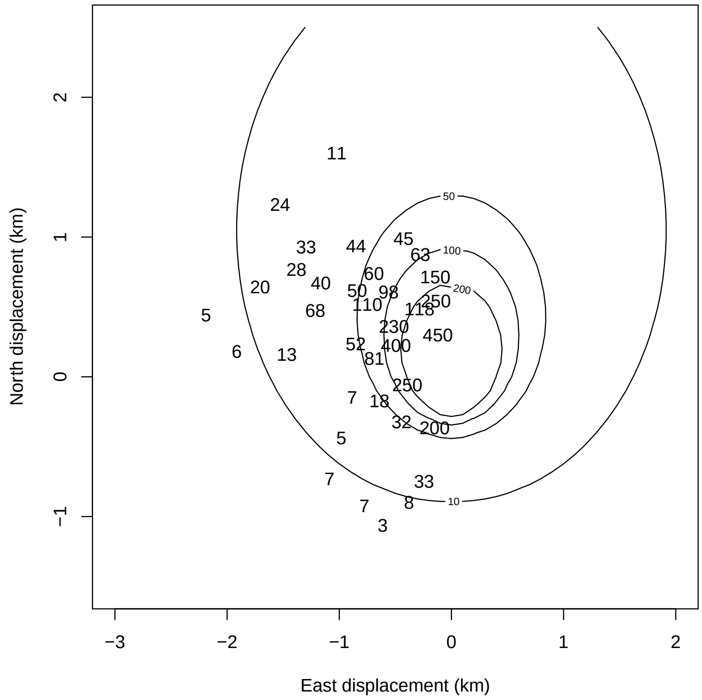

(ii) Semiempirical model (Gonzlalez-Mellado and De la Cruz-Reyna, 2010) (Equation 2.6)

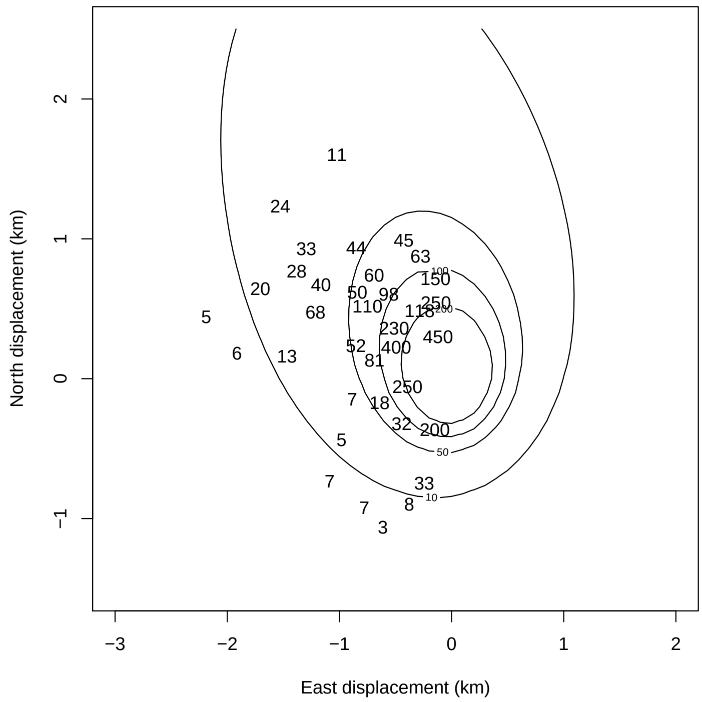

Figure 2.4: Observed vs. fitted thicknesses of the two semiempirical models using the Heimaey data.

(i) Directional attenuation relation (Rhoades et al., 2002) (Equation 2.5)

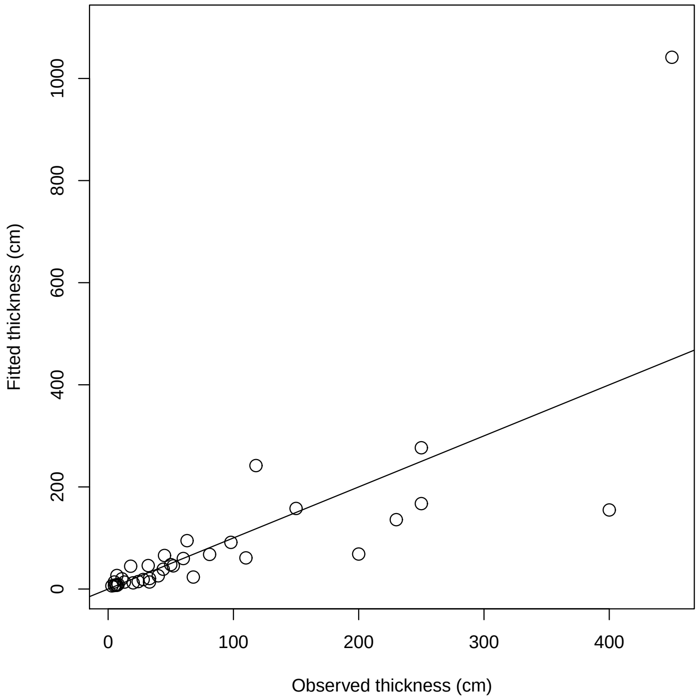

(ii) Semiempirical model (Gonzlalez-Mellado and De la Cruz-Reyna, 2010) (Equation 2.6)

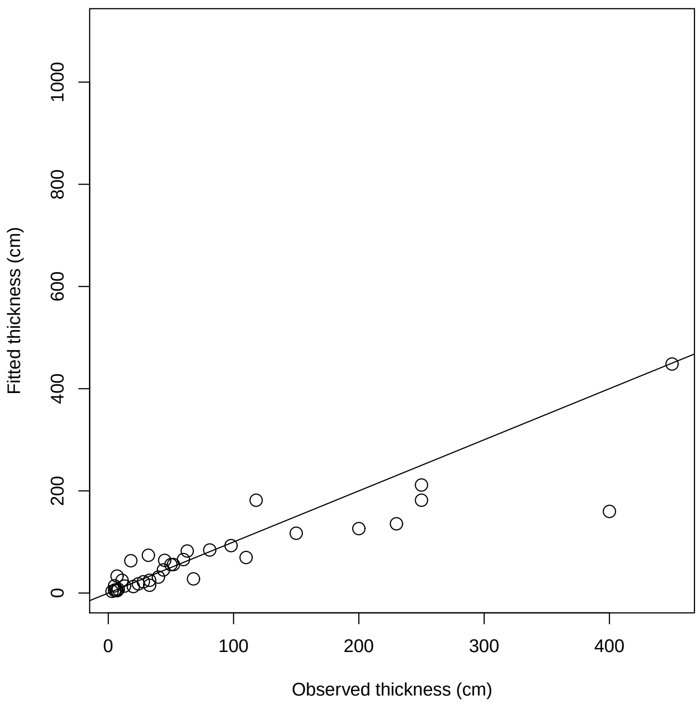

and, as the isopachs will be circular, the exponential model (Equation 2.2) becomes

$$T(r) = \gamma \exp(-\delta r) \tag{2.8}$$

(Gonzlalez-Mellado and De la Cruz-Reyna, 2010; Burden et al., 2013; Engwell et al., 2013).

The most popular method of estimating the model parameters has been least squares minimisation after appropriately linearising the model. Bonasia et al. (2010) and Bonadonna and Costa (2012) used weighted least squares. Gonzlalez-Mellado and De la Cruz-Reyna (2010) estimated their parameters by maximising the linear correlation coefficients between the observed and fitted data.

Burden et al. (2013) and Engwell et al. (2013) initially fitted Equation 2.8 to the entire tephra blanket. Later, as a compromise for the lack of directional effect they divided the raw data into quadrants and fitted a symmetric model such as Equations 2.7 and 2.8 to each. As in actuality, each data point has its own slope with distance dependent on its azimuth, the use of quadrants is an approximation. It allows different slopes for different quadrants but has to assume a constant slope within each quadrant. This can be improved further by increasing the number of sectors but the amount of available data in each sector will inevitably decreases. A further disadvantage of this approach is the subjectivity in dividing the data set into a predetermined number of sectors and the possibility that models produce inconsistent results at the edges of the two adjacent sectors.

2.2.5 Fresh versus old tephra

Tephra can be collected and sampled immediately after an eruption as fresh tephra or hundreds of years later as stale or weathered tephra. The thicknesses of tephra change over time due to erosion and reworking. In general thinner thicknesses are more likely to erode over time (Engwell et al., 2013). Bonadonna et al. (1998), Gonzlalez-Mellado and De la Cruz-Reyna (2010) and Engwell et al. (2013) investigated the suitability of the exponential and power law models on fresh and stale tephra deposits by fitting both models on the same data and comparing the fit of the two models. Engwell et al. (2013) found that the exponential model was preferred for the approximately 5,000-year-old Fogo A eruption in Sao Miguel. Gonzlalez-Mellado and De la Cruz-Reyna (2010) fitted their model to fresh deposits from El Chichon 1982 and stale deposits after several months of rain (Carey and Sigurdsson, 1986) and compared the fits. They found that fresh deposits are better described by the power law model and older deposits are better described by the exponential function. These findings agree with the weathering behaviour of the tephra. Because distal deposits erode over time and become thinner over time, stale deposits prefer the exponential model which decays slower at proximal and faster at distance. An illustration is given by Figure 2.5(i) showing the fresh 1973 Heimaey eruption tephra deposits for which the power law model fits better.

2.2.6 Volume estimation

The size of an eruption is an important variable to establish when assessing volcanic hazard. The eruptive volume of tephra deposits can be estimated based on its relationship with tephra thicknesses.

Unlike the other tephra fall attenuation models which are designed for tephra blanket from single eruptions, Rhoades et al. (2002) examined a data set of multiple eruptions from Taupo Volcano, thus incorporating volume. Equation 2.5 has a volume term in its model as an explicit parameter which can be estimated when fitting the model.

However, attenuation models such as Gonzlalez-Mellado and De la Cruz-Reyna (2010) and Bonadonna and Costa (2012) do not have a volume parameter in their models. There are a number of ways to estimate volume. The integration of one of the three

Figure 2.5: The relationship between thickness (cm) and distance (km) from the vent for the Heimaey eruption data.

(i) Fitted thicknesses from the power law model (Equation 2.7) and exponential model (Equation 2.8)

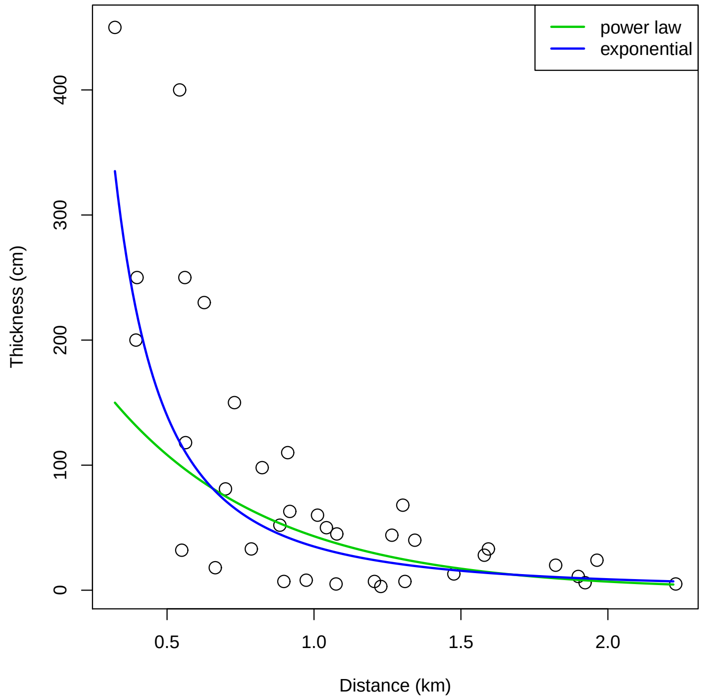

(ii) Fitted thicknesses vs. residuals from the power law model (left) and exponential model (right)

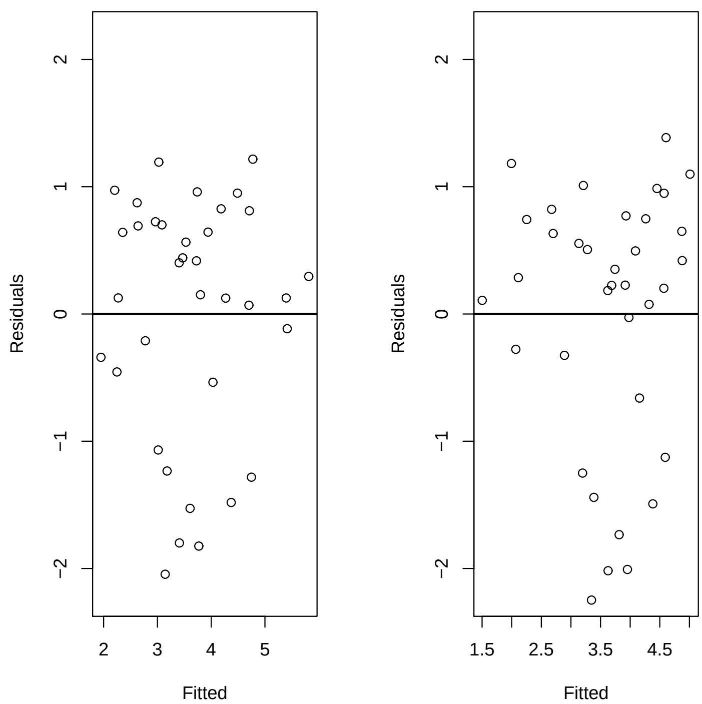

empirical models (Equations 2.2-2.4) at appropriate limits can produce volume estimates,

$$
\begin{aligned}
V &= \int_0^\infty T(\sqrt{A})\,\mathrm{d}\sqrt{A} \\
&= 2\int_0^\infty \sqrt{A}T(\sqrt{A})\,\mathrm{d}A,
\end{aligned}
$$

where T is the tephra thickness and A is the isopach area. The integration of the power law model requires selecting arbitrary integration limits as the model cannot be integrated between zero and infinity (Bonadonna and Costa, 2012). The proposed Weibull model (Bonadonna and Costa, 2012) is integrable between zero and infinity like the exponential model but can describe the thinning relationship well like the power law model, which the exponential model manages to do only with multiple segments.

With more sophisticated models (Equations 2.6-2.8) that give tephra thickness by location (x, y) instead of isopach area A the volume can be estimated by

$$
\begin{aligned}
V &= \iint\limits_R T(x,y)\,\mathrm{d}A \\
&= \lim_{L\to\infty}\int_0^{2\pi}\int_0^L T(r\cos\theta, r\sin\theta)r\,\mathrm{d}r\mathrm{d}\theta,
\end{aligned}
$$

where R is the circular area with an infinite radius. Note that the polar coordinate gains an r term when converted from the Cartesian coordinate since $\mathrm{d}A = r\,\mathrm{d}r\mathrm{d}\theta$.

Alternatively an approximation is to sum the fitted thicknesses over an appropriate region but the estimate is sensitive to the choice of limits for r.

There is yet to be one single model that has been accepted as the model to use in the literature. Hence fitting multiple models and comparing their fits has become more and more common. AshCalc (Daggitt et al., 2014) is software written in Python that fits the three most commonly used models; exponential, power law, and Weibull (Equations 2.2-2.4) and compares their suitability in a routine manner. The estimated volumes from the three models can be calculated, along with relative mean squared error measuring the accuracy of the estimates (Bonadonna and Costa, 2012). The comparison of the new estimates provided by AshCalc were in agreement with the previously published estimates (Daggitt et al., 2014).

Burden et al. (2013) produced volume estimates by summing the four integrations of the tephra models from the four quadrants. They followed the Bayesian method of Chen and Deely (1996) with non-informative priors to estimate the confidence intervals for their volume estimates. Previously published volume estimates based on isopachs were not included in the resulting confidence intervals.

2.2.7 Residuals, sensitivity analysis and robustness

Although sometimes the fitted thicknesses are plotted on top of the observed, checking of the regression assumptions is often neglected when least squares is used in the literature. Thickness is naturally strictly positive and hence right skewed. If least squares is used on the log scale then appropriateness of the log transformation should be checked in terms of normality and homogeneity of residuals.

When least squares is used and there is some wind effect present in the data, equal variance (for the symmetric models) cannot be assumed as the residuals will depend on direction as well as distance. Engwell et al. (2013) checked for homogeneity of error variance and found the residuals from the exponential model more symmetrically scattered than those from the power law model.

To give an example, although the fitted vs. residual plots do not indicate a major concern (Figure 2.5(ii)), the normality of the residuals is rejected with a p-value of 0.0015 and 0.0025, respectively, given by Shapiro-Wilk normality tests.

Rhoades et al. (2002) provides standard errors of the estimated parameters. Biass et al. (2014) produced a MATLAB package called TError to incorporate uncertainty that is propagated in modelling plume height and mass eruption rate as well as eruption volume from tephra deposits. TError allows the user to input the necessary parameters such as tephra thickness measurements and area of isopach contours, each with multiplicative error range. This uncertainty may be due to sampling error, measurement error and, in the construction of isopach contours, the subjectivity involved in the process. The necessary models that describe the relationship between input and output parameters come from the literature. The model parameters are estimated using least squares after linearising the appropriate side(s) of the equation. TError incorporates the uncertainty associated with each input parameter stochastically, one at a time, to produce output parameters with error. This is useful to assess the sensitivity of output parameters.

Bonadonna and Costa (2012) performed a sensitivity analysis by removing proximal, medial, and distal data one at a time. After comparing the robustness of their Weibull model against the exponential and power law models they were able to claim that their Weibull function is the most robust when proximal, medial, or distal data are missing. The ability to produce a good estimate in the absence of one type of data is desirable as proximal and distal areas are often not well-preserved (Bonadonna and Costa, 2012) due to inaccessibility and weathering.

2.2.8 Recreation of past events

Tephra attenuation models can be used to recreate a past eruption by estimating the model parameters or to simulate a potential tephra dispersal scenario around a volcano for a future explosive eruption. In order to do this empirical models require appropriate possible parameter values and numerical models require necessary additional information such as external conditions. Volcanic hazard forecasting will help with future planning by creating a spatial hazard map for tephra dispersal.

A volcanic eruption can also be simulated by applying the scenario of a different volcano with its estimated parameters. Gonzlalez-Mellado and De la Cruz-Reyna (2010) fitted their model to some of the recent eruptions at Popocatepetl and Colima volcanoes. The fitted model can be used to generate the tephra dispersal in a new eruption scenario and/or at another volcano by substituting the estimated parameters into the model.

Possible applications include estimating the relative likelihood of a tephra being sourced from different vents (Bebbington and Cronin, 2011) due to the feasibility of inverting the attenuation models. Bebbington et al. (2008) used the model of Rhoades et al. (2002) to produce a probabilistic tephra hazard model for potential impact of tephra fall on the electrical infrastructure in the Taranaki Region.

These tephra attenuation models are useful for civil defence purposes through spatial hazard maps and for simulating a past/future eruption given the necessary topographical, eruption, and meteorological parameters.

2.3 Dating methods

A number of radiometric and other dating methods are available to estimate the timing of eruptions. Different methods have different degrees of reliability due to their characteristics. For example, radiometric methods such as argon-argon and potassium-argon may have uncertainties in the range of thousands of years (Siebert et al., 2010). The precision of estimated ages also depends on the quality of the sample and the environment in which it is found and the time of dating as the techniques tend to improve over time. However these will always be estimates and the true ages are still unknown.

2.3.1 Radiocarbon dating

Radiocarbon (^{14}C) dating measures the decay rate of ^{14}C in the organic material usually found in tephra, to estimate the timing of an eruption. This is done by measuring the ratio of ^{14}C to ^{12}C or ^{13}C present in the sample. The normally distributed ^{14}C ages are expressed in the form mean $\pm$ error years before present (BP) where present is referred to as 1950 (Siebert et al., 2010). Since the half-life of ^{14}C is 5,730 years (Ramsey, 2014) the ages of samples older than 50,000 years cannot be accurately measured with the current technology due to an insufficient amount of ^{14}C left in them (Lindsay and Leonard, 2009).

The conventional ^{14}C ages are calibrated to be expressed in terms of calendar years BP. However the conversion is not as simple as adding the difference between the current year and 1950 due to inconsistencies in the proportion of ^{14}C in the atmosphere over time. Therefore ^{14}C ages are calibrated to be expressed in terms of calendar years BP using a calibration curve such as Figure 2.6. The curve is not monotonic, meaning there may not be a unique calendar age range for each ^{14}C age.

For example, a sample of charcoal from the base of a pit of Rangitoto (Davidson, 1972) dated 570 ± 38 ^{14}C age BP was converted into a calendar age interval using available software such as `http://radiocarbon.ldeo.columbia.edu/research/radcarbcal.htm` (Figure 2.7). The unimodal normally distributed ^{14}C age is plotted on the vertical axis and the derived calendar age on the horizontal axis shows a bimodal distribution. This means that the Rangitoto sample has two possible calendar age intervals.

2.3.2 Potassium-argon dating

Potassium-argon (K-Ar) dating measures the ratio of the radio active ^{40}K to the stable ^{40}Ar isotopes to evaluate the age of lava. This method is most commonly used for rocks aged older than 100,000 years (Dalrymple and Lanphere, 1969) and is used extensively for dating ages on older rocks (McDougall and Harrison, 1999). There is some disagreement about its applicability to younger samples due to the lack of ^{40}Ar (McDougall et al., 1969; Dalrymple and Lanphere, 1971).

2.3.3 Argon-argon dating

Argon-argon ($^{40}Ar/^{39}Ar$) dating measures the ratio of the radio active ^{39}Ar to the stable ^{40}Ar isotopes in the lavas. This technique is similar to K-Ar but considered more favourable due to the greater precision (Siebert et al., 2010). For very young rocks (less than 100,000 years), the reliability of this technique is less certain (Dalrymple and Lanphere, 1969; Cassata et al., 2008).

Figure 2.6: Calibration curve based on Southern Hemisphere tree-ring measurements SHCal04 with one standard deviation interval (McCormac et al., 2004).

(i) 0-1,000 cal BP

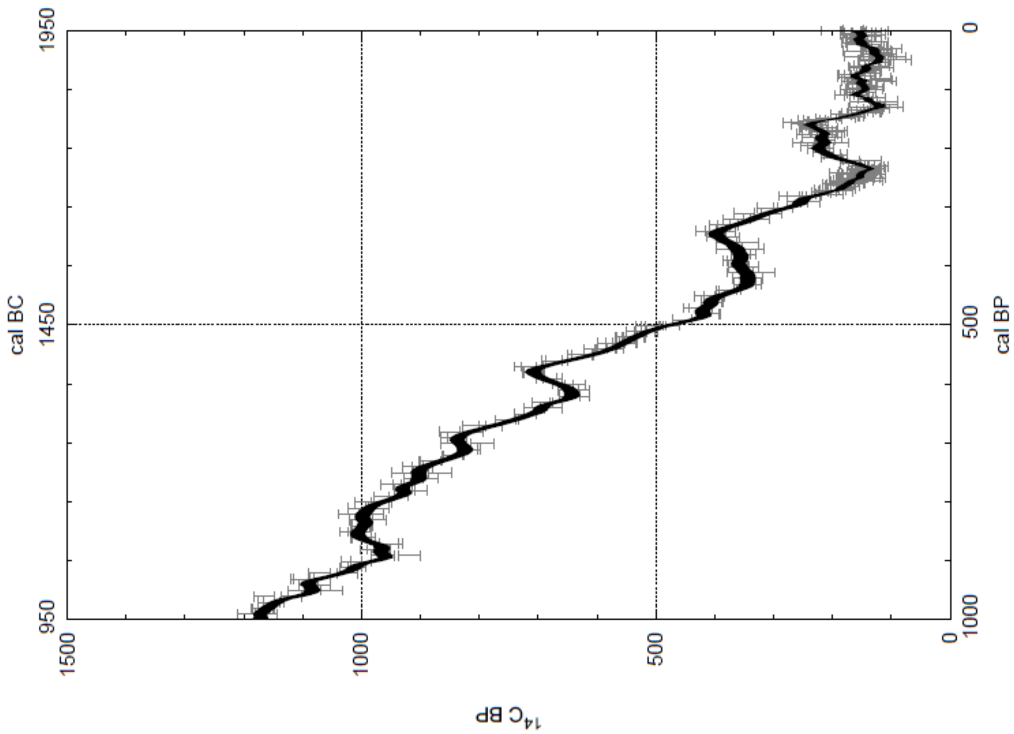

(ii) 1,000-2,000 cal BP

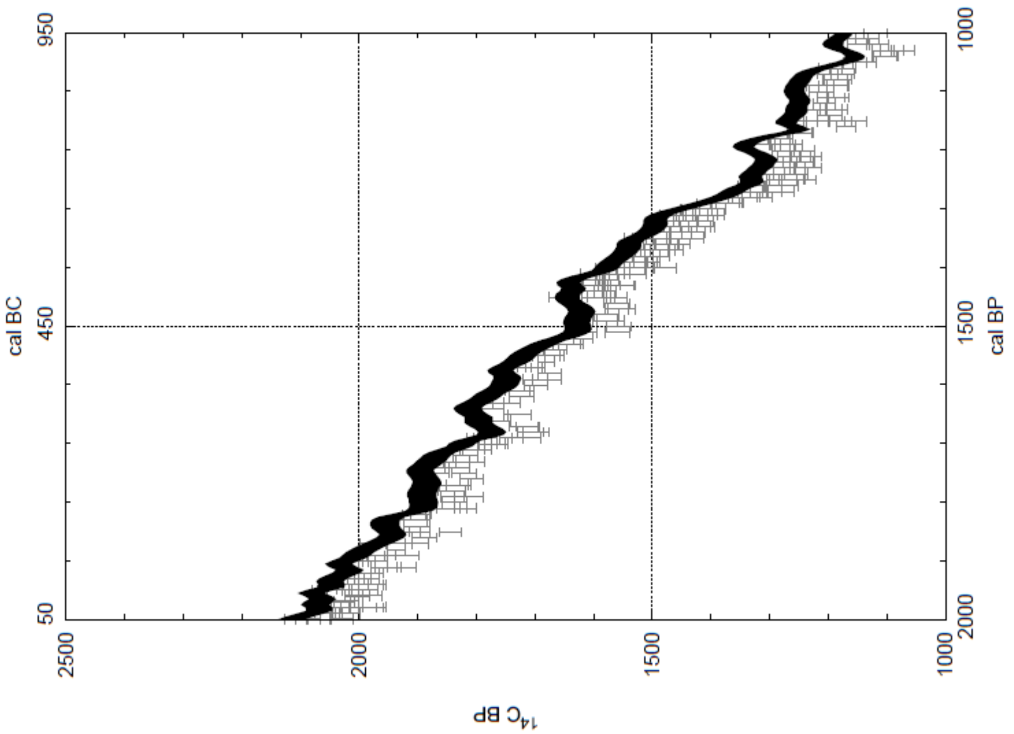

Figure 2.7: Radiocarbon age to calendar age conversion using `http://radiocarbon.ldeo.columbia.edu/research/radcarbcal.htm`.

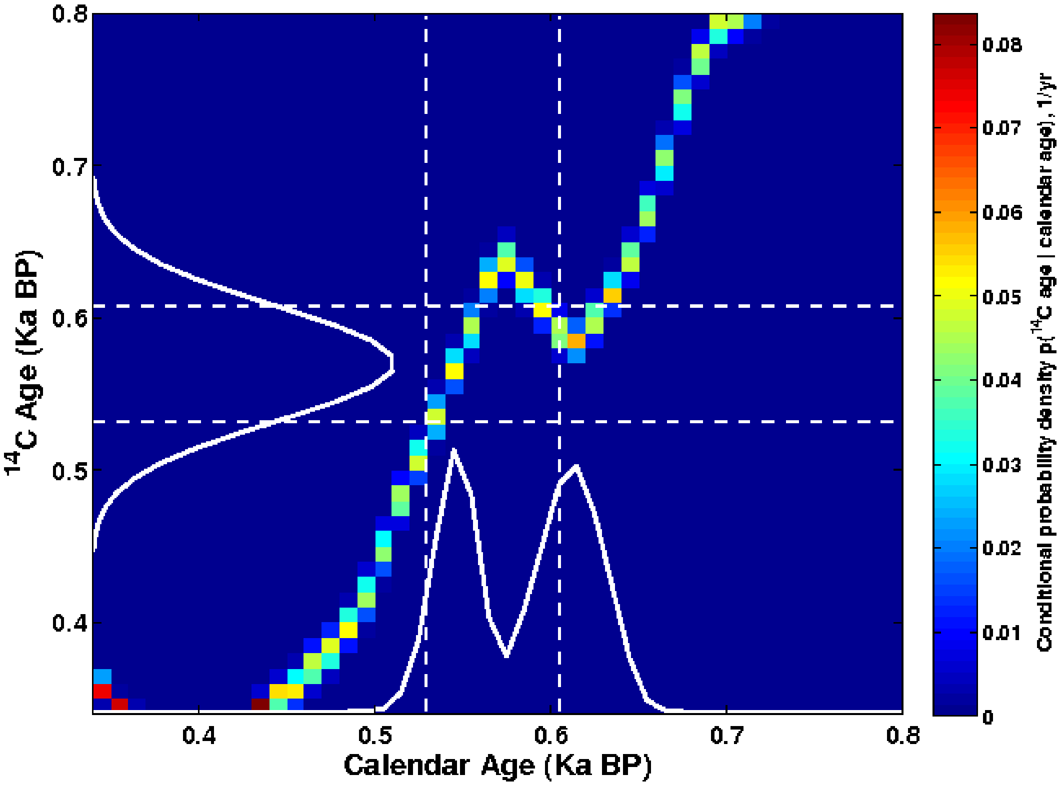

Figure 2.8: The two alternating states of the geomagnetic field (Bogue and Merrill, 1992).

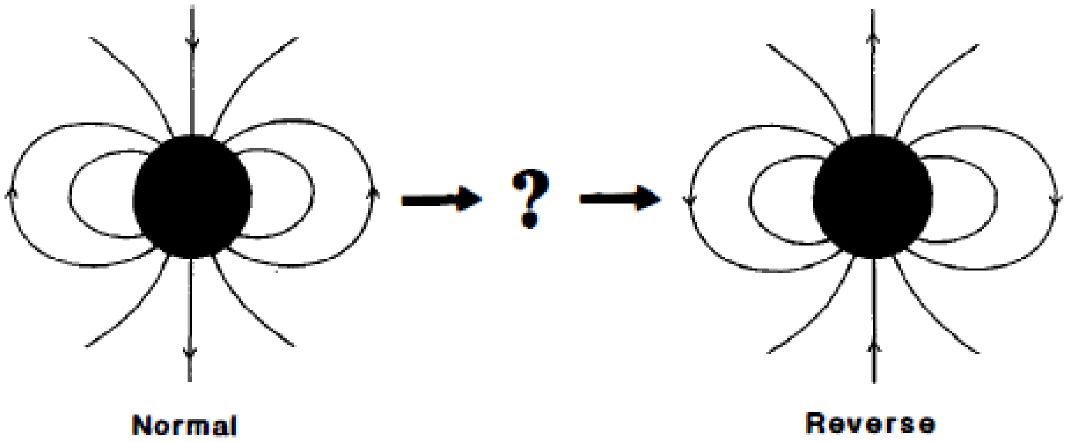

2.3.4 Paleomagnetic declination

At the Earth's surface the flow of the geomagnetic field has alternated between normal and reversed at particular times in the past (Cande and Kent, 1995) (Figure 2.8). A geomagnetic reversal (the right of Figure 2.8) is a temporary change in the magnetic field that swaps magnetic north to south and vice versa. Two particular reversal periods, the Laschamp excursion (40.4 ± 1.1ka) (Guillou et al., 2004) and the Mono Lake excursion (32.4 ± 0.3ka) (Cassidy, 2006; Singer, 2007; Cassata et al., 2008), are relevant in this thesis. The paleomagnetic declination is measured by comparing the measured paleomagnetic declinations against the known geomagnetic reversals in the geological record.

2.3.5 Optically stimulated luminescence dating

Optically stimulated luminescence (OSL) dating obtains its estimated ages by measuring the dose from ionising radiation in sediments. OSL dating determines the timing of the event directly, resulting in a higher likelihood of pinpointing the time of deposition (Aitken, 1985). Two quantities are required to date a sediment, the dose, and the equivalent dose required to produce the luminescence signal. The returned age is the time elapsed since the sampled sediment was last exposed to sunlight (Lindsay and Leonard, 2009). In general, Murray and Olley (2002) found the OSL ages to be accurate for up to 350ka, however, this method is sensitive to light (McKeever and Moscovitch, 2003).

2.3.6 Thermoluminescence dating

Thermoluminescence (TL) dating measures the amount of radiation from the crystalline minerals contained in lavas. Similarly to OSL, TL directly dates the time elapsed since the material was exposed to sunlight (Richter, 2007). Although TL (on heated rock material) shows robustness due to the stable internal dose rate in all samples, it has been criticised for the large uncertainties (Richter, 2007).

2.4 Summary

In this chapter the volcanological terminology and concepts have been reviewed. In particular, tephra has been defined and existing tephra dispersal models have been reviewed and discussed. The development of estimating eruptive volume from these models has also been discussed.

Chapter 3

Tephra Dispersal - One Component

Work regarding the Heimaey eruption discussed in this chapter and work regarding the Ukinrek eruption discussed in Chapter 4 are published in Kawabata et al. (2013).

3.1 Introduction

One of the major hazards from volcanic eruptions is the dispersal of tephra at considerable distances from the volcano. The thickness of tephra fall deposits usually decreases with distance from the source. Thus a tephra attenuation model as a function of distance and direction from the source can be useful in estimating tephra thickness at a given location. It can also incorporate thickness decay in an elliptical shape, caused by wind. In recent studies, isopachs have been generally fitted to the model, however, in this chapter, the models will be fitted to actual tephra measurements using maximum likelihood estimation (MLE). This way the sampling error in the thickness measurements can be expressed explicitly. Since tephra thickness is strictly non-negative, and larger measurements will generally produce larger absolute errors, a multiplicative error structure is assumed. Thus lognormal, Weibull, and gamma distributions have been considered to describe the variability for the thickness data. In order to determine a suitable distribution, a data set is required without the complications of multiple lobes or vents. We consider the basaltic explosive 1973 Heimaey eruption.

3.2 The Heimaey eruption

The eruption of Eldfell on Heimaey, Iceland, on 24 January 1973 provided appropriate data for studying the variability in deposited tephra thicknesses. The tephra dispersal data (Self et al., 1974) was collected from 24 January to 19 February 1973. The data consist of observed thicknesses at 36 locations, ranging between 3 and 450cm, as shown in Figure 3.1. Winds were blowing predominantly to the northwest and the northeast during the eruption, according to measurements from the Icelandic Meteorological Service at the Storhofdi Lighthouse. While the former wind direction resulted in measurable deposition on land, an estimated 65% of the tephra deposited under the influence of the westerly winds fell into the sea and were not measured. The resulting single-lobe pattern is ideal for this study.

3.3 Sampling error

The actual thickness observed at any given point differs from an expected thickness due to small random effects of wind strength and direction, but primarily due to local redistribution of fallen tephra by wind, rain, and slope processes (especially in highly irregular topography). This difference can be termed the ‘sampling error’ or ‘aleatory error’, which describes the inherent variability of the observations. The absolute error (or residual) at a point i is $A_i = O_i - E_i$, where O_i is the observed thickness at location i, and E_i is the expected thickness at location i. However, a multiplicative error structure is assumed here, such that the size of the error is proportional to the expected thickness. In other words, the focus is the ‘relative error’ $A_i/E_i \geq -1$. For reasons that will become obvious, it is shifted to become non-negative, and the (shifted)

Figure 3.1: The observed thickness (cm) and locations for the Heimaey eruption data. The vent is indicated by the triangle. The dotted line indicates the coast line prior to this eruption.

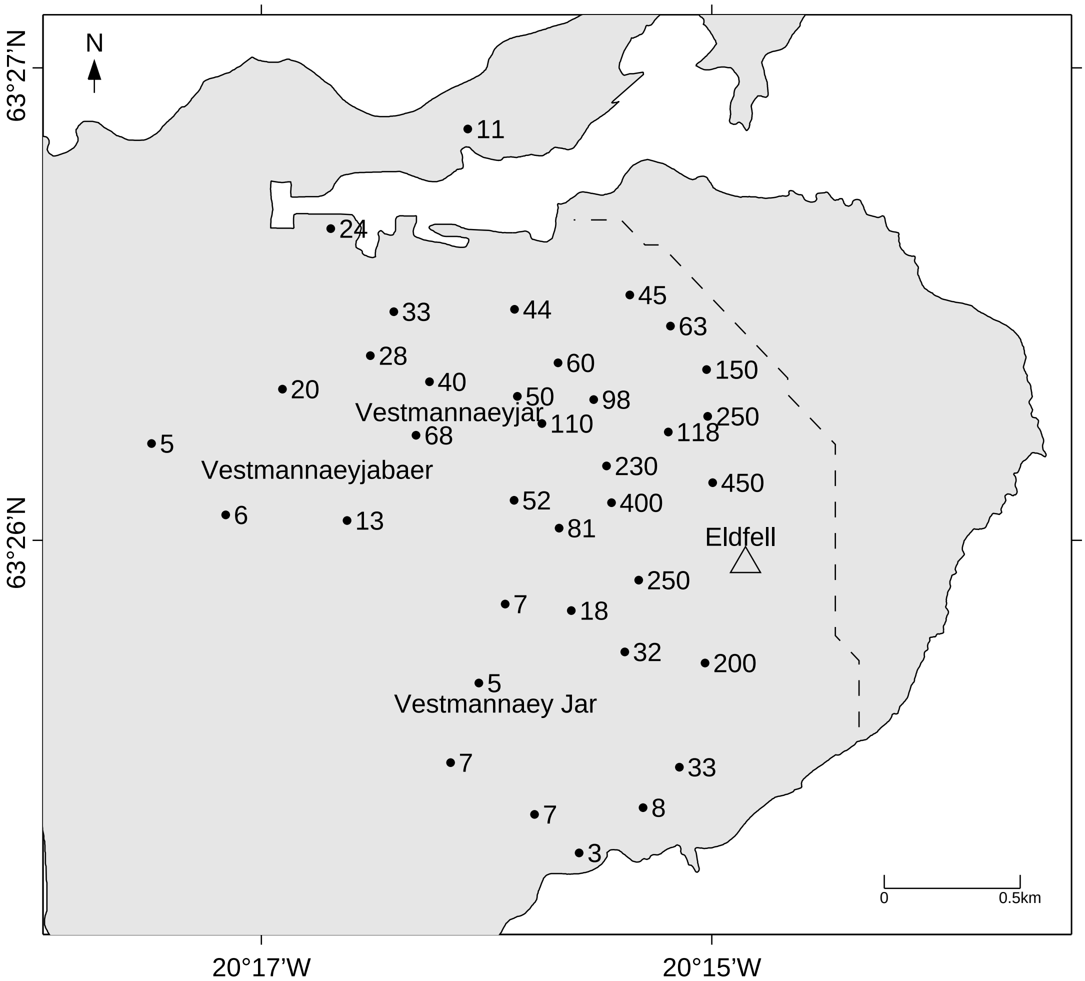

relative error is considered $R_i = A_i/E_i + 1 = O_i/E_i$. Thus, an observation that aligns exactly with expectation has a relative error of one. Values less than or greater than one indicate under- or over-thickening of the tephra, respectively.

The relative errors are all defined in terms of an expected value that is to be calculated from a parametric model. As the error is thus dependent on the model, and selection amongst multiple models is required, a model independent (nonparametric form) of the error distribution is initially estimated in order to discover candidate parametric distributions that might be suitable.

A leave-one-out cross-validation approach to estimating the expected thickness was applied. The observation at location i is omitted, and a surface is fitted to the remaining 35 data points using a triangulated C^1-continuous interpolating surface. The C^1 denotes a differentiable function whose derivative is continuous (except at the observed locations). The value of this surface at location i is taken to be E_i. This is repeated for all locations inside the convex hull of the data to obtain relative errors, as shown by the histogram in Figure 3.2(i). It is clear that the relative sampling error is non-negative and right-skewed, with a mode less than one. By denoting the relative error by R, the lognormal

$$f(R) = \frac{1}{R\sqrt{2\pi\sigma^2}} \exp\left[-\frac{(\log R - \mu)^2}{2\sigma^2}\right], \tag{3.1}$$

Weibull

$$f(R) = \frac{\kappa R^{\kappa-1}}{\lambda^\kappa} \exp\left[-\left(\frac{R}{\lambda}\right)^\kappa\right], \tag{3.2}$$

and gamma

$$f(R) = \frac{R^{\kappa-1}}{\lambda^\kappa \Gamma(\kappa)} \exp\left(\frac{-R}{\lambda}\right) \tag{3.3}$$

distributions are good exemplars of distributions that can be used to model such errors. All have two parameters: a location parameter μ and a scale parameter σ for the lognormal and a shape parameter κ and a scale parameter λ for the Weibull and gamma distributions. As can be seen from Equations 3.1-3.3, they differ mainly in the rate at which the tail decays. The gamma distribution decays much more rapidly than the lognormal, and the Weibull may decay faster or slower than the gamma, depending on the value of the shape parameter κ. Fitting these distributions to the nonparametric relative errors via MLE produces the densities superimposed on the histogram in Figure 3.2(i).

The lognormal density is less faithful to the data than the other two candidates, due primarily to the right-hand tail of the data not being thick enough, and this is quantified more clearly in Figure 3.2(ii). The maximum distance between the data (the step function) and the curve is the Kolmogorov-Smirnov statistic for the distance between distributions, with values of 0.156, 0.122, and 0.124 for the lognormal, Weibull, and gamma distributions, respectively. The critical value for testing against a uniform distribution is 0.264 at the 5% significance level. While all of the statistics are much smaller than this value, they do indicate that the Weibull and gamma distributions both fit the data well, and the lognormal slightly less well.

3.4 Tephra attenuation

The nonparametric relative errors have been shown to be consistent with the Weibull and gamma, and perhaps lognormal, distributions. Hence, these error distributions were embedded in the framework of a tephra dispersal model. For the reasons outlined in Section 3.1, an empirical model is required that has the facility to include a possible wind effect. Since the Rhoades et al. (2002) model is framed for a sample of multiple eruptions, the model of Gonzlalez-Mellado and De la Cruz-Reyna (2010) is preferred here.

The basic form of the Gonzlalez-Mellado and De la Cruz-Reyna (2010) model is that the expected tephra fall deposit thickness is the product of a power law decay with distance (Bonadonna et al., 2005) and a noncircular term based on wind direction. A power law decay with distance was preferred to an exponential primarily because it fits well in both the near and far field. It has also been shown that a simple exponential decay may

Figure 3.2: Nonparametric relative sampling error R and three fitted distributions.

(i) Density

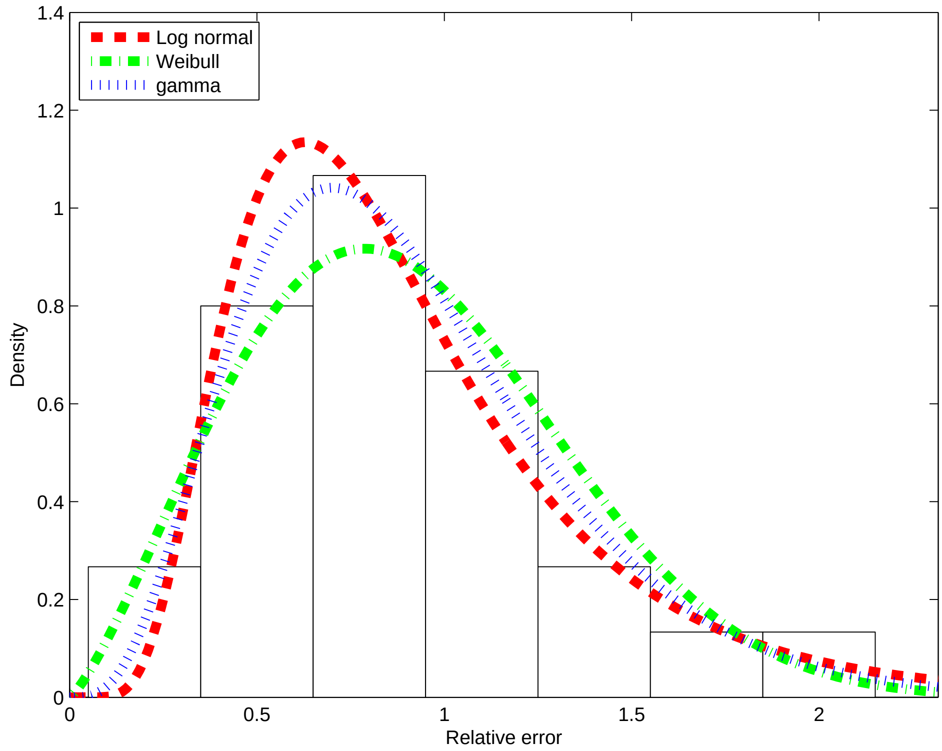

(ii) Distribution

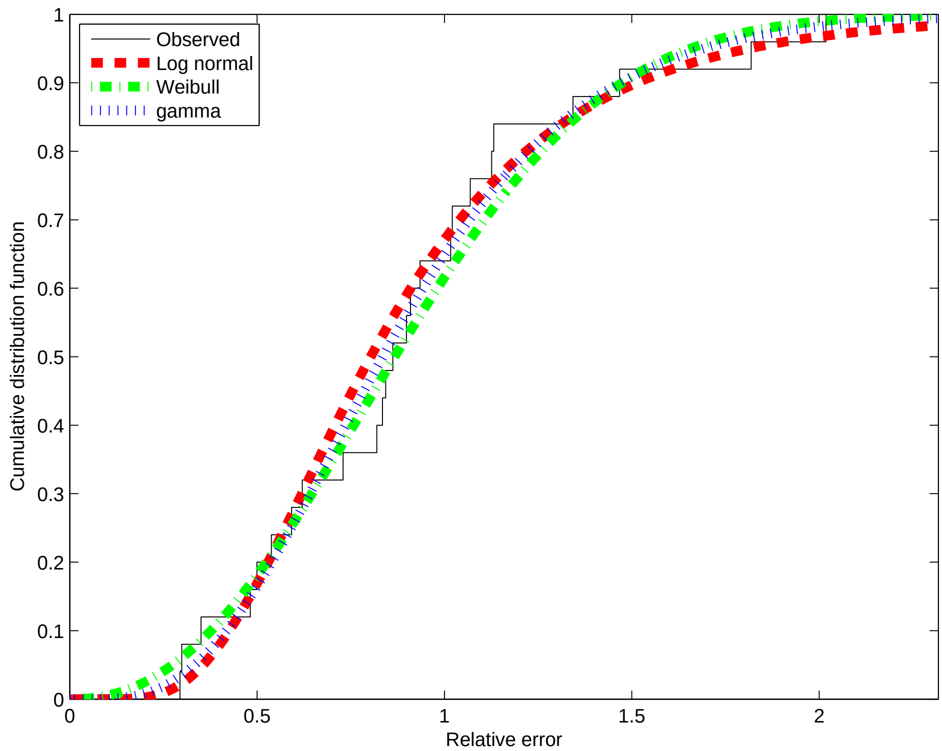

not well describe well-preserved tephra deposits, due to distal ash settling differently (Sparks et al., 1992; Rose, 1993). Using the three exponential segments necessary to model accurately the thinning of well-preserved deposits (Bonadonna et al., 2005) is also undesirable, because it would add another four parameters to the estimation problem.

The attenuation relation by Gonzlalez-Mellado and De la Cruz-Reyna (2010) is

$$T(r, \theta) = \gamma \exp\left[-\beta U r(1 - \cos\theta)\right] r^{-\alpha}, \tag{3.4}$$

where T is the tephra thickness (cm) at a distance from the vent r (km) in direction θ relative to the wind direction. If the supposed wind direction is given by ϕ, and that the direction from the vent to the deposit location is ξ (both measured in degrees anticlockwise from East), then $\theta = \xi - \phi$, and Equation 3.4 becomes

$$T(r, \xi) = \gamma \exp\{-\beta U r[1 - \cos(\xi - \phi)]\} r^{-\alpha}. \tag{3.5}$$

Note that the wind speed U (km/h) and direction ϕ are considered as the mean (with respect to the eruption rate) values of the predominant wind, and as such will be estimated from the data (the left-hand side of the equation).

The other parameters to be estimated are α, β, and γ. The latter is the expected thickness at 1km from the vent along the dispersal axis, which is a proxy for the eruption size. The dimensionless attenuation parameter α is non-negative, and β is inversely related to the diffusion coefficient, and thus can be regarded as a proxy for the grain size distribution. However, there is an identifiability issue, in that βU cannot be separately estimated, and so βU is considered as a single variable, reducing the number of parameters to be estimated to four. Moreover, βU (along with ϕ) is also a nuisance parameter, i.e., one that may or may not be present in the model. If there is no significant wind, then $U = 0$ and Equation 3.5 reduces to Equation 3.6:

$$T(r, \xi) = \gamma r^{-\alpha}, \tag{3.6}$$

with only two parameters to be estimated.

Gonzlalez-Mellado and De la Cruz-Reyna (2010) fitted their model to isopach data, thus avoiding the question of sampling error. However, the actual observed tephra thicknesses and locations are used in our formulation, rather than isopachs, and thus sampling error must be included in our fitting. By incorporating an error distribution, the model can be fitted using standard statistical MLE methods. This avoids the necessity of choosing a weighting scheme in the least-squares minimisation procedure. The choice of such a weighting scheme depends on the estimated uncertainties (Costa et al., 2009) and can strongly affect the results. In effect, the MLE treats the uncertainties explicitly, rather than approximately.

The error distributions are incorporated by treating the tephra thickness formula (Equation 3.5 or 3.6) as a link function giving the mean of the thickness distribution at the location (r, ξ). The shape parameter of the distribution (σ for the lognormal, κ for the Weibull, κ for the gamma) becomes an additional parameter to be estimated. Here the likelihood formulae for the various combinations of model and error distribution are derived. Let T denote the tephra thickness obtained from Equations 3.5 or 3.6.

Assume $T_i \sim$ lognormal (μ_{N_i}, σ_N) where μ_N is the location parameter and σ_{N_i} is the scale parameter of the conjugate normal distribution. Then $\mu_{LN_i} = \exp(\mu_{N_i} + \sigma_N^2/2)$ and $\sigma_{LN_i}^2 = [\exp(\sigma_N^2) - 1]\exp(2\mu_{N_i} + \sigma_N^2)$ by definition. Thus $\mu_{LN_i} = T(r_i, \xi_i)$ for the ith observation, and so $\mu_{N_i} = \log T_i - \sigma_N^2/2$. Note that the location parameter is no longer a constant, as it varies for each observation. The log likelihood function for the complete sample $i = 1, 2, \ldots, n$ is then obtained from Equation 3.1 as follows:

$$\log L = -\frac{n}{2}\left[\log(2\pi\sigma_N^2)\right] - \sum_{i=1}^{n} \log T_i - \frac{\sum_{i=1}^{n}(\log T_i - \mu_{N_i})^2}{2\sigma_N^2}. \tag{3.7}$$

Similarly, assume $T \sim$ Weibull (κ, λ) where κ is the shape parameter and λ is the scale parameter. Then $\mu_W = \lambda\Gamma(1 + 1/\kappa)$ and $\sigma_W = \lambda\sqrt{\Gamma(1 + 2/\kappa) - \Gamma^2(1 + 1/\kappa)}$ by definition. Thus $\mu_{W_i} = T(r_i, \xi_i)$ for the ith observation, and $\lambda_i = T_i/\Gamma(1 + 1/\kappa)$.

Again, the scale parameter is no longer a constant, as it varies for each observation. The log likelihood function for the complete sample $i = 1, 2, \ldots, n$ is then obtained from Equation 3.2 as follows:

$$\log L = n \log \kappa + (\kappa - 1) \sum_{i=1}^{n} \log T_i - \kappa \sum_{i=1}^{n} \log(\lambda_i) - \sum_{i=1}^{n} \left(\frac{T_i}{\lambda_i} \right)^{\kappa}. \tag{3.8}$$

Similarly, assume $T \sim$ gamma (κ, λ) where κ is the shape parameter and λ is the scale parameter. Then $\mu_G = \kappa\lambda$ and $\sigma_G = \sqrt{\kappa}\lambda$ by definition. So $\mu_{G_i} = T(r_i, \xi_i)$ for the ith observation, and $\lambda_i = T_i/\kappa$. Again, the scale parameter is no longer a constant. The log likelihood function for the complete sample $i = 1, 2, \ldots, n$ is then obtained from Equation 3.3 as follows:

$$\log L = (\kappa - 1) \sum_{i=1}^{n} \log T_i - \kappa \sum_{i=1}^{n} \log \lambda_i - n \log \Gamma(\kappa) - \sum_{i=1}^{n} \frac{T_i}{\lambda_i}. \tag{3.9}$$

To compare the distribution parameters of the three error distributions (the scale parameter for the lognormal distribution and the shape parameters for Weibull and gamma distributions) to be meaningfully compared, they can be converted into a coefficient of variation (CV = standard deviation divided by mean). Since we have $T_i = \mu_i R_i$,

$$\begin{aligned} CV[T_i] &= \frac{\sqrt{Var[T_i]}}{E[T_i]} \\ &= \frac{\mu_i^2 Var[R_i]}{\mu_i E[R_i]} \\ &= \frac{\sqrt{Var[R_i]}}{E[R_i]} \\ &= \frac{\sqrt{Var[R]}}{E[R]} \\ &= CV[R]. \end{aligned}$$

In each case, the CV is a function solely of the shape parameter (scale parameter in the lognormal case). In other words, the CV is a constant in all directions and at all distances, which is exactly the multiplicative error structure required. Hence, for the lognormal

$$\begin{aligned} \mathrm{CV} = \frac{\sigma_{LN}}{\mu_{LN}} &= \frac{\sqrt{[\exp(\sigma_N^2) - 1] \exp(2\mu_{N_i} + \sigma_N^2)}}{\exp\left(\mu_{N_i} + \sigma_N^2/2\right)} \\ &= \sqrt{\exp(\sigma_N^2) - 1}, \end{aligned} \tag{3.10}$$

Weibull

$$\begin{aligned} \mathrm{CV} = \frac{\sigma_W}{\mu_W} &= \frac{\lambda_i \sqrt{\Gamma\left(1 + 2/\kappa\right) - \Gamma^2\left(1 + 1/\kappa\right)}}{\left(\lambda_i \Gamma(1 + 1/\kappa)\right)} \\ &= \sqrt{\frac{\Gamma(1 + 2/\kappa)}{\Gamma^2(1 + 1/\kappa)} - 1}, \end{aligned} \tag{3.11}$$

and gamma

$$\mathrm{CV} = \frac{\sigma_G}{\mu_G} = \frac{\sqrt{\kappa}\lambda_i}{\kappa \lambda_i} = \frac{1}{\sqrt{\kappa}}. \tag{3.12}$$

Two baseline models (with and without wind) and three error distributions make for a total of six models to be fitted. This leaves the question of which model best describes the data. As all the error distributions have the same number of parameters, this can be decided on the basis of the likelihood. Equation 3.6 is nested within Equation 3.5, and so the model with more parameters can be justified using a likelihood ratio test. For comparison of models with and without wind, the Akaike Information Criterion (AIC) (Akaike, 1974) can be used instead:

$$\mathrm{AIC} = 2p - 2 \log L, \tag{3.13}$$

where p is the number of parameters, and $\log L$ the log likelihood. Smaller AICs indicate better models, with the effect of additional parameters being compensated for in order to avoid overfitting.

3.5 Results

Table 3.1 shows the estimated parameters from fitting each of the six possible models to the Heimaey tephra thickness data. To allow the shape parameters of the three error distributions, they have been converted into a CV, using Equations 3.10-3.12. The errors are calculated from the square root of the diagonal of the inverse of Hessian matrix of the likelihood function (Equations 3.7-3.9). It can be seen that the estimated parameters are fairly consistent for all distributions. In particular, the estimated wind direction ϕ is approximately north-northwest, in agreement with the meteorological data (Self et al., 1974).

The Weibull distribution has the smallest AIC, indicating that it is the best of the three distributions, but the gamma distribution is not significantly worse. However, the difference in AICs is sufficient to reject the lognormal distribution as a description of the sampling error. Moreover, the lognormal distribution systematically overestimates the volume of the eruption γ with respect to the other two distributions. It also has the highest CV, indicating a poorer absolute fit. Note that the CV decreases for all the error distributions with the introduction of wind effects. There is definitely an improvement from the model without wind (Equation 3.6), compared to the model incorporating wind (Equation 3.5). The χ^2 statistic (2 degrees of freedom) of twice the difference in the log likelihood ratios is significant for all three error distributions, with p-values less than 10^{-8} indicating that the model fit is significantly improved by including wind effects.

The AIC and likelihood ratio test tell us which model is better, but the question of whether the model is a good description of the data can only be answered by residual analysis, i.e., by examining the discrepancy between the data and the model. For a first visual inspection, Figure 3.3 shows the residual error (observation divided by the expected mean from the model) at each observation location. Small symbols indicate close to relative residual error of 1, which is desirable, while a large number of large

Table 3.1: Estimated parameters of the models with errors (1σ).

Baseline model	Parameter	Error distribution		
		lognormal	Weibull	gamma
Without wind	γ	54.0 ± 10.1	48.4 ± 5.6	48.6 ± 6.3
(Equation 3.6)	α	2.0 ± 0.3	2.0 ± 0.2	2.0 ± 0.3
	CV	1.18 ± 0.21	0.70 ± 0.09	0.78 ± 0.08
	$\log L$	-179.4	-175.5	-176.3
	AIC	364.8	357.0	358.5
With wind	γ	83.5 ± 16.0	71.0 ± 10.1	76.0 ± 12.8
(Equation 3.5)	βU	1.4 ± 0.2	1.5 ± 0.2	1.4 ± 0.2
	ϕ	114.1 ± 13.0	125.3 ± 12.1	119.2 ± 12.7
	α	1.6 ± 0.3	1.9 ± 0.2	1.8 ± 0.2
	CV	0.59 ± 0.08	0.45 ± 0.05	0.49 ± 0.06
	$\log L$	-160.1	-157.0	-157.9
	AIC	330.2	324.0	325.7

Table 3.2: Residual error statistics from the models.

Baseline model	Error distribution	Mean	SD
Without wind	lognormal	0.899	0.599
(Equation 3.6)	Weibull	1.004	0.669
	gamma	1.000	0.666
With wind	lognormal	0.978	0.461
(Equation 3.5)	Weibull	1.001	0.458
	gamma	1.000	0.463

symbols indicates a poor fit. The means and standard deviations of the residual errors are calculated in Table 3.2. The table shows that the residuals are much closer to one (smaller standard deviation) under the more complicated model (Equation 3.5). The lognormal overestimates thicknesses (the mean residual, or ratio of observed to estimated, is less than one), for reasons discussed above, while the Weibull and the gamma error distributions appear to be unbiased.

Although some of the residuals from our models are large, the aim is to explicitly quantify this variation. Whether the residuals are incompatible with the model can be evaluated by obtaining confidence bounds via Monte Carlo simulation. This uses repeated random sampling from the model with the estimated parameters to simulate possible thicknesses consistent with the model at each location. Figure 3.4 shows the

Figure 3.3: The relative errors from the two models. Top row is the model without wind (Equation 3.6) and bottom row the model with wind (Equation 3.5). Columns are for the lognormal, Weibull, and gamma error distributions, reading left to right. The displacements are relative to the vent location, indicated by the triangle.

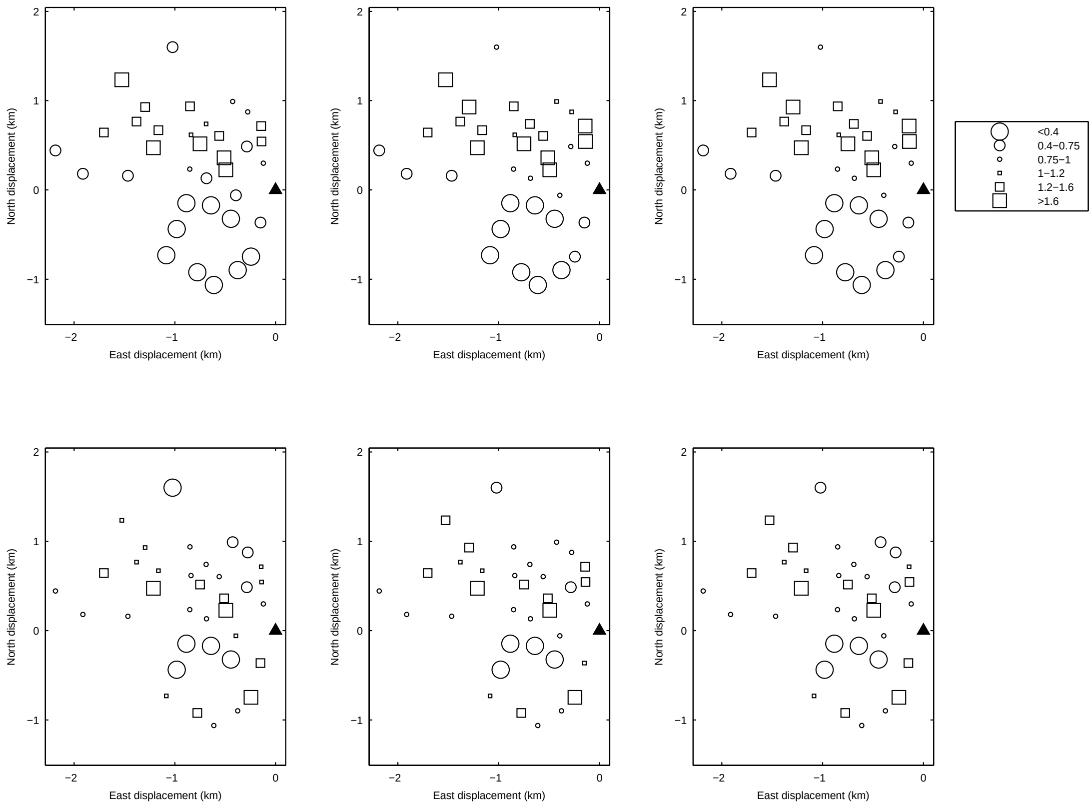

ratio between the simulated and observed thicknesses. A perfect fit is given by the horizontal line, which can be compared with the 90% point-wise coverage band. For the model without wind (Equation 3.6), there is a systematic trend with the ratio decreasing with observed thickness. This indicates that small thicknesses are being overestimated, and large thicknesses are underestimated. On the other hand, the baseline model (Equation 3.5) only slightly exhibits this behaviour; it also shows generally tighter bounds. All three error distributions exhibit behaviour consistent with the data, although it should be noted that the thick tail (producing occasional very large relative residuals) in the lognormal distribution is not being examined by this procedure.

Figure 3.4: The Monte Carlo residual bounds for tephra thickness. Top row is the model without wind (Equation 3.6) and bottom row the model with wind (Equation 3.5). Columns are for the lognormal, Weibull and gamma error distributions, reading left to right. Medians are shown by the dashed lines, 90% bounds by the filled areas.

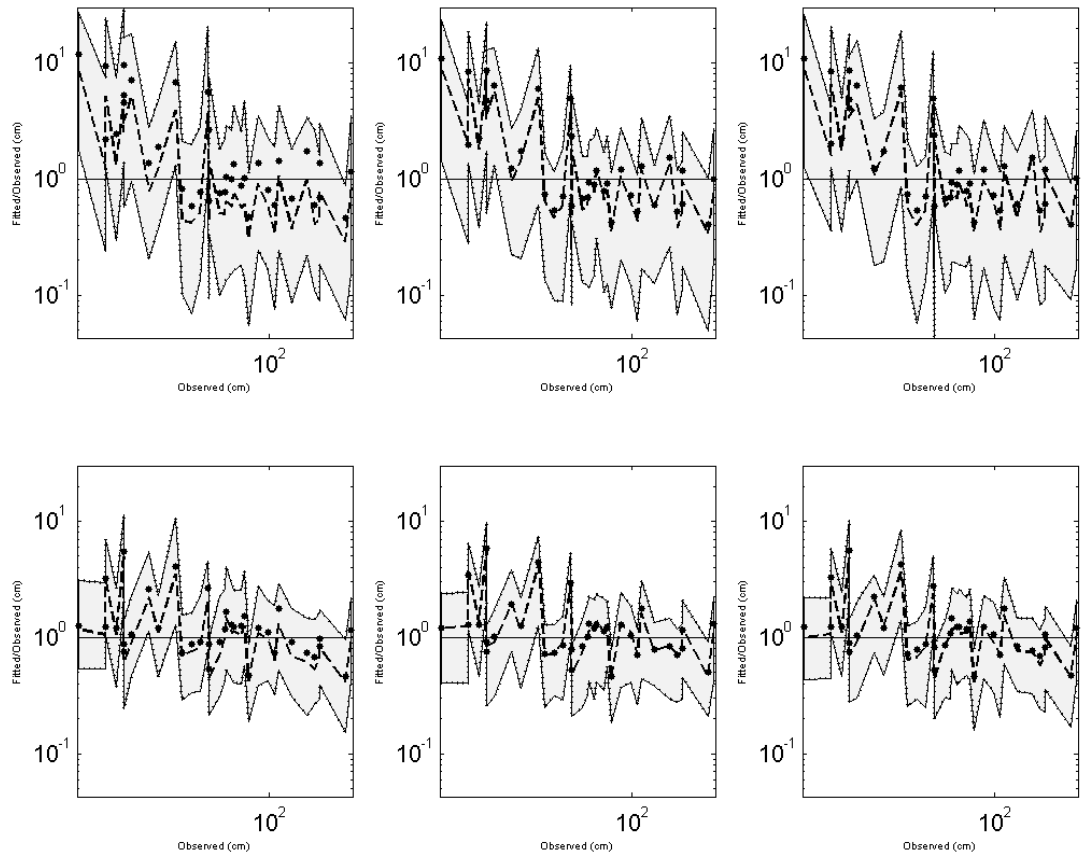

Table 3.3: Parameter estimates for the sensitivity analysis on the Heimaey data. Errors are 1σ.

No. of data deleted, N	Parameter γ	βU	ϕ	α
3	71.3 ± 2.5	1.48 ± 0.07	125.0 ± 4.3	1.88 ± 0.08
6	71.8 ± 4.6	1.49 ± 0.12	124.8 ± 6.9	1.87 ± 0.14
12	72.2 ± 6.0	1.51 ± 0.19	125.9 ± 9.4	1.88 ± 0.19
24	81.4 ± 22.1	1.84 ± 1.04	124.0 ± 19.2	1.85 ± 0.44

3.6 Sensitivity analyses

The fitted model may be sensitive to either variation in parameters and/or the data. The latter can be investigated by Monte Carlo simulation and refitting. The Heimaey data consists of 36 tephra thicknesses in the fall direction. Random samples of these measurements of various sizes (i.e., removing $N = 3, 6, 12,$ or 24) are refitted to the best model (Equation 3.5) with Weibull error distribution. The results of 100 random samples for each N are shown in Table 3.3. The table shows that the estimates are consistent, in that the means vary little for $N \leq 12$, and that the variability increases with decreasing amounts of data (N increasing). Deleting two thirds of the data ($N = 24$) is too much for the model, with a tendency to find more eccentric (higher βU) lobes in variable directions. It appears that a number of the simulations retain locations suggesting different fall direction, or possibly more than one such direction, with consequent instability in the other (coupled) parameters. The error distributions in the parameters are reasonably symmetric, apart from α, as would be expected. It can be concluded that the model is robust to the amount of data, provided that the data represents the fall pattern correctly; the robustness of the model is dependent on the quantity and quality of the data.

The sensitivity to the variation of individual parameters is investigated following an idea analogous to that of Scollo et al. (2008). Starting at the optimum solution, each parameter, one at a time, is varied in the best model with Weibull error distribution. Figure 3.5 shows the resulting likelihoods, demonstrating that the parameter values are

Figure 3.5: A sensitivity analysis on the estimated parameters. The maximum likelihood estimates are shown by the dashed lines.

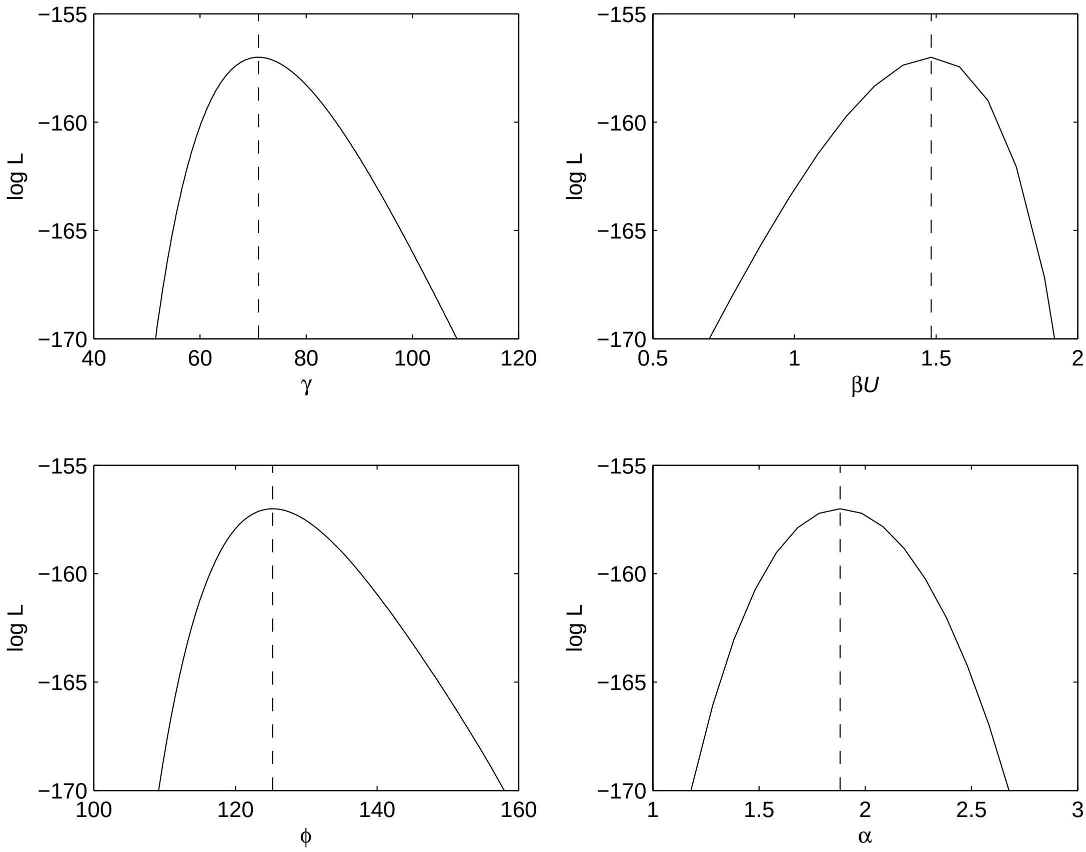

robustly estimated as indicated by the presence of a pronounced peak in the likelihood.

3.7 Discussion

Only the tephra thickness was considered in formulating our model as this is the most common directly measured quantity. In many respects, particularly the risk to built structures, the tephra loading can be a more important measure. Often, thickness is converted into loading by assuming an average particle bulk density and packing density; measured values are often in the range of 1,000 to 1,400kg/m^3 (Cronin et al., 1998). It is possible that a method similar to that above could be developed to model tephra loading directly, provided that an attenuation model can be formulated.

Gonzlalez-Mellado and De la Cruz-Reyna (2010) derived a number of empirical relationships based on fitting their model (Equation 3.4) to ten well-documented eruptions worldwide. In particular, they found that

$$\alpha = 2.535 - 0.051H, \tag{3.14}$$

giving an estimate of H, the height (km) of the eruption column (Figure 3.6(i)). It should be borne in mind that both α, which was estimated from the isopachs in Gonzlalez-Mellado and De la Cruz-Reyna (2010), and H have uncertainties associated with them besides those allowed for in their regression analysis, and so this relation is an approximation at best. The eruptions with large eruptive column heights, El Chichon-2 and Pinatubo-2, have large residuals, indicating that this relationship does not work well for eruptions with large eruptive column heights. This suggests that there might be different relationships between H and α for smaller and larger column heights. A much larger dataset is required to explore these relationships. Of course, the attenuation parameter α is also a function of total grain size distribution, which is weakly linked to column height. A second relationship between β and the column height,

$$\frac{1}{2\beta} = \begin{cases} 114.407 - 4.189H & \text{if } H < 15.5 \\ -770.17 + 52.822H & \text{otherwise} \end{cases},$$

which might otherwise allow us to separate the wind speed U from βU, appears to be an artifact of the inclusion of the Pinatubo-2 eruption, with its column height of 43km (Figure 3.6(ii)). Without this point, a quadratic regression has an adjusted R^2 of zero, indicating no relationship.

For Heimaey, calculating H from the estimated α via Equation 3.14, using the example of the Weibull error distribution and baseline model which had the best AIC, yields an estimated column height of $H = 2.44$km, in line with the observed 2 to 3km (Wilson et al., 1978). In this instance, the particle density is near-uniform across the deposit (mean $\pm$ standard deviation of 2.08 ± 0.29g/cm^3 from 99 measurements). Hence, the

Figure 3.6: Relationships between eruptive column height H and the attenuation parameters.

(i) Fitted linear regression (Gonzlalez-Mellado and De la Cruz-Reyna, 2010) between the estimated α and eruptive column heights of the ten volcanoes.

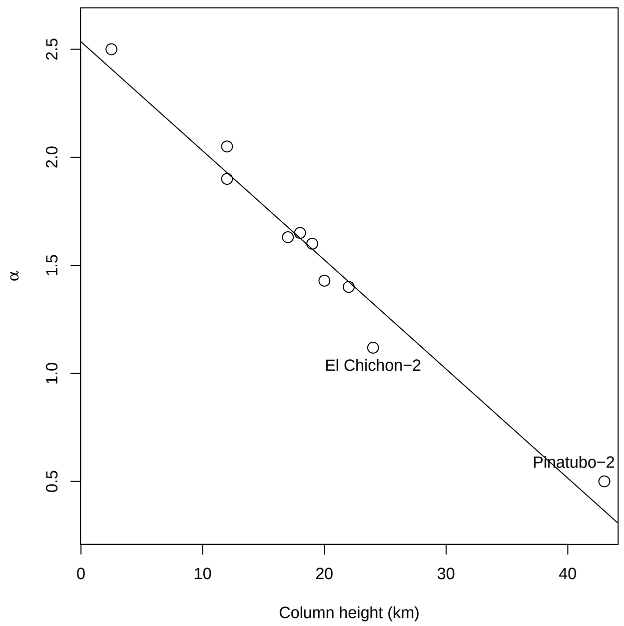

(ii) Fitted linear (Gonzlalez-Mellado and De la Cruz-Reyna, 2010) and quadratic regressions between the estimated $1/2\beta$ and eruptive column heights. The two quadratic regressions are fitted, first to the ten volcanoes including Pinatubo-2 (green) and then to the nine volcanoes excluding Pinatubo-2 (blue).

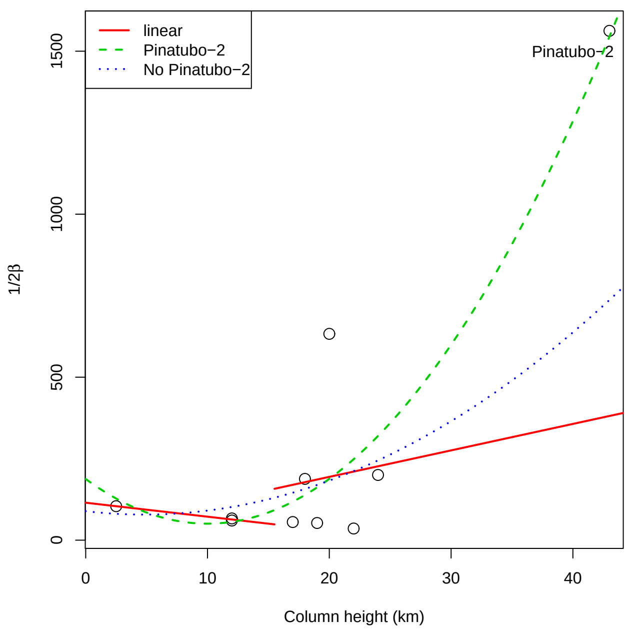

isopachs are a constant function of the isopleths which are usually used to estimate column height.

As the Heimaey eruption was observed, thus detailed observations of the eruption exist, the average wind velocity was observed to be to the northwest, which seems to have been on the order of 50km/h (Self et al., 1974). From the estimated $\beta U = 1.48$, this gives a value of $\beta = 0.03$ and, thus, an 'effective diffusion coefficient' (Gonzlalez-Mellado and De la Cruz-Reyna, 2010; Costa et al., 2013) $D = 17$km^2/h=4,700m^2/s, which appears reasonable.

The diffusion coefficient is also an empirical parameter in such 'semianalytical' models such as Tephra2 and HAZMAP, 'describing complex plume and atmospheric processes not captured in the physical model' (Volentik et al., 2010). Hence, the difference in 'physical reality' between physical and statistical models is one of degree rather than a hard boundary. The advantage of the statistical model is that there is an objective, consistent method of parameter estimation through MLE. The advantage of the physical model is that 'feasible', but perhaps not consistent, estimates of column height and mass eruption rate can be obtained, provided that grain size information and/or eruption duration is also available.

In estimating the actual volume, the fact that the power law produces an infinite thickness at $r = 0$ is an issue. To get around this, $r^{-\alpha}$ could possibly be replaced by $(r + \delta\gamma)^{-\alpha}$ following the lead of Rhoades et al. (2002). This is dimensionally correct, and gives a finite thickness at $r = 0$, at the price of adding one more parameter to the estimation problem. However, it is easier to simply exclude the area of the crater from calculations following, in effect, the suggestion of Bonadonna et al. (2005). Volume estimates can most easily be calculated by numerical integration of the Equation 3.4, using the estimated parameters.

3.8 Conclusion

A method is shown to combine a semiempiricial model of tephra deposition with an error distribution to produce a statistical model capable of being fitted to actual measurements rather than isopachs constructed from these measurements. This provides a ready-made inversion formula for the volume of the eruption and the average dispersal axis. In addition, it can be used to forecast the distribution of tephra at locations without data, and it provides an objective measure of goodness of fit to the data.

Applied to the 1973 Heimaey eruption, the model without wind effects was decisively rejected. The wind direction obtained with the other model corresponds well with the mean wind direction from the onshore wind that deposited the measured tephra thicknesses. The estimated attenuation parameter indicated a mean column height equal to that observed for the eruption (Wilson et al., 1978). For the error distribution, the Weibull and gamma distributions fitted the data similarly well but the lognormal distribution fitted less well. The sensitivity of the fitted models on the data and estimated parameters was then investigated.

Chapter 4

Tephra Dispersal - Multiple Components

Work regarding the Heimaey eruption discussed in Chapter 3 and work regarding the Ukinrek eruption discussed in this chapter are published in Kawabata et al. (2013). Work regarding the Al-Madinah eruption discussed in this chapter is published in Kawabata et al. (2015).

4.1 Introduction

Complex eruption episodes commonly produce several phases of tephra fall and/or concurrent falls from multiple vents, and these phases of eruption are challenging to reconstruct from the geological record alone. In this chapter, the tephra attenuation model discussed in Chapter 3 is implemented in a mixture framework to account for the multiple lobes and/or vents and identify the source and direction of tephra deposits. This framework is demonstrated using the tephra dispersal data from the 1977 Ukinrek Maars eruption from Alaska, US, consisting of two vents. The Weibull distribution has been found to be the best description for fresh tephra data such as of the Heimaey eruption (Chapter 3). Similarly to the Heimaey eruption the Ukinrek Maars eruption was also observed and tephra measurements were taken immediately after the eruption. Thus the Weibull distribution is considered for the Ukinrek Maars eruption as well. The directions of the phases and their sources have been closely observed and recorded by Self et al. (1980). Thus the components of the fitted model of the eruption can be evaluated against their observations.

In contrast to the well-described Heimaey and Ukinrek eruption sequences, the 1256 AD Al-Madinah eruption from Saudi Arabia has no detailed observations of individual timings and wind directions of eruption phases, and the tephra deposits were mapped over 750 years later. Thus, to model tephra dispersal for this eruption, the error distribution needs to be adopted to accommodate weathered tephra. Individual tephra lobe properties (the amount of empty space in the sediment, called porosity, and grain size distribution) in different sectors around the volcano varied only subtly (Kawabata et al., 2015). Thus, a method is needed to define the most likely number of explosive or tephra fall events that constructed the composite fall blanket. The complex Al-Madinah eruption sequence is a case study typical of the challenges in interpreting eruption scenarios from the geologic record in basaltic environments.

4.2 Data

4.2.1 The Ukinrek Maars eruption

The tephra thickness data shown in Figure 4.1 are taken from Self et al. (1980). Note that one thickness measurement of 37cm approximately 1km south east of the East Maar will be deleted, as it is the only measurement from that described and partly sketched southerly tephra lobe in Self et al. (1980). It is not possible to fit a component with four parameters to a single observation. High-level winds distributing fine tephra to distal areas were apparently not related to the proximal tephra distribution which was controlled only by the low-level winds under 2km of altitude (Kienle et al., 1980). The West Maar erupted first (30-31 March 1977), with two tephra fall units directed to the southeast and southwest, overlaid by surge deposits, which are thickest on the west-southwest edge of the crater (Kienle et al., 1980). The map of the deposits is in Self et al. (1980), which includes a slightly different chronology to that in Kienle et al. (1980). The eruption of the East Maar probably began on 1 April (Self et al., 1980), with tephra fallout to the north-northeast and north-northwest, with further eruptions on 5 April dispersing tephra to the northwest and north. Later, Strombolian phases of eruptions from 7-9 April produced tephra fall lobes to the northwest, east, and south-southeast (Kienle et al., 1980; Self et al., 1980). So, in mixture model terms, the source and direction of the observed components are

West Maar

- **w1:** SE (fall)
- **w2:** SW-WSW (surge plus fall)

East Maar

- **e1:** NNE (fall 2 April)
- **e2:** NW-NNW (fall 1 April, 5 April, and 7-9 April)
- **e3:** E (7-9 April)
- **e4:** WNW (surges throughout eruption)
- **e5:** SSE (7-9 April)

4.2.2 The Al-Madinah eruption

The alkali basaltic 1256 AD Al-Madinah eruption (Figure 4.2) formed an approximately 2.5-km-long roughly north-south striking fissure, with three small spatter cones (low, steep-sided hills (Fodor and Németh, 2014)) (Cones 1, 2, and 3 of Camp et al. 1987) and ramparts, as well as three larger cinder or scoria cones (Cones 4, 5, and 6 of Camp et al. 1987) which produced tephra. The eruption took place over 52 days with at least

Figure 4.1: The observed tephra thicknesses (cm) for the Ukinrek Maars eruption. The vents are indicated by the triangles.

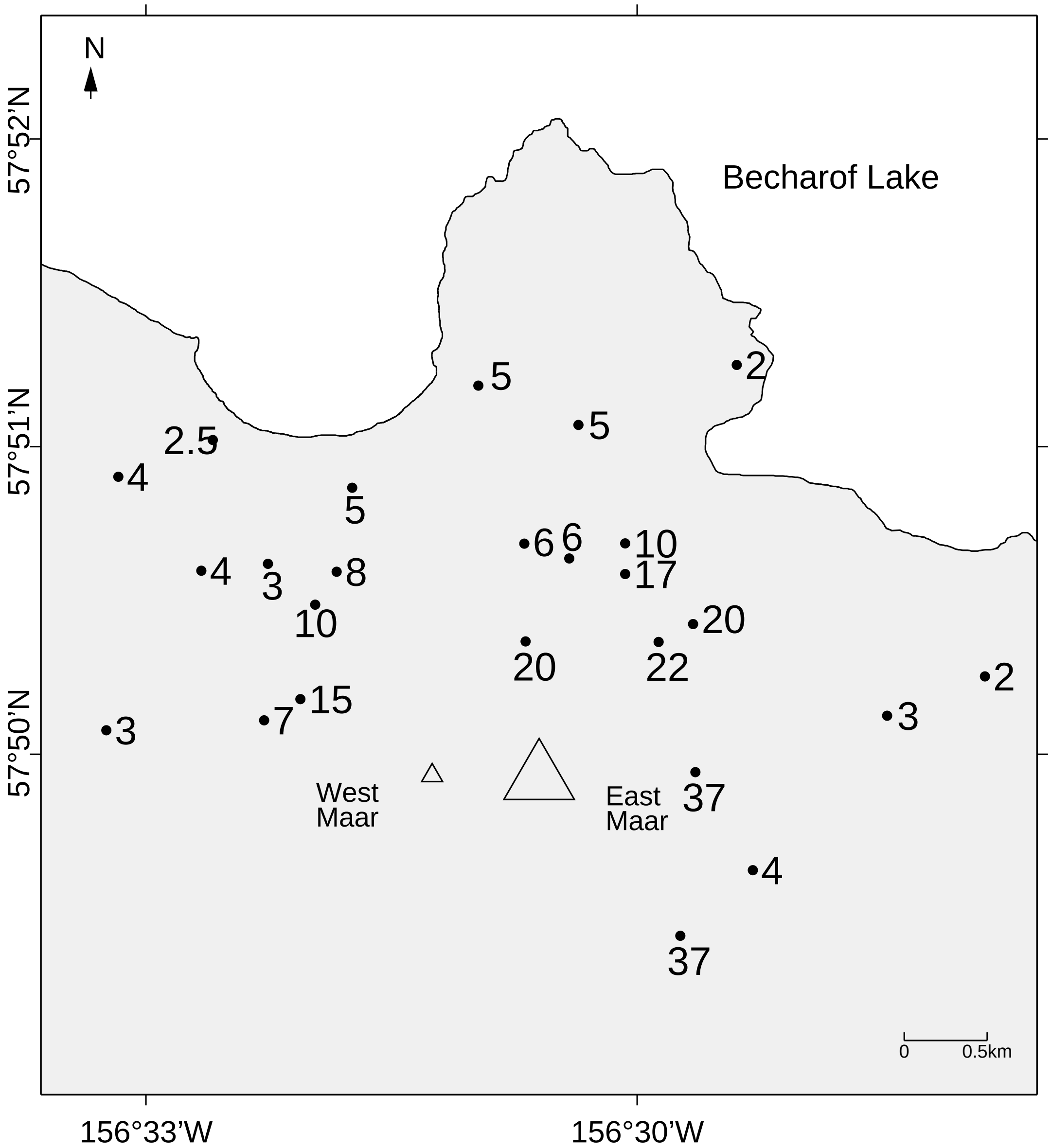

Figure 4.2: Oblique aerial view of the largest cones along the north-northwest aligned fissure system produced during the 1256 AD Al-Madinah eruption. The three cones show Cones 6, 5, and 4 are labelled.

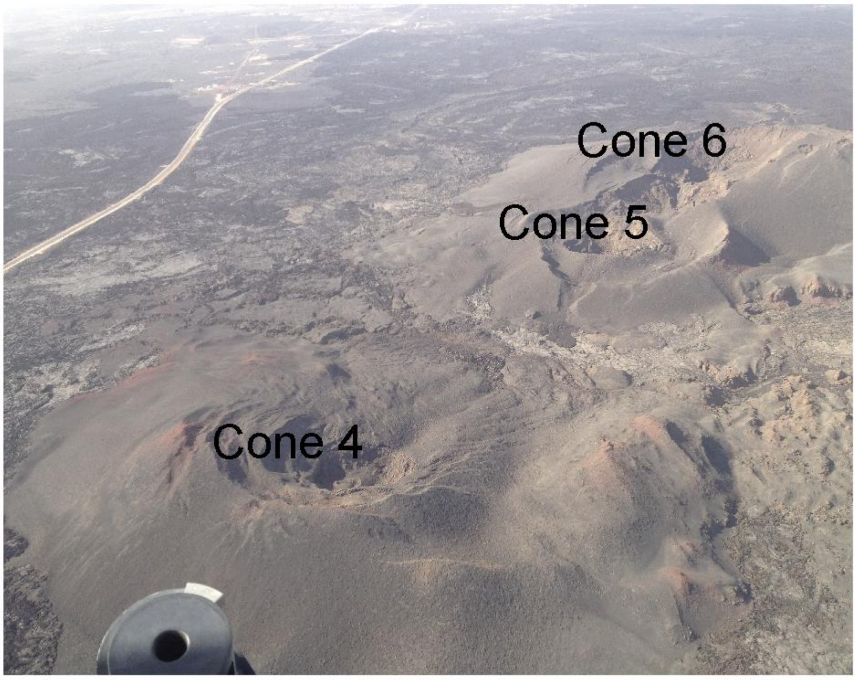

two separate episodes of tephra fall recorded by local written records (Camp et al., 1987).

The data consist of 121 spot thickness measurements (excluding bomb or ballistic beds in near-vent areas and the cones) securing the greatest degree of coverage possible, given the topography and overlaying lava fields. The map (Figure 4.3) confirms that tephra is dispersed in several sectors, implying that individual falls occurred at different times under diverse wind conditions. Rare surface floods and high winds have eroded much of the outer margins of the tephra blanket (tephra fall laid out on the ground), meaning that reliable measurements of falls extend only down to approximately 3cm thickness.

Figure 4.3: Tephra ash fall distribution map for the 1256 AD tephra blanket, with spot thickness measurements (cm) marked and automated isopachs drawn using a simple kriging process (Cleveland et al., 1992). The lava and spatter blankets are shown by the light and darker grey shading. The cones are indicated by the triangles. Inset map shows the position of the eruption in the Harrat Rahat lava field, western Saudi Arabia.

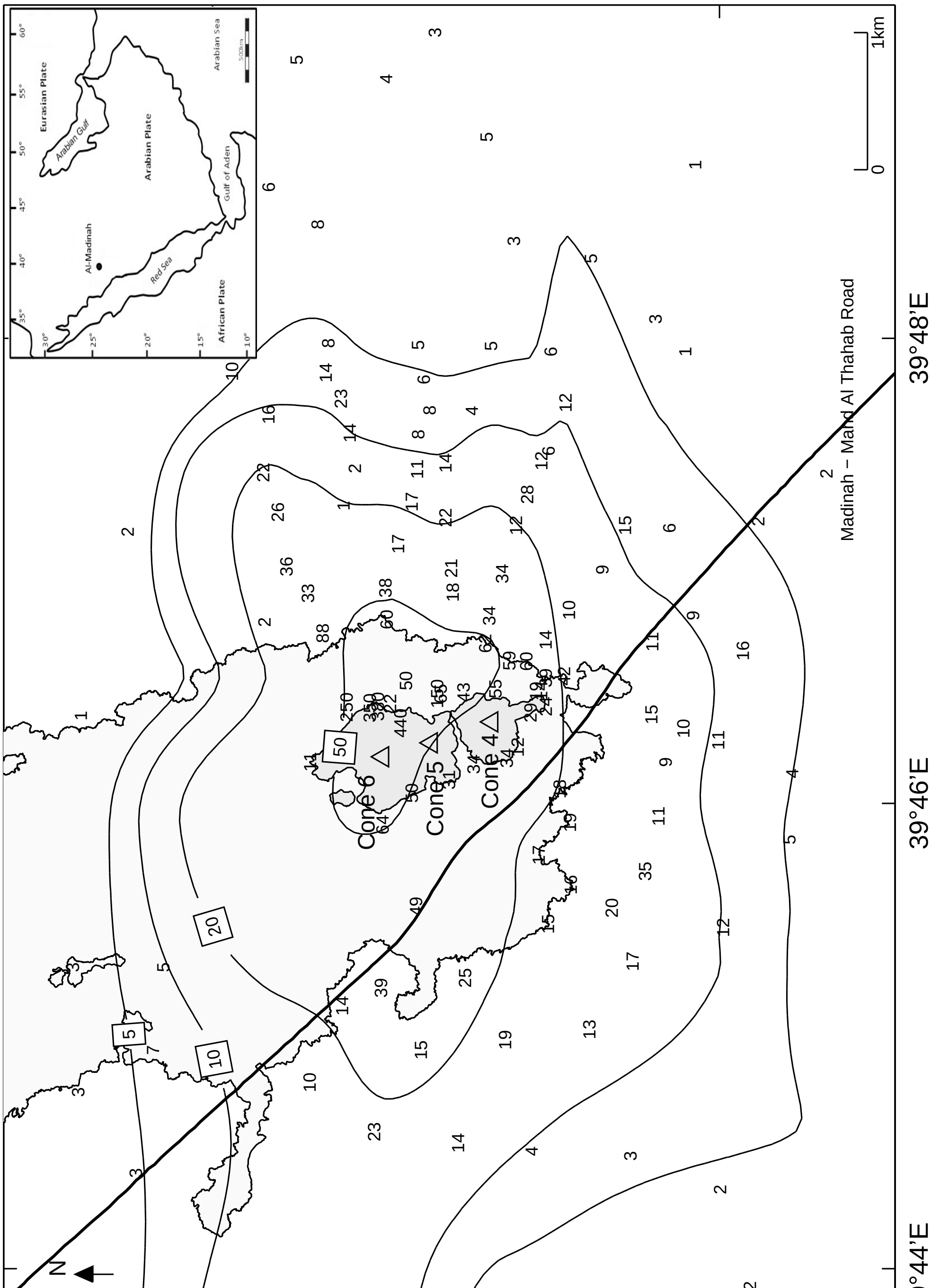

4.3 Methodology

4.3.1 Tephra modelling

To identify the direction of fall lobes from multiple sources the attenuation model will be extended to a mixture framework where each lobe is represented by a component in the mixture model of explosive phases.

Let us suppose that we have m vents, and that the ith vent has n_i components (lobes). The model (Equation 3.5) to prescribe the thickness at a given location then becomes

$$T(r_1, \ldots, r_m, \xi_1, \ldots, \xi_m) = \gamma \sum_{i=1}^{m} \sum_{j=1}^{n_i} P_{i,j} \exp\left\{-(\beta U)_{ij} r_i [1 - \cos(\xi_i - \phi_{ij})]\right\} r_i^{-\alpha_{ij}}, \tag{4.1}$$

where (r_i, ξ_i) is the distance and azimuth to the location from the ith vent, which has n_i explosive phases. Each component has its own α, βU, and ϕ parameters in place of those in Equation 3.5. There is only one γ as the differing sizes of the components are identified through the presence of the mixing distribution $P_{i,j}$, where $\sum_i \sum_j P_{i,j} = 1$. This is equivalent to summing over components with $\gamma_{i,j} = \gamma P_{i,j}$. The models can then be fitted to the data using maximum likelihood, in a minor elaboration of the technique described in Section 3.4.

The isopach produced by Equation 3.5 is an ellipse, which is the simplest geometrical approximation to most observed isopachs. Subjectively drawn isopachs have the flexibility of forming any shape. But to recreate such isopachs mathematically would require an arbitrarily large number of parameters. Ellipses can be considered to be the most sensible compromise and as building blocks from which a full isopach map can be constructed. Each ellipse represents an elliptical lobe, occurring in an approximately constant wind field.

This formulation gives rise to a total of $p = 4 \sum_i n_i$ parameters because the mixing proportions P_{ij} sum to unity. This approach allows incorporation of multiple vents and lobes and can be used to identify the most likely number of eruptive stages from each vent. The best fitting model can be identified by the model with the smallest Akaike Information Criterion (AIC) (Akaike, 1974). The AIC (Equation 3.13) finds the best balance between an improved model fit and excess parameters, and thus identifies the most likely number of lobes.

4.3.2 Data imputation

Recall that the number of parameters in Equation 4.1 is $4\sum_i n_i$, where $\sum_i n_i$ is the number of components. In the Ukinrek Maars eruption there are as many as seven components (Self et al., 1980) but the exact number is unknown. As it is numerically impossible to identify seven lobes from the 24 data points available (Figure 4.4) additional data are required. Imputation can be performed to estimate possible thicknesses at unobserved locations. But the imputed data must be smooth between observations to avoid introducing any new structure to the data. Hence, expected thicknesses will be interpolated at new locations by fitting a surface to the observed data using a triangulated C^1-continuous interpolating surface. In order to consider what would be expected, let us consider a parametric bootstrapping framework to interpolate (expected) thicknesses E at new locations. The best practice to obtain the interpolated thickness is to sample the relative error R_i^* $(= O_i/E_i)$ from a set of the existing or observed $\{R\}$ to obtain $O_i^* = R_i^* E_i$. This will achieve spatial independence between locations. However, instead $O_i^* = E_i$ were sampled at new locations on a grid in order not to introduce new features to the tephra blanket. This will mean that the errors are no longer independent but are spatially correlated. This achieves the preferred smooth interpolated thickness which is ideal for model testing. A grid (at a spacing of 0.25km) will be overlayed and the interpolated thicknesses at the grid points (Figure 4.4) will be used as our fitting data. Note that the grid is restricted within the convex hull of the observed data to avoid extrapolation. This results in approximately 150 data points, enough numerically to fit the required models.

Figure 4.4: The observed thicknesses (cm) are in large type while the interpolated thicknesses (see text) are in smaller type for the Ukinrek Maars data.

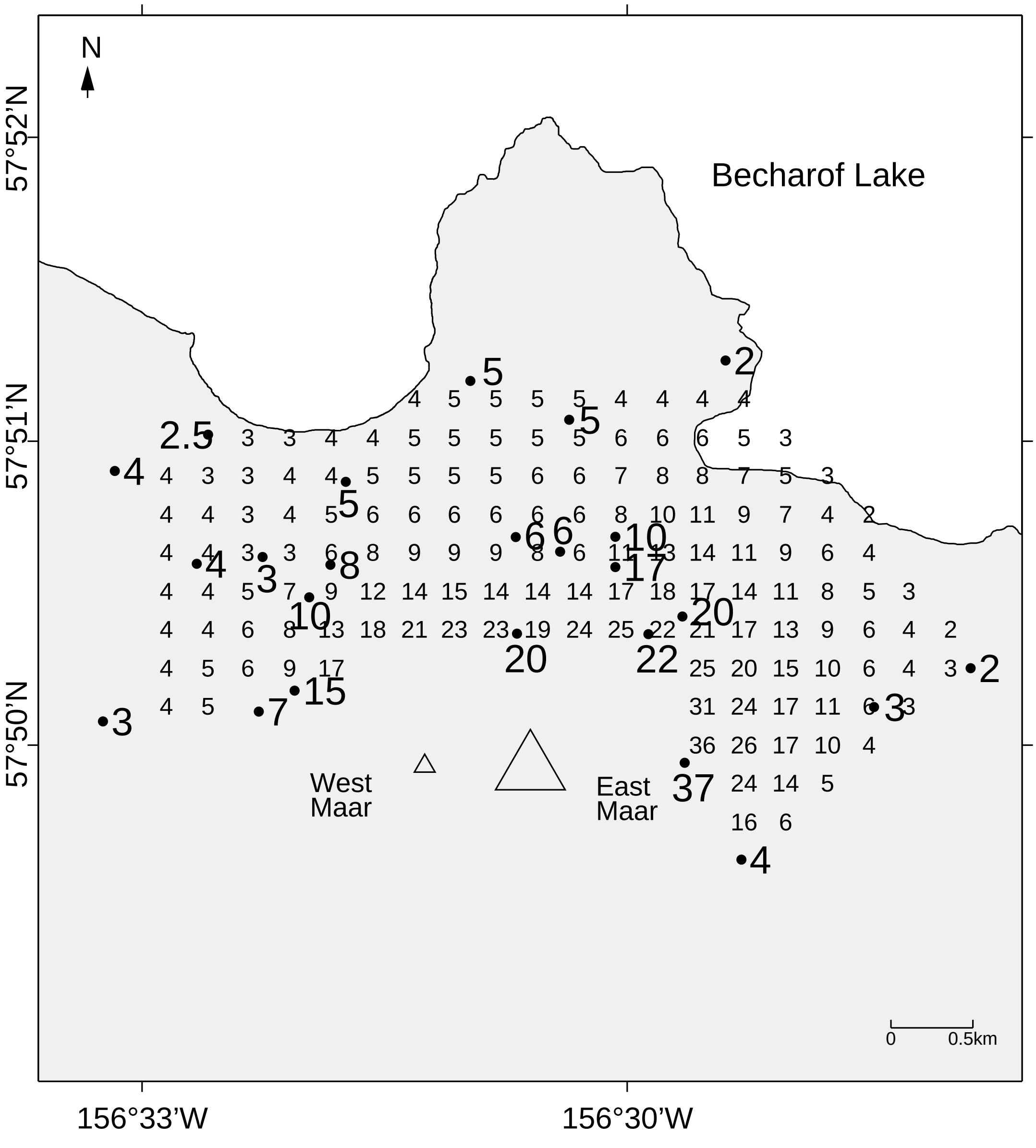

4.3.3 Error distribution for old deposits

In Section 2.2.5 different tephra attenuation models were used to deal with different states of tephra. The power law model was found to describe fresh tephra while the exponential model better described weathered tephra due to the absence of a large portion of the deposits. However a good model fit does not necessarily indicate reliability. Here the difference is dealt with by filtering out the noise of the weathering with an error distribution to obtain erupted tephra. This way the attenuation model can be retained. For the $>$ 750-year-old Al-Madinah eruption, we must account for the effects of compaction and erosion on the tephra blanket. The Heimaey case study showed that the Weibull (Equation 3.2) and gamma (Equation 3.3) distributions describe the inherent variability in the tephra thickness measurements well; where κ is the shape parameter, and λ the scale parameter of the respective distributions. Where Equations 3.2 and 3.3 differ is in the likelihood of observing unexpectedly large thicknesses. Since $\kappa < 1$ indicates mode at zero, it is almost certain that for tephra $\kappa > 1$, which indicates a positive mode of the thickness distribution(s) and hence a tendency for thicknesses to be consistent with a wind and distance decay model. By contrast, a mode at zero implies a more erratic deposition of tephra. Hence, Equation 3.2 is less likely to produce greatly over-thickened measurements and is preferred for modelling fresh tephra observations.

Considering that the 1256 AD tephra has been subject to erosion and reworking for several centuries, finer grained and thinner parts of the deposit are more likely to be eroded and reworked in comparison to coarser or thicker units as noted in Hawaii (Hay and Jones, 1972) and during the fieldwork (Kawabata et al., 2015). Hence, the variability should be greatest for the outer, thinner margins of the tephra blanket. The marginal thickness behaviour is controlled by T^{κ} in both Weibull and gamma distributions, while the greater thicknesses are controlled by $\exp[-(T/\lambda)^{\kappa}]$ in the Weibull distribution (Equation 3.2) and $\exp(-T/\lambda)$ in the gamma distribution (Equation 3.3). In the Weibull case, when thin tephra measurements disappear and κ changes, the thicker tail is lost also due to a coupling effect. Therefore, weathering in the small measurements would remove the large measurements, contradicting reality. By contrast in the gamma distribution, the tails are independent, and there is no link between κ and λ (Figure 4.5). This property means that the gamma distribution should be better suited for the description of weathered tephra deposits.

In order to test this idea, simulations can be run to see which of the Weibull and gamma distributions is preferred for old tephra thickness data. The Al-Madinah eruption data is an example of old deposits. A Weibull error distribution is fitted to the observed tephra thickness data from the eruption. This will give us the shape and scale parameters. Then a sample of hypothetical thicknesses of the same size ($n = 121$) will be simulated from the distribution at the given location. Weibull and gamma distributions are fitted to the simulated data through maximum likelihood estimation (MLE). The two likelihoods will be compared to evaluate whether the correct (Weibull) distribution is preferred. This is done by calculating the proportion of the 1,000 runs where the likelihood from the Weibull distribution is greater than that of the gamma distribution. The simulated thickness data are now thinned, where a tephra of thickness T is removed with a probability $\exp(5+T/2)/[1+\exp(5+T/2)]$; this represents a thinning probability of (0.99, 0.92, 0.5, 0.01) for deposited thicknesses of (1, 5, 10, 20)cm. Thus smaller measurements have a larger probability of disappearing. We now compare the two distributions after thinning by refitting the two distributions on the thinned data. Again the proportion of times that the correct distribution is identified is calculated. This process will be repeated, with a simulated gamma distribution fitted to the observed data this time, instead of a Weibull distribution. Now whether the gamma distribution is correctly identified as the preferred distribution is evaluated. Note that the coefficients of variation (CVs) are larger than 1 in both distributions as shown in the left column of Table 4.1. This entire process is repeated with the fresh tephra from the Ukinrek Maars eruption, which tend to produce CV < 1 (the right column of Table 4.1).

Figure 4.5: Aleatory uncertainty in tephra thickness subject to weathering and compaction. The original (f) densities have the same mean and variance. The new (w) densities are then found by multiplying κ by 1.5 (to thin out the small tephras), and retaining the same mean (i.e., tephra is redispersed).

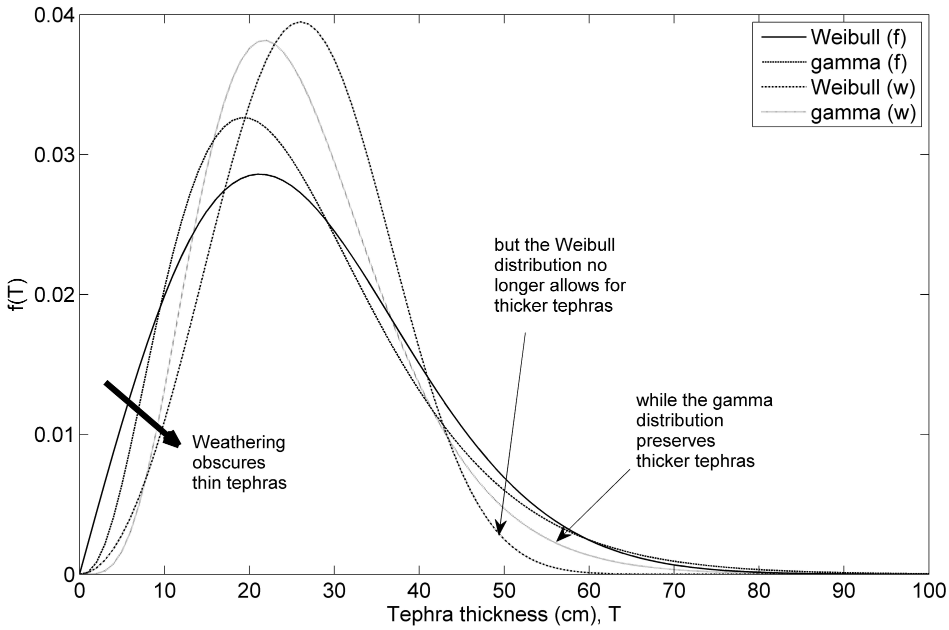

Table 4.1 shows the proportions of times the correct error distribution is identified before and after thinning of hypothetical fresh and old tephra deposits. The top row shows about two thirds of the time the correct distribution was identified in all cases before thinning.

4.4 Results

4.4.1 The Ukinrek Maars eruption

For the purposes of illustration, the results from only the Weibull error distribution are presented. The lognormal has already been shown to fit fresh tephra poorly, and while the gamma distribution is a viable alternative for one or two components with fresh tephra as we saw for the fresh Heimaey data, it performs increasingly poorly

Table 4.1: Proportion of correctly identifying the error distribution before and after thinning using hypothetical thickness data.

	Old deposits		Fresh deposits	
Distribution	Weibull	Gamma	Weibull	Gamma
CV	1.328	1.182	0.820	0.788
Before	0.651	0.656	0.648	0.645
After	0.011	0.993	0.26	0.79

relative to the Weibull as the number of components increases. This is understandable, as the thinner tail of the Weibull better describes the reduced sampling variation as excess thicknesses are ascribed to multiple components. Hence, the preferred model, as identified by AIC, will give the number of components (on each Maar). As the East Maar crater is approximately 16 times the volume of the West Maar crater (Kienle et al., 1980), at least one component is placed on the East Maar.

The estimated parameters for the Ukinrek eruption are shown in Table 4.2. The best model is clearly the 1-3 model, with one component on the West Maar (S), and three on the East Maar (NE, NNW, and E), the last three of which correspond quite closely to the sought-after e1, e2, and e3, respectively. The West Maar component appears to have (correctly) identified the aggregation of w1 and w2 from the scattering opposite to the dispersal axis. This will have been overlaid with e4. The remaining parameter estimates are given in Table 4.3, although further comment will be restricted to the preferred 1-3 model, which is illustrated in Figure 4.6. All the models assign a minimum weighting of 65% to the East Maar, while the preferred model assigns 80% weight to the East Maar. This volume apportioning is consistent with the relative sizes of the two maars and with the fact that the bulk of activity was observed from the later erupting East Maar (Kienle et al., 1980). The decay with distance α and the eccentricity βU indicate a wide proximal fall from the West Maar, while the East Maar contributes two narrower falls (e1 and e3) and a smaller wide deposit slowly thinning with distance (e2). Again, these are in excellent agreement with observations (Kienle et al., 1980; Self et al., 1980). In the residual plot for the best fitting model as shown in Figure 4.7; there

Table 4.2: The estimated AICs (lowest number indicates best fit) and model parameters for the imputed Ukinrek Maars thickness data.

Model (WM-EM)	AIC	γ	ϕ WM	EM
0-2	570.0	39.5		216, 39
1-1	538.9	44.8	90	30
0-3	514.5	78.7		27, 158, 96
1-2	498.9	67.0	94	12, 52
2-1	516.2	66.0	89, 42	18
1-3	**468.9**	**74.0**	**264**	**12, 52, 113**
2-2	477.0	78.3	297, 98	12, 52
0-4	484.9	78.7		15, 157, 99, 55

appear to be no systematic patterns. The fitted CV (Figure 4.7) for the actual (not imputed) data is 0.28, which is somewhat less than the 0.46 for the Heimaey example (Table 3.2). But an examination of Figure 3.3 suggests that more than one component might have been justified there, which would have lowered the CV.

4.4.2 The Al-Madinah eruption

Three main vent sites produced the majority of the widely dispersed tephra. These were identified by Camp et al. (1987) and confirmed during fieldwork, although it cannot be ruled out that small amounts of proximal tephra was produced in other locations along the fissure. Field mapping indicates that each of the three explosive vents (Cones 4, 5, and 6 of Camp et al. 1987 as shown in Figure 4.3) produced at least one phase of tephra fall. Hence, all combinations of eruptions were considered by adding new eruptive phases until the number of components (i.e., parameters) is no longer justified by the AIC values. Since the gamma distribution was preferred over the Weibull distribution for the weathered tephra found in the Al-Madinah eruption (Section 4.3.3) only the gamma distribution is considered for the error distribution. Models with more than six components, besides having worsening AIC, invariably produced a component tephra fall with an infinitesimal volume. This implies that up to a maximum of six phases best

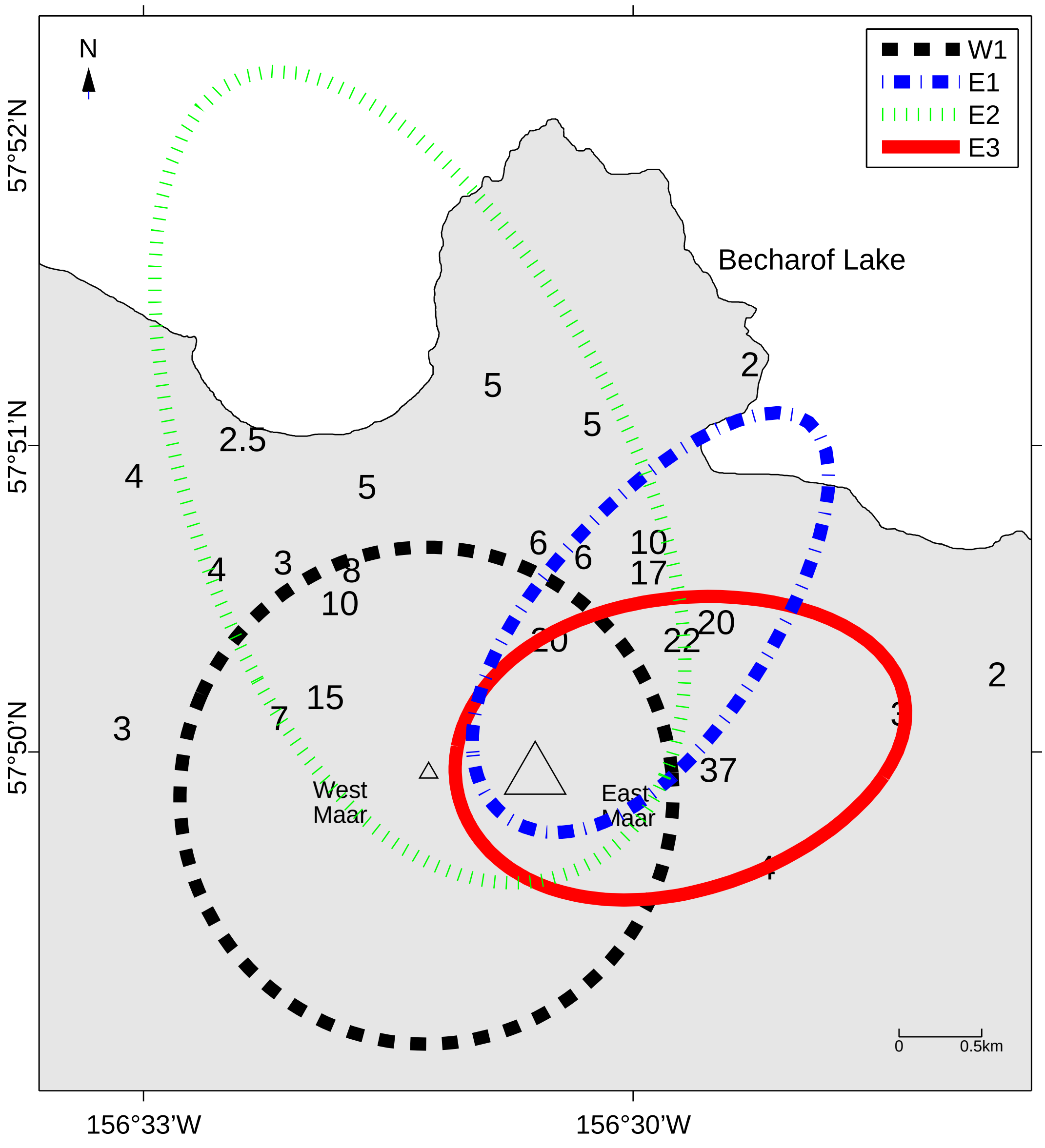

Figure 4.6: The 3cm isocontours for each component from the best 1-3 model are shown for the Ukinrek Maars eruption. W1 is the West Maar component, while the East Maar components are denoted E1-E3. Observed thicknesses (cm) and locations are also shown.

Figure 4.7: The relative errors at measurement locations for the best 1-3 model for the Ukinrek Maars data. The text is scaled by size of error.

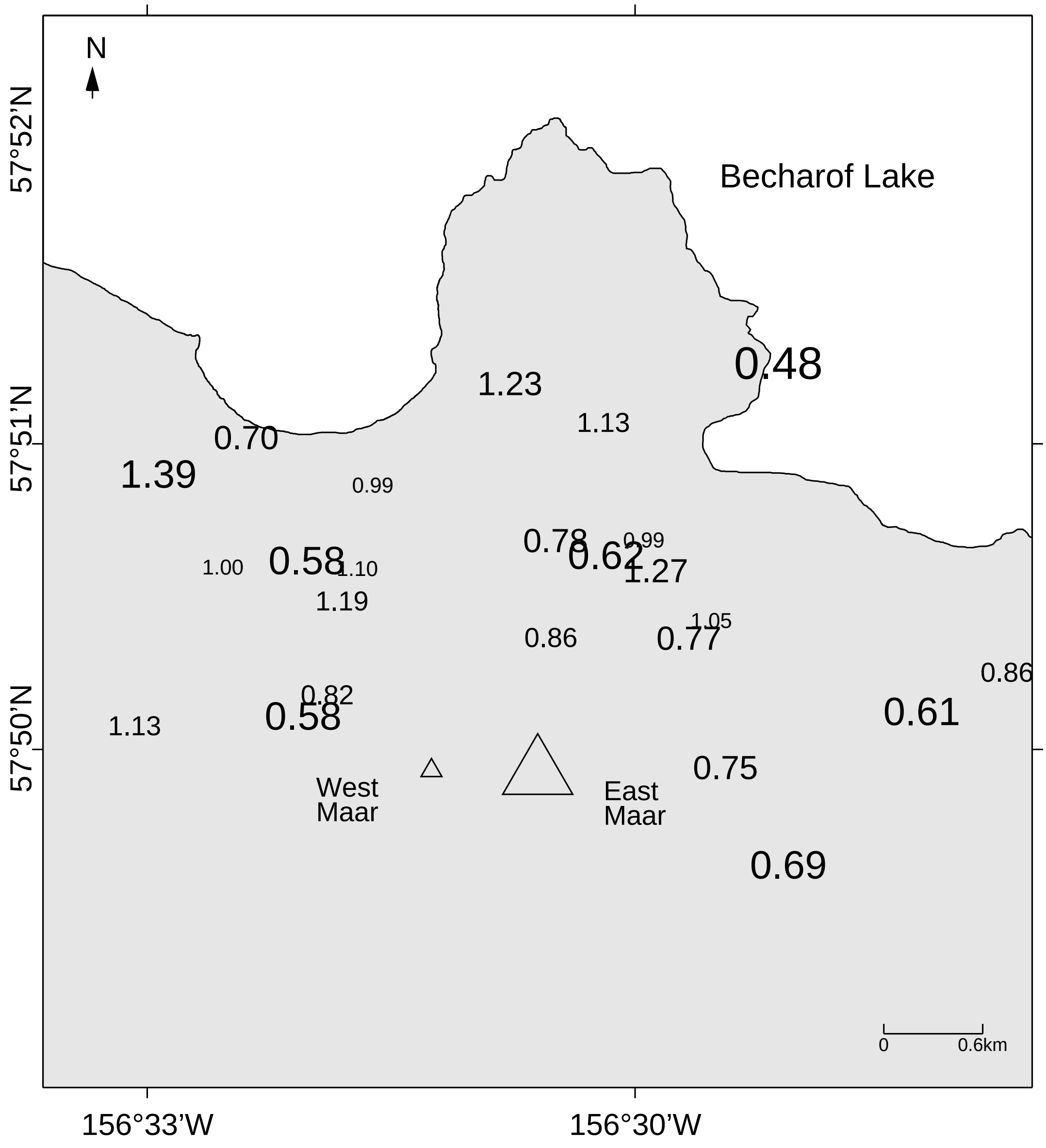

Table 4.3: The estimated model parameters for the imputed Ukinrek Maars thickness data.

Model	P		βU		α	
(WM-EM)	WM	EM	WM	EM	WM	EM
0-2		0.64, 0.36		0.1, 3.7		1.9, 2.3
1-1	0.28	0.72	0.3	1.8	1.5	2.5
0-3		0.46, 0.46, 0.08		1.9, 4.6, 0.9		2.6, 2.9, 0.4
1-2	0.21	0.56, 0.23	0.4	4.8, 5.2	1.6	3.1, 1.7
2-1	0.20, 0.15	0.65	0.4, 10.5	4.0	1.5, 1.0	3.2
1-3	**0.20**	**0.51**, **0.21**, **0.07**	**0.2**	**5.0**, **6.1**, **0.6**	**3.2**	**3.1**, **1.7**, **0.4**
2-2	0.23, 0.06	0.49, 0.21	0.3, 0.6	5.3, 5.6	2.9, 0.3	3.2, 1.7
0-4		0.42, 0.35, 0.13, 0.10		3.4, 4.5, 0.7, 9.9		2.7, 2.7, 1.1, 1.3

describes the tephra dispersal of the Al-Madinah eruption episode. The volumes (Table 4.4) were numerically integrated from the fitted attenuation model (Equation 4.1) for each component.

Among models with the same total number of components, the best models were always those with one component on each of Cones 5 and 4 and the remainder on Cone 6 (Table 4.4). The 4-1-1 model (four phases from Cone 6, and one from each of Cones 5 and 4) has the best AIC, but the improvement is only 1.0 from the 3-1-1 model. A value of 2.0 or more would indicate that the larger model is a significant improvement (Utsu, 1999). Therefore, the smaller, simpler, model best describes the situation, although both are considered likely. These two models (Figure 4.8) imply a series of eruptive phases of similar size, which is consistent with the similar grain size distributions, dispersal, isopleth distribution and porosity characteristics of the tephra in all dispersal directions (Kawabata et al., 2015). However, while the identified lobes are similar across all models, their vent assignment is not always consistent. For example, the northwest lobe is assigned to Cone 5 in the 3-1-1 model but it is assigned to Cone 6 in the 4-1-1 model. The estimated total tephra volume from this eruption can be numerically integrated from the fitted attenuation model (Equation 4.1), yielding values of 0.021-0.024km^3 (0.006 ± 0.001km^3 dense rock equivalent (DRE), after accounting for and removing the void space within the sample). The isopachs from the complete model (Figure 4.8) indicate that significant fall was distributed both east and west of the vents. The largest lobes are indicated to the west and south, but these also have the greatest errors in estimation and a lack of distal sampling locations make closing the isopachs difficult. Based on the physical properties of the tephras, the northeastern and western distributed lobes were likely sourced from the highest fountains and/or the strongest winds.

Figure 4.8: Model component tephra lobes estimated for the 1256 AD Al-Madinah eruption. The 3cm isopachs for each component of the 3-1-1 model (top) and the 4-1-1 model (bottom). The 5, 10, 20, and 50cm isopachs are generated from the complete model. The relative (aleatory) errors at measurement locations are shown by the shape and size of symbols.

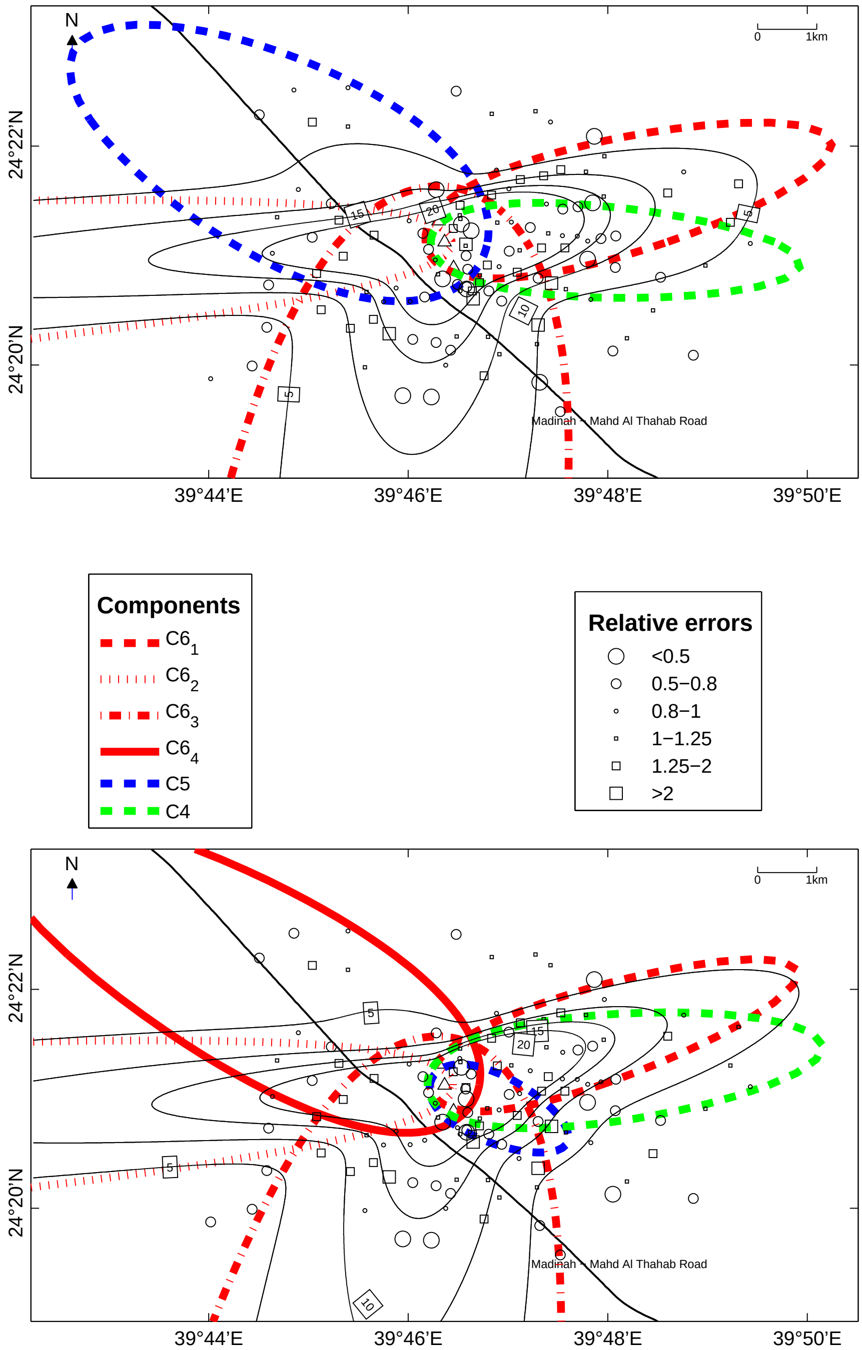

Table 4.4: The AICs and total bulk fall volumes (sum of numerically integrated volumes of all identified lobes) of the fitted models for the 1256 AD Al-Madinah data. Model notation is such that 4-1-1 indicates four phases on Cone 6, one at each of Cones 5 and 4.

Model	AIC	Total bulk fall volume (km^3)	Model	AIC	Total bulk fall volume (km^3)
1-1-1	831.7	0.017	4-1-1	812.3	0.024
2-1-1	817.0	0.021	3-2-1	816.1	0.023
1-2-1	818.2	0.020	3-1-2	817.6	0.024
1-1-2	824.7	0.022	2-3-1	822.1	0.021
3-1-1	813.3	0.021	2-2-2	822.1	0.021
2-2-1	814.8	0.020	2-1-3	825.4	0.024
2-1-2	818.1	0.023	1-4-1	825.7	0.022
1-3-1	817.7	0.022	1-3-2	825.7	0.022
1-2-2	819.2	0.022	1-2-3	827.1	0.022
1-1-3	829.3	0.025	1-1-4	837.3	0.025

4.5 Discussion

4.5.1 The Ukinrek Maars eruption

Equation 3.14 appears to break down for the Ukinrek model with αs greater than 2.535 (negative column height), or small enough ($\alpha = 0.3$) to correspond to a 44km column height. The observed column heights (Kienle et al., 1980) of 6.5km (West Maar) and 3.5km (East Maar) would require α values of 2.2 and 2.4, respectively. We note that the less complex models in Table 4.3 have α values much closer to these ideal values. Thus, the empirical relation (Equation 3.14) appears more likely to be valid where the deposit is a single lobe corresponding to the maximum column height, which are the conditions under which it was derived by Gonzlalez-Mellado and De la Cruz-Reyna (2010). The higher βU values observed for some of the components in Table 4.3 may reflect the generally higher wind velocity environment at Ukinrek, wind shear (a difference in wind speed and direction in close proximity) causing bent-over plumes, or directional control in the individual eruptions.

Since base surge deposits do not travel further than a few kilometres (Einsele, 2000) the attenuation parameter in $r^{-\alpha}$ could take an extra parameter in the form $r^{-\alpha_1}$ if $r > 3$km and $r^{-\alpha_2}$ otherwise. The main base surge directions identified in Self et al. (1980) were northwest, east, and west. The northwest and east directions as lobe directions (E2 and E3 in Figure 4.6) were successfully identified.

For the Heimaey eruption, the robustness of the parameters was investigated by varying the attenuation model parameters, one at a time, (Scollo et al., 2008) in Section 3.6. Although it was not performed in this thesis, a similar sensitivity analysis may be conducted even though there are more parameters due to multiple components.

The best model for the Ukinrek eruption produced a CV of 0.28 (Section 4.4) compared to 0.46 from the Heimaey eruption (Section 3.5). Further examination of the relative residuals from the Heimaey data (Figure 3.3) suggests that positive and negative residuals appear in close proximity, suggesting a second lobe may be justified. Moreover, the calculation of CV for the Ukinrek data involved only the measurements at the observed locations. These findings suggest that the lower CV from the Ukinrek model is not due to the smoothing method used for imputation.

Figure 4.4 shows that the interpolated thicknesses were produced only on the northern side of the maars and no extrapolation was done on the southern side. Yet Figure 4.6 shows that the best model identified W1, an almost symmetric lobe around the West Maar, which includes non-zero thicknesses on the southern side of the maars. This suggests a southern lobe based on the interpolated thicknesses from the north. This is also evidence that our imputation method is valid without sampling the relative error R^*.

Since the Ukinrek data contain only 24 data points to test whether the procedure can be used to identify separate lobes requires imputation to permit running the models. This was done without bootstrap errors R^* to produce smooth thickness data in order to avoid picking up fictitious lobes that might have arisen from an uneven surface. Nevertheless, the sensitivity of the imputed data on the preferred model was examined by varying the spacing of the grid over the region and thus changing the amount of imputed data.

Since the East Maar is much larger than the West Maar, it is reasonable to assume the bigger maar had more phases. So the models with the same or more number of phases on the East Maar, namely the 1-1, 1-2, and 1-3 models, are chosen and examined to check if the preferred model is consistent regardless of the spacing size. Initially imputation was done over a grid at a spacing of 0.25km. Now the spacing between neighbouring points is changed to a range of 0.1 to 1km, and the models are fitted to a combination of the observed and imputed data. The AICs obtained from Equation 3.13 are plotted in Figure 4.9(i). It shows that up to 0.6km spacing the 1-3 model is always most preferred, which is consistent with the findings earlier.

Figure 4.9(ii) examines the consistency in the estimated parameter values of the preferred 1-3 model at different spacings. The top left figure shows the modified (or average) AIC (Kagan and Knopoff, 1977) defined as:

$$\text{Modified AIC} = 2p - 2\log L\left(\frac{N}{N+M}\right),$$

where p is the number of model parameters, L is the likelihood, N is the number of observed data points, and M is the number of imputed data points. The modified AICs are fairly consistent for all spacing sizes, indicating that the model fits stay the same. Figure 4.9(ii) shows that none of the parameters show an obvious pattern between spacing and estimated values, indicating that smooth imputed data of any spacing size will identify the same lobes.

The effect of smoothing in the imputation procedure can be investigated by adding bootstrap errors R^* from parametric bootstrapping to the imputed data E so that the models are now fitted to $O^* = R^*E$ instead of $O^* = E$ as in Section 4.4.1. A suitable distribution of R^* can come from the distribution best describes the multiplicative error for the Heimaey data. After fitting three distributions (Equations 3.1-3.3) the Weibull distribution was found to best describe the error (Section 3.3) so it will be used to

Figure 4.9: Sensitivity analyses of imputation done for the Ukinrek Maars data.

(i) AIC values of the 1-1, 1-2, and 1-3 models for different spacings. Tow row shows the spacing increasing from 0.1km to 0.5km left to right and bottom row shows the spacing increasing from 0.6km to 1km.

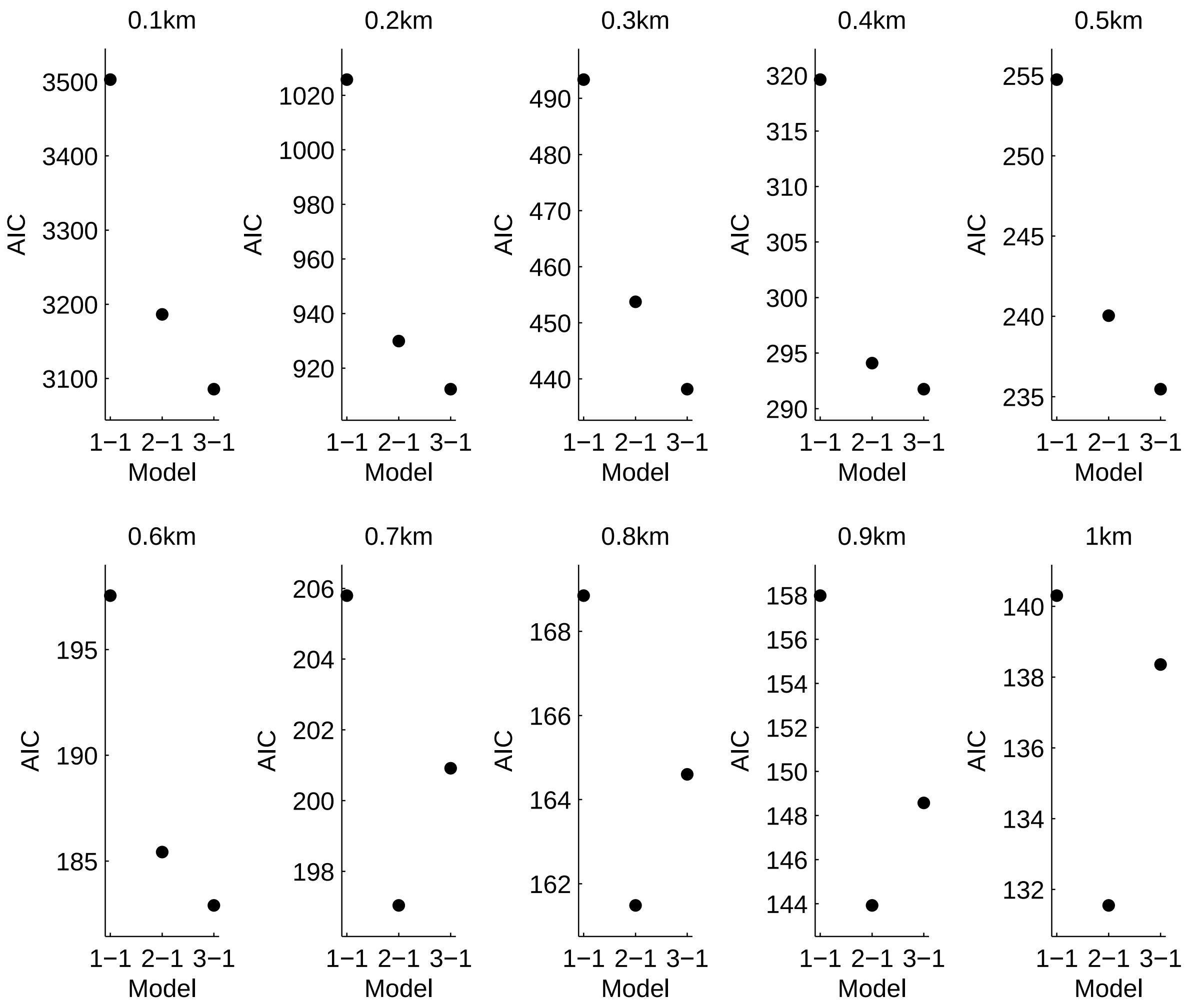

(ii) Estimated parameters of the best 1-3 model for different spacings. The left column shows the West Maar component while the rest shows the three components from the East Maar.

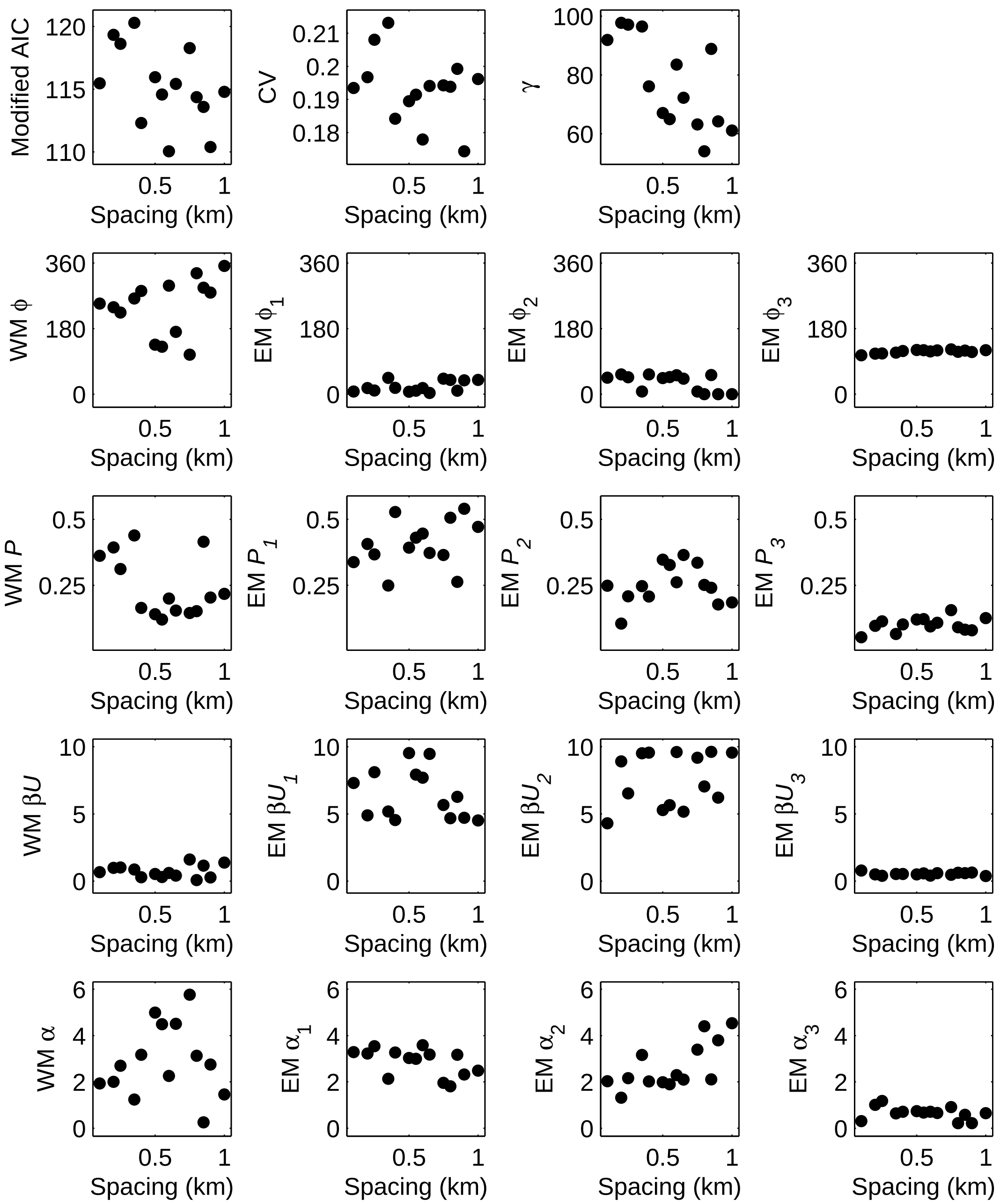

Table 4.5: The mean estimated parameters (with standard deviation) of the Ukinrek models fitted to the imputed data including bootstrap errors R^*.

Model		AIC	γ	ϕ		P		βU		α	
				WM	EM	WM	EM	WM	EM	WM	EM
1-1	Mean	762.1	43.4	94	31	0.28	0.72	0.6	2.3	1.5	2.7
	SD	16.0	7.0	39	7	0.06	0.06	0.9	1.0	0.5	0.4
1-2	Mean	760.1	62.9	164	27, 94	0.31	0.57, 0.12	1.9	3.6, 2.2	2.8	2.8, 0.6
	SD	16.4	14.8	71	18, 29	0.17	0.15, 0.07	2.1	1.8, 2.4	2.0	0.5, 0.6
1-3	Mean	760.9	70.4	152	22, 60, 119	0.20	0.48, 0.23, 0.09	2.0	5.8, 5.5, 1.9	3.5	2.9, 1.7, 0.6
	SD	16.2	11.8	70	33, 50, 39	0.08	0.11, 0.08, 0.04	2.3	2.3, 2.9, 2.1	2.4	0.6, 0.7, 0.4

simulate R^*. The spacing was kept constant at 0.25km between the grid points and the same three (i.e., 1-1, 1-2 and 1-3) models were fitted. Repeating this process 500 times produced the mean and standard deviation for each model parameter for the three models (Table 4.5). Unsurprisingly lack of smoothness in the data increased the AICs compared to the AICs obtained from the smoothed imputed data in Table 4.2. The estimated parameter values in Tables 4.2 and 4.3 were usually contained within the mean $\pm$ standard deviation although the preference of the 1-3 model is no longer obvious. However, provided that the choice of preferred model does not continue to increase with additional data, these sensitivity analyses demonstrate that the objective of the imputation has been achieved.

When applied to a catalogue of eruption data from a particular volcano our model can be used to identify the number of phases for each eruption. Then a probability could be assigned to each number of phases accordingly. We then have a way of estimating the number of phases in a stochastic model which would be particularly useful for unobserved eruptions.

4.5.2 The Al-Madinah eruption

The volume estimate from the kriged contours on Figure 4.3 using the method of Pyle (1989), as modified by Fierstein and Nathenson (1992), is 0.0077km^3 (Figure 4.10). This estimate is much smaller than the estimates shown in Table 4.4 as the former uses an area much smaller than the areas that were obtained by the lobes in Equation 4.1.

Compared to a single phase eruptive event where the tephra dispersal tends to concentrate only on one side of the vent, an eruption with multiple phases is more likely to deposit tephra in multiple directions due to the ever changing wind conditions (Jenkins et al., 2007). Our model offers the means to identify each phase and its wind direction and volume size (cf. Section 4.5.1).

Figure 4.10: The relationship between log thickness $\log T$ and square root of the area $\sqrt{A}$ (after Pyle 1989) for the entire modelled composite tephra fall. Integration yields a total volume estimate of 0.0077km^3 ($0.0024 \pm 0.0004\text{km}^3$ DRE).

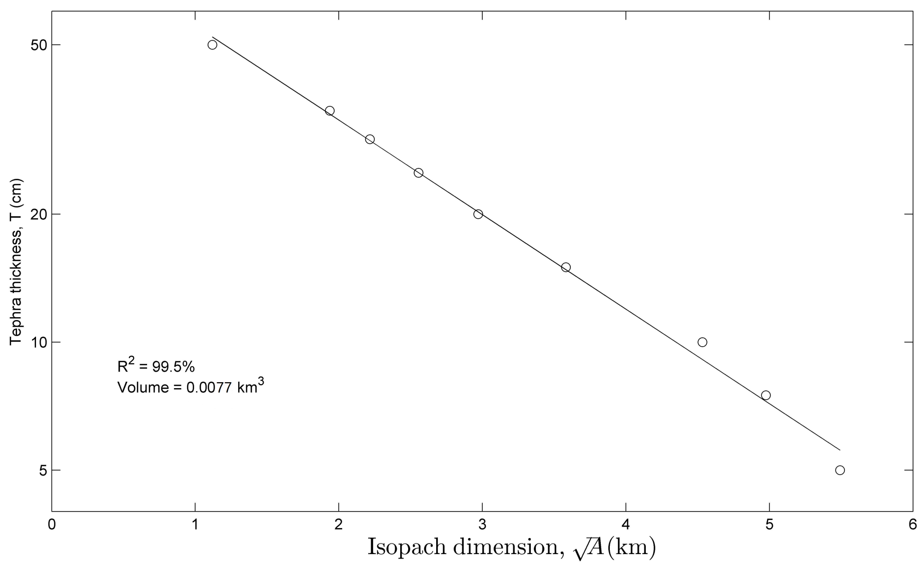

4.6 Conclusion

Elaborating the tephra attenuation model (Equation 3.5) further in a mixture framework enables the model to fit multiple lobes and/or vents. Applied to the 1977 Ukinrek Maars eruption, it was able to identify lobes in the correct directions, for which data exists, from each vent. The model therefore has obvious utility in studying unobserved eruptions with multiple vents.

Due to the lack of distinctive physical differences between fall lobes in different sectors surrounding the main eruptive vents, a statistical approach was developed to use spot fall thickness information to distinguish the multiple overlapping tephra lobes. This method can be used to distinguish the main tephra-producing phases produced during any similar multi-event and multi-source explosive basaltic eruption. The most likely set of vent and lobe combinations that comprise the 1256 AD Al-Madinah eruption including their most likely individual magnitudes. This information provides greater resolution to future tephra hazard models for this area.

Chapter 5

Auckland Volcanic Field

Work discussed in this chapter and Chapter 7 have been revised for Journal of Volcanology and Geothermal Research.

5.1 Introduction

Monogenetic volcanic fields are areas of distributed volcanism, where each new eruption typically occurs in a new location, rather than at an existing vent (Connor and Conway, 2000). The Auckland Volcanic Field (AVF) is a prominent example (Kermode et al., 1992; Allen and Smith, 1994; Kereszturi et al., 2013). The AVF (Figure 5.1) covers most of Auckland City in New Zealand. There have been 52 volcanoes identified (Allen and Smith, 1994; Hayward, Kenny and Grenfell, 2011*b*) as occurring during its active phase over the last 250,000 years (Shane and Hoverd, 2002).

In a monogenetic volcanic field, the main hazard to life is base surge (Sandri et al., 2012) in the vicinity of a new vent. However, effusive eruptions produce lava flows and explosive eruptions produce tephra, which both constitute a hazard to infrastructure. Tephra can also disrupt transport links, especially aviation, even in small amounts

(Miller and Casadevall, 2000). The estimation of the hazard from a monogenetic volcanic field, where each eruptive event creates a new volcano, is critically dependent on a likely reconstruction of past events. The age estimates for these events exist but many are inconsistent. In this chapter, a summary of the volcano age data and maar records available for the AVF is provided.

As Grafton Volcano (Hayward, Kenny, High and France, 2011) is considered an earlier phase of the Domain volcano, probably within a few decades, and its estimated volume is included in that of Domain (Kereszturi et al., 2013), the combination of them is treated as a single volcano leaving 51 volcanoes. Apart from this, and the two eruptions of Rangitoto (Needham et al., 2011), each volcano will be considered to have occurred in a single eruption.

The direct age-order model has been difficult to construct as only 11 of the volcanoes in the AVF are dated with reasonable reliability (Lindsay et al., 2011). Since eruptions from monogenetic fields are generally small, they do not often produce enough lava to overlay with neighbouring volcanoes, making it difficult to determine the stratigraphy of the volcanoes. Bebbington and Cronin (2011) used the maar data from Molloy et al. (2009) to construct an age model by correlating the volcanoes to the tephra deposits found in the maars.

5.2 Direct volcano age determinations

There have been many attempts to directly determine the ages of the volcanoes in the AVF, summarised in Lindsay et al. (2011). These involved various dating methods such as radiocarbon (^{14}C) (e.g., Fergusson et al. (1959); Grant-Taylor and Rafter (1963); Searle (1965); Polach et al. (1969); Grant-Taylor and Rafter (1971)), potassium-argon (K-Ar) (e.g., Stipp (1968); McDougall et al. (1969); Mochizuki et al. (2004, 2007)), argon-argon (^{40}Ar/^{39}Ar) (e.g., Shane and Sandiford (2003); Cassata et al. (2008)),

Figure 5.1: The Auckland Volcanic Field (Bebbington and Cronin, 2011). The cored maars are indicated by stars.

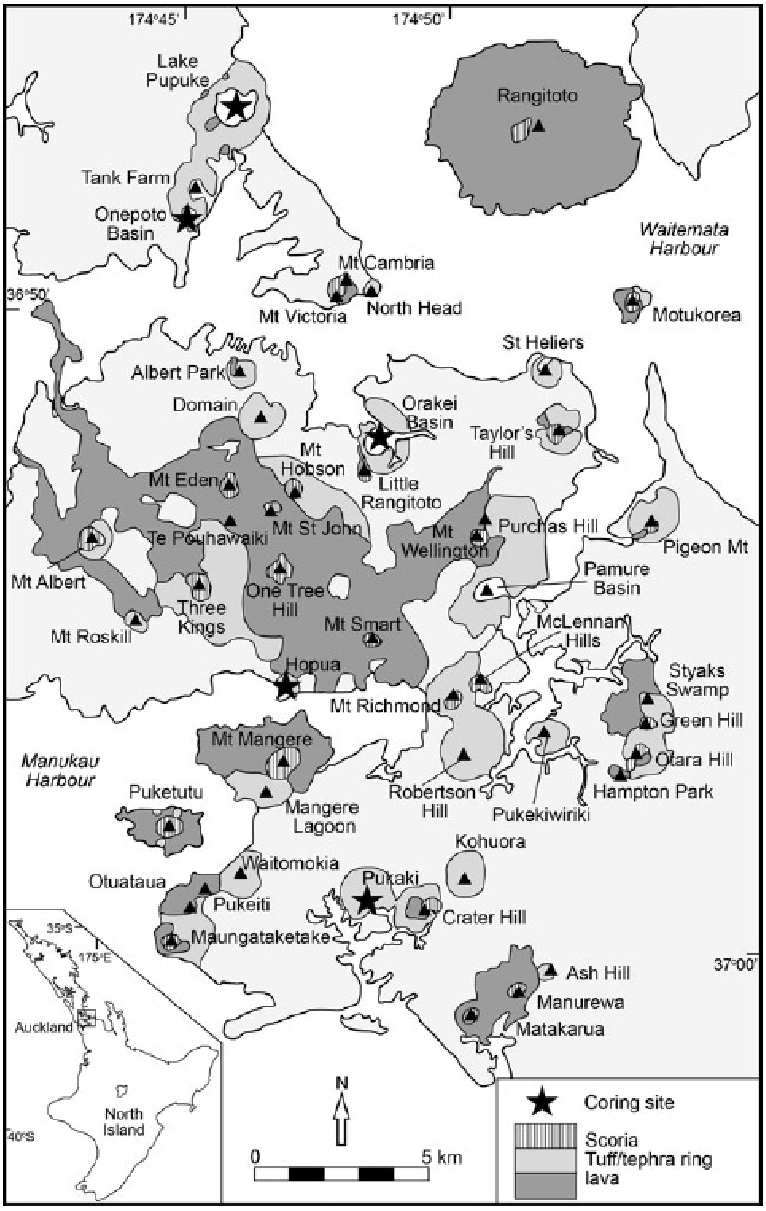

thermoluminescence (TL) (e.g., Adams (1986); Phillips (1989); Wood (1991)), tephrocholonology (e.g., Newnham et al. (1999)), optically stimulated luminescence (OSL) (e.g., Marra et al. (2006)), and paleomagnetism (e.g., Robertson (1983, 1986)). However many of the determined ages are contradictory (Allen and Smith, 1994; Lindsay and Leonard, 2009; Bebbington and Cronin, 2011; Lindsay et al., 2011). Paleomagnetic determinations, which limit the possible age of some volcanoes to a short excursion of the magnetic pole, based on the magnetism in the lavas, also contradict many of the ages. While the excess amount of Ar means that conventional K-Ar ages were unreliably overestimated (McDougall et al., 1969), more recent K-Ar experiments based on groundmass obtained significantly younger ages (Mochizuki et al., 2004, 2007), more in line with the ^{14}C ages. Even further improvement is shown in $^{40}Ar/^{39}Ar$ ages (Cassata et al., 2008).

One unambiguous source of data is stratigraphy from overlaying lavas. A core of lavas contains layers of lavas, each belonging to one distinct event with a unique chemical composition. Hence two layers of lavas are never identical and they can be distinguished. Since lavas in the core are solid and immobile, when two lavas from distinct vents overlap in the field, the source volcano which corresponds to the bottom layer must have erupted first. Hence the age order of some events in the field are reliably determined, and thus their ages can be constrained.

Table 5.1 shows the available determined ages from ^{14}C dating, involving dating organic materials in the tephra, or other radiometric dating from dating rocks directly. Additional information is provided by stratigraphy and the age of the oldest observed tephras in maars, which must postdate the eruption that formed the maar. Different standards were used until the conventional radiocarbon age (CRA) was defined in 1977 (Lindsay and Leonard, 2009). Pre 1980s ^{14}C determinations published in the literature are in calendar year ages which can be considered to be normally distributed. Later ^{14}C ages, of which these are few in the AVF, have to be converted to calendar years.

Table 5.1: The available determined ages for the AVF volcanoes. The minimum ages for Hopua and Orakei Basin follow from the oldest observed tephra found in their cores. "Sea level" means that the volcano occurred above or below a certain sea level, which can be used to constrain the age. Nine ^{14}C ages from Maungataketake and two ^{14}C ages from Panmure Basin were combined via the method of Ward and Wilson (1978) to arrive at a mean age and error shown in this table.

Volcano	Age (ka)	Dating method	References
Ash Hill	31.80 ± 0.16	^{14}C	Hayward (2008*a*)
Boggust Park	> 130	Sea level	Hayward, Kenny and Grenfell (2011*a*)
Crater Hill	33.33 ± 0.67	^{14}C	Searle (1965)
Domain	> 60	^{14}C	Grenfell and Kenny (1995)
Green Hill	199.83 ± 8.98	^{14}C methanol	Sameshima (1990)
Hampton Park	26.60 ± 8.10	$^{40}Ar/^{39}Ar$	Cassata et al. (2008)
Hopua	> 29	Oldest tephra	Molloy et al. (2009)
	< 33	Age of lava at base	Lindsay and Leonard (2009)
Kohuora	34.02 ± 0.27	^{14}C	Searle (1965); Grant-Taylor and Rafter (1971)
McLennan Hills	42.60 ± 3.80	$^{40}Ar/^{39}Ar$	Cassata et al. (2008)
Maungataketake	39.99 ± 0.53	^{14}C	Fergusson et al. (1959); Grant-Taylor and Rafter (1963); Polach et al. (1969); McDougall et al. (1969)
Motukorea	> 7	Sea level	Bryner (1991)
Mt Albert	> 30	^{14}C	Fergusson et al. (1959); Grant-Taylor and Rafter (1963)
Mt Eden	28.39 ± 0.35	^{14}C	East and George (2003)
Mt Mangere	21.94 ± 0.40	^{14}C	Searle (1959, 1965); Grant-Taylor and Rafter (1971)
Onepoto Basin	> 99.5	Oldest tephra	Molloy et al. (2009); Green et al. (2014)
Orakei Basin	> 83.1	Oldest tephra	Molloy et al. (2009)
	< 120	Sea level	Bruce Hayward, personal communication
Panmure Basin	31.73 ± 0.17	^{14}C	Fergusson et al. (1959); Grant-Taylor and Rafter (1963); Polach et al. (1969); McDougall et al. (1969)
Pukaki	> 67	Oldest tephra	Molloy et al. (2009)
Puketutu	33.60 ± 3.70	$^{40}Ar/^{39}Ar$	Cassata et al. (2008)
Pukewairiki	> 130	Sea level	Lindsay and Leonard (2009)
Lake Pupuke	207 ± 6	$^{40}Ar/^{39}Ar$	Cassata et al. (2008)
Roberston Hill	29.90 ± 0.60	^{14}C	Sandiford et al. (2002)
Three Kings	28.59 ± 0.38	^{14}C	Eade (2009)
Wiri Mountain	32.88 ± 0.67	^{14}C	Searle (1965); Grant-Taylor and Rafter (1971)

5.3 Volcano age constraints

The stratigraphy information from overlaying lavas can be used to stochastically order some ages. Table 5.2 shows pairs of volcanoes whose lavas are overlapped. Due to the typically small eruptions in the AVF many lavas do not overlap, thus the order of many pairs cannot be established.

Further age constraints arise through paleomagnetism. A magnetic excursion is a significant temporary change in the geomagnetic field. There were two excursions during the period for which tephra data exists (Shibuya et al., 1992). The first of the two AVF excursions has been identified with the Mono Lake excursion based on ^{40}Ar/^{39}Ar dating (Cassidy, 2006; Cassata et al., 2008). The Mono Lake excursion is usually found in the Northern Hemisphere (Benson et al., 2003) and is a period centred at 32.4 ± 0.3ka (Singer, 2007), that lasted approximately at most 1,000 years (Cassidy, 2006). Due to their similar abnormal magnetic field properties, Crater Hill, Mt Richmond, Puketutu, Taylors Hill, and Wiri Mountain were determined (Cassidy, 2006) to have erupted during the Mono Lake excursion. Taylors Hill occurred at a slightly different time to the others (Cassidy and Hill, 2009). We will interpret this to mean that Taylors Hill has to be the first or the last of the five eruptions. In addition to the five volcanoes above, Cemetery Hill, Hopua, and Little Rangitoto may be within the Mono Lake excursion (John Cassidy, personal communication), but other volcanoes cannot, either due to age constraints or normal remnant magnetism.

The earlier excursion is the Laschamp excursion (Guillou et al., 2004), which is estimated to be centred on an age which is normally distributed with $(40.4, 1.0^2)$ka, and is also approximately at most 1,000 years in duration. McLennan Hills, which has an estimated age of 42.6 ± 3.8ka (Cassata et al., 2008), is considered to have occurred during this excursion, and Little Rangitoto and Pukeiti may also be within the Laschamp excursion (John Cassidy, personal communication).

Based on anomalous palaeomagnetic declination and inclination, some other pairs of

Table 5.2: Stratigraphy and contemporaneous events. $A > B$ to indicate that eruption A occurred before eruption B. An equality indicates (near) contemporaneous events, which may also be ordered. Where no reference is given, see Bebbington and Cronin (2011).

Stratigraphy	References
Ash Hill > Wiri Mountain	
Green Hill > Styaks Swamp	Sibson (1968)
Kohuora > Crater Hill	
Mangere Lagoon > Mt Mangere	Kermode and Heron (1992)
Mt Albert > Mt Roskill	Searle (1962)
Mt Eden > Mt Hobson	
Mt Mangere > Mt Smart	Kermode and Heron (1992)
Mt Roskill > Three Kings	Allen and Smith (1994)
Mt St John > Three Kings	Eade (2009)
North Head > Mt Victoria	
One Tree Hill > Hopua	Allen and Smith (1994)
One Tree Hill > Mt Eden	
One Tree Hill > Mt Mangere	Hayward (2008*b*)
One Tree Hill > Mt Smart	Searle (1962); Hayward (2008*b*)
One Tree Hill > Three Kings	Hayward (2008*b*)
Orakei Basin > Little Rangitoto	Kermode et al. (1992)
Pukeiti > Otuataua	Searle (1959)
Te Pouhawaiki > Mt Eden	Affleck et al. (2001)
Waitomokia > Pukeiti	Searle (1959)
Wiri Mountain > Matukutureia	
Contemporaneous	**References**
Cemetery Hill ≥ Crater Hill	Károly Németh, personal communication
Otara Hill ≥ Hampton Park	Cassidy and Locke (2010)
Maungataketake ≥ Otuataua	Cassidy and Locke (2010)
Mt Cambria = Mt Victoria	

volcanoes are considered contemporaneous (Cassidy and Locke, 2010) as shown in Table 5.2. We interpret contemporaneity to mean they must have erupted within 100 years of each other. In addition to being contemporaneous, some pairs have an additional stratigraphic constraint, based on interleaved or overlapping lavas, as indicated in Table 5.2.

5.4 Maar data

Besides lavas, most of the eruptions produced tephra blankets. In Auckland maars are prone to becoming a swamp afterwards, preserving a sedimentary record including subsequent tephra falls. Sediment cores were recovered from five maars in Auckland, namely Lake Pupuke (Molloy et al., 2009), Onepoto Basin (Shane and Hoverd, 2002), Orakei Basin (Molloy et al., 2009), Hopua Crater (Molloy et al., 2009), and Pukaki Crater (Sandiford et al., 2002; Shane, 2005). These tephra records include proximal AVF events as well as distal Taupo, Okataina, Mayor Island, Taranaki (Egmont), and Tongariro events. Each distal source has a distinct chemical composition so the basaltic (AVF) events are easily distinguishable. At each maar a core containing tephras was collected and the thickness of each tephra layer was measured (Figure 5.2). These were subjectively correlated across the five cores by hand, resulting in 24 distinct AVF tephras (Molloy et al., 2009), approximately over the last 70,000 years.

In addition to the AVF tephras, a number of rhyolitic 'marker tephras' (Lowe et al., 2013) from Taupo and Okataina Volcanic Centres were found in the five maars. These have distinct petrological and chemical characteristics and separate the AVF events in the cores. As part of the process 10 marker tephras from other volcanoes were also correlated across the tephras. The same data, including the marker tephras, were used (Green et al., 2014) to perform a heuristic search over all possible combinations of tephras across the five cores, identifying 22 AVF tephras, each with a normally distributed age, as shown in Table 5.3. AVF 1 refers to the oldest tephra layer found

Figure 5.2: Examples of tephra layers in Auckland maar sediment cores (Molloy et al., 2009).

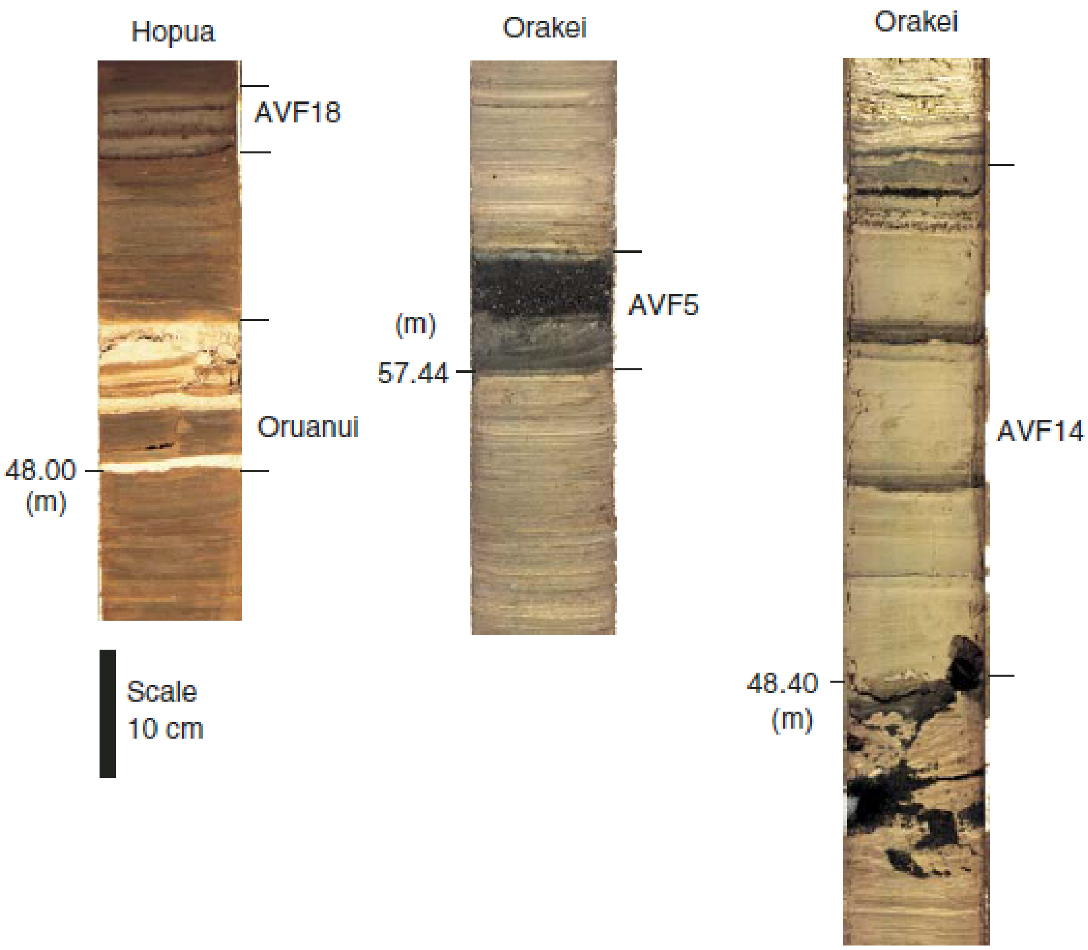

at the bottom of the core and AVF 22 refers to the youngest tephra layer at the top.

Since a maar is the result of an eruption, each is a volcano itself. An additional constraint is provided by the maar (volcano) being older than any of the tephras contained therein. The beginnings of the uncensored periods of maars are estimated to be earlier than 99.5ka, 83ka, 67ka, 55ka, and 29ka at Onepoto Basin, Orakei Basin, Pukaki Crater, Lake Pupuke, and Hopua Crater, respectively, based on the estimated age of the oldest tephra therein, which may not be from the AVF.

Table 5.3 also gives the observed tephra thicknesses at each maar for the 22 AVF tephras (Green et al., 2014). The actual tephra thicknesses may have been either over- or under-thickened depending on the site location. This site specific effect was quantified by Green et al. (2014) using distal tephras from the Taranaki volcano. Dividing thus by a factor (Green et al., 2014) of 0.88 (Lake Pupuke), 0.92 (Onepoto Basin), 1.21 (Orakei Basin), 1.07 (Hopua Crater), and 0.98 (Pukaki Crater) corrects for the mean thickness; individual tephra thicknesses are still likely to be overdispersed. The site specific ratios larger than one at Orakei Basin and Hopua Crater indicate the tephras were over-thickened there, probably due to inflow, and under-thickened at the other sites probably due to streams washing out. Table 5.3 shows the thicknesses before adjustment. Where the thickness is 0mm, the thickness is assumed to have been less than 0.5mm, this being the limit of resolution in the cores.

5.5 Spatio-temporal hazard estimates

Volcanic hazard estimation is important in making informed decisions in safety and financial planning. Safety planning includes ensuring the safety of nuclear power plants around the world (McBirney and Godoy, 2003). At some plants, such as Java in Indonesia, it is necessary to consider potential volcanic hazard as well as other natural hazards. Volcanic hazard is also important in emergency and land use planning in less critical areas.

Table 5.3: The posterior ages and thicknesses for the marker and AVF tephras found in the five cores in the AVF. The Maketu and Tahuna ages are from Molloy et al. (2009) and the Rotoehu from Danišík et al. (2012); other tephra ages are summarised by Lowe et al. (2013). Blank entries delineate the age limits of the recovered cores (censoring).

Source	Age (ka)		Thickness (mm)				
	Mean	SD	Pupuke	Onepoto	Orakei	Hopua	Pukaki
AVF 22	0.80	0.50	22				
Taupo	1.72	0.01	3				
Tahua	6.56	0.14	15		18	20	70
Mamaku	7.95	0.08	0		0	1	2
Rotoma	9.43	0.03	45	43	0	10	7
AVF 21	9.97	0.50	0	0	0	3	0
Opepe	10.00	0.05	0	2	0	2	4
Waiohau	14.01	0.04	2	2	0	3	3
AVF 20	15.45	0.53	0	0	0	0	1
Rotorua	15.64	0.09	45	20	8	25	20
Rerewhakaaitu	17.49	0.12	1.5	3	0	2	1.5
AVF 19	19.74	0.37	0	0	0	290	3
AVF 18	20.00	0.37	0	0	0	235	3
Okareka	21.86	0.06	2	2	3	15	4
AVF 17	23.25	0.51	0	0	8	0	0
AVF 16	23.64	0.38	0	0	5	0	1
AVF 15	24.35	0.38	0	0	12	0	0.5
Te Rere	24.89	0.26	0	0.5	0	0	0.5
AVF 14	24.67	0.39	0	0	340	0	50
AVF 13	24.97	0.36	0	0	740	40	0
Oruanui	25.36	0.04	25	27	10	60	22
Poihipi	28.41	0.16	1.5	1	0	1	1
AVF 12	28.46	0.26	7	12	410	335	70
Okaia	29.03	0.30	6	7	0		15
AVF 11	30.09	0.36	3	0	400		1
AVF 10	30.52	0.36	6	2	45		0
AVF 9	30.85	0.31	20	4	20		490
AVF 9A	30.85	0.31	20	4	0		0
AVF 9B	30.85	0.31	0	0	20		490
AVF 8	32.02	0.36	2	8	0		200
AVF 7	32.89	0.62	0	0	0		5
AVF 6	33.05	0.62	0	0	0		500
AVF 5	34.31	0.70	0	0	110		0
AVF 4	34.90	0.40	15	12	35		0
Maketu	36.37	0.29	60	40	40		25
Tahu	39.37	0.57	8	4	5		4
Rotoehu	45.10	0.79	630	530	70		430
AVF 3	48.61	3.00	0	0	120		0
AVF 2	56.84	6.03		0	510		0
AVF 1	69.45	7.36		4	40		

Traditionally eruption forecasting had been done deterministically (e.g., short-term (Voight and Cornelius, 1991; Hill et al., 2002; Kilburn, 2003) and long-term (Marzocchi, 1996; Sparks, 2003)) identifying one, often the worst, possible sequence of events. However, probabilistic volcanic hazard assessment (Marzocchi and Bebbington, 2012) is becoming increasingly popular.

Volcanic hazard estimation for a monogenetic volcanic field requires the estimation of the locations and timings of future eruptions. Due to the small eruption rates of monogenetic fields the biggest challenge is the lack of sufficient and accurate data. Often the locations of vents can be determined but the precise timings of past eruptions are very difficult to determine as these often go back hundreds of thousands of years.

The nonhomogeneous Poisson nearest-neighbour model (Connor and Hill, 1995) is a spatial-temporal model which estimates the recurrence rate $\lambda(x, y)$ of an eruption per unit time per unit area defined as:

$$\lambda(x, y) = \frac{m}{\sum_{i=1}^{m} u_i t_i},$$

where u_i is the area of a circle whose radius is the distance from the ith randomly chosen point to the nearest volcano, t_i is the time elapsed since the formation of the ith volcano, and m is the number of volcanoes. The hazard estimates from this model are very sensitive to the available age data (Bebbington, 2013).

A vent clustering model for spatio-temporal hazard assessments was used to identify possible clusters in the AVF (Magill et al., 2005). They considered only the age-order model of the eruptions from Allen and Smith (1994) and not the ages. Thus they constructed a spatial mixture renewal model to estimate the location of the next eruption, ignoring the timing of it, using a Monte Carlo simulation. Although these models require no assumption on the independence of the spatial and temporal components, the age-order of the vents is critical.

Allen and Smith (1994) had a default setting of placing geographically close centres after one another in their age-order model (Ian Smith, personal communication). After updating the ages, the independent simulation run by Bebbington and Cronin (2011) did not indicate any spatio-temporal dependencies in the AVF. Based on this finding the spatial and temporal components can be estimated separately (Figure 5.3). Hence they considered the temporal and spatio patterns in the AVF separately, fitting a triggering model for the clustered temporal pattern of the eruptions and considering the spatially correlated eruption locations.

Probabilistic event trees have been developed for short-term forecasting (Newhall and Hoblitt, 2002; Aspinall et al., 2003; Meloy, 2006; Marzocchi et al., 2008; Neri et al., 2008; Lindsay et al., 2010; Marzocchi and Bebbington, 2012). The most accessible version is the BET_EF (Bayesian Event Tree Eruption Forecasting) software (available from `http://bet.bo.ingv.it`). The BET scheme produces the probability of occurrence for each possible sequence of events (Marzocchi et al., 2004) based on the event trees (Newhall and Hoblitt, 2002), which lists all possible sequences such as the size and location of the next eruption in an event of unrest (Marzocchi et al., 2004; Neri et al., 2008). The BET model calculates the probability of occurrence of each possible outcome using a Monte Carlo simulation. Each probability will have an associated error (epistemic uncertainty), indicating the level of uncertainty involved in the prediction.

A more recent development has been the use of BET in long-term forecasting called BET_VH (BET Volcanic Hazard) (Marzocchi et al., 2010; Selva et al., 2010; Sandri et al., 2012). This uses prior knowledge from the volcanological record, coupled with a Poisson process hazard, although the latter assumption is being weakened (Garcia-Aristizabal et al., 2013). The BET_VH model has been applied to the AVF (Sandri et al., 2012), but the Poisson assumption means that the resulting hazard (Figure 5.4) is a long-term average rate multiplied by a detailed spatial hazard.

Figure 5.3: Temporal and spatial hazards in the AVF.

(i) Temporal hazard in the Auckland Volcanic Field (Bebbington and Cronin, 2012)

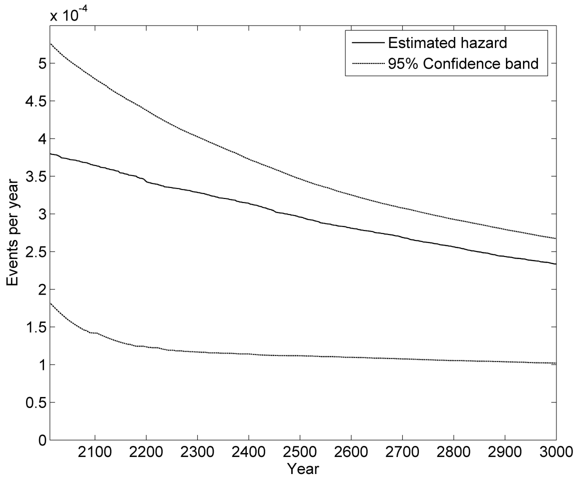

(ii) Spatial hazard in the AVF using Kernel smoothing estimation (Bebbington and Cronin, 2011). The probability contours at intervals of 0.001. Triangles represent eruption centres.

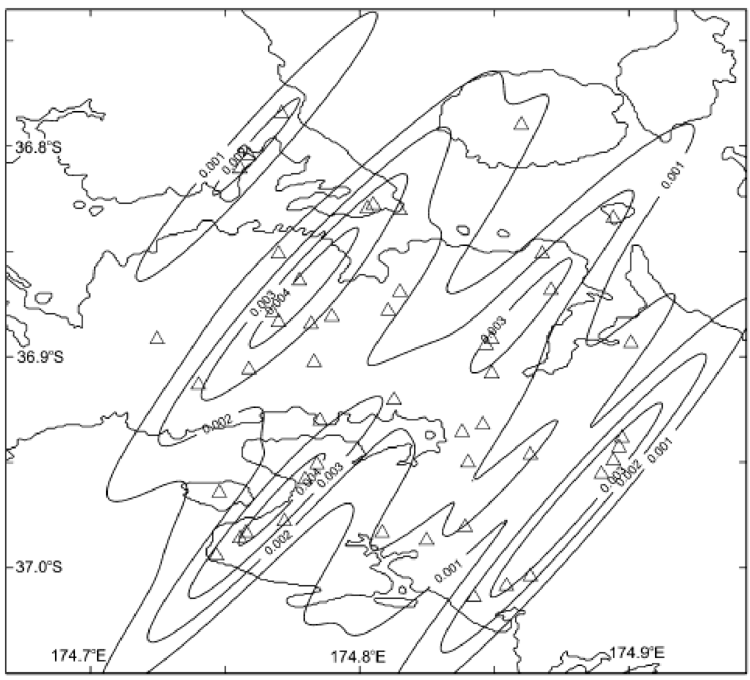

Figure 5.4: Long-term annual probability of base surge impact as estimated from BET_VH application (Sandri et al., 2012).

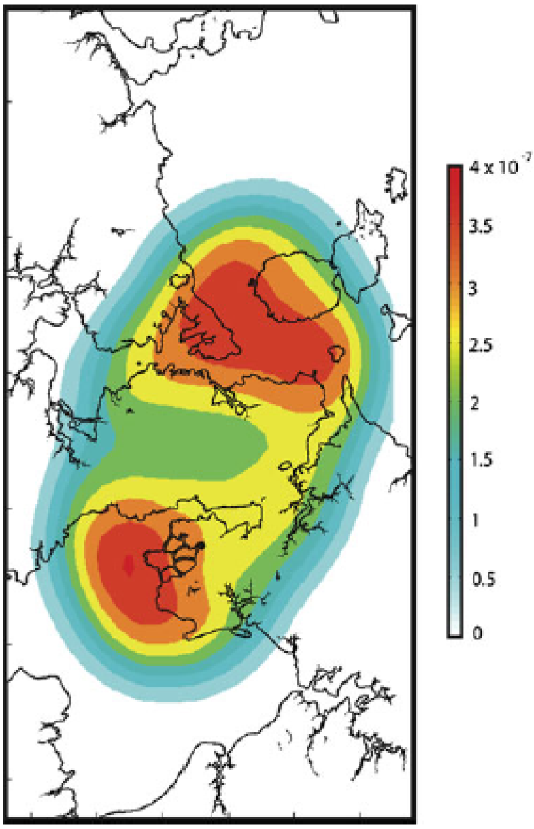

5.6 Tephra hazard estimates

Tephra spatial hazard models have been extended to evaluate the risk in terms of financial loss from a future volcanic eruption in the AVF. The Auckland Region may be affected by a local AVF volcano eruption or eruptions from distal large volume volcanoes. The source probabilities of the next eruption, regardless of time, are the local AVF (0.0169), distal volcanoes such as Tuhua (0.019), Taupo (0.067), Tongariro (0.053), Okataina (0.156), and Egmont (0.536) (Newnham and Lowe, 1991; Newnham et al., 1999; Sandiford et al., 2001; Shane and Hoverd, 2002; Turner et al., 2002) based on geological evidence (Magill, Hurst, Hunter and Blong, 2006; Magill, Blong and McAneney, 2006). However, these probabilities may not reflect the recent development in the Holocene ages of the distant volcanoes (Shane, 2007). Other forms of hazards are discussed in Sandri et al. (2012) for base surge and Kereszturi et al. (2012, 2014) for lava flow.

Magill, Hurst, Hunter and Blong (2006) used the tephra dispersal model ASHFALL (Hurst and Turner, 1999) to generate possible tephra fallout from simulated volcanic events for the Auckland Region. The model requires the eruption column height, total eruption volume, and wind information. They proposed that the 1977 Ukinrek eruption (Self et al., 1980) was analogous to a typical eruption in the AVF (Magill, Hurst, Hunter and Blong, 2006) and so they randomly sampled column heights and eruption volumes based on the observations from the Ukinrek eruption. The wind profiles were collected at Auckland Airport which are found to be consistent across the entire region (Rhoades et al., 2002; Magill, Hurst, Hunter and Blong, 2006).

ASHFALL was also used by Magill, Blong and McAneney (2006) to produce a database of possible tephra thicknesses for the Auckland Region, from local and distal volcanoes, with associated probabilities of occurrences based on the geological record. VolcaNZ is a probabilistic volcanic loss model that can be used to estimate the expected replacement cost for damaged buildings and their associated clean up costs for the Auckland Region

(Magill, Blong and McAneney, 2006). It evaluates the cost with consideration to the exposure, vulnerability, and value of the buildings based on the simulated tephra fall scenario. Although the model fails to consider climate changes, which can greatly influence the tephra dispersal occurred over the time window in the region (Shane, 2007), the VolcaNZ model can be updated when relevant data become available (Magill, 2007) including meteorological data.

Hurst and Smith (2010) discuss the volcanic hazard risk from ash fallout from volcanic eruptions in New Zealand including Auckland. Their model estimates the probability of an eruption of volume greater than a selected amount based on the volume-frequency relationship of the past eruptions. However, the contribution from the AVF, which accounts for about half of the total risk in the area, was not done in any great detail.

5.7 Correlating tephras to volcanoes

To have a forecast of the next eruption in the AVF requires a reconstruction of past eruptions. Forecasting the location of the next eruption requires us to consider the temporal aspect of the existing volcanoes. The correlation exercise between tephras and volcanoes in the AVF will allow an improvement in the age-order model and age estimates of some of the volcanoes.

An ad-hoc, rather than optimal, record was constructed (Bebbington and Cronin, 2011) using a tephra thickness attenuation model (Rhoades et al., 2002) to link estimated eruption volumes (Allen and Smith, 1994) with the tephra thicknesses (Molloy et al., 2009) via the locations of source volcano and deposition location. The procedure worked from the largest and most wide-spread tephras to the smallest. The source with the best apparent fit to the distance and thickness data was assigned to that tephra unless the ages were inconsistent. Some back-tracking from infeasible solutions was required. The estimated ages of the volcanoes were used only as constraints and were not evaluated against the ages of the tephras, which were linearly interpolated, independently for each maar, by Molloy et al. (2009). No wind direction information was used.

Bebbington and Cronin (2012) updated the matching algorithm to better reflect the paleomagnetic results, and produced 1,000 Monte Carlo age sequences for the 51 volcanoes in the field. Besides being used to show that there appeared to be no significant spatio-temporal dependence in the AVF (Bebbington and Cronin, 2011, 2012), these sequences were used by Bebbington (2013) to test various spatio, temporal, and spatio-temporal models. Le Corvec et al. (2013) also used the data to examine whether the chemical evolution of the field could be correlated with the temporal (inter-event time) or spatial (inter-event distance).

Chapter 6

Bayesian Age Reconciliation

6.1 Introduction

The Auckland Volcanic Field (AVF) has produced at least 52 volcanoes during its active phase over the last 250,000 years. Age data for many of these exist, from radiocarbon or other radiometric methods, dosimetric methods such as thermoluminescence or optically stimulated luminescence, and paleomagnetism. However, the results are often inconsistent. For example, a number of age estimates are available for Maungataketake from four different dating methods. Radiocarbon (^{14}C) dating on the samples and thermoluminescence date the volcano to be about 30-50ka while potassium-argon and optically stimulated luminescence estimate Maungataketake to be over 100ka. The available mean ages for Puketutu are also inconsistent with argon-argon and thermoluminescence estimating it to be around 20-40ka but the two of the potassium-argon ages provided 16ka (Mochizuki et al., 2007) and 77ka (McDougall et al., 1969).

This chapter discusses how best to reconcile these inconsistent data and arrive at an optimum age-model for the AVF in a Bayesian paradigm. The aim is to estimate the true ages for the AVF volcanoes. In the process the reliability of each dating method will also be evaluated. Informative priors will be obtained, via expert elicitation, on both the individual ages, and the reliabilities of the dating methods. The inconsistencies in the estimated ages between the dating methods may be dealt with by assigning a weight of reliability for each method.

6.2 Expert elicitation

To obtain priors for our Bayesian age reconciliation model, expert elicitation was performed in which experts in the AVF and/or dating samples were asked for their opinions on the ages of the volcanic eruptions in the AVF and the reliabilities of the dating methods used on dating samples collected from the AVF. They were asked to provide their personal or subjective opinion to cover the breadth of expert opinion.

In 2013, 35 experts worldwide, 25 from New Zealand who are/have been working on the AVF and the rest from overseas, mainly from Asia, were asked to participate. Most of the New Zealanders were researchers or PhD students from Massey University, the University of Auckland, or the University of Canterbury and a couple were from GNS Science. International experts were also invited to provide their opinions on the reliabilities of dating methods based on their experiences in general. As the independence between the experts' responses were important, the participants, who were likely to be colleagues, were asked not to communicate with anyone about this questionnaire.

Figure 6.1 shows the questionnaire that was sent out to each of the 35 experts. The first part contained questions about the reliability of the dating methods used in the AVF and the second part asked the AVF volcano estimated ages.

Out of 35 experts, 15 returned the questionnaire with their opinions, with only six making an attempt at the second part. All international experts and most of the local experts opted out of it citing their unfamiliarity with the specific volcanoes in the AVF as the main reason. Overall the response rate was extremely disappointing.

Figure 6.1: The questionnaire template.

Auckland Volcanic Field Questionnaire

Thank you for taking part in the following short questionnaire. Please feel free to leave blank any sections you are unable to answer. ***Please do not confer with any other respondents.***

Question 1: Radiocarbon dating

Please circle one response for each item.

If ^{14}C dating returns an age in the following intervals, how reliable would you consider the returned age to be?

	Unreliable				Reliable
a. 0 – 20 ka	1	2	3	4	5
b. 20 – 40 ka	1	2	3	4	5
c. 40 – 60 ka	1	2	3	4	5
d. 60 – 120 ka	1	2	3	4	5
e. 120 – 240 ka	1	2	3	4	5

If the true age is in the following intervals, how reliable do you believe ^{14}C dating would be in returning that age?

	Unreliable				Reliable
a. 0 – 20 ka	1	2	3	4	5
b. 20 – 40 ka	1	2	3	4	5
c. 40 – 60 ka	1	2	3	4	5
d. 60 – 120 ka	1	2	3	4	5
e. 120 – 240 ka	1	2	3	4	5

Question 2: K-Ar dating

Please circle one response for each item.

If K-Ar dating returns an age in the following intervals, how reliable would you consider the returned age to be?

	Unreliable				Reliable
a. 0 – 20 ka	1	2	3	4	5
b. 20 – 40 ka	1	2	3	4	5
c. 40 – 60 ka	1	2	3	4	5
d. 60 – 120 ka	1	2	3	4	5
e. 120 – 240 ka	1	2	3	4	5

1

If the true age is in the following intervals, how reliable do you believe K-Ar dating would be in returning that age?

	Unreliable				Reliable
a. 0 – 20 ka	1	2	3	4	5
b. 20 – 40 ka	1	2	3	4	5
c. 40 – 60 ka	1	2	3	4	5
d. 60 – 120 ka	1	2	3	4	5
e. 120 – 240 ka	1	2	3	4	5

Question 3: ^{40}Ar-^{39}Ar dating

Please circle one response for each item.

If ^{40}Ar-^{39}Ar dating returns an age in the following intervals, how reliable would you consider the returned age to be?

	Unreliable				Reliable
a. 0 – 20 ka	1	2	3	4	5
b. 20 – 40 ka	1	2	3	4	5
c. 40 – 60 ka	1	2	3	4	5
d. 60 – 120 ka	1	2	3	4	5
e. 120 – 240 ka	1	2	3	4	5

If the true age is in the following intervals, how reliable do you believe ^{40}Ar-^{39}Ar dating would be in returning that age?

	Unreliable				Reliable
a. 0 – 20 ka	1	2	3	4	5
b. 20 – 40 ka	1	2	3	4	5
c. 40 – 60 ka	1	2	3	4	5
d. 60 – 120 ka	1	2	3	4	5
e. 120 – 240 ka	1	2	3	4	5

Question 4: Paleomagnetic declination

Please circle one response for each item.

If paelomagnetic declination returns an age in the following intervals, how reliable would you consider the returned age to be?

	Unreliable				Reliable
a. 0 – 20 ka	1	2	3	4	5
b. 20 – 40 ka	1	2	3	4	5
c. 40 – 60 ka	1	2	3	4	5
d. 60 – 120 ka	1	2	3	4	5
e. 120 – 240 ka	1	2	3	4	5

If the true age is in the following intervals, how reliable do you believe paleomagnetic declination would be in returning that age?

	Unreliable				Reliable
a. 0 – 20 ka	1	2	3	4	5
b. 20 – 40 ka	1	2	3	4	5
c. 40 – 60 ka	1	2	3	4	5
d. 60 – 120 ka	1	2	3	4	5
e. 120 – 240 ka	1	2	3	4	5

Question 5: Optically stimulated luminescence dating

Please circle one response for each item.

If OSL dating returns an age in the following intervals, how reliable would you consider the returned age to be?

	Unreliable				Reliable
a. 0 – 20 ka	1	2	3	4	5
b. 20 – 40 ka	1	2	3	4	5
c. 40 – 60 ka	1	2	3	4	5
d. 60 – 120 ka	1	2	3	4	5
e. 120 – 240 ka	1	2	3	4	5

If the true age is in the following intervals, how reliable do you believe OSL dating would be in returning that age?

	Unreliable				Reliable
a. 0 – 20 ka	1	2	3	4	5
b. 20 – 40 ka	1	2	3	4	5
c. 40 – 60 ka	1	2	3	4	5
d. 60 – 120 ka	1	2	3	4	5
e. 120 – 240 ka	1	2	3	4	5

Question 6: Thermoluminescence dating

Please circle one response for each item.

If thermoluminescence dating returns an age in the following intervals, how reliable would you consider the returned age to be?

	Unreliable				Reliable
a. 0 – 20 ka	1	2	3	4	5
b. 20 – 40 ka	1	2	3	4	5
c. 40 – 60 ka	1	2	3	4	5
d. 60 – 120 ka	1	2	3	4	5
e. 120 – 240 ka	1	2	3	4	5

If the true age is in the following intervals, how reliable do you believe thermoluminescence dating would be in returning that age?

	Unreliable				Reliable
a. 0 – 20 ka	1	2	3	4	5
b. 20 – 40 ka	1	2	3	4	5
c. 40 – 60 ka	1	2	3	4	5
d. 60 – 120 ka	1	2	3	4	5
e. 120 – 240 ka	1	2	3	4	5

Question 7: Ages and errors

Please give your interpretation of the most likely age and error in calendar years for each of the following volcano centres in the Auckland Volcanic Field (complete only for those that you feel you have some geological evidence for, e.g., stratigraphy, relative age, weathering, unpublished dates or geological information etc.).

1. Domain: ____________________ ± ____________________
2. Albert Park: ____________________ ± ____________________
3. St Heliers: ____________________ ± ____________________
4. Onepoto Basin: ____________________ ± ____________________
5. Tank Farm: ____________________ ± ____________________
6. Lake Pupuke: ____________________ ± ____________________
7. Mt Cambria: ____________________ ± ____________________
8. Mt Victoria: ____________________ ± ____________________
9. North Head: ____________________ ± ____________________
10. Mt Albert: ____________________ ± ____________________
11. Mt Roskill: ____________________ ± ____________________
12. Panmure Basin: ____________________ ± ____________________
13. McLennan Hills: ____________________ ± ____________________
14. Mt Richmond: ____________________ ± ____________________
15. Roberston Hill: ____________________ ± ____________________
16. Pukekiwiriki: ____________________ ± ____________________
17. Waitomokia: ____________________ ± ____________________
18. Maungataketake: ____________________ ± ____________________
19. Pukeiti: ____________________ ± ____________________
20. Otuataua: ____________________ ± ____________________
21. Matakarua: ____________________ ± ____________________
22. Ash Hill: ____________________ ± ____________________
23. Kohuora: ____________________ ± ____________________
24. Crater Hill: ____________________ ± ____________________
25. Wiri Mountain: ____________________ ± ____________________
26. Puketutu: ____________________ ± ____________________
27. Pigeon Mountain: ____________________ ± ____________________
28. Taylors Hill: ____________________ ± ____________________

5

29. Pukaki: ____________________________ ± ____________________________
30. Mt Smart: ____________________________ ± ____________________________
31. Styakes Swamp: ____________________________ ± ____________________________
32. Green Hill: ____________________________ ± ____________________________
33. Otara Hill: ____________________________ ± ____________________________
34. Hampton Park: ____________________________ ± ____________________________
35. Mangere Lagoon: ____________________________ ± ____________________________
36. Mt Mangere: ____________________________ ± ____________________________
37. One Tree Hill: ____________________________ ± ____________________________
38. Three Kings: ____________________________ ± ____________________________
39. Hopua: ____________________________ ± ____________________________
40. Te Pouhawaiki: ____________________________ ± ____________________________
41. Mt Eden: ____________________________ ± ____________________________
42. Mt St John: ____________________________ ± ____________________________
43. Mt Hobson: ____________________________ ± ____________________________
44. Little Rangitoto: ____________________________ ± ____________________________
45. Orakei Basin: ____________________________ ± ____________________________
46. Purchas Hill: ____________________________ ± ____________________________
47. Mt Wellington: ____________________________ ± ____________________________
48. Motukorea: ____________________________ ± ____________________________
49. Rangitoto: ____________________________ ± ____________________________

Any further comments:

Thank you for taking your valuable time to share your knowledge.

6

6.2.1 Volcano ages

In the first part, the questionnaire asked the experts to estimate the ages (with error) of 51 AVF volcanoes. Six experts provided their opinions on the ages of at least one of them. Some of them provided ages only on the well known volcanoes, hence each volcano has at most six estimates, usually much less.

Each of the returned estimated ages was in one of the two forms $\mu \pm \sigma$ or a range of a to b. If the former, an assumption was made that the estimated age follows a normal distribution. For some volcanoes this assumption inevitably includes a negative age when simulating from the distribution. For example, one expert's estimated age for North Head was 11.5 ± 20ka. On the other hand, if an estimate is given as a range or only contains a minimum age a, then the age is assumed to follow a uniform distribution with a lower limit of a and an upper limit of b or 250ka if not given.

For these experts' age estimates to be used as priors, they must be combined to obtain a single prior distribution for each volcano. O'Hagan et al. (2006) details the linear pooling method where the resulting consensus prior distribution is the weighted average of the individual distributions. Here, without asking the experts to rate their own opinions, there is no good way of putting different weights, especially with only six (or fewer) responses. Hence equal weighting is implicitly assumed. Following `http://blog.revolutionanalytics.com/2014/01/forecasting-by-combining-expert-opinion.html`, 10,000 values were generated from each expert's distribution and they were combined and plotted in a histogram for each volcano (Figure 6.2). Volcanoes such as Pigeon Mountain were provided with only one normally distributed estimate, and hence its simulated values form a typical normal bell-shaped distribution. Some volcanoes have a bimodal distribution as a result of at least two normal ages with distinct means. Wiri Mountain received four estimated ages, 30.9 ± 0.4, 32 ± 1, 32.4 ± 1.3, and 33 ± 0.5ka. The first formed the left peak and the rest contributed to the right peak.

This bimodality is largely due to the lack of number of estimates provided by the experts, which is the biggest limitation in forming the priors. If more responses were available the individual estimates may combine to give a unimodal, possibly normal, distribution. Puketutu is an example of such a case where similar estimates, 32 ± 1, 32.4 ± 1.3, 33 ± 0.5, and 33 ± 0.5ka, form a smooth unimodal distribution.

Treating the combined generated values as data, Figure 6.2 shows a suitable distribution fitted to the simulated ages to obtain a prior distribution for each volcano. Volcanoes such as Boggust and Grafton received only one estimated age range. Simply a uniform distribution is fitted for these volcanoes. For the rest of the volcanoes a gamma distribution is considered for its ability to handle non-negative values. The experts are fairly certain about the ages of the volcanoes whose mean ages are younger than 35ka. Hence these young volcanoes, including the Mono Lake volcanoes, have fairly tight priors. On the other hand, the ages of volcanoes such as Hopua and Waitomokia are not agreed well between the experts. When there is an expert who is fairly certain that the volcano is fairly young, another expert's uncertainty results in almost a flat prior.

The bimodality present in some of the histograms was ignored as it is assumed to be due to the small number of responses. If more responses were received from the experts and the bimodality is still present a mixture of two distributions may be fitted. However, the fitted distributions should be adequate for the purpose of building a Bayesian age-order model.

6.2.2 Dating method reliability

In order to combine the determined ages of various dating method, the reliability of the dating methods is also evaluated. The six dating methods used on samples from the AVF are explained in Section 2.3. They are

1. radiocarbon (^{14}C) dating

2. potassium-argon (K-Ar) dating

Figure 6.2: Histograms of generated volcano ages from the expert elicitation and fitted densities. The number in the parenthesis indicates the number of experts who provided an age estimate.

(i) Albert Park (3)

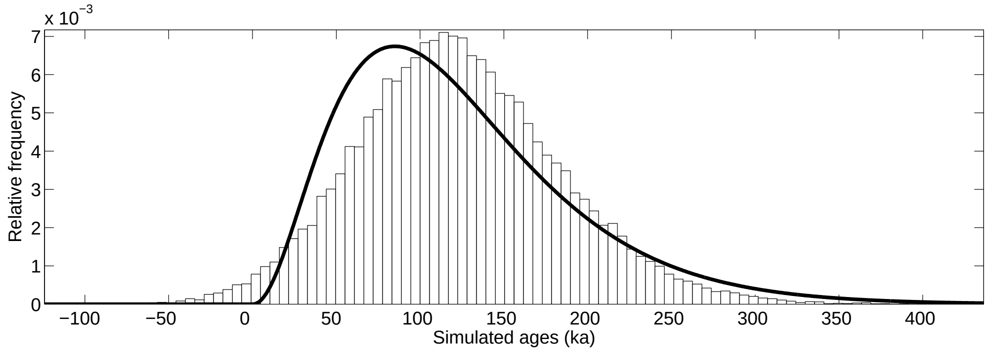

(ii) Ash Hill (4)

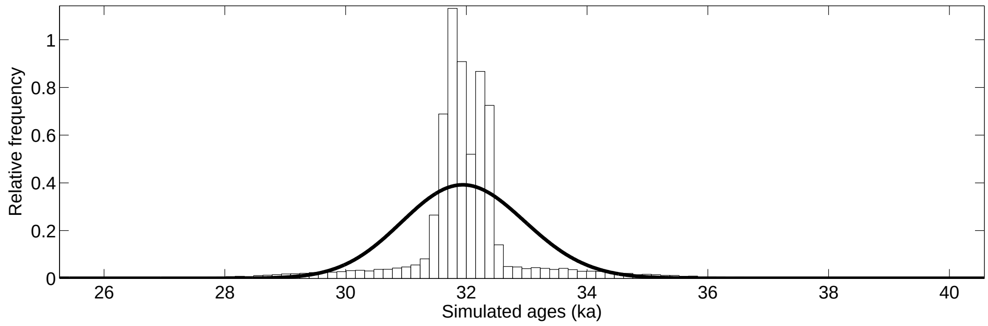

(iii) Boggust (1)

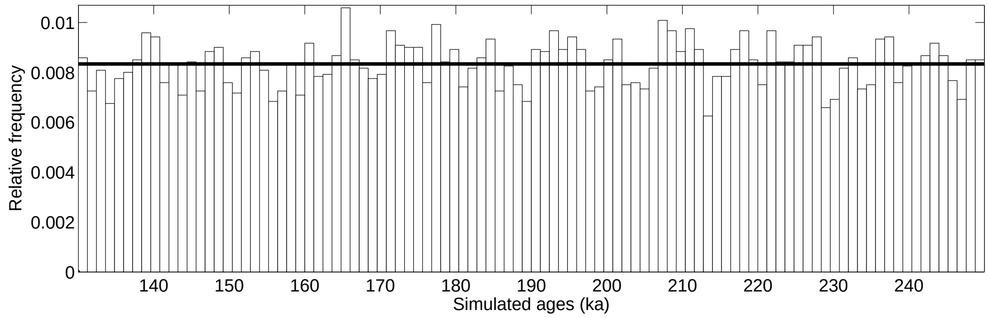

(iv) Crater Hill (4)

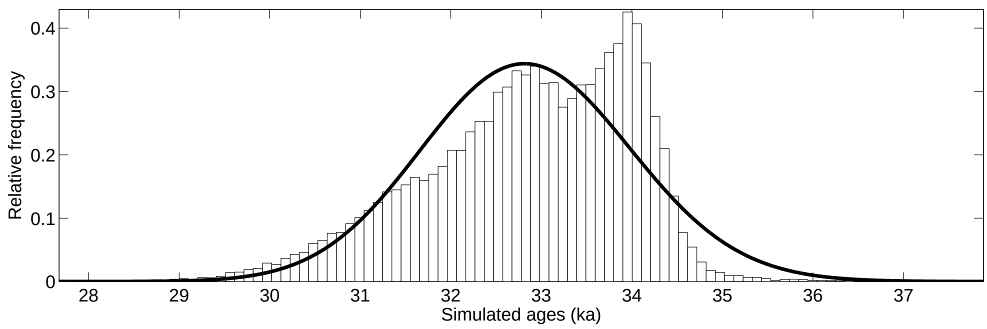

(v) Domain (5)

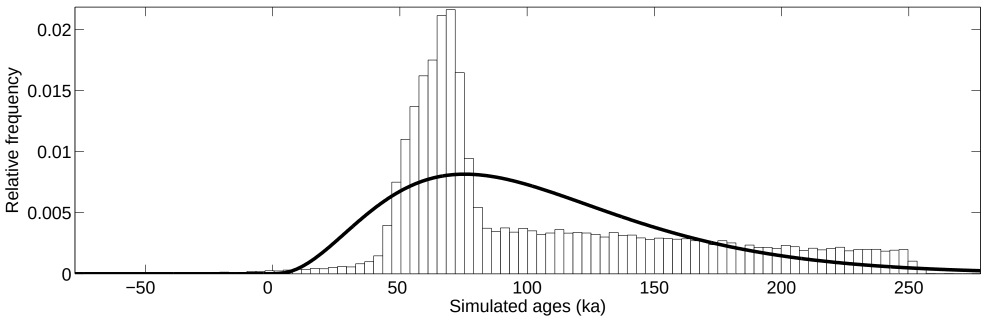

(vi) Grafton (1)

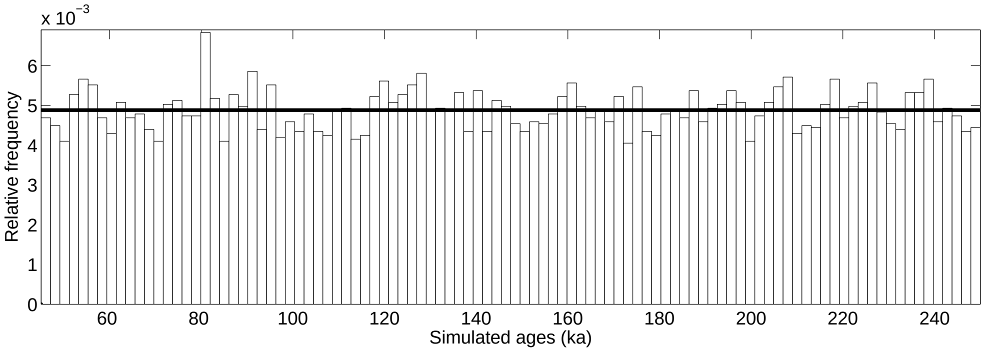

(vii) Green Hill (3)

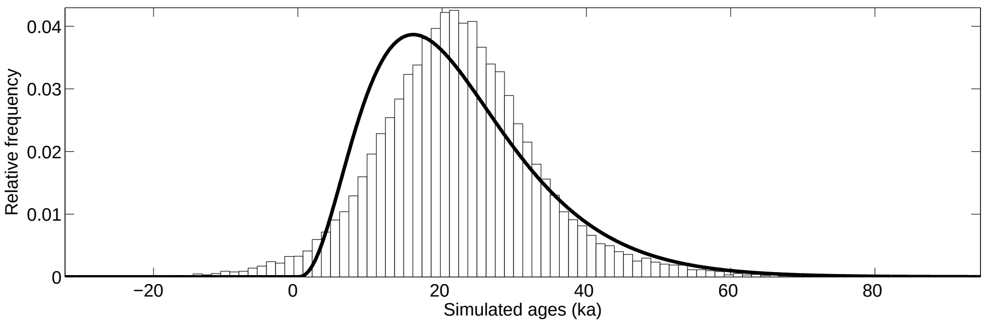

(viii) Hampton Park (4)

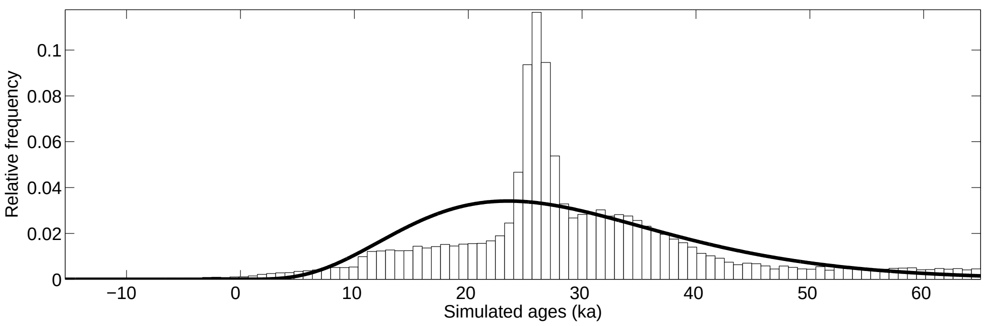

(ix) Hopua (4)

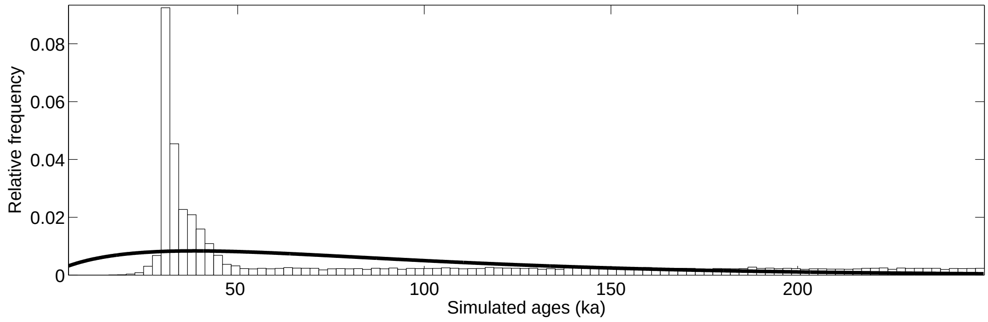

(x) Kohuora (4)

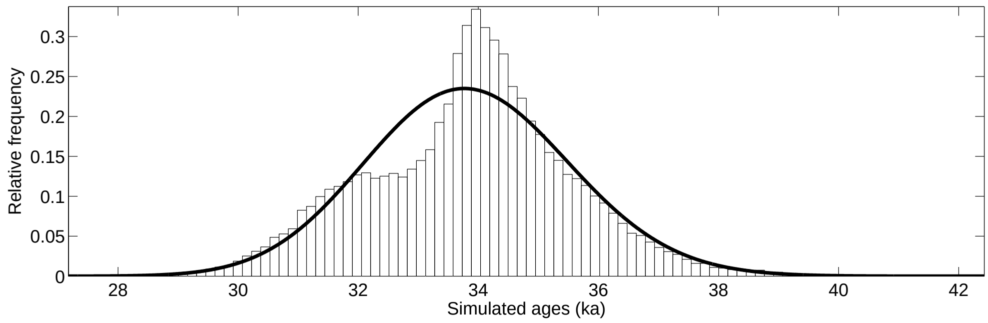

(xi) Lake Pupuke (6)

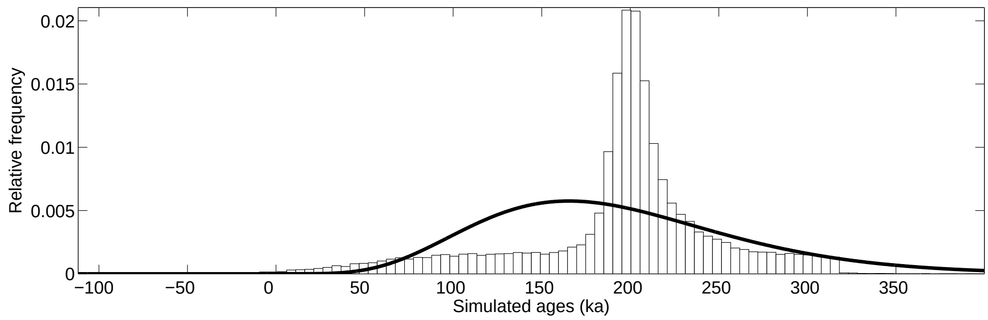

(xii) Little Rangitoto (2)

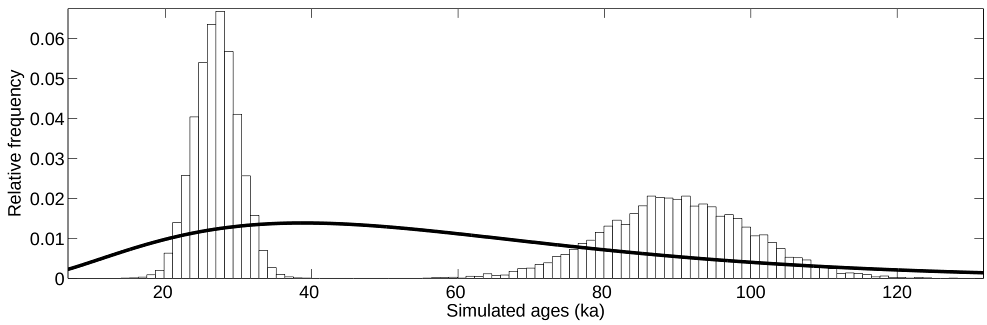

(xiii) Mangere Lagoon (3)

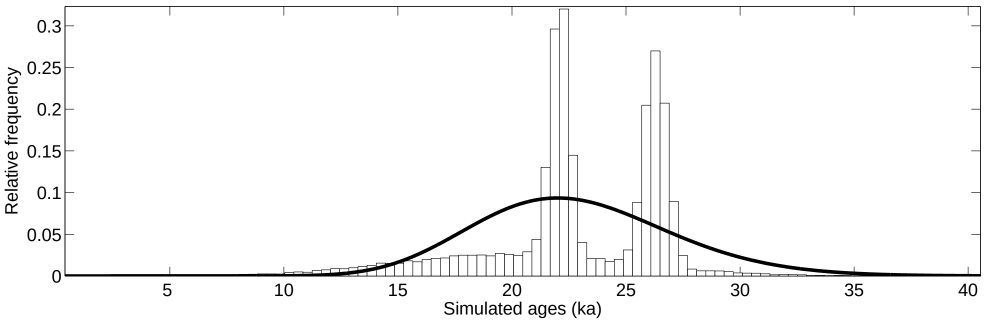

(xiv) Matukutureia (1)

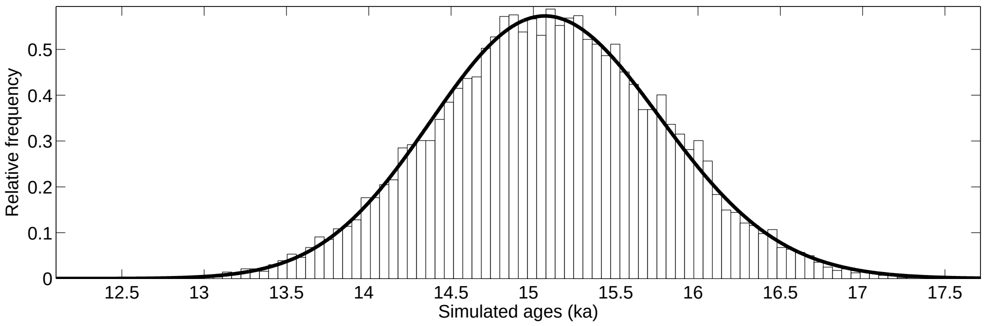

(xv) Maungataketake (4)

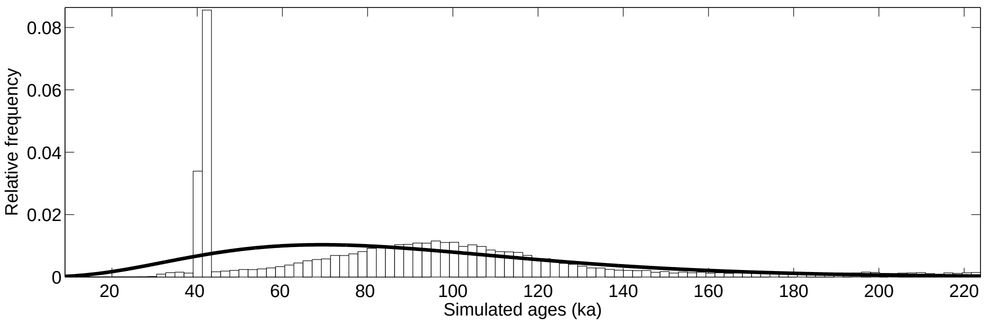

(xvi) McLennan Hills (4)

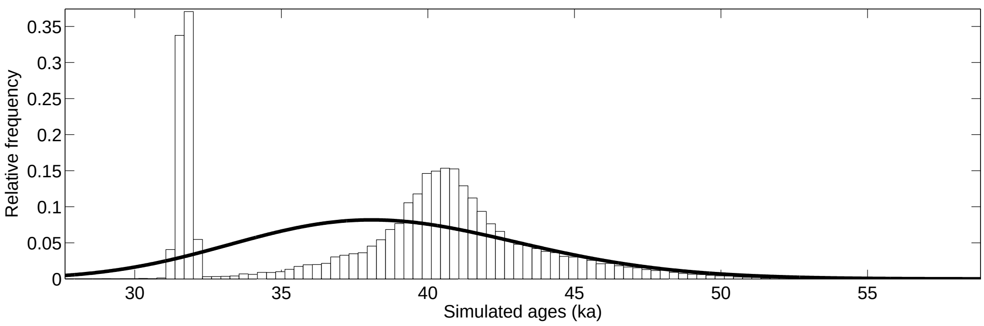

(xvii) Motukorea (3)

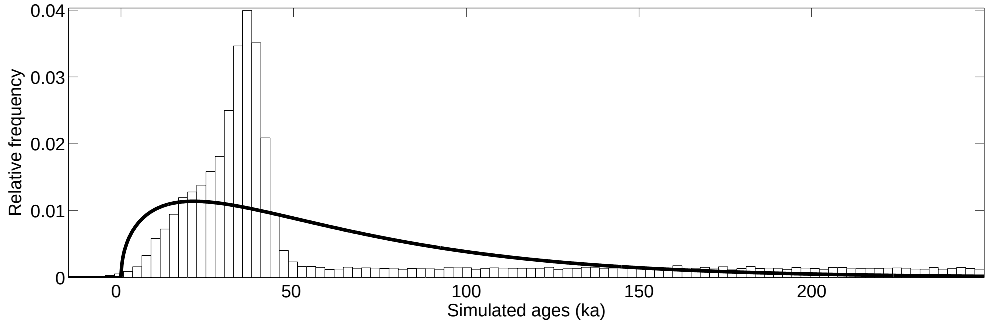

(xviii) Mt Albert (3)

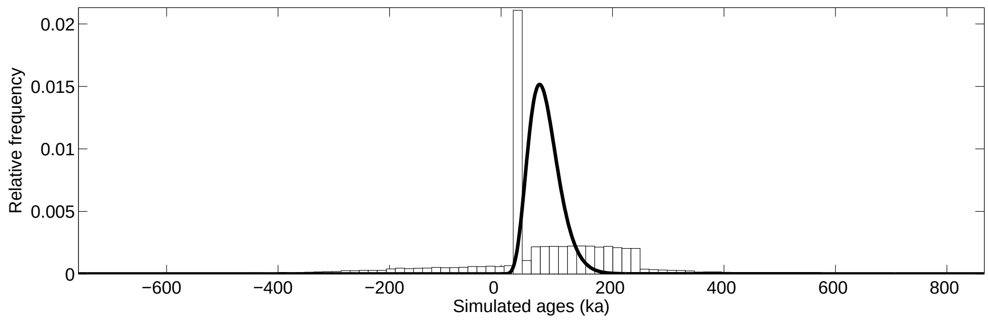

(xix) Mt Cambria (2)

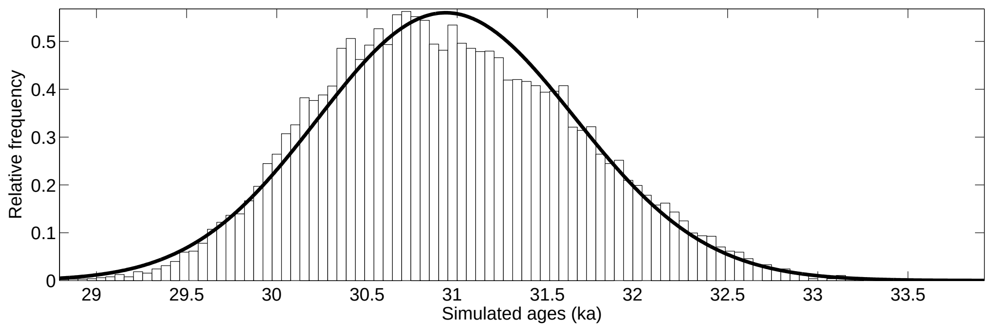

(xx) Mt Eden (4)

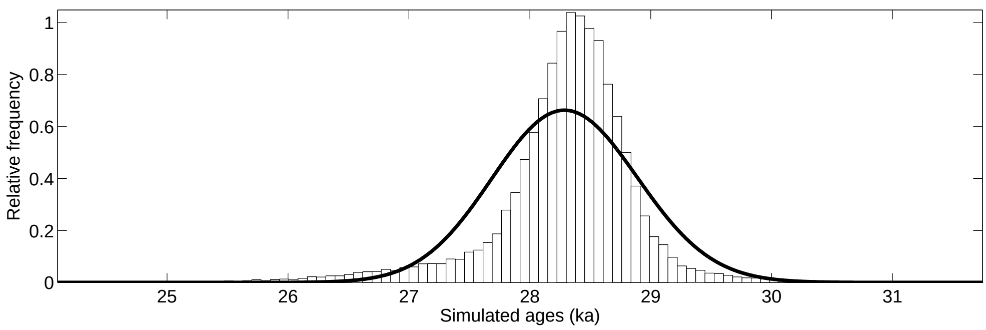

(xxi) Mt Hobson (3)

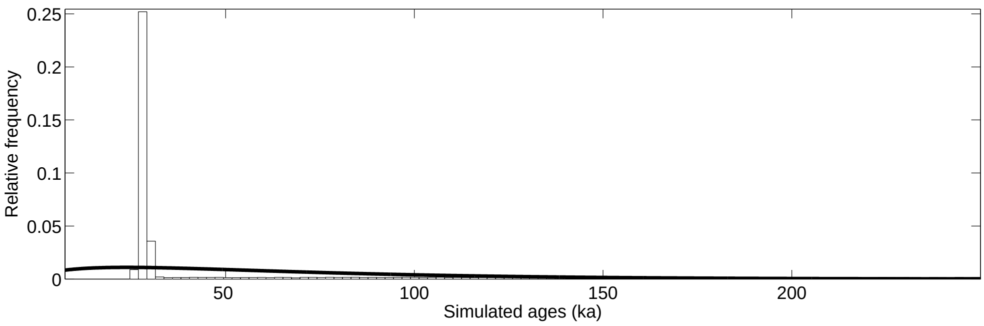

(xxii) Mt Mangere (3)

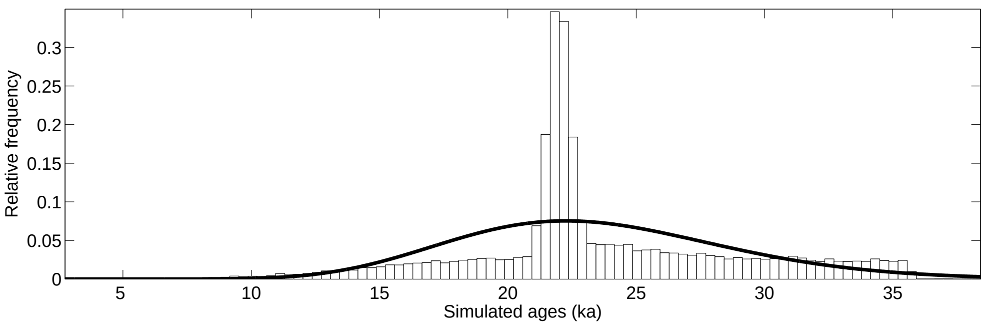

(xxiii) Mt Richmond (4)

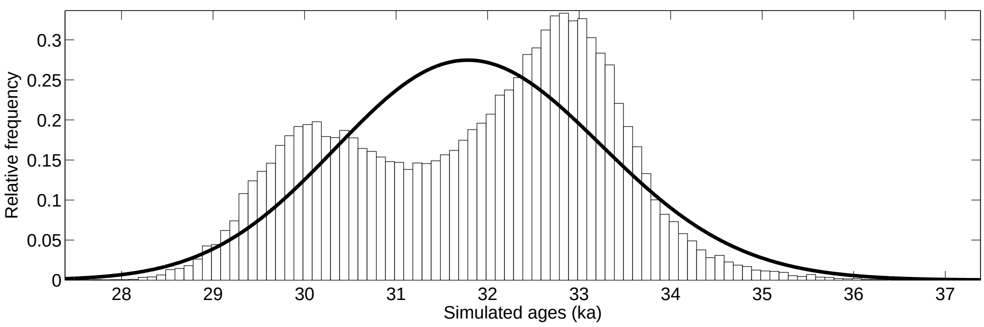

(xxiv) Mt Roskill (1)

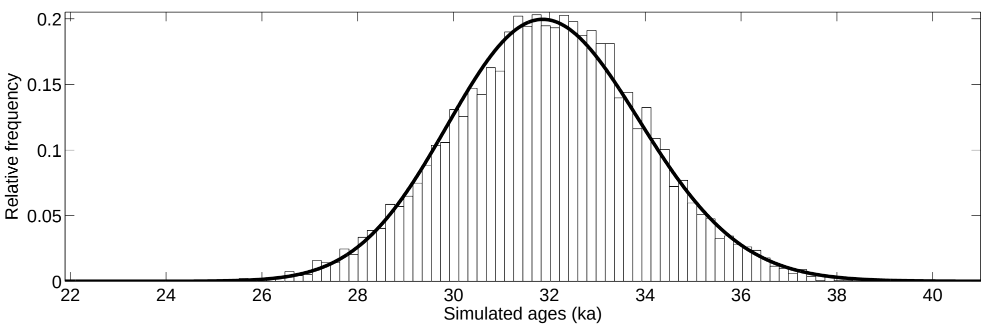

(xxv) Mt Smart (1)

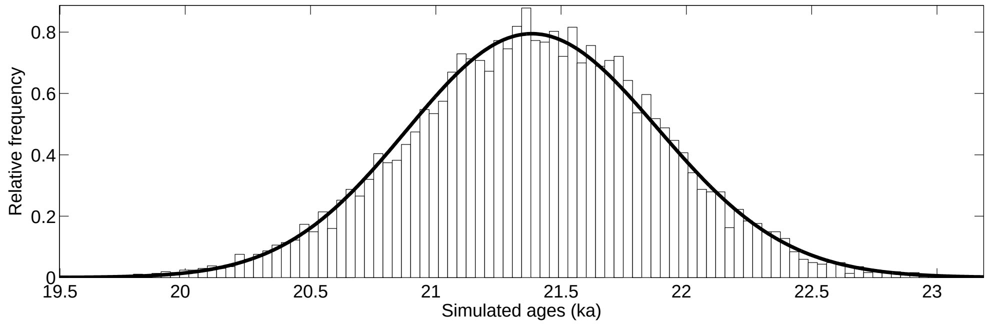

(xxvi) Mt St John (4)

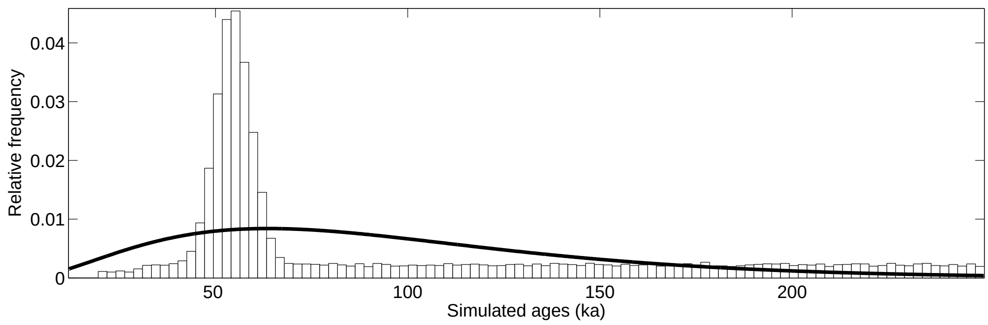

(xxvii) Mt Victoria (2)

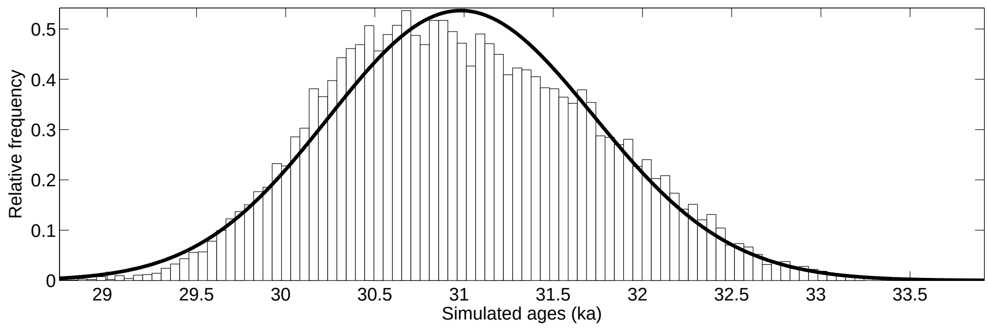

(xxviii) Mt Wellington (5)

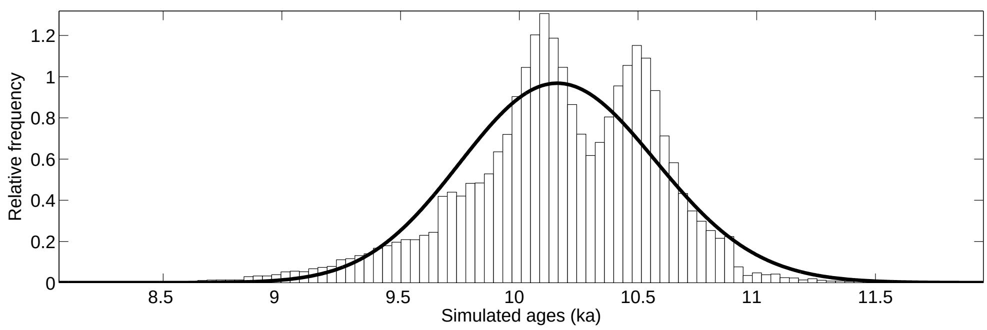

(xxix) North Head (2)

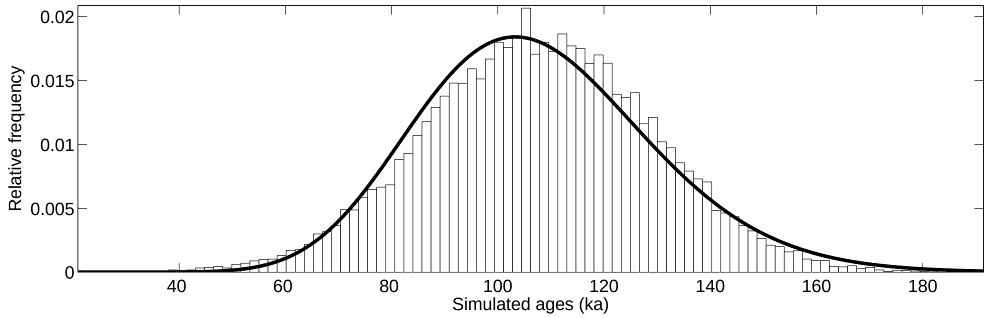

(xxx) One Tree Hill (3)

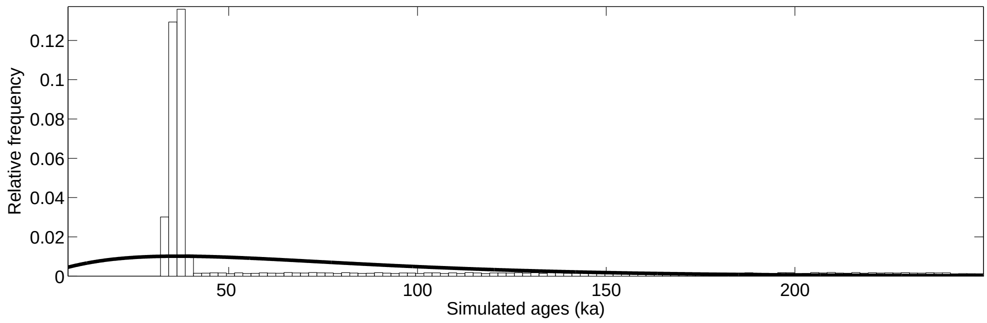

(xxxi) Onepoto Basin (6)

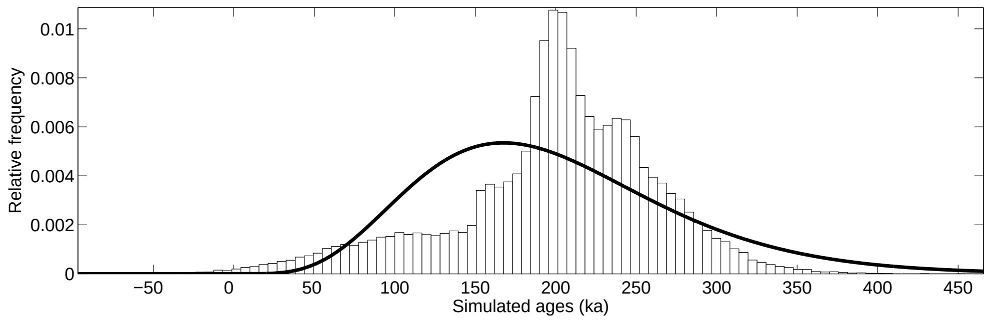

(xxxii) Orakei Basin (4)

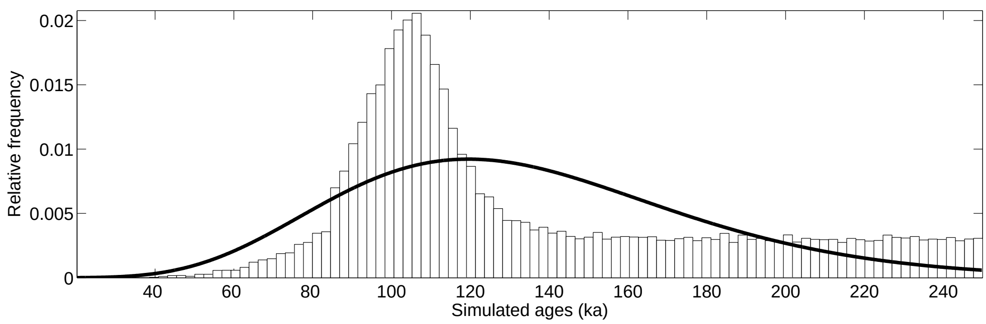

(xxxiii) Otara Hill (3)

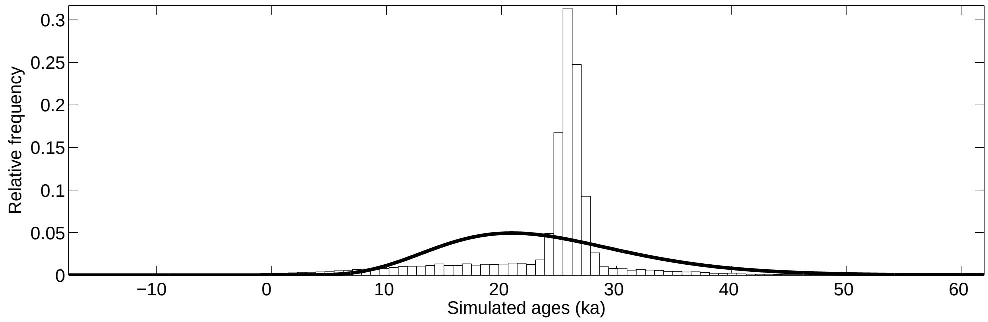

(xxxiv) Otuataua (2)

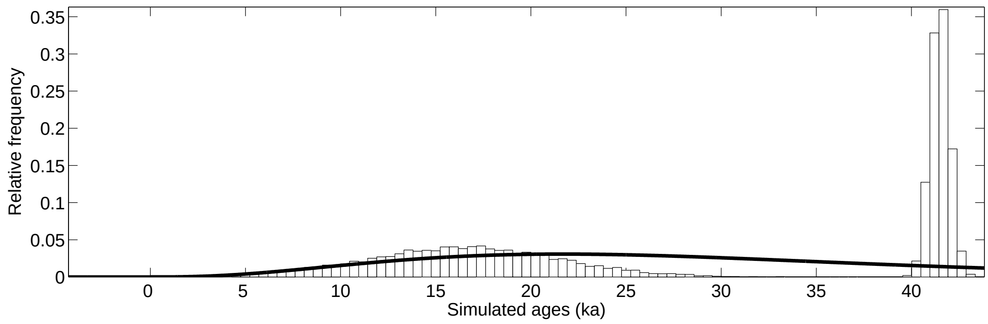

(xxxv) Panmure Basin (4)

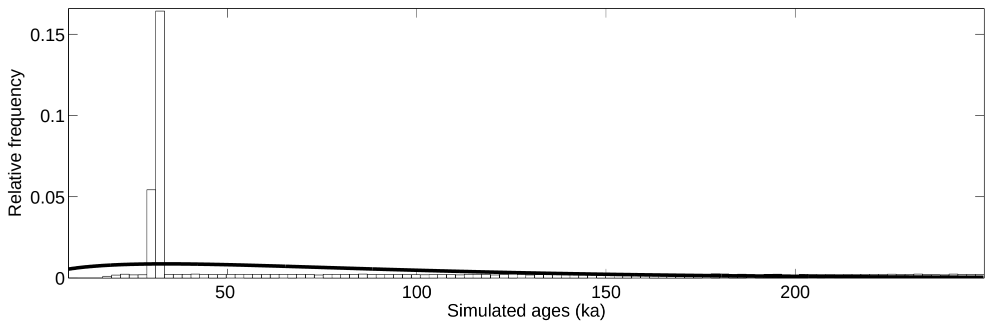

(xxxvi) Pigeon Mountain (1)

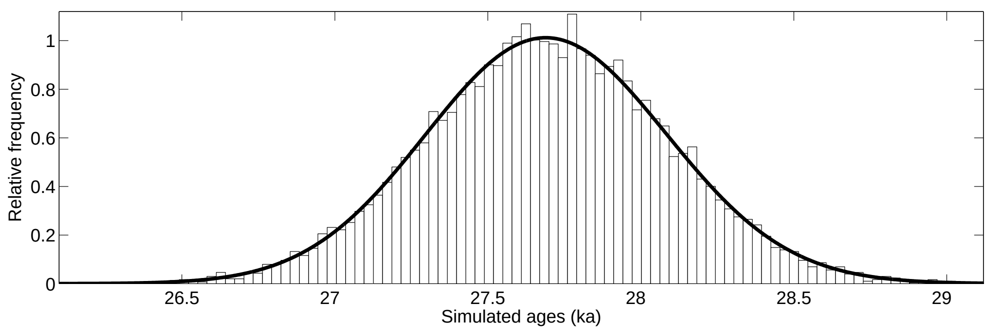

(xxxvii) Pukaki (5)

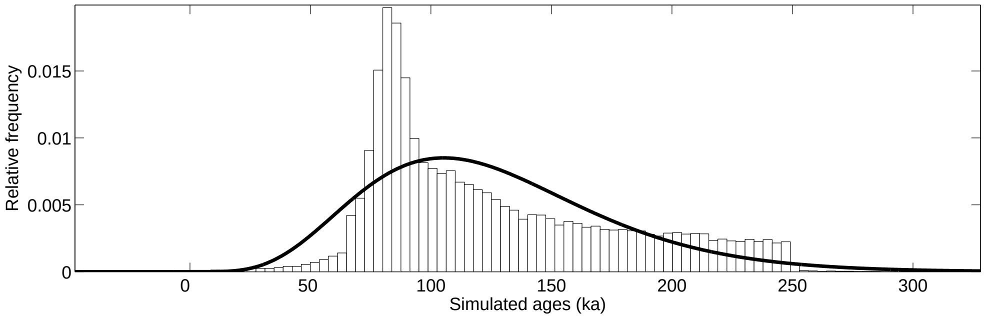

(xxxviii) Pukeiti (1)

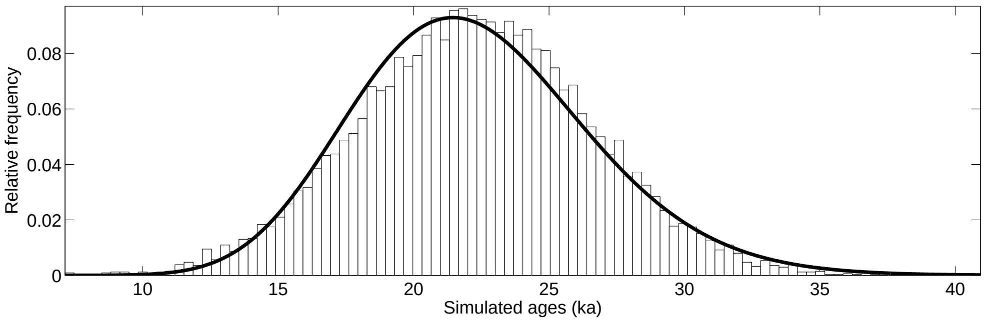

(xxxix) Puketutu (4)

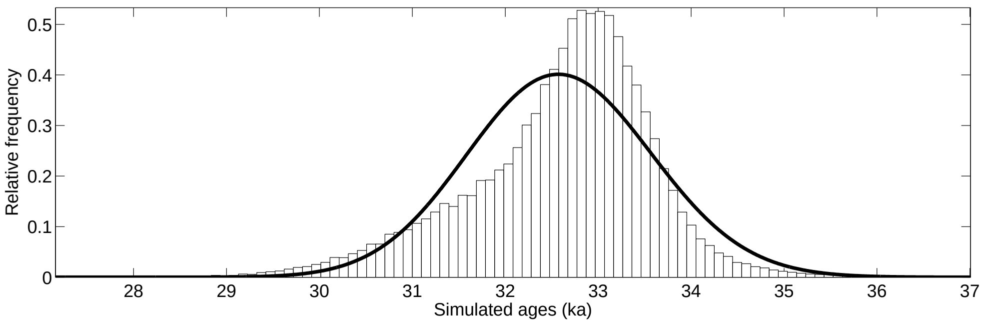

(xl) Pukewairiki (2)

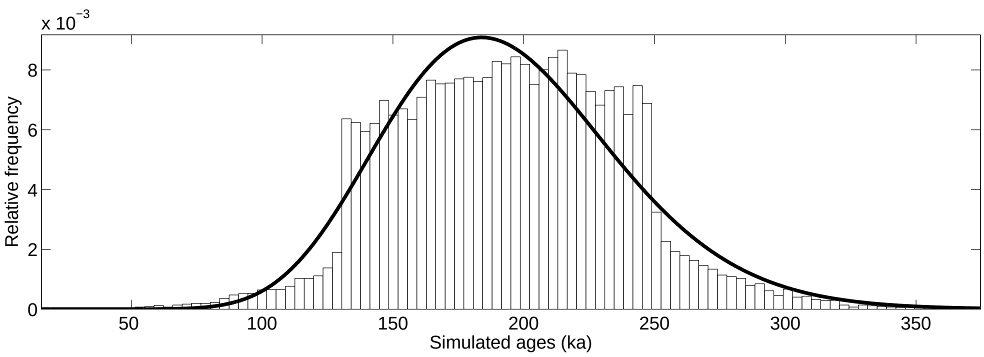

(xli) Purchas Hill (4)

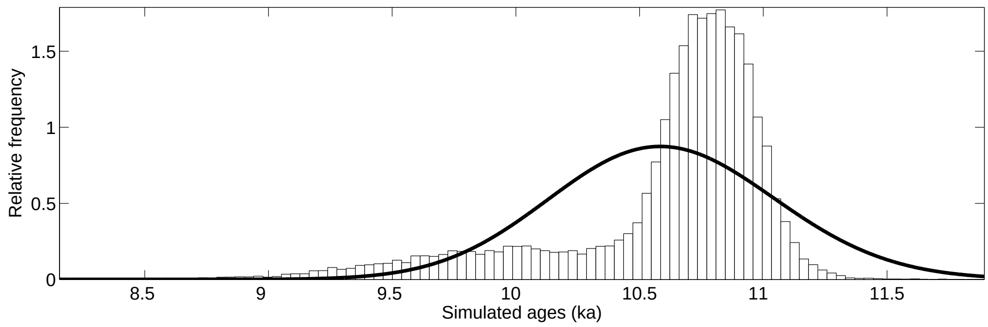

(xlii) Rangitoto (5)

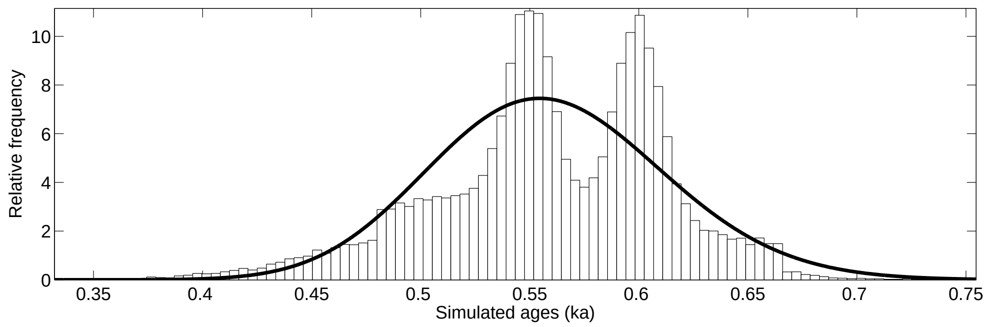

(xliii) Robertson Hill (2)

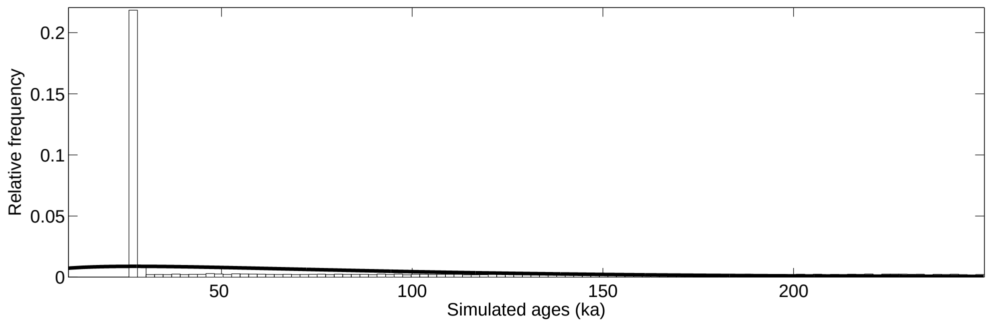

(xliv) St Heliers (4)

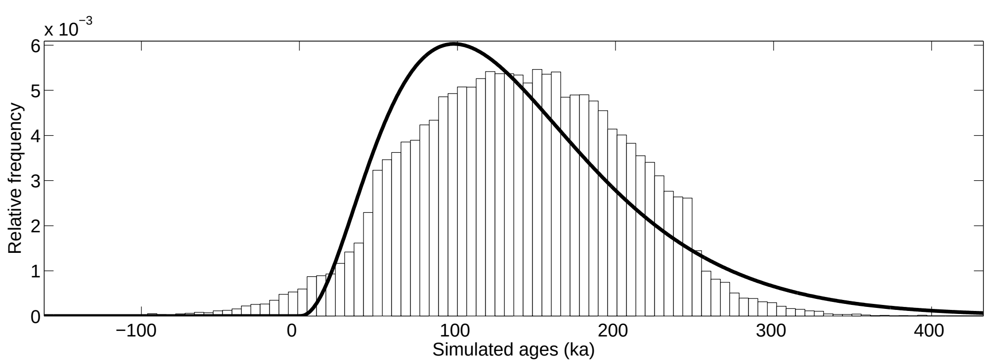

(xlv) Styaks Swamp (2)

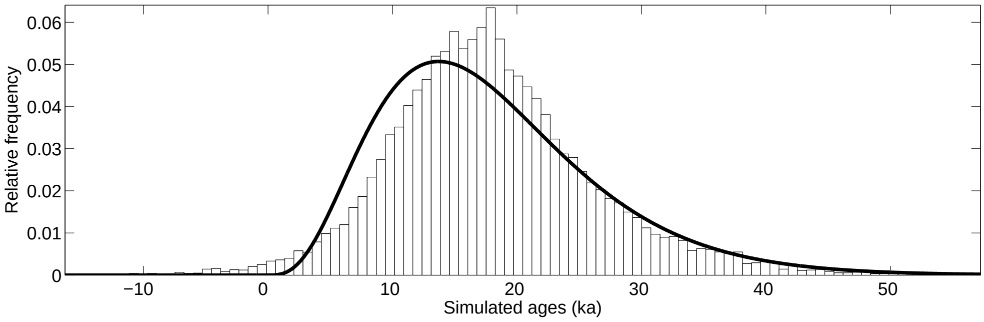

(xlvi) Tank Farm (3)

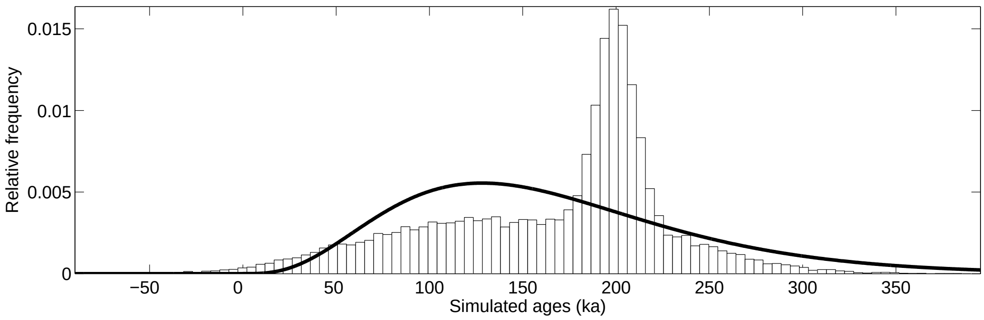

(xlvii) Taylors Hill (4)

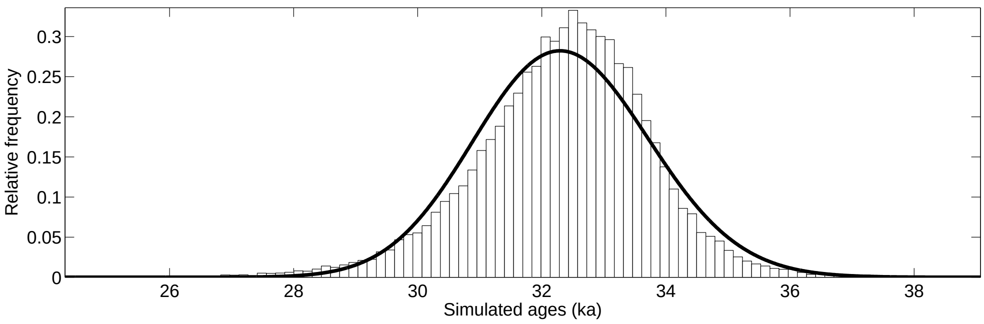

(xlviii) Te Pouhawaiki (2)

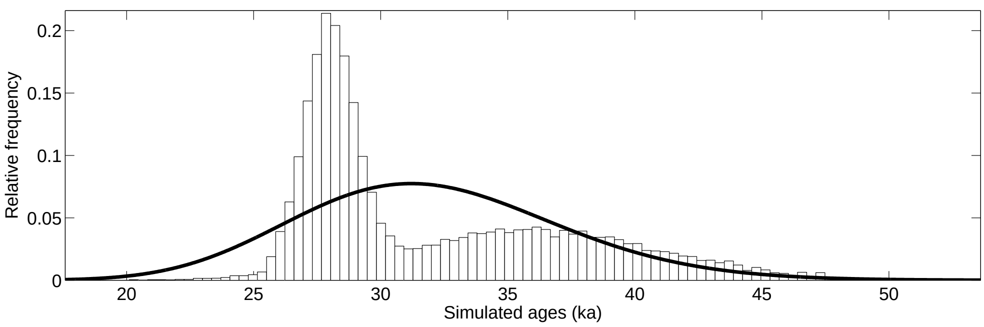

(xlix) Three Kings (4)

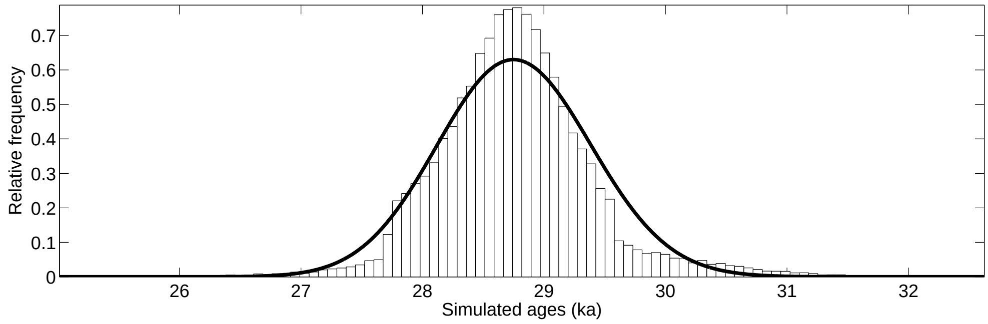

(l) Waitomokia (3)

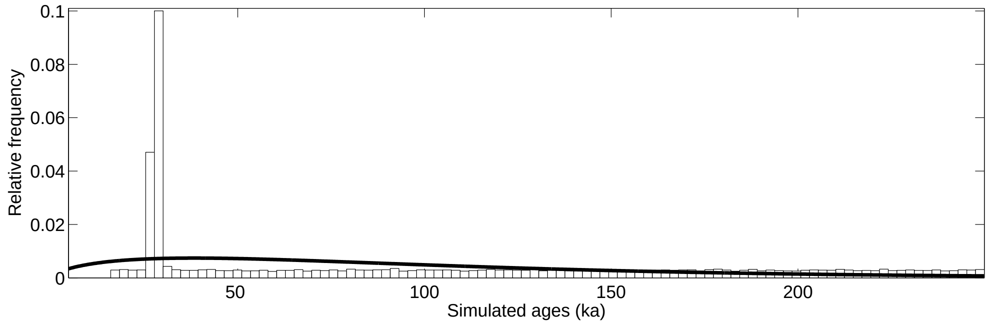

(li) Wiri Mountain (4)

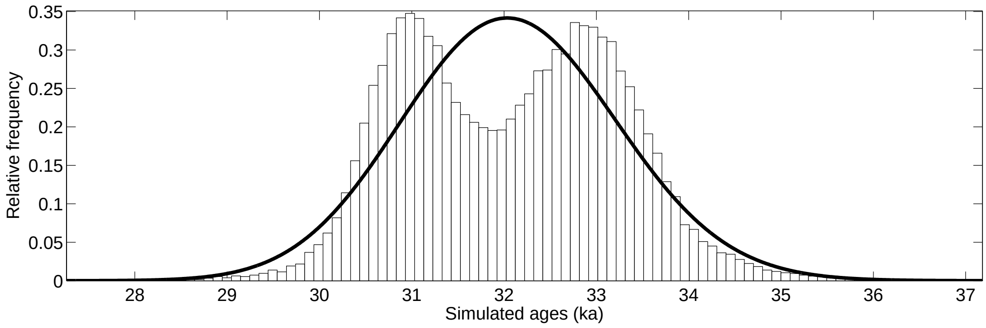

3. argon-argon (^{40}Ar/^{39}Ar) dating
4. paleomagnetic declination
5. optically stimulated luminescence (OSL) dating
6. thermoluminescence (TL) dating.

The reliability may change depending on the ages. The entire activity period of the AVF is divided into five age intervals, separating the last 60ka into three intervals of equal length due to the rapid improvement in the accuracy in some of these dating methods as the past becomes more recent and dividing the rest into two intervals, 60-120ka and 120-240ka.

Two questions were asked for each dating method and age interval (Figure 6.1). Each was rated on a five point Likert scale where 1 indicates unreliable and 5 indicates reliable. The first question was "If the dating method returns an age in the age interval, how reliable would you consider the returned age to be?" This question asks the expert to rate the reliability of the sample given its estimated age is in an age interval. This will be used as the prior for the reliability of the dating method. The second question is "If the true age is in the age interval, how reliable do you believe the dating method would be in returning that age?" This asks about the reliability of the dating method given that the true age is in an age interval. This will be used as initial points for the reliability posteriors when estimating the parameters.

The responses to the two questions are shown in stacked bar charts in Figure 6.3. The reliability of radiometric dating methods such as ^{14}C, K-Ar, and ^{40}Ar/^{39}Ar is time sensitive to the volcano and sample ages while the other methods such as paleomagnetic declination, OSL, and TL dating remain similar across all age intervals. Some experts struggled with the difference between the two questions. Figure 6.4 shows the strong correlation in their responses between the two questions, given the age interval and dating method. Most responses were perfectly correlated following on a straight, upward line and only a few deviate from the line. The common comment received from the experts was that the reliability of dating depends on the material and the time of dating. The latter means a sample that is dated today will be more reliable than the same sample that was dated 50 years ago.

6.3 Discussion

This chapter discusses a possible way to set up priors and initial points for a Bayesian age reconciliation model. One suitable model is based on a regular Bayesian approach using WinBUGS. However, currently due to the lack of consistent volcano age data available and the low response rate from the expert elicitation, no model is implemented in practice. In order to evaluate the reliability of age data the volcanoes can be correlated with the better dated tephras. Since the tephras have better age estimates, with tighter upper and lower limits provided by stratigraphy in the cores, the assigned volcanoes will have another good source of age estimates.

Figure 6.3: Stacked bar charts of the reliabilities of the dating methods. The left is the reliability of returned sample and the right is the reliability of returning the correct age.

(i) ^{14}C

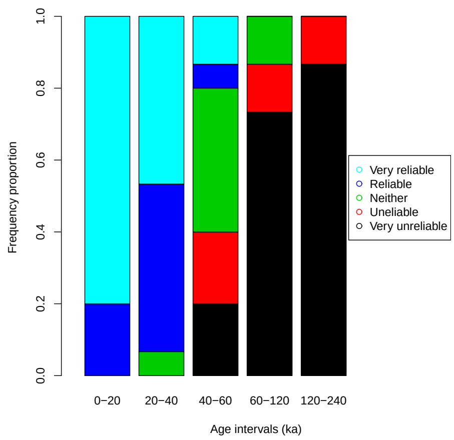

(ii) ^{14}C

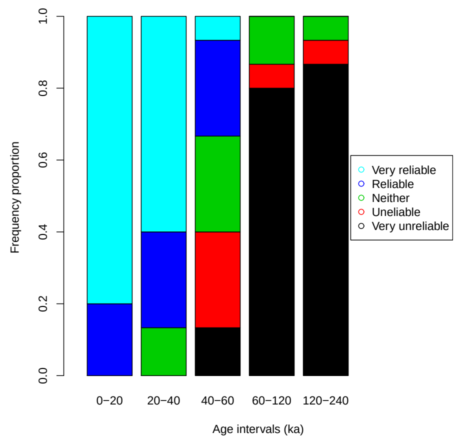

(iii) K-Ar

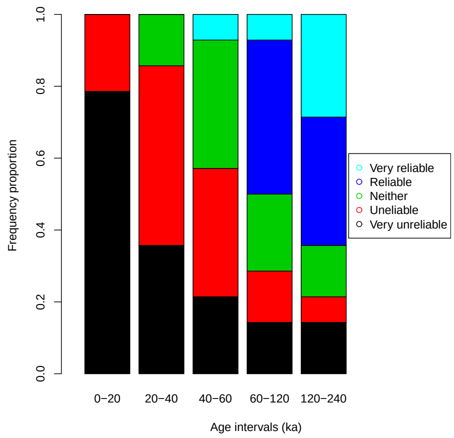

(iv) K-Ar

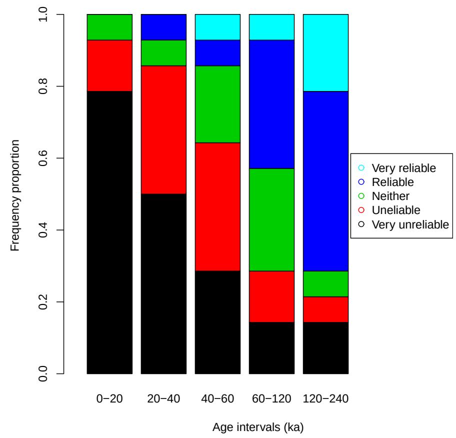

(v) ^{40}Ar/^{39}Ar

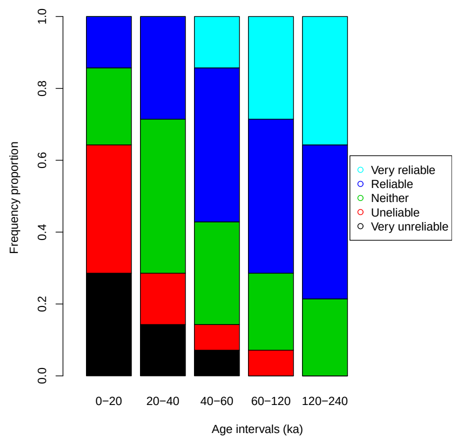

(vi) ^{40}Ar/^{39}Ar

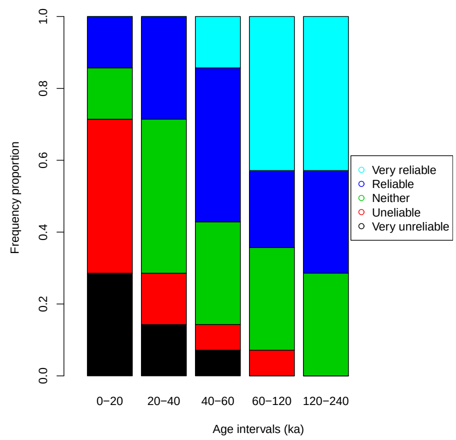

(vii) Paleomagnetic declination

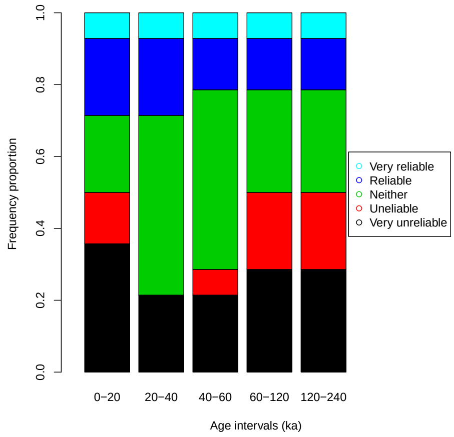

(viii) Paleomagnetic declination

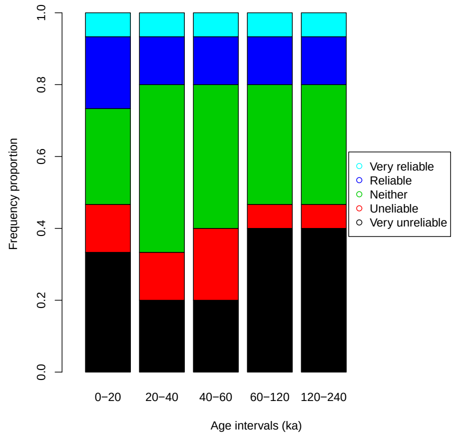

(ix) OSL

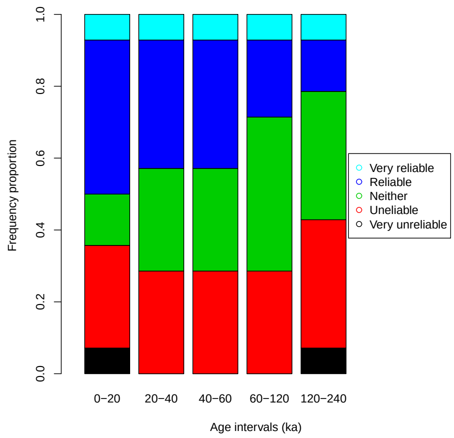

(x) OSL

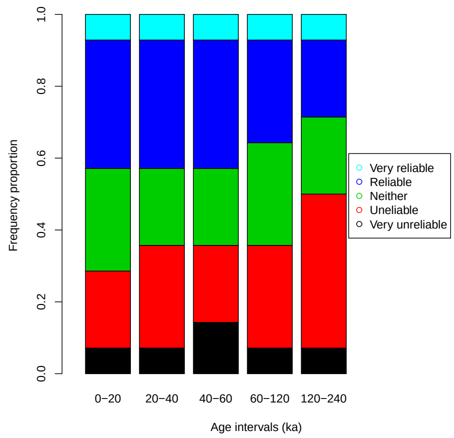

(xi) TL

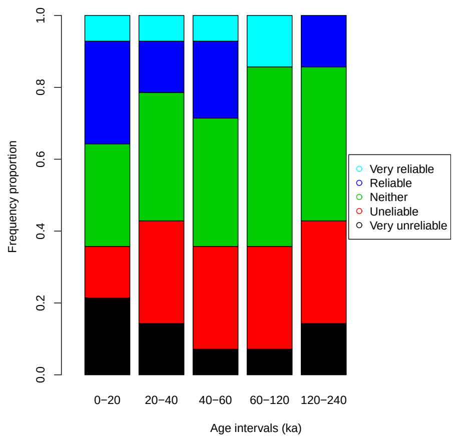

(xii) TL

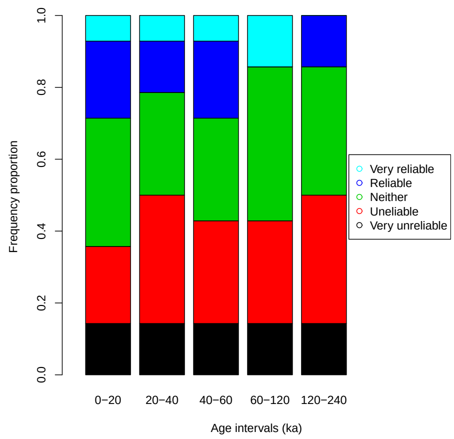

Figure 6.4: Scatterplots showing the correlation in the responses between the two reliability questions on the dating methods. Each dot represents a response from an expert.

(i) ^{14}C

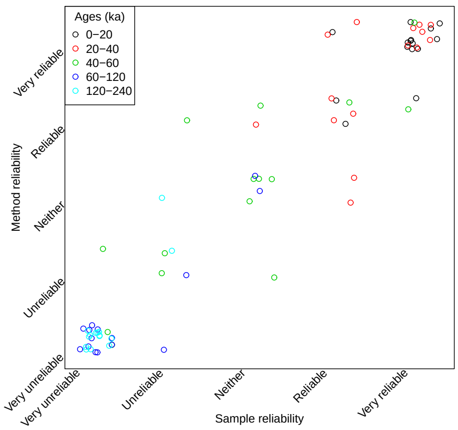

(ii) K-Ar

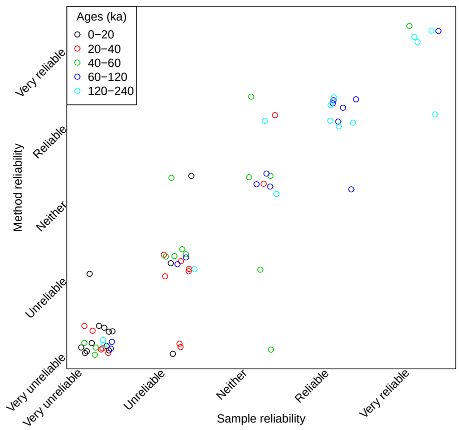

(iii) $^{40}Ar/^{39}Ar$

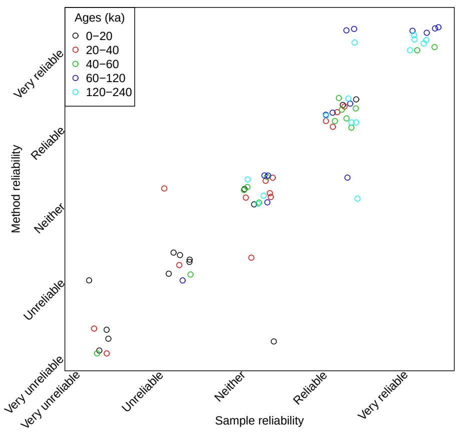

(iv) Paleomagnetic declination

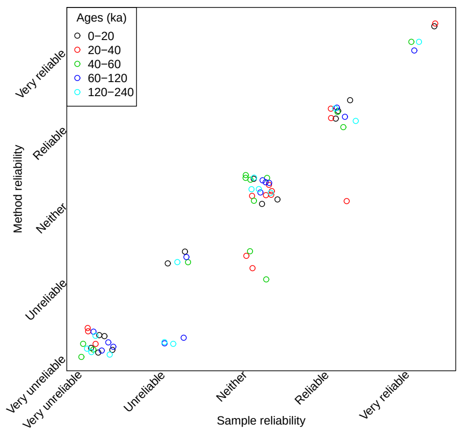

(v) OSL

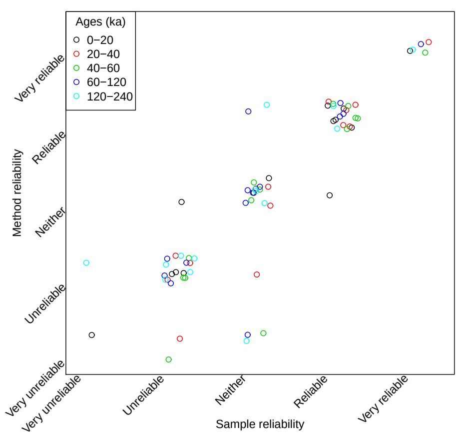

(vi) TL

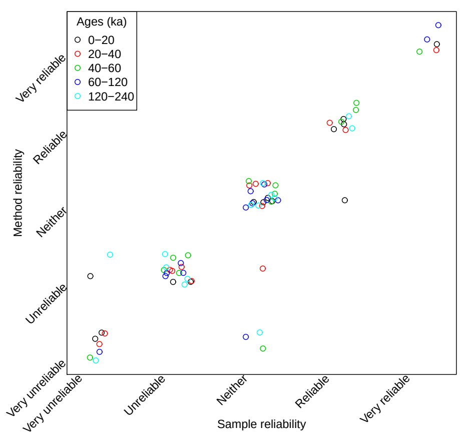

Chapter 7

Tephra ID matching

Work discussed in this chapter and Chapter 5 have been revised for Journal of Volcanology and Geothermal Research.

7.1 Introduction

Eruptions in volcanic fields are usually infrequent with a temporal rate of 10^{-4} to 10^{-6} eruptions per year (Connor and Conway, 2000) and since the next eruption will most likely occur at a new location, hazard estimation requires a spatial, as well as temporal, component. In particular, the estimation of spatial intensity is important for evacuation and land use planning purposes (Marzocchi and Bebbington, 2012). While the locations of many previous vent locations are usually available, the aim of estimating present day hazard is critically dependent on an assessment of any spatio-temporal dependence in the record. It is actively detrimental to have a forecast weighted towards past, rather than future, behaviour. Assessing such dependence requires a record of vent ages, not just locations. In order to avoid complicating factors such as multiple vent eruptions (Runge et al., 2014) or multiple eruption vents from a central volcano as at Jeju in South Korea, the (relatively) well-dated Auckland Volcanic Field (AVF) will be considered as an example.

To come up with an age-order model, the best possible volcanic record of times (Sections 5.2 and 5.3) and locations of past volcanic events (Figure 7.1) must be constructed. Partial records of these are available from five deposition locations within the field formed by maars (eruptive craters in-filled by sediment) (Section 5.4). However, there is no direct link between the deposit(s) and a particular source volcano. The direct unique correlations based on the chemical and geochemical aspects of the tephra deposits are made difficult by the non-uniqueness of magma composition in the individual volcanoes (Smith et al., 2008).

In this chapter, the improved attenuation model that explicitly provides a likelihood for thickness from a single eruption, discussed in Chapter 3, is used to calculate the likelihood of any combination(s) of source volcanoes and tephras. The single lobe model discussed in Section 3.4 is used to capture the single most dominant dispersal direction, due to only having at most five tephra deposits. Wind strength and direction was not estimated from the data for the same reason, though Section 7.3.2 discusses how they can be incorporated in the model. In order to include the contribution of the tephra and volcano ages into the likelihood, pseudo prior age distributions will be generated, by simulation, including stratigraphy.

The rhyolitic marker tephras as discussed in Section 5.4 are all well-dated from many locations outside the AVF, and thus can be used to further constrain some combinations of source(s) and tephra(s). The resulting age likelihood was combined with the spatial likelihood to form a likelihood function which will be used to produce the most statistically likely matching arrangement of the volcanoes and tephras through maximum likelihood estimation (MLE). The calculations required to maximise this likelihood function are performed in a linear programming framework. Since the tephras are better dated than the volcanoes we will thus improve the age estimates of the assigned volcanoes.

Figure 7.1: The Auckland Volcanic Field. The cored maars are indicated by circles and bold text. Volcanoes in italics were not considered as candidates in the matching procedure. Symbols scale with the cube root of the tephra volume.

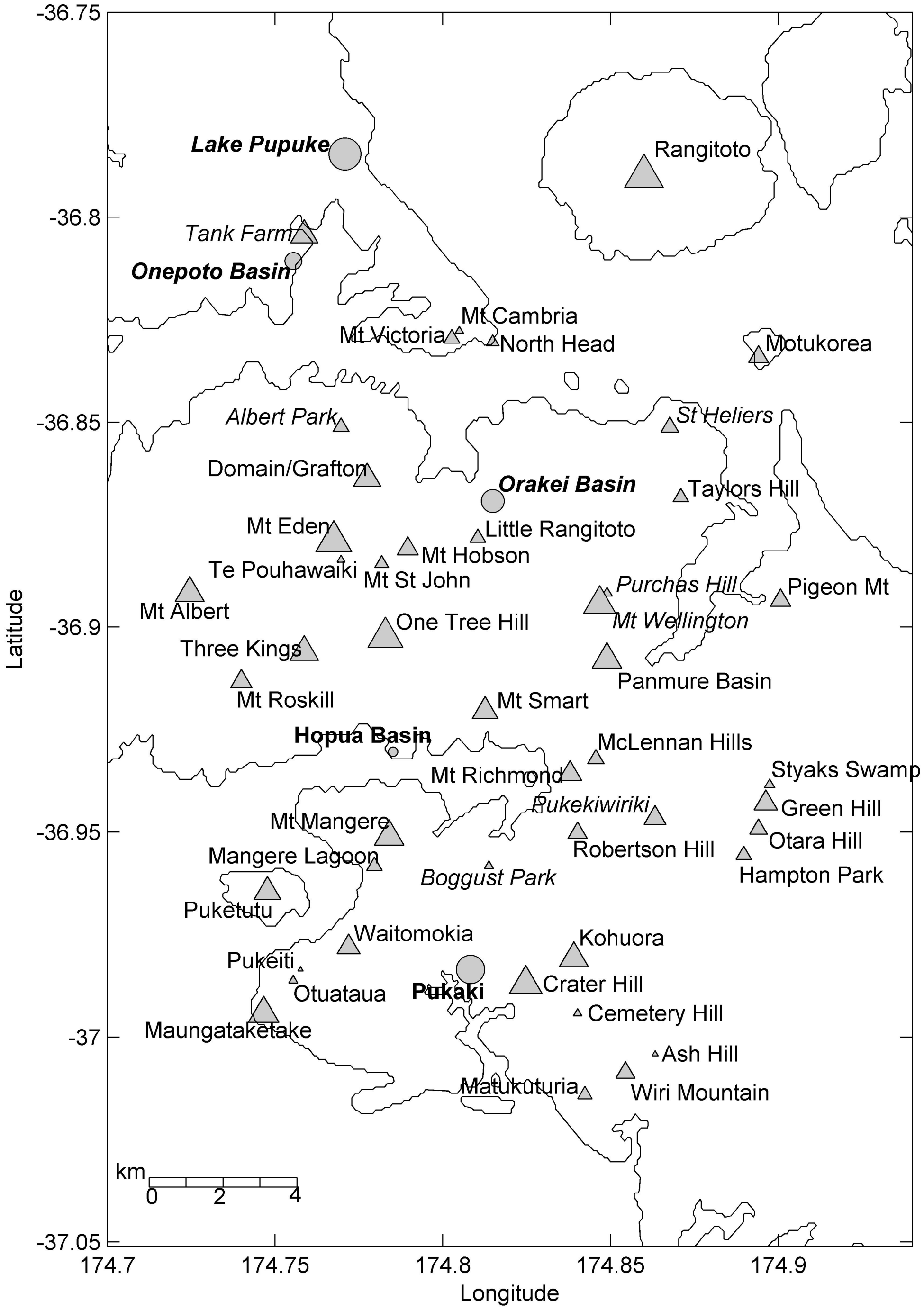

7.2 Other volcano data

In addition to data described in Chapter 5, Table 7.1 lists several other types of data, in particular the erupted volume and dispersal axis, relevant to our problem of constructing an age-order model. The probable wind direction ϕ (degrees anticlockwise from East) at the time of the eruption is identified by the highest point on the crater rims (Hayward, Murdoch and Maitland, 2011), where available.

A LiDAR survey-based digital surface model has been used to estimate the volume of scoria cones, tuff rings, and lava flows (Kereszturi et al., 2013). As distal tephra could not be measured, they used a regression relation between volume and vent diameter from Sato and Taniguchi (1997). However, this includes many points of high leverage with volumes many orders larger than those from the AVF, and is consequently inappropriate, as the linear relationship breaks down at smaller volumes. Although limitations and uncertainty exist for constructing an empirical function between tephra volume and tuff and scoria volumes, data from a number of well-studied small-scale eruptions (the 1959 Kilauea Iki (Richter et al., 1970), 1973 Heimaey (Self et al., 1974), 1977 Ukinrek Maars (Self et al., 1980), and 1256 AD Al-Madinah (Chapter 4) eruptions) suggest that the distal tephra volume can be estimated by

$$V^{\text{DRE}} = 0.5V_{\text{tuff}}^{\text{DRE}} + 1.5V_{\text{scoria}}^{\text{DRE}},$$

where V, V_{tuff}, and V_{scoria} are the bulk tephra, bulk tuff, and bulk scoria volumes (all measured in 10^6m^3), respectively. Dense rock equivalent (DRE) means the corrected volume by accounting for and removing the void space within the sample. Correcting from DRE to the bulk volumes relevant to thicknesses then results in the relation

$$\begin{aligned} V &= \frac{0.5 \times 0.83V_{\text{tuff}} + 1.5 \times 0.41V_{\text{scoria}}}{0.66} \\ &= 0.63V_{\text{tuff}} + 0.93V_{\text{scoria}}, \end{aligned} \tag{7.1}$$

Table 7.1: Wind directions (degrees anticlockwise from East) and volcano tephra volumes estimated from volcano tuff and scoria volumes ([a]Allen and Smith (1994) [b]Kereszturi et al. (2013)) using Equation 7.1.

Volcano	Wind direction (ϕ)	Bulk volume (10^6m^3) Tuff (V_{tuff})	Scoria (V_{scoria})	Tephra (V)
Ash Hill	10	0.25[a]		0.16
Cemetery Hill		0.66[b]		0.41
Crater Hill	160	28.01[b]	3.82[a]	21.17
Domain	0	19.33[a]	0.28[b]	12.42
Green Hill		1.71[a]	7.51[b]	8.07
Hampton Park	0	0.50[a]	1.99[b]	2.17
Hopua	0	1.47[b]		0.92
Kohuora		24.29[b]		15.27
Little Rangitoto			2.50[b]	2.33
Mangere Lagoon	30	3.37[b]	0.06[b]	2.18
Matukutureia		2.43[b]	0.49[b]	1.98
Maungataketake	330	20.93[b]	4.36[a]	17.23
McLennan Hills	270	2.00[b]	1.86[b]	2.99
Motukorea	60	3.13[b]	2.87[b]	4.64
Mt Albert	350	1.67[a]	15.13[b]	15.15
Mt Cambria	45		0.49[b]	0.45
Mt Eden	280		29.72[b]	27.7
Mt Hobson	350		6.00[b]	5.59
Mt Mangere	270		16.55[b]	15.42
Mt Richmond	350	5.57[b]	3.80[b]	7.04
Mt Roskill	180	0.08[a]	6.87[b]	6.45
Mt Smart	270		11.72[b]	10.92
Mt St. John	350		2.00[b]	1.87
Mt Victoria			2.88[b]	2.69
North Head		2.00[a]	0.18[b]	1.43
One Tree Hill	0		28.52[b]	26.57
Orakei Basin	315	17.97[b]		11.3
Otara Hill		0.53[a]	3.49[b]	3.58
Otuataua	120		0.53[b]	0.5
Panmure Basin	20	22.12[b]	1.50[b]	15.31
Pigeon Mountain	70	6.33[a]	1.38[b]	5.27
Pukaki	45	33.82[b]		21.27
Pukeiti	315		0.12[b]	0.12
Puketutu	110	14.30[a]	2.39[b]	11.22
Roberston Hill	340	4.81[b]	1.20[a]	4.14
Styaks Swamp	320	1.17[a]		0.74
Taylors Hill	290	2.23[a]	0.91[b]	2.25
Te Pou Hawaiki			0.40[a]	0.37
Three Kings			15.02[b]	14
Waitomokia	280	10.95[b]	0.54[a]	7.39
Wiri Mountain	45	0.40[a]	4.32[a]	4.28

as shown in Table 7.1. Here bulk distal tephra and scoria are assumed to contain 34 and 59% void space, respectively (Kereszturi et al., 2013). Bulk tuff has at least 1% void space (Kereszturi et al., 2013), and is denser than bulk distal tephra; the midpoint of 17% is used here, but later results are not sensitive within the range.

7.3 Age-order model

We have 22 AVF tephras that need to be uniquely assigned to one of the 51 AVF volcanoes. Since the age of the oldest AVF tephra in the maars is only some 70,000 years, many of the volcanoes can be eliminated from consideration before matching to the tephras. In addition to Grafton, a further 11 volcanoes can be eliminated from consideration; the age of Lake Pupuke is estimated to be 207 ± 6ka (Cassata et al., 2008); Albert Park is considered very old on the basis of geomorphology (Searle, 1962); Pukewairiki is older than 130,000 years (Lindsay and Leonard, 2009); Boggust is at least 130ka as it was breached during the last interglacial (Hayward, Kenny and Grenfell, 2011*a*); St Heliers is much older than 45ka on the basis of geomorphology (Lindsay and Leonard, 2009); Onepoto Basin and Orakei Basin contain AVF 1 and thus must be older than AVF 1; and Tank Farm is the same or older than Onepoto Basin (Lindsay et al., 2011). These eight volcanoes are thus considered too old for any of the AVF tephras. However, Orakei Basin will be included in the model to limit the upper age of Little Rangitoto as indicated by Table 5.2. The two youngest AVF tephras are known to correspond to Rangitoto and Mt Wellington; Rangitoto is assigned to the youngest tephra AVF 22 since it is known to have happened around 0.7ka (Molloy et al., 2009). Similarly Mt Wellington is assigned to AVF 21 (Molloy et al., 2009; Bebbington and Cronin, 2011). As Purchas Hill is only slightly older than Mt Wellington (Lindsay and Leonard, 2009) at around 10.9ka or contemporaneous to Mt Wellington (AVF 21), it is too young to correspond to AVF 20 or any older tephras. This leaves 41 volcanoes (the remaining 40 and Orakei Basin) to be considered to be matched to the 20 AVF tephras.

Now the aim is to find the most statistically likely arrangement which matches each tephra to a unique volcano through MLE. A likelihood function for matching the 41 volcanoes and 20 tephras will be constructed to evaluate the tephra locations and ages of the tephras and volcanoes. To do this two things need modelling: the attenuation of tephra thickness with distance and direction, and the complexity and interdependence of the volcano and tephra age distributions.

7.3.1 Likelihood equation

First the notations used in Sections 7.3.1-7.3.5 are summarised in Table 7.2.

Table 7.2: Notations for the age-order model.

Notation	Definition
V_i	Tephra volume (10^6m^3) for the ith volcano
ϕ_i	Wind direction (degrees anticlockwise from East) for the ith volcano
T_{jk}	Observed tephra thickness (cm) for the jth AVF tephra at Maar k
r_{ik}	Distance (km) between Volcano i and Maar k
ξ_{ik}	Direction (degrees) from Volcano i to Maar k
$\hat{T}_{ik}$	Estimated tephra thickness (cm) for the ith volcano at Maar k
γ_i	Constraint to fix volume at estimated value for the ith volcano
α, βU	Constant attenuation parameters for column height and wind speed
s_i^n	Generated pseudo prior age for Volcano i for the nth iteration
(μ_j, σ_j^2)	Normal age (ka) of the jth AVF tephra
$(\mu_{j^*}, \sigma_{j^*}^2)$	Normal age (ka) of the j^*th named marker tephra
C_k	Uncensored period of Maar k
P_{ij}	Proportion of the 10,000 runs where Volcano i is assigned to AVF tephra j

For each nth iteration, the likelihood function for evaluating each pair of Volcano i and AVF tephra j is

$$\log L_{ij}^n = \begin{cases} \sum_{k=1}^5 \log u_{ijk}(T_{jk}) + \log f_j^n(s_i^n) + \sum_{j^*=1}^{10} \log g_{j,j^*}^n(s_i^n) & \text{if } j = 1, \dots, 20 \\ \sum_{k=1}^5 \log v_{ik}^n(T_{jk}) & \text{if } j = 0 \end{cases}, \tag{7.2}$$

where $j^* = 1, \dots, 10$ (oldest to youngest) denotes the number of marker tephras between AVF 1 and 20 as shown in Table 5.3. The term u_{ijk} is the likelihood of AVF eruption

j depositing a thickness T_{jk} at location k if the source were i, f_j is the likelihood of Volcano i erupting at the time consistent with when AVF tephra j was deposited, g_{j,j^*} is the likelihood of Volcano i and AVF tephra j both being younger/older than Marker Tephra $j*$, given the stratigraphy of the marker and AVF tephras in the cores, and v_{ik} is the likelihood of Volcano i not depositing any tephra at Maar k. The terms u_{ijk} and v_{ik} are summed over all maars k while g^n_{j,j^*} is summed over all marker tephras j^* to obtain the likelihood for each i and j pair. Each component of Equation 7.2 is discussed in Sections 7.3.2 and 7.3.3.

7.3.2 Tephra attenuation model

The likelihood of Volcano i producing the observed thickness of tephra j, T_{jk}, given the locations of Volcano i and Maar k, u_{ijk}, depends on the amount of observed tephra thickness T_{jk} and whether or not Maar k is censored at that age. The observed thicknesses $T_{jk} > 0$ indicates that some tephra was observed at an uncensored maar k. Then the likelihood is the probability of observing $\hat{T}_{ik}$ given the observed thickness T_{jk} obtained from a lognormal probability density function. When no tephra is observed at an uncensored Maar k ($T_{jk} = 0$) we treat it as $T_{jk} < 0.05$cm. When Maar k is censored and there is no possibility of finding any tephra ($T_{jk} =$ NA), we set $u_{ijk} = 1$ as a mathematical convenience. The likelihood function thus becomes

$$u_{ijk}(T_{jk}) = \begin{cases} \frac{1}{T_{jk}\sqrt{2\pi\sigma_N^2}} \exp\left[-\frac{(\log T_{jk} - \mu_{N_{ik}})^2}{2\sigma_N^2}\right] & \text{if } T_{jk} > 0.05 \\ \frac{1}{\sqrt{2\pi\sigma_N^2}} \int_0^{0.05} \frac{1}{t} \exp\left\{-\frac{[\log(t) - \mu_{N_{ik}}]^2}{2\sigma_N^2}\right\} \mathrm{d}t & \text{if } 0 \leq T_{jk} \leq 0.05 \\ 1 & \text{if } T_{jk} = NA \end{cases}, \tag{7.3}$$

where $\mu_{N_{ik}} = \log(\hat{T}_{ik}) - \sigma_N^2/2$ and $\sigma_N = \sqrt{\log\{(\mathrm{CV})^2 + 1\}}$. The coefficient of variation is set at CV = 0.5 again following the Heimaey eruption example (Chapter 3). Note that the higher CV (cf. Ukinrek example in Section 4.4) allows for the possibility of multiple lobes.

The ideal (i.e., without sampling error) tephra thickness $\hat{T}_{ik}$ (cm) at each maar location

k given the location of the source volcano i and the appropriate parameters in the attenuation model can be described by the semiempirical model (Gonzlalez-Mellado and De la Cruz-Reyna (2010), Section 3.4)

$$\hat{T}_{ik}(r_{ik}, \xi_{ik}) = \gamma_i \exp\{-(\beta U)_i r_{ik}[1 - \cos(\xi_{ik} - \phi_i)]\} r_{ik}^{-\alpha_i}, \tag{7.4}$$

where Maar k lies at a distance r_{ik} (km) and azimuth ξ_{ik} from Volcano i, which has an observed wind direction ϕ_i as shown in Table 7.1. If Volcano i has no observed wind direction, then $\beta U = 0$ in Equation 7.4 yielding a symmetric power law decay model (Pyle, 1989; Bonadonna et al., 1998)

$$\hat{T}_{ik}(r_{ik}, \xi_{ik}) = \gamma_i r_{ik}^{-\alpha_i}. \tag{7.5}$$

Equation 7.4 produces elliptic isopachs while Equation 7.5 produces radially symmetric deposits around the vent (circular isopachs).

The constant γ_i is the thickness at 1km from the source on the dispersal axis, which will be determined so that the tephra volume V_i matches that in Table 7.1. γ_i is determined by:

$$\begin{aligned} \gamma_i &= \frac{V_i}{\int_{r \in R} \hat{T}_{ir} \, \mathrm{d}r} \\ &\approx \frac{10,000 V_i}{\sum_{r \in R} \hat{T}_{ir}}, \end{aligned}$$

where R is a 20km radius circle, excluding a 0.1km radius circle, around the vent, divided into a uniform grid with 0.1km spacing. The differences in the units yield 10,000 in the numerator.

Due to insufficient data, the eruptive column height represented by α_i (smaller α indicates a higher column), and the product of diffusivity and wind speed $(\beta U)_i$ are treated as constant across all volcanoes. Since there can be at most five data points for each eruption there is not enough data to estimate all of these parameters. Although there is risk involved in using a similar eruption to estimate the parameters, this will be overcome by trialling a range of values for α and βU (henceforth 'environmental conditions') informed by the 1973 Heimaey eruption (Self et al., 1974) which was similar to the AVF eruptions in terms of eruption style and size. Based on $\alpha \approx 1.9$ for the Heimaey eruption (Section 3.5) $\alpha \in \{1.5, 2, 2.5\}$ will be considered, constant for all eruptions. As the average wind speed in the AVF can be supposed to have been about half of the 60km/h that was recorded at Heimaey (Self et al., 1974), i.e., $\beta U \approx 1.5$ (Section 3.5), thus $\beta U \in \{0.5, 1\}$ will be considered.

To evaluate u_{ijk} given the locations of Volcano i and Maar k, requires an error distribution for the spatial deposit of the tephra. A lognormal distribution ($T \sim$ lognormal (μ_N, σ_N)) is used (cf. Rhoades et al. (2002)) for our AVF tephras because of their overdispersed thicknesses. See Chapters 3 and 4 for more discussion.

Since we have 41 volcanoes and only 20 AVF tephras, only 20 volcanoes will be assigned to a tephra and the remaining 21 volcanoes (one of which will be Orakei Basin) will be unassigned. Intuitively, large eruptions are more likely to deposit tephra and hence be assigned to a tephra. So if a large volume volcano is unassigned it should be penalised more than a small volume volcano, all other things being equal. The likelihood function for Volcano i not depositing any observed tephra at Maar k is

$$v_{ik}^n(T_{jk}) = \begin{cases} \frac{1}{\sqrt{2\pi\sigma_N^2}} \int_0^{0.05} \frac{1}{t} \exp\left\{-\frac{[\log(t)-\mu_{N_{ik}}]^2}{2\sigma_N^2}\right\} \mathrm{d}t & \text{if } s_i^n \in C_k \\ 1 & \text{otherwise} \end{cases}, \tag{7.6}$$

where s_i^n is the generated pseudo prior age for Volcano i from the nth iteration and C_k is the uncensored period of Maar k and $\mu_{N_{ik}}$ and σ_N are evaluated in the same way as for Equation 7.3. Equation 7.6 depends on whether Maar k is censored at the time of the eruption s_i^n to observe any tephra. If Maar k became uncensored before the eruption $s_i^n \in C_k$ then the maar could have observed some tephra from the volcano. But 21 unassigned volcanoes did not leave enough tephra to be observed. The likelihood function penalises each of the volcanoes for their non-zero estimated tephra thickness

$\hat{T}_{ij}$ at the uncensored maars. At a censored maar there is no penalty for not observing tephra, in which case we set $v_{ik}^n = 1$.

7.3.3 Age model

The spatial likelihood function using the attenuation model is heavily influenced by the volcano volumes. Volcanoes with large volumes are more likely to be assigned to the tephras regardless of their age compatibility. However it is unreasonable to link a pair when their ages are very different. In order to evaluate the temporal likelihood of any pair of volcano and tephra we need age distributions for the volcanoes and tephras. To do this requires constructing prior age distributions for the volcanoes from the available record of determined volcano ages and errors and stratigraphy.

To account for the temporal aspect, the temporal component will be included in our likelihood function as,

$$f_j^n(s_i^n) = \frac{1}{\sqrt{2\pi\sigma_j^2}} \exp\left[-\frac{(s_i^n - \mu_j)^2}{2\sigma_j^2}\right],$$

where μ_j and σ_j are the parameters of the normally distributed AVF tephra ages from Table 5.3 and s_i^n is the generated volcano age, treated here as data. This probability density of the volcano ages is treated as the likelihood.

Even if a pair of a tephra and a volcano have similar age estimates, if they are on different sides (older/younger) of a marker tephra they may be unlikely to be a match. The likelihood of Volcano i being on the correct side of Marker Tephra j^* given the stratigraphy of j^* and AVF j from the cores is evaluated as

$$g^n_{j,j^*}(s^n_i) = \begin{cases} Pr(j^* < s^n_i) & \\ \quad = \frac{1}{\sqrt{2\pi\sigma^2_{j^*}}} \int_{-\infty}^{s^n_i} \exp\left[-\frac{(t-\mu_{j^*})^2}{2\sigma^2_{j^*}}\right] \mathrm{d}t & \text{if AVF } j \text{ older than } j^* \\ Pr(j^* > s^n_i) & \\ \quad = 1 - \frac{1}{\sqrt{2\pi\sigma^2_{j^*}}} \int_{-\infty}^{s^n_i} \exp\left[-\frac{(t-\mu_{j^*})^2}{2\sigma^2_{j^*}}\right] \mathrm{d}t & \text{otherwise} \end{cases},$$

where μ_{j^*} and σ_{j^*} are the parameters of the normally distributed marker tephra ages from Table 5.3. The stratigraphy in the cores tell us if the AVF tephra is older or younger than the marker tephra.

To generate the volcano ages s^n_i, the age data in Tables 5.1 and 5.2 and the information about the excursions are used to compile a list of candidate age distributions for the 41 volcanoes (the remaining 40 and Orakei Basin) (Table 7.3). Where there is no minimum age limit 1ka is assumed because all volcanoes must be older than Rangitoto at around 0.7ka (Molloy et al., 2009). If there is no maximum age limit 250ka is assumed as the beginning of the AVF (Shane and Hoverd, 2002). These prior distributions were formulated conservatively so all possible ages are covered.

For a normally distributed candidate age distribution it is simply generated from a normal distribution with its given parameters. Similarly a uniform distribution is generated for a volcano with a uniform candidate age distribution. Since the Mono Lake excursion lasted approximately at most 1,000 years (Cassidy, 2006) and Taylors Hill occurred at a slightly different time to the others (Cassidy and Hill, 2009), we will interpret this to mean that Taylors Hill has to be the first or the last of the five eruptions and the time between the first and last Mono Lake eruptions must be at most 1,000 years. Without reliable age determinations Mt Richmond is assigned to be somewhere within two standard deviations of the Mono Lake excursion (i.e., 31.3-33.5ka). Taylors Hill is a special case in that its candidate age distribution is bimodal as it could be at the beginning or the end of the Mono Lake excursion (Cassidy and Hill, 2009). Since the centre of the 1,000-year-long Mono Lake excursion is estimated to be 32.4 ± 0.3ka

(Singer, 2007) the estimated Mono Lake excursion is 31.9-32.9ka. This means Taylors Hill should be centred either at 31.9 or 32.9ka (with error 300 years) with equal probability. To achieve this a normal distribution (31.9, 0.3^2) is generated for the end of the excursion and add 1,000 years to the generated age of Taylors Hill 50% of the time. If a pair of volcanoes are contemporaneous they are assumed to have erupted within 100 years of each other, and so first one of the ages is generated, then add, depending on stratigraphy, a $\mathrm{U}(-0.1, 0.1)$ or $\mathrm{U}(0, 0.1)$ variate to obtain the other. For instance, Hampton Park is generated from normal (26.6, 8^2) and Otara Hill, thought to be contemporaneous to Hampton Park, should always be within 100 years of it. So a possible age for Hampton Park is generated first. Then a uniform distribution $(-0.1, 0.1)$ is generated and added it to Hampton Park's pseudo prior age for Otara Hill.

Now a prior age can be generated for each volcano from the age distributions presented in Table 7.3. When a set of 41 volcano ages is generated these ages must be ensured to be feasible using the stratigraphy, magnetic excursion, and tephra conditions. In addition, there must be enough volcano ages in a given age range (between each set of marker tephras) to match the number of observed AVF tephras (see below). If the set satisfies all of these conditions the whole set of ages is considered as one feasible sequence of volcano ages. This procedure is repeated 10,000 times ($n = 1, \ldots,$ 10,000) to get 10,000 possible such sequences. Thus 10,000 replications of a sequence of volcano ages will be produced, each of which is a valid arrangement. Note that the means of the volcano ages may not themselves be a valid arrangement. For each n, s_i^n is defined to be the generated pseudo prior age for volcanoes ($i = 1, \ldots, 41$) where the volcanoes are sorted in the chronological order of their pseudo prior ages. This means that the corresponding volcano for each i will differ for each replication n. This ordering only becomes relevant in Section 7.3.4.

Each set of ages must follow all of the following stratigraphy and excursion conditions:

- If the stratigraphy of a pair of volcanoes is known then the ages must be in the correct order.

Table 7.3: Prior age distributions for each vent in the AVF, obtained from the available age determinations (Section 5.2). Where the age is given as an addition to that of another volcano these are the contemporaneous events.

Volcano	Prior age distribution (ka)
Ash Hill	$\sim \mathrm{N}(31.8, 0.16^2)$
Cemetery Hill	$\sim \mathrm{U}(0, 0.1)+$ Crater Hill
Crater Hill	$\sim \mathrm{N}(33.3, 0.6^2)$
Domain	$\sim \mathrm{U}(60, 250)$
Green Hill	$\sim \mathrm{N}(19.827, 8.98^2)$
Hampton Park	$\sim \mathrm{N}(26.6, 8^2)$
Hopua	$\sim \mathrm{U}(29, 33)$
Kohuora	$\sim \mathrm{N}(34, 0.3^2)$
Little Rangitoto	$\sim \mathrm{U}(1, 120)$
Mangere Lagoon	$\sim \mathrm{U}(21, 250)$
Matukutureia	$\sim \mathrm{U}(1, 34)$
Maungataketake	$\sim \mathrm{N}(39.99, 0.53^2)$
McLennan Hills	$\sim \mathrm{N}(42.6, 3.8^2)$
Motukorea	$\sim \mathrm{U}(7, 250)$
Mt Albert	$\sim \mathrm{U}(30, 250)$
Mt Cambria	$\sim \mathrm{U}(-0.1, 0.1)+$ Mt Victoria
Mt Eden	$\sim \mathrm{N}(28.39, 0.345^2)$
Mt Hobson	$\sim \mathrm{U}(1, 30)$
Mt Mangere	$\sim \mathrm{N}(21.94, 0.395^2)$
Mt Richmond	$\sim \mathrm{U}(31.9 - 2 * 0.3, 32.9 + 2 * 0.3)$
Mt Roskill	$\sim \mathrm{U}(27, 250)$
Mt Smart	$\sim \mathrm{U}(10, 23)$
Mt St. John	$\sim \mathrm{U}(27, 250)$
Mt Victoria	$\sim \mathrm{U}(1, 250)$
North Head	$\sim \mathrm{U}(1, 250)$
One Tree Hill	$\sim \mathrm{U}(29, 250)$
Orakei Basin	$\sim \mathrm{U}(83, 120)$
Otara Hill	$\sim \mathrm{U}(-0.1, 0.1)+$ Hampton Park
Otuataua	$\sim \mathrm{U}(-0.1, 0)+$ Maungataketake
Panmure Basin	$\sim \mathrm{N}(31.73, 0.17^2)$
Pigeon Mountain	$\sim \mathrm{U}(1, 250)$
Pukaki	$\sim \mathrm{U}(65, 250)$
Pukeiti	$\sim \mathrm{U}(38, 250)$
Puketutu	$\sim \mathrm{N}(33.6, 3.7^2)$
Roberston Hill	$\sim \mathrm{N}(29.9, 0.6^2)$
Styaks Swamp	$\sim \mathrm{U}(1, 125)$
Taylors Hill	$\sim \mathrm{N}(31.9, 0.3^2) + \mathrm{Bern}(0.5)$
Te Pouhawaiki	$\sim \mathrm{U}(27, 250)$
Three Kings	$\sim \mathrm{N}(28.59, 0.381^2)$
Waitomokia	$\sim \mathrm{U}(38, 250)$
Wiri Mountain	$\sim \mathrm{N}(32.879, 0.67^2)$

- Crater Hill, Mt Richmond, Puketutu, Taylors Hill, and Wiri Mountain must be within the Mono Lake excursion. This means that there cannot be more than 1,000 years between the first and last of these ages. In addition Taylors Hill must be the first or last of the five volcanoes. If the generated ages for Cemetery Hill, Hopua, and Little Rangitoto fall within the Mono Lake excursion period, i.e., within 1,000 years of Taylors Hill in the excursion, these are considered to be in the Mono Lake excursion as well. Otherwise they are not. No other volcanoes may fall within the excursion due to the difference in the magnetic field properties.

- The centre of the Laschamp excursion is also generated where McLennan Hills' age is constrained to be within 500 years of it, since McLennan Hills must be in the excursion. Little Rangitoto and Pukeiti will be considered as part of the Laschamp excursion if their generated ages fall within 500 years on either side of the centre of the Laschamp excursion. No other volcano can fall within 500 years of the centre of the Laschamp excursion.

Since the existence of a tephra requires an eruptive vent at least one vent is required in the appropriate age range (as defined by well-dated marker tephras in Table 5.3) of each AVF tephra. We condition this in the following way.

- Since AVF 1 left tephra in Orakei Basin it must be younger than Orakei Basin (83-120ka). Hence AVF 1 is at the oldest 83ka. We assume that Rotoehu, the marker tephra just above AVF 3, is older than the Laschamp excursion. Since McLennan Hills is occurred during the excursion it must be younger than Rotoehu. Thus there must be at least three volcanoes between 83ka and McLennan Hills (exclusive) for AVF 1-3.

- Preliminary analysis (see also Bebbington and Cronin (2011)) suggested that one of Mt Eden or Three Kings corresponds to the widespread AVF 12 tephra, due to the highly constrained ages, central position, and large volumes. Hence at least 11 volcanoes are required between Orakei Basin and the younger of Three Kings and Mt Eden (exclusive), for AVF 1-11.

- If Three Kings is older than AVF 12 (Jenni Hopkins, personal communication) then there must be at least eight volcanoes younger than Mt Eden for AVF 13-20.

- The earliest observed tephra in Hopua Crater is AVF 12, hence Hopua cannot be assigned to AVF 12 or younger. Thus there must be at least nine volcanoes younger than Hopua for AVF 12-20.

- AVF 4-11 are placed between marker tephras Maketu and Okaia. Thus there must be at least eight volcanoes between these marker terphas. To be conservative three standard deviations are chosen. Similarly, AVF 13-17 are placed between marker tephras Oruanui and Okareka. Then there must be at least five volcanoes between these marker tephras for AVF 13-17. Similarly, AVF 13-19 are placed between marker tephras Oruanui and Rerewhakaaitu. Then there must be at least seven volcanoes between these marker tephras for AVF 13-19. Similarly, AVF 18-19 are placed between marker tephras Okareka and Rerewhakaaitu. Then there must be at least two volcanoes between these marker tephras for AVF 18-19. Similarly, AVF 20 is placed just above marker tephra Rotorua and it must be older than AVF 21. Then there must be at least one volcano between Rotorua and AVF 21 for AVF 20.

Figure 7.2 shows the marginal pseudo prior ages of certain selected volcanoes from the 10,000 runs. The prior ages for Wiri Mountain and Three Kings are generated from normal distributions but the histogram of the generated ages for Wiri Mountain shows that the symmetry has been replaced by left skewness due to the additional stratigraphy, Mono Lake, and marker tephra constraints. Taylors Hill is bimodal representing the two possibilities at the beginning and end of the Mono Lake excursion. Little Rangitoto, North Head, and Mt Victoria have the same uniform candidate age distribution but their histograms show the effects of the additional constraints. The peaks around 30ka are due to the requirement that there be enough volcanoes to match tephras AVF 4-11.

Figure 7.2: Simulated ages (histograms) of selected volcanoes resulting from the constraints outlined in the text. Note the different vertical scale for Mt Victoria.

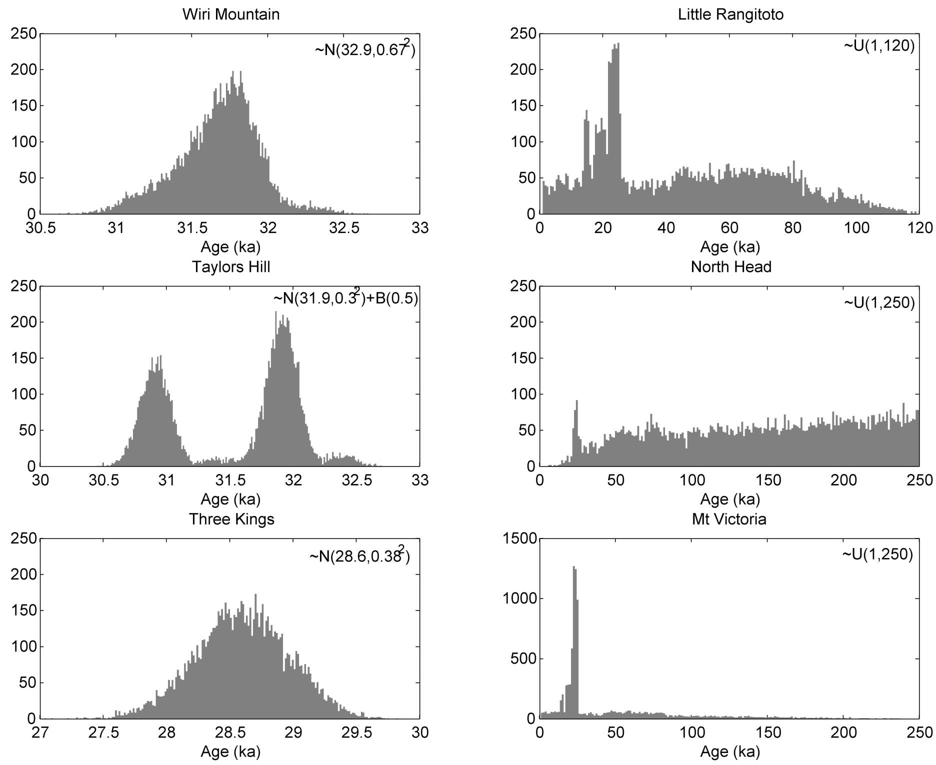

Little Rangitoto is limited above by Orakei Basin which is at least 83.1ka, while North Head must be older than Mt Victoria.

7.3.4 Linear programming

Since each pair of a tephra and a volcano has two outcomes, either assigned or not assigned, this problem can be formulated in a linear programming framework to find the most statistically likely matching arrangement for each feasible set of prior ages through MLE.

In order to find the maximum likelihood arrangement a unique volcano must be assigned to each AVF tephra and the remaining 21 volcanoes to the unassigned AVF tephra, which we denote as AVF 0. This problem will be treated in a binary integer programming framework by creating 41 $\times$ 21 variables x_{ij} for $i = 1, \ldots, 41$ and $j = 0, \ldots, 20$. Each x_{ij} is binary, either 0 or 1. It takes the value 1 if Volcano i is assigned to Tephra j, 0 otherwise. For each feasible set of prior volcano ages n our objective function becomes

$$\log L^n = \sum_{i=1}^{41} \sum_{j=1}^{20} x_{ij}^n \left[\sum_{k=1}^{5} \log u_{ijk}(T_{jk}) + \log f_j^n(s_i^n) + \sum_{j^*=1}^{10} \log g_{j,j^*}^n(s_i^n) \right] + \sum_{i=1}^{41} \sum_{k=1}^{5} x_{i0}^n \log v_{ik}^n(T_{jk}). \tag{7.7}$$

While maximising the above objective function the following constraints must be observed to ensure that our solution remains feasible: First

$$\sum_{j=0}^{20} x_{ij}^n = 1 \quad \forall i = 1, \ldots, 41, \tag{7.8}$$

which ensures that each volcano is assigned to either an AVF tephra or the 'unassigned' AVF 0 tephra. Second

$$\sum_{i=1}^{41} x_{ij}^n = 1 \quad \forall j = 1, \ldots, 20, \tag{7.9}$$

which ensures that each AVF tephra is assigned to a volcano. Equations 7.8 and 7.9 together ensure that each volcano-tephra assignment is unique, that no volcano will be assigned to two AVF tephras and vice versa. Also, we require that

$$\sum_{i=1}^{41} x_{i0}^n = 21 \tag{7.10}$$

ensuring that all 21 unassigned volcanoes are assigned to AVF 0, and

$$\sum_{i=1}^{41} (i x_{i,j+1}^n - i x_{ij}^n) > 0 \quad \forall j = 1, \ldots, 19, \tag{7.11}$$

which ensures that the stratigraphy is maintained. Since the volcanoes are ordered by the simulated ages s_i^n and the AVF tephras are ordered in the cores, both from oldest to youngest, Volcano 1 is older than Volcano 2 and AVF 1 is older than AVF 2 and so on. Equation 7.11 ensures that the volcano that is assigned to the younger AVF tephra $j+1$ is younger (smaller i) than the volcano that is assigned to the older AVF tephra j (larger i). For example, if Volcano 5 is assigned to AVF 3 then Volcano 7 may be assigned to AVF 4, making the left-hand side of Equation 7.11 equal to $7-5$ as $5x_{53} = 5$ and $7x_{74} = 7$ when $j = 3$. However if we try to assign a younger Volcano 3 to AVF 4 instead Equation 7.11 breaks down as $3 - 5 \ngtr 0$.

Further constraints derive from the data itself: As AVF 1 was observed in Orakei Basin, Orakei Basin and any volcanoes whose prior age is older must be assigned to AVF 0. Since AVF 2 was observed in Pukaki Crater it can only be assigned to AVF 1 or 0. The presence of AVF 12 in Hopua Crater means that Hopua cannot be assigned to AVF 12 or a younger tephra.

7.3.5 Age model averaging

Maximising the objective function (Equation 7.7) subject to the above constraints (Equations 7.8-7.11) produces the maximum likelihood arrangement for matching the AVF volcanoes and tephras for each n. The 10,000 arrangements must be combined to find the global best arrangement. Importance sampling was considered, weighting the arrangements by their likelihood values L^n to produce posterior distributions but by construction every age set is equally likely and more likely age sets will be produced more frequently and thus will be more heavily represented in the sample. Thus each age set will be treated with equal weight, and another linear programming problem will be solved to find the best global arrangement. Let us define P_{ij} to be the proportion of times Volcano i is assigned to AVF tephra j from the 10,000 runs, then the multinomial log likelihood is maximised

$$\sum_{j=0}^{20}\sum_{i=1}^{41} x_{ij}[\log P_{ij} + \sum_{k\neq j}\log(1-P_{ik})]. \qquad (7.12)$$

This can be solved as a linear programming problem with constraints similar to Equations 7.8-7.11 to ensure a feasible arrangement.

7.4 Results

Solving Equation 7.7 according to Constraints 7.8-7.11 produces solutions such as Table 7.4 for each environmental condition as described in Section 7.3. These are the proportions of times Volcano i is assigned to AVF tephra j from the 10,000 runs. They are marginal probabilities, for each Volcano i and AVF tephra j (each column/row sums to 1). Table 7.4 shows the proportions for $\alpha = 2.0$ and $\beta U = 0.5$. The proportions for the rest of the environmental conditions are tabulated in Appendix A. We can consider these as the posterior probabilities as they are derived from the prior age distributions. Three Kings is a viable match for AVF 9-12 due to its highly constrained ages, central position, and large volume, in agreement with Bebbington and Cronin (2011). Similarly Crater Hill is always assigned to one of AVF 5-11. On the other hand, Pukeiti and Waitomokia are almost certainly not matched to any of the tephras. Volcanoes such as Green Hill, Little Rangitoto, Mt Victoria, and North Head are feasible matches for all AVF tephras due to their central positions, relatively large eruptive volumes, and the lack of age constraints.

The global matching assignment obtained from Equation 7.12 is indicated by bold type in Table 7.4. We see that for AVF 13, 18, and 20 the volcanoes with the largest marginal probabilities were not selected. This is because the likelihood of the overall matching assignment was maximised and sometimes individual matches are compromised to improve the overall likelihood. For example, Little Rangitoto is the best match for both AVF 1 and 2. The next best for AVF 1 is Domain and for AVF 2 is One Tree Hill.

Since the pair of AVF 1 and Domain is relatively better than the pair of AVF 2 and One Tree Hill, AVF 1 is assigned to Domain to allow for Little Rangitoto to be matched to AVF 2. Similarly Mt Mangere and Mt Smart had the largest probabilities in more than one AVF tephra.

The first column in Table 7.5 shows the global arrangement of the 20 pairs of volcanoes and tephras obtained from Equation 7.12 for the six environmental conditions. A remarkable number of the tephras have a single preferred source under all environmental conditions, so can be considered robust assignments. Looking at these in detail:

AVF 3 (48.61 ± 3.00ka) is always assigned to Otuataua (contemporaneous to 39.99 ± 0.53ka). This eruption deposited tephra at Orakei Basin, situated northeast of Otuataua, but not at Pukaki Crater, situated closer and directly east of the volcano. This is not implausible as Otuataua had an estimated wind direction of north-northwest and is a relatively small volume volcano. However, the prior age distribution for Otuataua has a vanishingly small probability of being older than 43ka, making this an apparently unlikely match time-wise. There appears to be no better option, but this will be reexamined later.

AVF 4 (34.90 ± 0.40ka) is always assigned to Kohuora (34 ± 0.3ka). The eruption left no tephra at Pukaki Crater, the closest core to Kohuora, but deposited small amounts at the northern sites of Orakei Basin, Lake Pupuke, and Onepoto Basin. This is unlikely to be explained by the different probabilities of observing a distal tephra across the five maars (Green et al., 2014). It is possible that the wind was blowing strongly to the north, and this is obscured by the unusual three-lobed nature of the explosion crater(s) at Kohuora (Hayward, Murdoch and Maitland, 2011).

AVF 5 (31.31 ± 0.70ka) is always assigned to Panmure Basin (31.73 ± 0.17ka). Panmure Basin is a relatively large volume volcano which erupted in a east-northeast wind direction, away from any of the core locations (Figure 7.1). Orakei Basin,

Table 7.4: Marginal posterior probabilities for a volcano to have produced a given tephra for the baseline scenario with $\alpha = 2.0$, $\beta U = 0.5$. The global best arrangement is indicated by bold type.

Volcano	AVF tephra (AVF 0 = 'unmatched') 0	1	2	3	4	5	6	7	8	9	10	11	12	13	14	15	16	17	18	19	20
Ash Hill	.8011					.0004	.1612	.0373													
Cemetery Hill	.0329				.0002	.0170	.1326	.1716	**.5343**	.1106	.0008										
Crater Hill	0					.0001	.0150	.0068	.2779	**.5690**	.1301	.0011									
Domain	.7589	**.1326**	.0870	.0215																	
Green Hill	.0102	.0007	.0031	.0162	.0255	.0160	.0059	.0003	.0004	.0037	.0376	.0164	.0555	**.1900**	.1223	.1029	.0775	.0874	.1098	.0878	.0308
Hampton Park	.3939					.0001								.0648	.1480	**.1912**	.1051	.0693	.0167	.0070	.0039
Hopua Basin	.8042			.0003		.0639	.0499	.0359	.0003	.0021	.0413	.0021									
Kohuora	.0001	.0001	.0018	.0171	**.8619**	.0656	.0514	.0010	.0010												
Little Rangitoto	.0440	.1987	**.1923**	.1444	.0215	.0117	.0013	.0009	.0008	.0025	.0133	.0056	.0182	.0497	.0383	.0288	.0208	.0317	.0488	.0530	.0737
Mangere Lagoon	.7382	.0450	.0609	.0558	.0005	.0077	.0022	.0003		.0006	.0053	.0038	.0047	.0254	.0216	.0158	.0096	.0026			
Matukutureia	.0209									.0008	.0076	.0032	.0067	.1381	.1007	.0861	.0683	.0642	.0950	.2123	.1961
Maungataketake	.9943	.0012		.0034		.0002	.0009														
McLennan Hills	.9259		.0162	.0435		.0128	.0009	.0007													
Motukorea	.9494	.0023	.0007	.0002		.0019					.0006			.0065	.0008	.0029	.0021	.0276	.0010	.0016	.0024
Mt Albert	.8857	.0585	.0360	.0184	.0007	.0005	.0001				.0001										
Mt Cambria	.7322	.0105	.0238	.0175	.0035	.0083					.0050			.0329	.0103	.0492	.0156	**.0888**	.0012	.0011	.0001
Mt Eden	.0442									.0006	.0363	.3759	**.5430**								
Mt Hobson	.1233										.0002	.0038	.0184	.1215	.0880	.0743	.0609	.0841	**.1128**	.1302	.1825
Mt Mangere	.0095													.0048	.0431	.1439	**.3543**	.3037	.1366	.0041	
Mt Richmond	.7783					.0013	.0717	.1487													
Mt Roskill	.9408	.0185	.0261	.0022	.0001	.0067	.0001	.0004			.0051										
Mt Smart	.0099														.0004	.0050	.0266	.0786	.2761	**.3807**	.2227
Mt St John	.7185	.0571	.1123	.0907	.0002	.0128	.0007	.0002		.0001	.0052	.0022									
Mt Victoria	.1755	.0696	.0735	.0718	.0136	.0070	.0030	.0001	.0001	.0018	.0043	.0050	.0076	.1063	.1252	.0652	.0846	.0173	.0773	.0382	.0530
North Head	.7306	.1006	.0624	.0508	.0077	.0036	.0004	.0001	.0001	.0003	.0050	.0015	.0050	.0112	.0062	.0041	.0028	.0026	.0019	.0015	.0016
One Tree Hill	.6754	.0843	.1248	.0981	.0023	.0109	.0009	.0002	.0001	.0003	.0018	.0009									
Otara Hill	.0057	.0004	.0006	.0075	.0052	.0030	.0020			.0008	.0073	.0040	.0112	.2147	**.2664**	.1806	.1282	.0605	.0686	.0251	.0082
Otuataua	.6472	.0065	.0601	**.2341**	.0477	.0040	.0002	.0002													
Panmure Basin	.1300		.0001	.0004	.0004	**.7081**	.0807	.0568		.0004	.0231										
Pigeon Mountain	.7722	.0307	.0443	.0358	.0005	.0047					.0062			.0225	.0122	.0161	.0074	.0281	.0039	.0036	.0118
Pukaki	.9114	.0886																			
Pukeiti	1																				
Puketutu	.0270				.0006	.0033	.0383	.0496	.1623	.2245	**.4942**	.0002									
Robertson Hill	.9995						.0005														
Styaks Swamp	.5310													.0116	.0165	.0339	.0362	.0535	.0503	.0538	**.2132**
Taylors Hill	.5495			.0001		.0198	**.2255**	.2043			.0008										
Te Pouhawaiki	.7341	.0941	.0740	.0702	.0079	.0063	.0011	.0003	.0003	.0004	.0087	.0026									
Three Kings	0									.0032	.0954	**.5717**	.3297								
Waitomokia	1																				
Wiri Mountain	.3945					.0023	.1535	**.2843**	.0224	.0783	.0647										

the only core to contain the AVF 5 tephra, is located north-northwest of Panmure Basin.

AVF 7 (32.89 ± 0.62ka) is always assigned to Wiri Mountain (32.88 ± 0.67ka). Pukaki Crater is the only core containing AVF 7 tephra, and is situated close to and northwest of Wiri Mountain, which erupted to the northeast.

AVF 8 (32.02 ± 0.36ka) is always assigned to Cemetery Hill (contemporaneous to 33.3 ± 0.6ka). The Pukaki core contains AVF 8 tephra (a large thickness of 20cm) and is located close to Cemetery Hill.

AVF 9 (30.85 ± 0.31ka) is always assigned to Crater Hill (33.3 ± 0.6ka). This eruption left a very thick tephra layer (49cm) at Pukaki Crater. Crater Hill was a much larger eruption than Cemetery Hill, and is closer to Pukaki Crater, and so the assignments of Crater Hill to the thicker AVF 9 and Cemetery Hill to the thinner AVF 8 are sensible and in keeping with the known stratigraphy.

AVF 10 (30.52 ± 0.36ka) is always assigned to Puketutu (33.6 ± 3.7ka). This eruption left no detectable tephra at Pukaki Crater, located close to and east-southeast of Puketutu but deposited some tephra at Orakei Basin, located north-northeast of the Puketutu. As Puketutu erupted in a north-northwest direction this seems feasible.

AVF 13 (24.97 ± 0.36ka) is always assigned to Green Hill (19.83 ± 8.98ka). It deposited tephra at Orakei Basin and Hopua Crater, which the two cores located closest to Green Hill in the northwest direction.

AVF 14 (24.67 ± 0.39ka) is always assigned to Otara Hill (contemporaneous to 26.6 ± 8ka). While Otara Hill has no discernable wind direction, it does seem unlikely that such thick tephras at such distances were not reflected in a deposit at Hopua Crater, which is about the same distance away on an azimuth between the other two maars. While this may be the most likely match, further investigation appears warranted.

AVF 15 (24.35 ± 0.3ka) is always assigned to Hampton Park (26.6 ± 8ka). Orakei Basin, situated northwest of the volcano, and Pukaki Crater, situated southwest of the volcano, each contain some AVF 15 tephra. However, in this case the thicknesses are much less than for AVF 14, and so its apparent absence in Hopua Crater is not as concerning. While Hampton Park is estimated to have erupted towards the east, all five cores are located to the west of the volcano.

AVF 16 (23.64 ± 0.38ka) is always assigned to Mt Mangere (21.94 ± 0.40ka). As Mt Mangere erupted to the south away from Orakei Basin, this may seem illogical. However, Mt Mangere has a tightly constrained age and a very large tephra volume, making it very unlikely that it was not observed somewhere.

AVF 17 (23.25 ± 0.51ka) is always assigned to Mt Cambria (1-250ka). While it may appear odd that the smaller, and less directionally favoured, Mt Cambria is preferred to the larger contemporaneous Mt Victoria, this is explained by reference to Table 7.4. Mt Cambria is preferred for this eruption because Mt Victoria is preferentially mapped to other tephras: AVF 17 is its least preferred match from AVF 13 to 20 inclusive.

AVF 20 (15.45 ± 0.53ka), observed only at Pukaki Crater, is always assigned to Styaks Swamp (1-125ka) largely due to the stratigraphy constraint on Styaks Swamp (younger than Green Hill).

The rest of the matches are less robust, depending on the environmental conditions.

AVF 1 (69.45 ± 7.36ka) is assigned to Little Rangitoto (1-120ka) in a strong wind, or for a high eruption column in a weak wind, and to Domain (60-250ka) otherwise. This tephra left 4cm of tephra at Orakei Basin which is situated close to both, especially Little Rangitoto. Little Rangitoto seems to be a plausible match for AVF 1 unless it is selected for the even thicker AVF 2.

AVF 2 (56.84 ± 6.03ka) is assigned to One Tree Hill (29-250ka) in a strong wind, or for a high eruption column in a weak wind, and to Little Rangitoto (1-120ka) otherwise. One Tree Hill is further (but in the right direction) from Orakei Basin and larger than Little Rangitoto (Table 5.3 and Figure 7.1), so a strong wind or high eruption column favours it as a source.

AVF 6 (33.05 ± 0.62ka) is assigned to Taylors Hill (31.9 ± 0.3ka or 32.9 ± 0.3ka) in a weaker wind, and to Ash Hill (31.8 ± 0.16ka) under a stronger wind condition. Pukaki Crater, the only core to contain AVF 6 tephra, is located closer to the smaller volume Ash Hill than the larger volume Taylors Hill. As Taylors Hill appears to have erupted in a southerly direction towards Pukaki Crater, while Ash Hill erupted in a easterly direction away from it, a stronger wind naturally favours Taylors Hill to produce AVF 6.

AVF 11 (30.09 ± 0.36ka) is apparently a large volume event, as 40cm of tephra was observed at Orakei Basin. Three Kings (28.59 ± 0.38ka) and Mt Eden (28.39 ± 0.35ka) have similar locations (relative to Orakei Basin), sizes, and estimated ages. Three Kings has no discernable wind direction, so as Mt Eden erupted in a southerly direction away from Orakei Basin, AVF 11 tends to identify with Three Kings in a weak wind condition and Mt Eden in stronger winds.

AVF 12 (28.46 ± 0.26ka) is another large event, with tephra observed in all five cores. Hence Three Kings is favoured under strong wind conditions, as Mt Eden is then erupting away from the three northern cores. Note that the AVF 11 and 12 matches are robustly assigned to Three Kings and Mt Eden in some order. The stratigraphy is silent on this point, unfortunately.

AVF 18 (20.00 ± 0.37ka) is observed at both Hopua Crater and Pukaki Crater, and is assigned to Mt Hobson (1-30ka) under weak wind conditions with a medium to high eruption column and to Mt Smart (10-23ka) under stronger wind conditions. Mt Smart is closer to both cores, and produced a larger eruption directly towards Pukaki Crater, which is best explained by looking at the AVF 19 match below.

AVF 19 (19.74 ± 0.3ka) is assigned to Mt Smart (10-23ka) in a weak wind field with a medium to high eruption column, and to Matukutureia (1-34ka) for low eruption column or a strong wind field. This is another very thick tephra in Hopua Crater, which is very close to Mt Smart. Essentially, Mt Smart matches to one of AVF 18 or 19, which the actual best match (and the consequent match to the other tephra) determined by the details of the wind speed and column height.

7.5 Sensitivity analyses

The data we have considered so far to produce the global solutions is based on the published data in the literature but there are some recent, mainly unpublished, data which slightly differ. The above scenario is considered as a baseline and investigate the robustness of its solution under the same set of environmental conditions.

Firstly, Maungataketake may be much older than the radiocarbon (^{14}C) determined age (39.99 ±0.53ka) at 87.4 ± 2.4ka (Agustín-Flores et al., 2014) based on the unpublished argon-argon (^{40}Ar/^{39}Ar) age data (Graham Leonard, personal communication), and the unconstrained North Head (1-250ka) may be constrained to 80-120ka (Agustín-Flores et al., 2015). Consequently Otuataua, which is contemporaneous to Maungataketake, must also be older. Since the oldest tephra AVF 1 is estimated at 69.45 ± 7.36ka the three volcanoes must be too old to match AVF 1. The second column of Table 7.5 shows differences for AVF 1-3 and AVF 16-17 (the rest are the same) as a result. Otuataua, which used to be matched to AVF 3, is now only considered for AVF 1 under the high wind condition. Little Rangitoto, which was previously matched to AVF 1, is assigned to AVF 3. The central location and the reasonable size of Little Rangitoto with the weak age constraint of 1-120ka makes it a viable match for AVF 3. The minor perturbations in the youngest tephra assignments are a consequence of the feasibility requirements; with Maungataketake and North Head no longer in the critical age bands, other volcanoes are more or less likely to be as close in age to the younger tephras.

Secondly, Three Kings might match either to AVF 9 or 10 based on the geochemical

Table 7.5: Best global arrangement of assigning Volcano i to AVF tephra j. Scenarios are outlined in the sensitivity analysis section (Section 7.5). M stands for Maungatake-take, NH stands for North Head; and TK stands for Three Kings. The six parameter sets are A = $\{\alpha = 1.5,\ \beta U = 0.5\}$; B = $\{\alpha = 2,\ \beta U = 0.5\}$; C = $\{\alpha = 2.5,\ \beta U = 0.5\}$; D = $\{\alpha = 1.5,\ \beta U = 1\}$; E = $\{\alpha = 2,\ \beta U = 1\}$; and F = $\{\alpha = 2.5,\ \beta U = 1\}$.

Tephra	Volcano	Scenario				
		Baseline	M and NH older	TK is AVF 9	TK is AVF 10	AVF 9 split in two
AVF 1	Domain	BC	ABC	B		B
	Little Rangitoto	ADEF		ACDEF	All	ACDEF
	Otuataua		DEF			
AVF 2	Little Rangitoto	BC		B		B
	OneTreeHill	ADEF	All	ACDEF	All	ACDEF
AVF 3	Little Rangitoto		All			
	Otuataua	All		All	All	All
AVF 4	Kohuora	All	All	All	All	All
AVF 5	Panmure Basin	All	All	All	All	All
AVF 6	Ash Hill	DEF	DEF			EF
	Cemetery Hill			F		
	Crater Hill			CDE		
	Taylors Hill	ABC	ABC		DEF	ABCD
	Wiri Mountain			AB	ABC	
AVF 7	Cemetery Hill			AB	ABCD	A
	Wiri Mountain	All	All	CDEF	EF	BCDEF
AVF 8	Cemetery Hill	All	All			BCDEF
	Crater Hill			AB	All	A
	Puketutu			CDEF		
AVF 9	Crater Hill	All	All			
	Puketutu				All	
	Three Kings			All		
AVF 9A	Crater Hill					BCDEF
	Wiri Mountain					A
AVF 9B	Puketutu					All
AVF 10	Hopua			DEF		All
	Puketutu	All	All			
	Robertson Hill			ABC		
	Three Kings				All	
AVF 11	Hopua			ABC	All	
	Mt Eden	DEF	DEF	DEF		DEF
	Three Kings	ABC	ABC			ABC
AVF 12	Green Hill			DEF		
	Mt Eden	ABC	ABC	ABC	All	ABC
	Three Kings	DEF	DEF			DEF
AVF 13	Green Hill	All	All	ABC	All	All
	Mt Hobson			DEF		
AVF 14	Otara Hill	All	All	All	All	All
AVF 15	Hampton Park	All	All	All	All	All
AVF 16	Matukutureia		AB			
	Mt Mangere	All	CDEF	All	All	All
AVF 17	Mt Cambria	All		BCDEF	All	All
	Mt Hobson		CDEF	A		
	Mt Mangere		AB			
AVF 18	Mt Hobson	AB	AB		A	AB
	Mt Smart	CDEF	CDEF	All	BCDEF	CDEF
AVF 19	Matukutureia	CDEF	CDEF	All	BCDEF	CDEF
	Mt Smart	AB	AB		A	AB
AVF 20	Styaks Swamp	All	All	All	All	All

evidence (Jenni Hopkins, personal communication). The third and fourth columns of Table 7.5 show the results of forcing Three Kings to match AVF 9 and 10 respectively. Consequently the Mono Lake volcanoes (from AVF 6 to Three Kings) scramble to accommodate the shortening of the excursion period and Robertson Hill and Hopua are selected as replacements for AVF 10 and 11.

Finally, we can look at the spatial distribution of the tephra thicknesses, which was not incorporated in the tephra matching done based on age by Green et al. (2014). We note that AVF 9 left 49cm at the most southern maar, Pukaki Crater, and that the observed thicknesses decrease moving north: 1.6cm at Orakei Basin and 0.44cm at Onepoto Basin. However the most northern maar Lake Pupuke contains 2.2cm, more than Onepoto Basin and Orakei Basin. The possibility that AVF 9 belongs to two distinct events, which will be called AVF 9A (Onepoto Basin and Lake Pupuke) and AVF 9B (Orakei Basin and Pukaki Crater) (Table 5.3) will be considered. This results in a perturbation of assignments to the tephras AVF 6-10 as a consequence of finding a new volcano to match the extra tephra (the last column of Table 7.5). Puketutu, which was originally assigned to AVF 10, is now matched to AVF 9B and Hopua is now identified with AVF 10.

7.6 Discussion

The attenuation parameters have necessarily been simplified by assuming a constant wind direction ϕ for each volcano and constant α and βU across all volcanoes. By assuming a constant wind direction the former represents the mean direction. The assumption of constant values for the latter parameters are necessary due to the lack of data to estimate individual values. Hence the volcanoes are distinguished by whether they have a preferred deposition direction, and in which direction it is. Another consequence is that the ability for a larger volcano to leave tephra in a wider region is underestimated hence it might be that the likelihood of matching larger volcanoes to

AVF tephras is underestimated. However, the comparison of the eruption volumes in Table 7.1 and the assignments in Table 7.5 shows that still the larger volcanoes were often selected for AVF tephras. The exceptions are: Maungataketake, Pukaki, Mt Albert, and Mt Roskill. Maungataketake is disadvantaged by a smaller but contemporaneous and closely situated Otuataua due to Otuataua's preferred wind direction. Pukaki (65-250ka), Mt Albert (30-250ka), and Mt Roskill (27-250ka) are usually too old to match to any tephras. Mt Albert has a favourable dispersal direction without any stratigraphic constraints so any new dating information to suggest this volcano is younger than 80ka would almost certainly match to an AVF tephra. Domain (60-250ka) is a feasible match only to AVF 1, which prefers a much smaller Little Rangitoto for its closely located position to Orakei Basin.

A base surge is the over-thick deposit in the close proximity of the source volcano. Orakei Basin, Hopua Crater, and Pukaki Crater observed some severely thick tephras in their cores but these are too many to be all base surges so it makes more sense to consider them as over-thickening or remobilisation of tephra, causing local overestimation of thickness. The additional error in the thicknesses can be accounted for by increasing the CV. To check the robustness of our solutions the baseline scenario was run once more with CV = 1 and produced the same global results for all six combinations of environmental conditions.

The Mono Lake excursion is the exclusive interval containing only the Mono Lake volcanoes, of which Taylors Hill must either be first or last. The baseline results indicate that the Mono Lake excursion started with Taylors Hill at AVF 6 (33.05 ± 0.62ka) under a weak wind condition and no later than AVF 7 (32.89 ± 0.62ka) under a strong wind condition. And the excursion ended no earlier than AVF 10 (30.52 ± 0.36ka) for all wind conditions. This suggests that the excursion is likely to have lasted longer than 1,000 years and Taylors Hill is most likely to be the first volcano to have erupted during the excursion. In a weak wind condition Taylors Hill is assigned to a tephra approximately 45% of the time. Given that it is assigned, the proportion of the time Taylors Hill is assigned to AVF 10 is less than 0.1%. Similarly, in a strong wind condition Taylors Hill is assigned to a tephra approximately 55% of the time, but almost never to a tephra older than AVF 7.

A remarkable number of solutions were robust for all wind conditions. These were dominating matches and other arrangements were significantly less likely. However there were cases where different volcanoes were matched under different environmental conditions. This is often due to the lack of dominating matches and small differences in the likelihoods between the top candidate volcanoes. Some volcanoes such as Little Rangitoto, One Tree Hill, and Mt Cambria have considerably variable prior age distributions and it is unknown how many replications are required to acquire a representative sample. Due to computational limitations only 10,000 replications were run, each replication taking about 20 seconds to generate simulated ages.

Turner et al. (2009) and Green et al. (2014) have considered the distribution of titanomagnetites (TiO_2, MgO, and Al_2O_3) in ash samples. Should titanomagnetite chemistry data become available from the volcanoes and tephras in this problem, they could be incorporated in the likelihood-based matching.

The most statistically likely arrangement of tephras and volcano sources were produced conditional on the prior age distributions. Bebbington and Cronin (2011) and Bebbington and Cronin (2012), who updated the paleomagnetism ages, matched the volcanoes to the 24 tephras identified by Molloy et al. (2009). Table 7.6 compares the results of the present work and those of Bebbington and Cronin (2011, 2012). Note that AVF 7 did not have an equivalent in the Molloy et al. (2009) data but Crater Hill is a very likely candidate. While many volcanoes appear in both lists, there are many differences in the assignments. The main discrepancies are due to inconsistencies in the volume estimates. While Bebbington and Cronin (2012) based their volume estimates on Allen and Smith (1994) some of them were updated from Kereszturi et al. (2013) for this thesis. Green Hill, Otara Hill, and Hampton Park due to their larger new volumes made appearances in our list while Mangere Lagoon and Mt St John disappeared. The remaining differences are due to the consideration of full prior age distributions for the volcanoes in our objective approach.

This matching exercise is of interest because the Bebbington and Cronin (2011, 2012) arrangement was used as the basis of a Monte Carlo age algorithm that underpinned investigations into the spatio-temporal evolution of the field (Bebbington and Cronin, 2011), its forecasting (Bebbington, 2013), and the geochemical and volume correlations between successive eruptions (Le Corvec et al., 2013). The algorithm substituted the more precise tephra ages for the sometimes unknown volcano ages, and then simulated the remaining ages from the volcano data available. In principle the same could be done with the results of this work, and the subsequent studies re-visited. However, this is only appropriate if age sequences can be simulated from our assignment. The implicit constraints as a result of our probabilistic assignment mean that the environmental conditions need to be incorporated and randomised for each sequence. Even if a deterministic assignment can be agreed upon generating age sequences with such tight constraints will be very computationally challenging and is beyond the scope of this thesis.

7.7 Conclusion

An optimal likelihood-based method for matching volcanic sources and tephras is constructed based on the differences between the age distributions of the volcanoes and tephras and the attenuation model for the tephra thickness based on the estimated tephra volumes, locations of source and deposit, and wind effects. Feasible sequences of volcano ages called 'pseudo age sequences' were generated in a Monte Carlo simulation from determined age distributions, improved by known stratigraphic ordering and paleomagnetic excursions. These prior ages were then evaluated against the normally distributed tephra ages. This likelihood was maximised in the linear programming

Table 7.6: Comparison of event order models.

Tephra	Baseline model, this work	Bebbington and Cronin (2012)
AVF 1	Little Rangitoto/Domain	Pukaki
AVF 2	One Tree Hill/Little Rangitoto	Domain
AVF 3	Otuataua	Mt St John
AVF 4	Kohuora	One Tree Hill
AVF 5	Panmure Basin	Motukorea
AVF 6	Taylors Hill/Ash Hill	Kohuora
AVF 7	Wiri Mountain	
AVF 8	Cemetery Hill	Puketutu
AVF 9	Crater Hill	Hopua
AVF 10	Puketutu	North Head
AVF 11	Three Kings/Mt Eden	Panmure Basin
AVF 12	Three Kings/Mt Eden	Three Kings
AVF 13	Green Hill	Mt Eden
AVF 14	Otara Hill	Mt Hobson
AVF 15	Hampton Park	Little Rangitoto
AVF 16	Mt Mangere	Pigeon Mountain
AVF 17	Mt Cambria	Mangere Lagoon
AVF 18	Mt Hobson/Mt Smart	Mt Mangere
AVF 19	Mt Smart/Matakutureia	Mt Smart
AVF 20	Styaks Swamp	Styaks Swamp

framework to find the optimal matching arrangement for each prior age sequence. Assuming more likely age sequences will be produced more frequently the multinomial likelihood of the different matches provided the global optimal matching arrangement. These results were shown to be robust across possible ranges for the environmental conditions and possible over-thickening of the deposits in the AVF.

Chapter 8

Conclusions and Future Work

The thesis first considered statistical modelling of tephra attenuation, and then used this as a central part of a statistical estimation of age-ordering in the Auckland Volcanic Field.

8.1 Statistical attenuation modelling

The attenuation of tephra fall thickness is most commonly estimated after contouring isolated and often irregular field measurements into smooth isopachs, with varying degrees of subjectivity introduced in the process. These isopach maps can be used to identify tephra lobes but accurately identifying the number of lobes can be difficult depending on the smoothness of the isopachs. When hand drawn, the degree of smoothness is due to the subjectivity introduced during the production. If the map is too smoothed out then similar multiple lobes may not be distinguished and too rough contours mean a lobe will be difficult to be identified. Even if the lobes were identified, multiple phases cannot be separated within a single lobe from tephra data and the isopach map alone if their wind directions do not vary much.

A semiempirical model of tephra deposition with wind effect incorporated, combined with an error distribution, was shown to produce a statistical model capable of being fitted to actual measurements rather than isopachs. This provides a ready-made inversion formula for the volume of the eruption and the average wind direction. In addition, it can be used to forecast the distribution of tephra at locations without data, and provides an objective measure of goodness of fit to the data.

Applied to the 1973 Heimaey eruption, the model without wind effects was decisively rejected. The wind direction obtained from the model with wind effects corresponds well with the mean wind direction from the onshore wind that deposited the measured tephra thicknesses. The estimated attenuation parameter indicated a mean column height equal to the observed for the eruption (Wilson et al., 1978).

Elaborating the semiempirical tephra attenuation model further in a mixture framework enables the model to fit multiple fall lobes and/or vents through maximum likelihood estimation (MLE). Applied to the 1977 Ukinrek Maars eruption, it was able to identify lobes in the correct directions, for which data existed, from each vent. This statistical method is more sensitive to slight changes in dispersal patterns than isopach maps. This has obvious utility in studying unobserved eruptions with multiple vents.

When attempting to precisely reconstruct past eruptions from the geological record, separate phases from a composite tephra blanket are often indistinguishable due to a lack of obvious distinct physical or chemical characteristics. This method can be used to distinguish the main tephra-producing phases produced during any similar multi-event and multi-source explosive basaltic eruption. The most likely sequence of tephra-fall phases could be identified for the unobserved 1256 AD Al-Madinah eruption including their most likely individual volumes. This information provides greater resolution to future tephra hazard models for this area.

8.2 Statistical age ordering in volcanic fields

Assessment of spatio-temporal dependence in a monogenetic field such as the Auckland Volcanic Field (AVF) requires a record of vent ages, not just locations. To come up with an age-order model, the best possible volcanic record of times and locations of past volcanic events must be constructed. Partial records of these are available from five deposition locations within the field formed by maars. However, there is no direct link between the deposit(s) and a particular source volcano.

Age data for many of the volcanoes in the AVF exist, from radiocarbon or other radiometric methods, dosimetric methods and paleomagnetism. However, the results are often inconsistent. The age order of some pairs is also known due to the overlaying of lavas (stratigraphy). A Bayesian age-model can be explored to reconcile these inconsistent data and arrive at an optimum age model for the AVF, with an objective to estimate the true ages for the AVF volcanoes. The reliability of each dating method was also evaluated in the process. Informative priors, via expert elicitation, were obtained on both the individual ages, and the reliabilities of the dating methods and the inconsistent determined volcano ages from dating samples were used as data. The inconsistencies were dealt with by assigning a weight of reliability for each dating method. Although the idea showed some promise, the available data and expert opinions were insufficient for it to give reliable results. Hence it became necessary to use data available from maar records, which give good ages for past eruptions in the last approximately 80kyr, but do not identify which volcano erupted.

An optimal likelihood-based method was constructed for matching volcanic sources and tephras based on the differences between the age distributions of the volcanoes and tephras and the attenuation model for the tephra thickness, as a function of the estimated tephra volumes, locations of source and deposit, and wind effects. Feasible sequences of volcano ages called 'pseudo age sequences' were generated in a Monte Carlo simulation from determined age distributions, filtered by known stratigraphic ordering and paleomagnetic excursions. These prior ages were then evaluated against the normally distributed tephra ages. This likelihood was maximised in the linear programming framework to find the optimal matching arrangement for each prior age sequence. Assuming more likely age sequences will be produced more frequently the multinomial likelihood of the different matches provides a global optimal matching arrangement. These results were found to be robust across possible ranges of the environmental conditions and possible over-thickening of the deposits in the AVF.

8.3 Future work

8.3.1 Bayesian age reconciliation model

The matching procedure between the AVF volcanoes and their tephra deposits (Chapter 7) can be incorporated into the Bayesian age model (Chapter 6). The MLE matching procedure could be treated as an iterative step within the model using the posterior volcano ages from the previous iteration each time. But this would run very slowly. Alternatively, the results from the matching algorithm could be used as another prior. These allow the matching procedure to use improved volcano ages by incorporating the expert elicitation and dating method reliabilities, not just the available dated samples. However, an appropriate methodology is required for reconciling the two types of priors, the pseudo prior ages available from the matching procedure and the estimated ages from the expert elicitation. A careful consideration of how to weigh the two priors is required.

Another issue is in using the same information twice in the combined model. The determined ages are used as priors in the matching algorithm and data in the Bayesian model. One possible way to resolve this would be to update the experts' priors at every iteration based on the results from the matching procedure as in a Delphi algorithm. However this is obviously impractical and would lower the already low response rate of the experts.

A consideration for handling the results from different possible environmental scenarios and possible dated age scenarios (Section 7.5) would also be required.

8.3.2 Grain size

The investigations in my thesis open the way to future work in statistical modelling of volcanic tehpra deposition and hazard. The semiempirical model is constructed for tephra thickness and does not consider grain size data. However future work may branch out in this direction. Grain size contains information about physical eruption parameters such as column height (Pyle, 1989), and hence the magnitude of the eruption (Sigurdsson et al., 1999). Numerical models (Section 2.2.2) contain a grain size distribution as one of their parameters. In order to put this in a statistical model as I did in Chapters 3 and 4, the simulated grain size distribution from an extensive simulation of suitable advection diffusion models such as Tephra2 (Connor et al., 2001) can be analysed to construct an empirical model, equivalent to the semiempirical model for tephra thicknesses (Gonzlalez-Mellado and De la Cruz-Reyna, 2010). The additional information provided by grain size should also provide more sensitivity in identifying phases.

8.3.3 Stochastic models for monogenetic volcanism

The methodology outlined in Chapter 4 to identify the most likely combination of multiple lobes and multiple vents for a volcanic field from tephra data alone can be used as a building block for modelling the number of phases and their sizes. A stochastic model for estimating these characteristics will be made possible given more eruption data are available. If enough eruptions are recorded the tephra data are relatively easily obtained. The freshness, weathering or maar deposits can be accounted for with an appropriate error distribution (Chapters 3 and 4). Given enough eruptions, a frequency table of number of phases in the past can be created. Then probabilities for different numbers of phases can be used to simulate possible numbers of phases. Similarly, the probabilities for the eruption parameters, such as γ, α, and βU from Equation 4.1, can be obtained. The wind direction ϕ can be obtained from local weather data. The durations of eruptions can usually be obtained from observation as approximately how many days each phase lasted is usually available. A simulated hazard model can be constructed by incorporating above. The practical limitation is the lack of past eruptions from monogenetic fields, which have very small eruption rates compared to polygenetic volcanoes, to build a reasonable model.

8.3.4 Wind direction

Although intuitively the maximum thickness occurs at the vent it is often offset by wind. Hence the thickest location may not be at the source vent, i.e., $r = 0$. Thus it is inappropriate to estimate a constant thinning parameter. One way to handle this feature is to add an offset parameter following the lead of Rhoades et al. (2002) which allowed for a finite thickness at the source.

A more interesting problem is the effect on wind shifts in tephra hazard estimation. This is easily handled in numerical models, but an investigation is required for a statistical model. One way is to predict the wind effects over time using an appropriate time series model, which may be used to model a composite tephra blanket for a given time period in a dynamic model. This model accounts for the time dependences using differential equations and will break the hazard simulation into short periods. This way the changes in wind speed and direction over time can be accounted for, not just the average of an entire eruption.

Glossary

Bulk density Density ‘in-situ’. 50

Cinder/scoria cone The most common and smallest type of volcano. 10, 57

Column height The maximum height to which tephra is ejected. 7, 14, 51, 74, 98, 137, 162

Conduit The below-ground path used by the tephra or lava. 10

Dense rock equivalent Volume that the ejecta would occupy if the same mass were in dense rock form. 72, 132

Isopach A contour of equal tephra thickness. 4, 13, 35, 61, 137, 161

Lava flow Molten rock expelled from a non-explosive eruption. 10, 83, 132

Maar A low-relief crater caused by a phretomagmatic eruption. 10, 84, 130, 163

Marker tephra Has distinct peterological and chemical characteristics and has relatively reliable age estimates. 90, 130

Tephra Collective term for all particles ejected during an eruption. 3, 11, 35, 55, 83, 125, 130, 161

Tuff ring A volcanic crater created as a result of an interaction between magma and shallow water. 10, 132

Bibliography

Adams, M. R. (1986), Thermoluminescence dating of plagioclase feldspar, PhD thesis, University of Auckland, Auckland.

Affleck, D. K., Cassidy, J. and Locke, C. A. (2001), Te Pouhawaiki Volcano and pre-volcanic topography in central Auckland: Volcanological and hydrogeological implications, *New Zealand Journal of Geology and Geophysics* **44**(2), 313–321.

Agustín-Flores, J., Németh, K., Cronin, S., Lindsay, J. M. and Kereszturi, G. (2015), Construction of the North Head (Maungauika) tuff cone: a product of Surtseyan volcanism, rare in the Auckland Volcanic Field, New Zealand, *Bulletin of Volcanology* **77**(2), 1–17.

Agustín-Flores, J., Németh, K., Cronin, S., Lindsay, J. M., Kereszturi, G., Brand, B. D. and Smith, I. E. (2014), Phreatomagmatic eruptions through unconsolidated coastal plain sequences, Maungataketake, Auckland Volcanic Field (New Zealand), *Journal of Volcanology and Geothermal Research* **276**, 46–63.

Aitken, M. J. (1985), *Thermoluminescence dating*, Academic press.

Akaike, H. (1974), A new look at the statistical model identification, *Automatic Control, IEEE Transactions on* **19**(6), 716–723.

Allen, S. and Smith, I. E. (1994), Eruption styles and volcanic hazard in the Auckland Volcanic Field, New Zealand, **20**, 5–14.

Armienti, P., Macedonio, G. and Pareschi, M. (1988), A numerical model for simulation of tephra transport and deposition: Applications to May 18, 1980, Mount St. Helens eruption, *Journal of Geophysical Research: Solid Earth (1978–2012)* **93**(B6), 6463–6476.

Aspinall, W., Woo, G., Voight, B. and Baxter, P. (2003), Evidence-based volcanology: Application to eruption crises, *Journal of Volcanology and Geothermal Research* **128**(1), 273–285.

Barberi, F., Macedonio, G., Pareschi, M. and Santacroce, R. (1990), Mappping the tephra fallout risk: an example from Vesuvius, Italy, *Nature* **344**, 142–144.

Barsotti, S., Neri, A. and Scire, J. (2008), The VOL-CALPUFF model for atmospheric ash dispersal: 1. Approach and physical formulation, *Journal of Geophysical Research: Solid Earth (1978–2012)* **113**(B3).

Baxter, P., Ing, R., Falk, H. and et al (1981), Mount St Helens eruptions, May 18 to June 12, 1980: an overview of the acute health impact, *Journal of the American Medical Association* **246**(22), 2585–2589.

Bebbington, M. (2013), Assessing spatio-temporal eruption forecasts in a monogenetic volcanic field, *Journal of Volcanology and Geothermal Research* **252**, 14–28.

Bebbington, M. and Cronin, S. (2011), Spatio-temporal hazard estimation in the Auckland Volcanic Field, New Zealand, with a new event-order model, *Bulletin of Volcanology* **73**(1), 55–72.

Bebbington, M. and Cronin, S. (2012), Paleomagnetic and geological updates to an event-order model for the Auckland Volcanic Field, *in* 'Proceedings of the 4th International Maar Conference, Geoscience Society of New Zealand Miscellaneous Publication A', Vol. 131, pp. 5–6.

Bebbington, M., Cronin, S., Chapman, I. and Turner, M. (2008), Quantifying volcanic ash fall hazard to electricity infrastructure, *Journal of Volcanology and Geothermal Research* **177**(4), 1055–1062.

Benson, L., Liddicoat, J., Smoot, J., Sarna-Wojcicki, A., Negrini, R. and Lund, S. (2003), Age of the Mono Lake excursion and associated tephra, *Quaternary Science Reviews* **22**(2), 135–140.

Biass, S., Bagheri, G., Aeberhard, W. and Bonadonna, C. (2014), TError: Towards a better quantification of the uncertainty propagated during the characterization of tephra deposits, *Statistics in Volcanology* **1**(2), 1–27.

Bogue, S. W. and Merrill, R. T. (1992), The character of the field during geomagnetic reversals, *Annual Review of Earth and Planetary Sciences* **20**, 181–219.

Bonadonna, C. (2006), *Probabilistic modelling of tephra dispersion*, Geological Society, London, pp. 243–259.

Bonadonna, C., Biass, S. and Costa, A. (2015), Physical characterization of explosive volcanic eruptions based on tephra deposits: Propagation of uncertainties and sensitivity analysis, *Journal of Volcanology and Geothermal Research* **296**, 80–100.

Bonadonna, C., Connor, C. B., Houghton, B. F., Connor, L., Byrne, M., Laing, A. and Hincks, T. K. (2005), Probabilistic modeling of tephra dispersal: Hazard assessment of a multiphase rhyolitic eruption at Tarawera, New Zealand, *Journal of Geophysical Research: Solid Earth* **110**(B3).

Bonadonna, C. and Costa, A. (2012), Estimating the volume of tephra deposits: a new simple strategy, *Geology* **40**(5), 415–418.

Bonadonna, C., Ernst, G. and Sparks, R. (1998), Thickness variations and volume estimates of tephra fall deposits: the importance of particle Reynolds number, *Journal of Volcanology and Geothermal Research* **81**(34), 173–187.

Bonadonna, C. and Houghton, B. (2005), Total grain-size distribution and volume of tephra-fall deposits, *Bulletin of Volcanology* **67**(5), 441–456.

Bonasia, R., Macedonio, G., Costa, A., Mele, D. and Sulpizio, R. (2010), Numerical inversion and analysis of tephra fallout deposits from the 472 AD sub-Plinian eruption at Vesuvius (Italy) through a new best-fit procedure, *Journal of Volcanology and Geothermal Research* **189**(34), 238–246.

Brenna, M., Cronin, S., Smith, I. E., Sohn, Y. K. and Maas, R. (2012), Spatio-temporal evolution of a dispersed magmatic system and its implications for volcano growth, Jeju Island Volcanic Field, Korea, *Lithos* **148**, 337–352.

Bryner, V. (1991), Motukorea: the evolution of an eruption centre in the Auckland Volcanic Field, PhD thesis, University of Auckland, Auckland.

Burden, R., Chen, L. and Phillips, J. (2013), A statistical method for determining the volume of volcanic fall deposits, *Bulletin of Volcanology* **75**(6), 1–10.

Bursik, M. (1998), Tephra dispersal, *Geological Society, London, Special Publications* **145**(1), 115–144.

Bursik, M., Sparks, R. S. J., Gilbert, J. and Carey, S. (1992), Sedimentation of tephra by volcanic plumes: I. Theory and its comparison with a study of the Fogo A plinian deposit, Sao Miguel (Azores), *Bulletin of Volcanology* **54**(4), 329–344.

Camp, V., Hooper, P., Roobol, M. and White, D. (1987), The Madinah eruption, Saudi Arabia: Magma mixing and simultaneous extrusion of three basaltic chemical types, *Bulletin of Volcanology* **49**(2), 489–508.

Cande, S. C. and Kent, D. V. (1995), Revised calibration of the geomagnetic polarity timescale for the Late Cretaceous and Cenozoic, *Journal of Geophysical Research: Solid Earth (1978–2012)* **100**(B4), 6093–6095.

Carey, S. and Sigurdsson, H. (1986), The 1982 eruptions of El Chichón volcano, Mexico (2): Observations and numerical modelling of tephra-fall distribution, *Bulletin of Volcanology* **48**(2-3), 127–141.

Carey, S. and Sparks, R. S. J. (1986), Quantitative models of the fallout and dispersal of tephra from volcanic eruption columns, *Bulletin of Volcanology* **48**(2-3), 109–125.

Cas, R. and Wright, J. (1987), *Volcanic successions, modern and ancient: a geological approach to processes, products and successions*, Chapman & Hall.

Cassata, W. S., Singer, B. S. and Cassidy, J. (2008), Laschamp and Mono Lake geomagnetic excursions recorded in New Zealand, *Earth and Planetary Science Letters* **268**(1), 76–88.

Cassidy, J. (2006), Geomagnetic excursion captured by multiple volcanoes in a monogenetic field, *Geophysical Research Letters* **33**(21).

Cassidy, J. and Hill, M. J. (2009), Absolute palaeointensity study of the Mono Lake excursion recorded by New Zealand basalts, *Physics of the Earth and Planetary Interiors* **172**(3), 225–234.

Cassidy, J. and Locke, C. A. (2010), The Auckland volcanic field, New Zealand: Geophysical evidence for structural and spatio-temporal relationships, *Journal of Volcanology and Geothermal Research* **195**(24), 127–137.

Chen, M.-H. and Deely, J. J. (1996), Bayesian analysis for a constrained linear multiple regression problem for predicting the new crop of apples, *Journal of Agricultural, Biological, and Environmental Statistics* pp. 467–489.

Cleveland, W. S., Grosse, E. and Shyu, W. M. (1992), Local regression models, *Statistical Models in S* pp. 309–376.

Connor, C. B. and Conway, F. M. (2000), Basaltic volcanic fields, *in* H. Sigurdsson, ed., 'Encyclopedia of volcanoes', Academic Press, New York, pp. 331–343.

Connor, C. B. and Hill, B. E. (1995), Three nonhomogeneous Poisson models for the probability of basaltic volcanism: Application to the Yucca Mountain region, Nevada, *Journal of Geophysical Research: Solid Earth* **100**(B6), 10107–10125.

Connor, C. B., Hill, B., Winfrey, B., Franklin, N. and Femina, P. (2001), Estimation of volcanic hazards from tephra fallout, *Natural Hazards Review* **2**(1), 33–42.

Connor, L. and Connor, C. B. (2006), *Inversion is the key to dispersion understanding eruption dynamics by inverting tephra fallout*, Geological Society Publishing House, chapter .

Costa, A., Dell'Erba, F., Vito, M., Isaia, R., Macedonio, G., Orsi, G. and Pfeiffer, T. (2009), Tephra fallout hazard assessment at the Campi Flegrei caldera (Italy), *Bulletin of Volcanology* **71**(3), 259–273.

Costa, A., Folch, A. and Macedonio, G. (2013), Density-driven transport in the umbrella region of volcanic clouds: Implications for tephra dispersion models, *Geophysical Research Letters* **40**(18), 4823–4827.

Costa, A., Macedonio, G. and Folch, A. (2006), A three-dimensional Eulerian model for transport and deposition of volcanic ashes, *Earth and Planetary Science Letters* **241**(34), 634–647.

Cronin, S., Hedley, M. J., Neall, V. E. and Smith, R. G. (1998), Agronomic impact of tephra fallout from the 1995 and 1996 Ruapehu Volcano eruptions, New Zealand, *Environmental Geology* **34**(1), 21–30.

Daggitt, M. L., Mather, T. A., Pyle, D. and Page, S. (2014), AshCalc - a new tool for the comparison of the exponential, power-law and Weibull models of tephra deposition, *Journal of Applied Volcanology* **3**(1), 7.

Dalrymple, G. B. and Lanphere, M. A. (1969), Potassium-argon dating: Principles, techniques and applications to geochronology, *in* 'Freeman', p. 258.

Dalrymple, G. B. and Lanphere, M. A. (1971), ^{40}Ar/^{39}Ar technique of KAr dating: a comparison with the conventional technique, *Earth and Planetary Science Letters* **12**(3), 300–308.

Danišík, M., Shane, P., Schmitt, A. K., Hogg, A., Santos, G. M., Storm, S., Evans, N. J., Fifield, L. K. and Lindsay, J. M. (2012), Re-anchoring the late Pleistocene tephrochronology of New Zealand based on concordant radiocarbon ages and combined $^{238}U/^{230}Th$ disequilibrium and (U–Th)/He zircon ages, *Earth and Planetary Science Letters* **349**, 240–250.

Davidson, J. M. (1972), Archaeological investigations on Motutapu Island, New Zealand, *Records of the Auckland Institute and Museum* **9**, 1–14.

Eade, J. G. (2009), Petrology and correlation of lava flows from the central part of the Auckland Volcanic Field, PhD thesis, University of Auckland, Auckland.

East, G. and George, A. (2003), The construction of the Auckland Central Remand Prison on the Mt Eden basalt flow, *in* 'Geotechnics on the Volcanic Edge: Tauranga, March 2003, New Zealand Geotechnical Society Symposium', Institution of Professional Engineers New Zealand, p. 387.

Einsele, G. (2000), *Sedimentary basins: Evolution, facies, and sediment budget*, Springer Science & Business Media, Berlin.

El Difrawy, M., Runge, M., Moufti, M., Cronin, S. and Bebbington, M. (2013), A first hazard analysis of the Quaternary Harrat Al-Madinah volcanic field, Saudi Arabia, *Journal of Volcanology and Geothermal Research* **267**, 39–46.

Engwell, S., Sparks, R. S. J. and Aspinall, W. (2013), Quantifying uncertainties in the measurement of tephra fall thickness, *Journal of Applied Volcanology* **2**(1), 1–12.

Fergusson, G., Grant-Taylor, T. and Rafter, T. (1959), New Zealand radiocarbon age measurements-4, *New Zealand Journal of Geology and Geophysics* **2**, 208–241.

Fierstein, J. and Nathenson, M. (1992), Another look at the calculation of fallout tephra volumes, *Bulletin of Volcanology* **54**(2), 156–167.

Fodor, E. and Németh, K. (2014), Spatter cone, *in* 'Encyclopedia of planetary landforms', Springer New York, pp. 1–9.

Folch, A. (2012), A review of tephra transport and dispersal models: Evolution, current status, and future perspectives, *Journal of Volcanology and Geothermal Research* **235**, 96–115.

Folch, A., Costa, A. and Macedonio, G. (2009), FALL3D: a computational model for transport and deposition of volcanic ash, *Computers and Geosciences* **35**(6), 1334–1342.

Froese, D. G., Lowe, D. J., Knott, J. R. and Slate, J. L. (2008), Global tephra studies: John Westgate and Andrei Sarna-Wojcicki commemorative volume, *Quaternary International* **178**(1), 1–3.

Garcia-Aristizabal, A., Selva, J. and Fujita, E. (2013), Integration of stochastic models for long-term eruption forecasting into a Bayesian event tree scheme: a basis method to estimate the probability of volcanic unrest, *Bulletin of Volcanology* **75**(2), 1–13.

Gonzlalez-Mellado, A. O. and De la Cruz-Reyna, S. (2010), A simple semi-empirical approach to model thickness of ash-deposits for different eruption scenarios, *Natural Hazards and Earth System Science* **10**(11), 2241–2257.

Gornitz, V. (2008), *Encyclopedia of paleoclimatology and ancient environments*, Springer Science & Business Media, New York.

Grant-Taylor, T. L. and Rafter, T. (1963), *New Zealand natural radiocarbon measurements IV*, American Journal of Science.

Grant-Taylor, T. and Rafter, T. (1971), New Zealand radiocarbon age measurements–6, *New Zealand Journal of Geology and Geophysics* **14**(2), 364–402.

Green, R. M., Bebbington, M., Cronin, S. and Jones, G. (2014), Automated statistical matching of multiple tephra records exemplified using five long maar sequences younger than 75ka, Auckland, New Zealand, *Quaternary Research* **82**(2), 405–419.

Grenfell, H. and Kenny, J. (1995), Another piece in the Auckland Volcanic Field jigsaw puzzle - or are we stumped, *Geological Society New Zealand Newsletter* **107**, 42–43.

Guillou, H., Singer, B. S., Laj, C., Kissel, C., Scaillet, S. and Jicha, B. R. (2004), On the age of the Laschamp geomagnetic excursion, *Earth and Planetary Science Letters* **227**(3), 331–343.

Hay, R. and Jones, B. (1972), Weathering of basaltic tephra on the island of Hawaii, *Geological Society of America Bulletin* **83**(2), 317–332.

Hayward, B. (2008*a*), Ash Hill Volcano, Wiri, *Panmure Basin Tuff Ring Bruce Hayward, Helen Holzer* p. 8.

Hayward, B. (2008*b*), Subject of Hochstetter and Heaphy debate site becomes reserve, *Geological Society New Zealand Newsletter* **147**, 15–19.

Hayward, B., Kenny, J. and Grenfell, H. (2011*a*), More volcanoes recognised in Auckland Volcanic Field, *GeoScience Society of New Zealand Newsletter* **5**, 11–16.

Hayward, B., Kenny, J. and Grenfell, H. (2011*b*), Puhini craters, *Geocene* pp. 1–6.

Hayward, B., Kenny, J., High, R. and France, S. (2011), Grafton volcano, *Geocene* pp. 12–17.

Hayward, B., Murdoch, G. and Maitland, G. (2011), Volcanoes of Auckland: the essential guide, *New Zealand Science Review* **68**, 123–124.

Heiken, G., Murphy, M., Hackett, W. and Scott, W. (1998), *Volcanic hazards and energy infrastructure, U. S.*, DIANE Publishing Company.

Hill, D., of Mines, C. D. and Geology (2002), *Response plan for volcano hazards in the Long Valley Caldera and Mono Craters region, California*, U.S. Geological Survey bulletin, US Department of the Interior, US Geological Survey.

Hurst, A. W. and Turner, R. (1999), Performance of the program ASHFALL for forecasting ashfall during the 1995 and 1996 eruptions of Ruapehu volcano, *New Zealand Journal of Geology and Geophysics* **42**(4), 615–622.

Hurst, T. and Smith, W. (2004), A Monte Carlo methodology for modelling ashfall hazards, *Journal of Volcanology and Geothermal Research* **138**(34), 393–403.

Hurst, T. and Smith, W. (2010), Volcanic ashfall in New Zealand - probabilistic hazard modelling for multiple sources, *New Zealand Journal of Geology and Geophysics* **53**(1), 1–14.

Jenkins, S. F., Magill, C. and McAneney, K. J. (2007), Multi-stage volcanic events: a statistical investigation, *Journal of Volcanology and Geothermal Research* **161**(4), 275–288.

Johnson, R. and Threlfall, N. (1937), *Volcano town: the 1937-43 Rabaul eruptions*, Robert Brown and Associates, Bathurst.

Johnston, E., Phillips, J., Bonadonna, C. and Watson, I. (2012), Reconstructing the tephra dispersal pattern from the Bronze Age eruption of Santorini using an advection-diffusion model, *Bulletin of Volcanology* **74**(6), 1485–1507.

Kagan, Y. and Knopoff, L. (1977), Earthquake risk prediction as a stochastic process, *Physics of the Earth and Planetary Interiors* **14**(2), 97–108.

Kawabata, E., Bebbington, M., Cronin, S. and Wang, T. (2013), Modeling thickness variability in tephra deposition, *Bulletin of Volcanology* **75**(8), 1–14.

Kawabata, E., Cronin, S., Bebbington, M., Moufti, M., El-Masry, N. and Wang, T. (2015), Identifying multiple eruption phases from a compound tephra blanket: an example of the AD1256 Al-Madinah eruption, Saudi Arabia, *Bulletin of Volcanology* **77**(1).

Kereszturi, G., Cappello, A., Ganci, G., Procter, J., Németh, K., Del Negro, C. and Cronin, S. (2014), Numerical simulation of basaltic lava flows in the Auckland Volcanic Field, New Zealand - implication for volcanic hazard assessment, *Bulletin of Volcanology* **76**(11), 1–17.

Kereszturi, G., Németh, K., Cronin, S., Agustín-Flores, J., Smith, I. E. and Lindsay, J. M. (2013), A model for calculating eruptive volumes for monogenetic volcanoes implication for the Quaternary Auckland Volcanic Field, New Zealand, *Journal of Volcanology and Geothermal Research* **266**(0), 16–33.

Kereszturi, G., Procter, J., Cronin, S., Németh, K., Bebbington, M. and Lindsay, J. M. (2012), LiDAR-based quantification of lava flow susceptibility in the City of Auckland (New Zealand), *Remote Sensing of Environment* **125**, 198–213.

Kermode, L. and Heron, D. (1992), *Geology of the Auckland Urban Area: Sheet R11: 1: 50 000*, Institute of Geological & Nuclear Sciences.

Kermode, L., Smith, I. E., Moore, C., Stewart, R., Ashcroft, J., Nowell, S. and Hayward, B. (1992), Inventory of Quaternary volcanoes and volcanic features of Northland, South Auckland and Taranaki, *Geological Society of New Zealand Miscellaneous Publication* **61**, 100.

Kienle, J., Kyle, P. R., Self, S., Motyka, R. J. and Lorenz, V. (1980), Ukinrek Mars, Alaska, I. April 1977 eruption sequence, petrology and tectonic setting, *Journal of Volcanology and Geothermal Research* **7**(12), 11–37.

Kilburn, C. R. (2003), Multiscale fracturing as a key to forecasting volcanic eruptions, *Journal of Volcanology and Geothermal Research* **125**(34), 271–289.

Klawonn, M., Houghton, B. F., Swanson, D. A., Fagents, S. A., Wessel, P. and Wolfe, C. J. (2014), From field data to volumes: Constraining uncertainties in pyroclastic eruption parameters, *Bulletin of Volcanology* **76**(7), 1–16.

Kratzmann, D. J., Carey, S. N., Fero, J., Scasso, R. A. and Naranjo, J.-A. (2010), Simulations of tephra dispersal from the 1991 explosive eruptions of Hudson volcano, Chile, *Journal of Volcanology and Geothermal Research* **190**(34), 337–352.

Krumbein, W. C. (1934), Size frequency distributions of sediments, *Journal of Sedimentary Research* **4**(2).

Le Corvec, N., Bebbington, M., Lindsay, J. M. and McGee, L. E. (2013), Age, distance, and geochemical evolution within a monogenetic volcanic field: Analyzing patterns in the Auckland Volcanic Field eruption sequence, *Geochemistry, Geophysics, Geosystems* **14**(9), 3648–3665.

Legros, F. (2000), Minimum volume of a tephra fallout deposit estimated from a single isopach, *Journal of Volcanology and Geothermal Research* **96**(1), 25–32.

Lindsay, J. M. and Leonard, G. (2009), Age of the Auckland Volcanic Field, Technical report, Institute of Earth Science and Engineering.

Lindsay, J. M., Leonard, G., Smid, E. and Hayward, B. (2011), Age of the Auckland Volcanic Field: a review of existing data, *New Zealand Journal of Geology and Geophysics* **54**(4), 379–401.

Lindsay, J. M., Marzocchi, W., Jolly, G., Constantinescu, R., Selva, J. and Sandri, L. (2010), Towards real-time eruption forecasting in the Auckland Volcanic Field: Application of BET_EF during the New Zealand National Disaster Exercise 'Ruaumoko', *Bulletin of Volcanology* **72**(2), 185–204.

Lorenz, V. (1985), Maars and diatremes of phreatomagmatic origin; a review, *South African Journal of Geology* **88**(2), 459–470.

Lorenz, V. (1986), On the growth of maars and diatremes and its relevance to the formation of tuff rings, *Bulletin of Volcanology* **48**(5), 265–274.

Lowe, D. J., Blaauw, M., Hogg, A. G. and Newnham, R. M. (2013), Ages of 24 widespread tephras erupted since 30,000 years ago in New Zealand, with re-evaluation of the timing and palaeoclimatic implications of the Lateglacial cool episode recorded at Kaipo bog, *Quaternary Science Reviews* **74**, 170–194.

Macedonio, G., Costa, A. and Longo, A. (2005), A computer model for volcanic ash fallout and assessment of subsequent hazard, *Computers and Geosciences* **31**(7), 837–845.

Macedonio, G., Pareschi, M. T. and Santacroce, R. (1988), A numerical simulation of the Plinian fall phase of 79 A.D. eruption of Vesuvius, *Journal of Geophysical Research: Solid Earth* **93**(B12), 14817–14827.

Magill, C. (2007), Reply to comments on 'Probabilistic tephra fall simulation for the Auckland region, New Zealand by', *Journal of Volcanology and Geothermal Research* **159**(4), 423–424.

Magill, C., Blong, R. and McAneney, J. (2006), VolcaNZ - a volcanic loss model for Auckland, New Zealand, *Journal of Volcanology and Geothermal Research* **149**(3), 329–345.

Magill, C., Hurst, A., Hunter, L. and Blong, R. (2006), Probabilistic tephra fall simulation for the Auckland Region, New Zealand, *Journal of Volcanology and Geothermal Research* **153**(34), 370–386.

Magill, C., McAneney, K. and Smith, I. E. (2005), Probabilistic assessment of vent locations for the next Auckland volcanic field event, *Mathematical Geology* **37**(3), 227–242.

Mannen, K. (2006), Total grain size distribution of a mafic subplinian tephra, TB-2, from the 1986 Izu-Oshima eruption, Japan: an estimation based on a theoretical model of tephra dispersal, *Journal of Volcanology and Geothermal Research* **155**(12), 1–17.

Marra, M., Alloway, B. and Newnham, R. (2006), Paleoenvironmental reconstruction of a well-preserved Stage 7 forest sequence catastrophically buried by basaltic eruptive deposits, northern New Zealand, *Quaternary Science Reviews* **25**(17), 2143–2161.

Marzocchi, W. (1996), Chaos and stochasticity in volcanic eruptions the case of Mount Etna and Vesuvius, *Journal of Volcanology and Geothermal Research* **70**(34), 205–212.

Marzocchi, W. and Bebbington, M. (2012), Probabilistic eruption forecasting at short and long time scales, *Bulletin of Volcanology* **74**(8), 1777–1805.

Marzocchi, W., Sandri, L., Gasparini, P., Newhall, C. and Boschi, E. (2004), Quantifying probabilities of volcanic events: the example of volcanic hazard at Mount Vesuvius, *Journal of Geophysical Research: Solid Earth* **109**(B11).

Marzocchi, W., Sandri, L. and Selva, J. (2008), BET_EF: a probabilistic tool for long- and short-term eruption forecasting, *Bulletin of Volcanology* **70**(5), 623–632.

Marzocchi, W., Sandri, L. and Selva, J. (2010), BET_VH: a probabilistic tool for long-term volcanic hazard assessment, *Bulletin of Volcanology* **72**(6), 705–716.

McBirney, A. and Godoy, A. (2003), Notes on the IAEA guidelines for assessing volcanic hazards at nuclear facilities, *Journal of Volcanology and Geothermal Research* **126**(1), 1–9.

McCormac, F. G., Hogg, A. G., Blackwell, P. G., Buck, C. E., Higham, T. F. and Reimer, P. J. (2004), SHCal04 Southern Hemisphere calibration, 0–11.0 cal kyr BP, *Radiocarbon* **46**(3), 1087–1092.

McDougall, I. and Harrison, T. M. (1999), *Geochronology and thermochronology by the $^{40}Ar/^{39}Ar$ method*, Oxford University Press.

McDougall, I., Polach, H. and Stipp, J. (1969), Excess radiogenic argon in young subaerial basalts from the Auckland volcanic field, New Zealand, *Geochimica et Cosmochimica Acta* **33**(12), 1485–1520.

McKeever, S. and Moscovitch, M. (2003), Topics under debate - on the advantages and disadvantages of optically stimulated luminescence dosimetry and thermoluminescence dosimetry, *Radiation Protection Dosimetry* **104**(3), 263–270.

Meloy, A. F. (2006), Arenal-type pyroclastic flows: a probabilistic event tree risk analysis, *Journal of Volcanology and Geothermal Research* **157**(1), 121–134.

Miller, T. and Casadevall, T. (2000), *Volcanic ash hazards to aviation*, Encyclopedia of Volcanoes, Academic Press, San Diego, California, USA.

Mochizuki, N., Tsunakawa, H., Shibuya, H., Tagami, T., Ozawa, A., Cassidy, J. and Smith, I. E. (2004), K-Ar ages of the Auckland geomagnetic excursions, *Earth, Planets, and Space* **56**(2), 283–288.

Mochizuki, N., Tsunakawa, H., Shibuya, H., Tagami, T., Ozawa, A. and Smith, I. E. (2007), Further K-Ar dating and paleomagnetic study of the Auckland geomagnetic excursions, *Earth, Planets, and Space* **59**(7), 755–761.

Molloy, C., Shane, P. and Augustinus, P. (2009), Eruption recurrence rates in a basaltic volcanic field based on tephra layers in maar sediments: Implications for hazards in the Auckland volcanic field, *Geological Society of America Bulletin* **121**(11-12), 1666–1677.

Murray, A. S. and Olley, J. M. (2002), Precision and accuracy in the optically stimulated luminescence dating of sedimentary quartz: a status review, *Geochronometria* **21**(1), 1–16.

Needham, A., Lindsay, J. M., Smith, I. E., Augustinus, P. and Shane, P. (2011), Sequential eruption of alkaline and sub-alkaline magmas from a small monogenetic volcano in the Auckland Volcanic Field, New Zealand, *Journal of Volcanology and Geothermal Research* **201**(1), 126–142.

Neri, A., Aspinall, W., Cioni, R., Bertagnini, A., Baxter, P., Zuccaro, G., Andronico, D., Barsotti, S., Cole, P., Ongaro, T. E., Hincks, T., Macedonio, G., Papale, P., Rosi, M., Santacroce, R. and Woo, G. (2008), Developing an event tree for probabilistic hazard and risk assessment at Vesuvius, *Journal of Volcanology and Geothermal Research* **178**(3), 397–415.

Newhall, C. and Hoblitt, R. (2002), Constructing event trees for volcanic crises, *Bulletin of Volcanology* **64**(1), 3–20.

Newnham, R. M. and Lowe, D. J. (1991), Holocene vegetation and volcanic activity, Auckland isthmus, New Zealand, *Journal of Quaternary Science* **6**(3), 177–193.

Newnham, R. M., Lowe, D. J. and Alloway, B. V. (1999), Volcanic hazards in Auckland, New Zealand: a preliminary assessment of the threat posed by central North Island silicic volcanism based on the Quaternary tephrostratigraphical record, *Geological Society, London, Special Publications* **161**(1), 27–45.

O'Hagan, A., Buck, C. E., Daneshkhah, A., Eiser, J. R., Garthwaite, P. H., Jenkinson, D. J., Oakley, J. E. and Rakow, T. (2006), *Uncertain judgements: Eliciting experts' probabilities*, John Wiley & Sons.

Pfeiffer, T., Costa, A. and Macedonio, G. (2005), A model for the numerical simulation of tephra fall deposits, *Journal of Volcanology and Geothermal Research* **140**(4), 273–294.

Phillips, D. (1989), *Aspects of thermoluminescence dating of plagioclase feldspars*, University of Auckland, Auckland.

Polach, H., Chappell, J. and Lovering, J. (1969), ANU radiocarbon date list III, *Radiocarbon* **11**(2), 245–262.

Pyle, D. (1989), The thickness, volume and grainsize of tephra fall deposits, *Bulletin of Volcanology* **51**(1), 1–15.

Pyle, D. (2000), *Sizes of volcanic eruptions*, Encyclopedia of Volcanoes, Academic Press, San Diego, California, USA.

Ramsey, C. B. (2014), Radiocarbon dating in paleoseismology, *Encyclopedia of Earthquake Engineering* .

Rhoades, D., Dowrick, D. and Wilson, C. (2002), Volcanic hazard in New Zealand: Scaling and attenuation relations for tephra fall deposits from Taupo Volcano, *Natural Hazards* **26**(2), 147–174.

Richter, D. (2007), Advantages and limitations of thermoluminescence dating of heated flint from Paleolithic sites, *Geoarchaeology* **22**(6), 671–683.

Richter, D. H., Eaton, J., Murata, K., Ault, W. and Krivoy, H. (1970), *Chronological narrative of the 1959-60 eruption of Kilauea volcano, Hawaii*, US Government Printing Office.

Robertson, D. (1986), A paleomagnetic study of Rangitoto Island, Auckland, New Zealand, *New Zealand Journal of Geology and Geophysics* **29**(4), 405–411.

Robertson, D. J. (1983), Paleomagnetism and geochronology of volcanics in the northern North Island, New Zealand, PhD thesis, University of Auckland.

Rose, W. (1993), Comment on 'another look at the calculation of fallout tephra volumes' by Judy Fierstein and Manuel Nathenson, *Bulletin of Volcanology* **55**(5), 372–374.

Runge, M. G., Bebbington, M., Cronin, S., Lindsay, J. M., Kenedi, C. L. and Moufti, M. (2014), Vents to events: Determining an eruption event record from volcanic vent structures for the Harrat Rahat, Saudi Arabia, *Bulletin of Volcanology* **76**(3), 1–16.

Sameshima, T. (1990), Chemical and dating data on some of the monogenetic volcanoes of Auckland, *in* 'Geological Society of New Zealand'.

Sandiford, A., Alloway, B. and Shane, P. (2001), A 28 000-6600 cal yr record of local and distal volcanism preserved in a paleolake, Auckland, New Zealand, *New Zealand Journal of Geology and Geophysics* **44**(2), 323–336.

Sandiford, A., Horrocks, M., Newnham, R., Ogden, J. and Alloway, B. (2002), Environmental change during the last glacial maximum (c. 25 000-c. 16 500 years BP) at Mt Richmond, Auckland Isthmus, New Zealand, *Journal of the Royal Society of New Zealand* **32**(1), 155–167.

Sandri, L., Jolly, G., Lindsay, J. M., Howe, T. and Marzocchi, W. (2012), Combining long- and short-term probabilistic volcanic hazard assessment with cost-benefit analysis to support decision making in a volcanic crisis from the Auckland Volcanic Field, New Zealand, *Bulletin of Volcanology* **74**(3), 705–723.

Sato, H. and Taniguchi, H. (1997), Relationship between crater size and ejecta volume of recent magmatic and phreato-magmatic eruptions: Implications for energy partitioning, *Geophysical research letters* **24**(3), 205–208.

Scollo, S., Carlo, P. D. and Coltelli, M. (2007), Tephra fallout of 2001 Etna flank eruption: Analysis of the deposit and plume dispersion, *Journal of Volcanology and Geothermal Research* **160**(12), 147–164.

Scollo, S., Tarantola, S., Bonadonna, C., Coltelli, M. and Saltelli, A. (2008), Sensitivity analysis and uncertainty estimation for tephra dispersal models, *Journal of Geophysical Research: Solid Earth* **113**(B6).

Searle, E. J. (1959), The volcanoes of Ihumatao and Mangere, Auckland, *New Zealand Journal of Geology and Geophysics* **2**(5), 870–888.

Searle, E. J. (1962), The volcanoes of Auckland city, *New Zealand Journal of Geology and Geophysics* **5**(2), 193–227.

Searle, E. J. (1965), Auckland volcanic district, *New Zealand Department of Scientific and Industrial Research* **49**, 90–103.

Self, S., Kienle, J. and Huot, J.-P. (1980), Ukinrek Maars, Alaska, II. Deposits and formation of the 1977 craters, *Journal of Volcanology and Geothermal Research* **7**(12), 39–65.

Self, S., Sparks, R. S. J., Booth, B. and Walker, G. P. L. (1974), The 1973 Heimaey strombolian scoria deposit, Iceland, *Geological Magazine* **111**, 539–548.

Selva, J., Costa, A., Marzocchi, W. and Sandri, L. (2010), BET_VH: Exploring the influence of natural uncertainties on long-term hazard from tephra fallout at Campi Flegrei (Italy), *Bulletin of Volcanology* **72**(6), 717–733.

Shane, P. (2005), Towards a comprehensive distal andesitic tephrostratigraphic framework for New Zealand based on eruptions from Egmont volcano, *Journal of Quaternary Science* **20**(1), 45–57.

Shane, P. (2007), Comment on: 'probabilistic tephra fall simulation for the Auckland region, New Zealand by', *Journal of Volcanology and Geothermal Research* **159**(4), 421–422.

Shane, P. and Hoverd, J. (2002), Distal record of multi-sourced tephra in Onepoto Basin, Auckland, New Zealand: Implications for volcanic chronology, frequency and hazards, *Bulletin of Volcanology* **64**(7), 441–454.

Shane, P. and Sandiford, A. (2003), Paleovegetation of marine isotope stages 4 and 3 in Northern New Zealand and the age of the widespread Rotoehu tephra, *Quaternary Research* **59**(3), 420–429.

Shibuya, H., Cassidy, J., Smith, I. E. and Itaya, T. (1992), A geomagnetic excursion in the Brunhes epoch recorded in New Zealand basalts, *Earth and planetary science letters* **111**(1), 41–48.

Sibson, R. H. (1968), Late Pleistocene volcanism in the East Tamaki district, PhD thesis, University of Auckland, Auckland.

Siebert, L., Simkin, T. and Kimberly, P. (2010), *Volcanoes of the World*, 3rd edn, University of California Press, California.

Sigurdsson, H., Houghton, B., Rymer, H., Stix, J. and McNutt, S. (1999), *Encyclopedia of volcanoes*, Academic Press.

Singer, B. S. (2007), Polarity transitions: Radioisotopic dating, *in* 'Encyclopedia of Geomagnetism and Paleomagnetism', Springer, pp. 834–839.

Smith, I. E., Blake, S., Wilson, C. and Houghton, B. (2008), Deep-seated fractionation during the rise of a small-volume basalt magma batch: Crater Hill, Auckland, New Zealand, *Contributions to Mineralogy and Petrology* **155**(4), 511–527.

Sparks, R. S. J. (1986), The dimensions and dynamics of volcanic eruption columns, *Bulletin of Volcanology* **48**(1), 3–15.

Sparks, R. S. J. (2003), Forecasting volcanic eruptions, *Earth and Planetary Science Letters* **210**(12), 1–15.

Sparks, R. S. J., Bursik, M., Ablay, G., Thomas, R. and Carey, S. (1992), Sedimentation of tephra by volcanic plumes. Part 2: Controls on thickness and grain-size variations of tephra fall deposits, *Bulletin of Volcanology* **54**(8), 685–695.

Sparks, R. S. J., Bursik, M., Carey, S., Gilbert, J., Glaze, L., Sigurdsson, H. and Woods, A. (1997), *Volcanic plumes*, Wiley, Chichester.

Stewart, C., Johnston, D., Leonard, G., Horwell, C., Thordarson, T. and S.Cronin (2006), Contamination of water supplies by volcanic ashfall: a literature review and simple impact modelling, *Journal of Volcanology and Geothermal Research* **158**(34), 296–306.

Stipp, J. J. (1968), *The geochronology and petrogenesis of the Cenozoic volcanics of North Island, New Zealand*, Australian National University.

Sulpizio, R. (2005), Three empirical methods for the calculation of distal volume of tephra-fall deposits, *Journal of Volcanology and Geothermal Research* **145**(34), 315–336.

Suzuki, T. (1983), A theoretical model for dispersion of tephra, *Arc Volcanism, Physics and Tectonics* pp. 95–113.

Thórarinsson, S. (1954), *The tephra-fall from Hekla on March 29th 1947*, HF Leiftur.

Turner, G., Robinson, N. and Verosub, K. (2002), Preliminary palaeomagnetic results from the holocene sediments of Lake Pupuke, Auckland, New Zealand, *Eos Transactions AGU Western Pacific Geophysics Meeting Supplement* **83**, 125.

Turner, M., Bebbington, M., Cronin, S. and Stewart, R. (2009), Merging eruption datasets: Building an integrated Holocene eruptive record for Mt Taranaki, New Zealand, *Bulletin of Volcanology* **71**(8), 903–918.

Utsu, T. (1999), Representation and analysis of the earthquake size distribution: a historical review and some new approaches, *Pure and Applied Geophysics* **155**(2-4), 509–535.

Vespermann, D. and Schmincke, H.-U. (2000), *Scoria cones and tuff rings*, Academic Press, San Diego, pp. 683–694.

Voight, B. and Cornelius, R. (1991), Prospects for eruption prediction in near real-time, *Nature* **350**, 695–698.

Volentik, A. C., Bonadonna, C., Connor, C. B., Connor, L. and Rosi, M. (2010), Modeling tephra dispersal in absence of wind: Insights from the climactic phase of the 2450 BP Plinian eruption of Pululagua volcano (Ecuador), *Journal of Volcanology and Geothermal Research* **193**(12), 117–136.

Walker, G. P. (1993), Basaltic-volcano systems, *Geological Society, London, Special Publications* **76**(1), 3–38.

Ward, G. and Wilson, S. (1978), Procedures for comparing and combining radiocarbon age determinations: a critique, *Archaeometry* **20**(1), 19–31.

Wentworth, C. K. and Macdonald, G. A. (1953), Structures and forms of basaltic rocks in Hawaii, Technical report, US Government Printing Office.

Wentworth, C. K. and Williams, H. (1932), *The classification and terminology of the pyroclastic rocks*, Place of publication not identified.

Wilson, L., Sparks, R. S. J., Huang, T. C. and Watkins, N. D. (1978), The control of volcanic column heights by eruption energetics and dynamics, *Journal of Geophysical Research: Solid Earth* **83**(B4), 1829–1836.

Wood, I. A. (1991), Thermoluminescence dating of the Auckland and Kerikeri basalt fields, PhD thesis, University of Auckland, Auckland.

Appendix A

The marginal posterior probabilities of matching AVF volcanoes and their tephras

Table 7.4 showed the marginal probabilities for a volcano to have produced a given tephra for the baseline scenario with B = $\{\alpha = 2.0,\ \beta U = 0.5\}$. Five other environmental conditions were considered, namely A = $\{\alpha = 1.5,\ \beta U = 0.5\}$; C = $\{\alpha = 2.5,\ \beta U = 0.5\}$; D = $\{\alpha = 1.5,\ \beta U = 1.0\}$; E = $\{\alpha = 2.0,\ \beta U = 1.0\}$; F = $\{\alpha = 2.5,\ \beta U = 1.0\}$. In addition to the baseline scenario, four other scenarios were considered, namely Maungataketake and North Head are too old for any tephras; Three Kings is assigned to AVF 9; Three Kings is assigned to AVF 10; and AVF 9 is split into AVF 9A and 9B. The marginal probabilities for these environmental conditions and scenarios are tabulated here.

Table A.1: Marginal posterior probabilities for a volcano to have produced a given tephra for the baseline scenario with A = $\{\alpha = 1.5, \beta U = 0.5\}$.

Volcano	AVF tephra (AVF 0 = 'unmatched')																				
	0	1	2	3	4	5	6	7	8	9	10	11	12	13	14	15	16	17	18	19	20
Ash Hill	0.8327	0.0000	0.0000	0.0000	0.0000	0.0003	0.1354	0.0316	0.0000	0.0000	0.0000	0.0000	0.0000	0.0000	0.0000	0.0000	0.0000	0.0000	0.0000	0.0000	0.0000
Cemetery Hill	0.0382	0.0000	0.0000	0.0000	0.0002	0.0171	0.1406	0.1915	0.5150	0.0969	0.0005	0.0000	0.0000	0.0000	0.0000	0.0000	0.0000	0.0000	0.0000	0.0000	0.0000
Crater Hill	0.0000	0.0000	0.0000	0.0000	0.0000	0.0001	0.0158	0.0068	0.3024	0.5595	0.1148	0.0006	0.0000	0.0000	0.0000	0.0000	0.0000	0.0000	0.0000	0.0000	0.0000
Domain	0.7601	0.1289	0.0917	0.0193	0.0000	0.0000	0.0000	0.0000	0.0000	0.0000	0.0000	0.0000	0.0000	0.0000	0.0000	0.0000	0.0000	0.0000	0.0000	0.0000	0.0000
Green Hill	0.0139	0.0007	0.0033	0.0178	0.0237	0.0166	0.0062	0.0003	0.0002	0.0040	0.0384	0.0158	0.0504	0.1906	0.1220	0.1010	0.0774	0.0843	0.1103	0.0917	0.0314
Hampton Park	0.3732	0.0000	0.0000	0.0000	0.0000	0.0000	0.0000	0.0000	0.0000	0.0000	0.0000	0.0000	0.0000	0.0668	0.1519	0.2027	0.1087	0.0694	0.0162	0.0073	0.0038
Hopua	0.8020	0.0000	0.0000	0.0002	0.0000	0.0645	0.0490	0.0346	0.0003	0.0020	0.0453	0.0021	0.0000	0.0000	0.0000	0.0000	0.0000	0.0000	0.0000	0.0000	0.0000
Kohuora	0.0000	0.0001	0.0017	0.0139	0.8775	0.0602	0.0456	0.0005	0.0005	0.0000	0.0000	0.0000	0.0000	0.0000	0.0000	0.0000	0.0000	0.0000	0.0000	0.0000	0.0000
Little Rangitoto	0.0571	0.1972	0.1897	0.1462	0.0183	0.0127	0.0014	0.0010	0.0009	0.0023	0.0145	0.0045	0.0160	0.0496	0.0379	0.0287	0.0213	0.0301	0.0481	0.0521	0.0704
Mangere Lagoon	0.7233	0.0497	0.0632	0.0636	0.0005	0.0069	0.0022	0.0002	0.0000	0.0006	0.0067	0.0028	0.0053	0.0251	0.0213	0.0154	0.0105	0.0027	0.0000	0.0000	0.0000
Matukutureia	0.0254	0.0000	0.0000	0.0000	0.0000	0.0000	0.0000	0.0000	0.0000	0.0007	0.0079	0.0026	0.0056	0.1381	0.0990	0.0853	0.0685	0.0645	0.0934	0.2046	0.2044
Maungataketake	0.9954	0.0014	0.0000	0.0028	0.0000	0.0000	0.0004	0.0000	0.0000	0.0000	0.0000	0.0000	0.0000	0.0000	0.0000	0.0000	0.0000	0.0000	0.0000	0.0000	0.0000
McLennan Hills	0.9345	0.0000	0.0138	0.0411	0.0000	0.0096	0.0006	0.0004	0.0000	0.0000	0.0000	0.0000	0.0000	0.0000	0.0000	0.0000	0.0000	0.0000	0.0000	0.0000	0.0000
Motukorea	0.9466	0.0024	0.0015	0.0001	0.0000	0.0019	0.0000	0.0000	0.0000	0.0000	0.0008	0.0000	0.0000	0.0072	0.0009	0.0046	0.0023	0.0268	0.0010	0.0016	0.0023
Mt Albert	0.8821	0.0612	0.0377	0.0175	0.0008	0.0005	0.0001	0.0000	0.0000	0.0000	0.0001	0.0000	0.0000	0.0000	0.0000	0.0000	0.0000	0.0000	0.0000	0.0000	0.0000
Mt Cambria	0.7500	0.0075	0.0112	0.0157	0.0032	0.0065	0.0000	0.0000	0.0000	0.0000	0.0016	0.0000	0.0000	0.0346	0.0102	0.0551	0.0173	0.0847	0.0012	0.0011	0.0001
Mt Eden	0.0249	0.0000	0.0000	0.0000	0.0000	0.0000	0.0000	0.0000	0.0000	0.0009	0.0362	0.3823	0.5557	0.0000	0.0000	0.0000	0.0000	0.0000	0.0000	0.0000	0.0000
Mt Hobson	0.1328	0.0000	0.0000	0.0000	0.0000	0.0000	0.0000	0.0000	0.0000	0.0000	0.0002	0.0035	0.0176	0.1205	0.0879	0.0731	0.0603	0.0826	0.1115	0.1320	0.1780
Mt Mangere	0.0084	0.0000	0.0000	0.0000	0.0000	0.0000	0.0000	0.0000	0.0000	0.0000	0.0000	0.0000	0.0000	0.0047	0.0421	0.1346	0.3430	0.3226	0.1404	0.0042	0.0000
Mt Richmond	0.7788	0.0000	0.0000	0.0000	0.0000	0.0016	0.0708	0.1488	0.0000	0.0000	0.0000	0.0000	0.0000	0.0000	0.0000	0.0000	0.0000	0.0000	0.0000	0.0000	0.0000
Mt Roskill	0.9432	0.0209	0.0259	0.0019	0.0001	0.0053	0.0001	0.0002	0.0000	0.0000	0.0024	0.0000	0.0000	0.0000	0.0000	0.0000	0.0000	0.0000	0.0000	0.0000	0.0000
Mt Smart	0.0128	0.0000	0.0000	0.0000	0.0000	0.0000	0.0000	0.0000	0.0000	0.0000	0.0000	0.0000	0.0000	0.0000	0.0004	0.0046	0.0233	0.0747	0.2733	0.3823	0.2286
Mt StJohn	0.7140	0.0562	0.1180	0.0906	0.0001	0.0126	0.0008	0.0002	0.0000	0.0001	0.0062	0.0012	0.0000	0.0000	0.0000	0.0000	0.0000	0.0000	0.0000	0.0000	0.0000
Mt Victoria	0.1820	0.0695	0.0812	0.0636	0.0107	0.0078	0.0032	0.0000	0.0000	0.0013	0.0071	0.0028	0.0070	0.1042	0.1275	0.0627	0.0845	0.0178	0.0772	0.0384	0.0515
North Head	0.7403	0.0946	0.0613	0.0500	0.0063	0.0040	0.0004	0.0001	0.0001	0.0005	0.0051	0.0011	0.0043	0.0113	0.0059	0.0041	0.0031	0.0023	0.0020	0.0017	0.0015
One Tree Hill	0.6773	0.0829	0.1275	0.0954	0.0017	0.0111	0.0008	0.0002	0.0001	0.0003	0.0020	0.0007	0.0000	0.0000	0.0000	0.0000	0.0000	0.0000	0.0000	0.0000	0.0000
Otara Hill	0.0074	0.0003	0.0007	0.0074	0.0049	0.0027	0.0019	0.0000	0.0000	0.0008	0.0073	0.0039	0.0101	0.2129	0.2640	0.1764	0.1349	0.0601	0.0706	0.0252	0.0085
Otuataua	0.6340	0.0057	0.0601	0.2518	0.0458	0.0026	0.0000	0.0000	0.0000	0.0000	0.0000	0.0000	0.0000	0.0000	0.0000	0.0000	0.0000	0.0000	0.0000	0.0000	0.0000
Panmure Basin	0.1189	0.0000	0.0001	0.0004	0.0002	0.7201	0.0825	0.0479	0.0000	0.0004	0.0295	0.0000	0.0000	0.0000	0.0000	0.0000	0.0000	0.0000	0.0000	0.0000	0.0000
Pigeon Mountain	0.7696	0.0321	0.0431	0.0370	0.0005	0.0047	0.0000	0.0000	0.0000	0.0000	0.0063	0.0001	0.0000	0.0225	0.0124	0.0167	0.0079	0.0274	0.0043	0.0038	0.0116
Pukaki	0.8863	0.1137	0.0000	0.0000	0.0000	0.0000	0.0000	0.0000	0.0000	0.0000	0.0000	0.0000	0.0000	0.0000	0.0000	0.0000	0.0000	0.0000	0.0000	0.0000	0.0000
Puketutu	0.0394	0.0000	0.0000	0.0000	0.0005	0.0037	0.0279	0.0574	0.1537	0.2348	0.4826	0.0000	0.0000	0.0000	0.0000	0.0000	0.0000	0.0000	0.0000	0.0000	0.0000
Robertson Hill	0.9994	0.0000	0.0000	0.0000	0.0000	0.0000	0.0006	0.0000	0.0000	0.0000	0.0000	0.0000	0.0000	0.0000	0.0000	0.0000	0.0000	0.0000	0.0000	0.0000	0.0000
Styaks Swamp	0.5371	0.0000	0.0000	0.0000	0.0000	0.0000	0.0000	0.0000	0.0000	0.0000	0.0000	0.0000	0.0000	0.0119	0.0166	0.0350	0.0370	0.0500	0.0505	0.0540	0.2079
Taylors Hill	0.5258	0.0000	0.0000	0.0001	0.0000	0.0186	0.2555	0.1991	0.0000	0.0000	0.0009	0.0000	0.0000	0.0000	0.0000	0.0000	0.0000	0.0000	0.0000	0.0000	0.0000
Te Pouhawaiki	0.7693	0.0750	0.0683	0.0636	0.0050	0.0061	0.0011	0.0003	0.0003	0.0003	0.0084	0.0023	0.0000	0.0000	0.0000	0.0000	0.0000	0.0000	0.0000	0.0000	0.0000
Three Kings	0.0000	0.0000	0.0000	0.0000	0.0000	0.0000	0.0000	0.0000	0.0000	0.0029	0.0954	0.5737	0.3280	0.0000	0.0000	0.0000	0.0000	0.0000	0.0000	0.0000	0.0000
Wiri Mountain	0.3638	0.0000	0.0000	0.0000	0.0000	0.0022	0.1571	0.2789	0.0265	0.0917	0.0798	0.0000	0.0000	0.0000	0.0000	0.0000	0.0000	0.0000	0.0000	0.0000	0.0000

Table A.2: Marginal posterior probabilities for a volcano to have produced a given tephra for the baseline scenario with C = $\{\alpha = 2.5, \beta U = 0.5\}$.

Volcano	AVF tephra (AVF 0 = ‘unmatched’)																				
	0	1	2	3	4	5	6	7	8	9	10	11	12	13	14	15	16	17	18	19	20
Ash Hill	0.7850	0.0000	0.0000	0.0000	0.0000	0.0007	0.1745	0.0398	0.0000	0.0000	0.0000	0.0000	0.0000	0.0000	0.0000	0.0000	0.0000	0.0000	0.0000	0.0000	0.0000
Cemetery Hill	0.0292	0.0000	0.0000	0.0000	0.0003	0.0165	0.1307	0.1672	0.5341	0.1207	0.0013	0.0000	0.0000	0.0000	0.0000	0.0000	0.0000	0.0000	0.0000	0.0000	0.0000
Crater Hill	0.0007	0.0000	0.0000	0.0000	0.0000	0.0001	0.0157	0.0088	0.2737	0.5564	0.1435	0.0011	0.0000	0.0000	0.0000	0.0000	0.0000	0.0000	0.0000	0.0000	0.0000
Domain	0.7562	0.1380	0.0826	0.0232	0.0000	0.0000	0.0000	0.0000	0.0000	0.0000	0.0000	0.0000	0.0000	0.0000	0.0000	0.0000	0.0000	0.0000	0.0000	0.0000	0.0000
Green Hill	0.0075	0.0007	0.0032	0.0155	0.0262	0.0154	0.0061	0.0003	0.0004	0.0043	0.0364	0.0171	0.0591	0.1888	0.1248	0.1032	0.0784	0.0880	0.1099	0.0862	0.0285
Hampton Park	0.4120	0.0000	0.0000	0.0000	0.0000	0.0001	0.0000	0.0000	0.0000	0.0000	0.0000	0.0000	0.0000	0.0608	0.1508	0.1823	0.0973	0.0700	0.0161	0.0066	0.0040
Hopua	0.8009	0.0000	0.0000	0.0004	0.0000	0.0691	0.0492	0.0356	0.0005	0.0029	0.0391	0.0023	0.0000	0.0000	0.0000	0.0000	0.0000	0.0000	0.0000	0.0000	0.0000
Kohuora	0.0013	0.0001	0.0019	0.0192	0.8585	0.0668	0.0487	0.0013	0.0021	0.0001	0.0000	0.0000	0.0000	0.0000	0.0000	0.0000	0.0000	0.0000	0.0000	0.0000	0.0000
Little Rangitoto	0.0351	0.2041	0.1886	0.1442	0.0230	0.0106	0.0012	0.0009	0.0008	0.0026	0.0134	0.0054	0.0191	0.0492	0.0393	0.0284	0.0206	0.0331	0.0497	0.0520	0.0787
Mangere Lagoon	0.7443	0.0426	0.0615	0.0525	0.0005	0.0072	0.0023	0.0003	0.0000	0.0008	0.0041	0.0044	0.0046	0.0259	0.0213	0.0165	0.0088	0.0024	0.0000	0.0000	0.0000
Matukutureia	0.0162	0.0000	0.0000	0.0000	0.0000	0.0000	0.0000	0.0000	0.0000	0.0008	0.0074	0.0035	0.0082	0.1381	0.1020	0.0875	0.0674	0.0653	0.0979	0.2165	0.1892
Maungataketake	0.9936	0.0012	0.0000	0.0029	0.0000	0.0002	0.0020	0.0001	0.0000	0.0000	0.0000	0.0000	0.0000	0.0000	0.0000	0.0000	0.0000	0.0000	0.0000	0.0000	0.0000
McLennan Hills	0.9194	0.0000	0.0183	0.0473	0.0000	0.0129	0.0013	0.0008	0.0000	0.0000	0.0000	0.0000	0.0000	0.0000	0.0000	0.0000	0.0000	0.0000	0.0000	0.0000	0.0000
Motukorea	0.9478	0.0020	0.0009	0.0003	0.0001	0.0019	0.0000	0.0000	0.0000	0.0000	0.0023	0.0000	0.0000	0.0063	0.0008	0.0026	0.0020	0.0281	0.0010	0.0016	0.0023
Mt Albert	0.8904	0.0575	0.0335	0.0171	0.0007	0.0006	0.0001	0.0000	0.0000	0.0000	0.0001	0.0000	0.0000	0.0000	0.0000	0.0000	0.0000	0.0000	0.0000	0.0000	0.0000
Mt Cambria	0.7375	0.0114	0.0282	0.0171	0.0036	0.0090	0.0000	0.0000	0.0000	0.0000	0.0064	0.0000	0.0000	0.0310	0.0115	0.0352	0.0138	0.0929	0.0012	0.0011	0.0001
Mt Eden	0.0536	0.0000	0.0000	0.0000	0.0000	0.0000	0.0000	0.0000	0.0000	0.0008	0.0374	0.3778	0.5304	0.0000	0.0000	0.0000	0.0000	0.0000	0.0000	0.0000	0.0000
Mt Hobson	0.1122	0.0000	0.0000	0.0000	0.0000	0.0000	0.0000	0.0000	0.0000	0.0000	0.0003	0.0041	0.0193	0.1234	0.0872	0.0764	0.0600	0.0876	0.1124	0.1296	0.1875
Mt Mangere	0.0108	0.0000	0.0000	0.0000	0.0000	0.0000	0.0000	0.0000	0.0000	0.0000	0.0000	0.0000	0.0000	0.0048	0.0456	0.1523	0.3675	0.2818	0.1331	0.0041	0.0000
Mt Richmond	0.7793	0.0000	0.0000	0.0000	0.0000	0.0013	0.0708	0.1486	0.0000	0.0000	0.0000	0.0000	0.0000	0.0000	0.0000	0.0000	0.0000	0.0000	0.0000	0.0000	0.0000
Mt Roskill	0.9442	0.0147	0.0268	0.0021	0.0001	0.0064	0.0001	0.0004	0.0000	0.0000	0.0052	0.0000	0.0000	0.0000	0.0000	0.0000	0.0000	0.0000	0.0000	0.0000	0.0000
Mt Smart	0.0076	0.0000	0.0000	0.0000	0.0000	0.0000	0.0000	0.0000	0.0000	0.0000	0.0000	0.0000	0.0000	0.0000	0.0004	0.0054	0.0291	0.0828	0.2811	0.3802	0.2134
Mt StJohn	0.7180	0.0577	0.1121	0.0907	0.0003	0.0125	0.0005	0.0002	0.0000	0.0001	0.0054	0.0025	0.0000	0.0000	0.0000	0.0000	0.0000	0.0000	0.0000	0.0000	0.0000
Mt Victoria	0.1710	0.0697	0.0717	0.0734	0.0155	0.0058	0.0029	0.0001	0.0001	0.0029	0.0034	0.0050	0.0085	0.1092	0.1176	0.0734	0.0842	0.0179	0.0751	0.0377	0.0549
North Head	0.7266	0.1032	0.0639	0.0502	0.0091	0.0031	0.0002	0.0000	0.0001	0.0003	0.0052	0.0013	0.0054	0.0111	0.0061	0.0042	0.0029	0.0023	0.0021	0.0015	0.0012
One Tree Hill	0.6779	0.0824	0.1219	0.1009	0.0021	0.0107	0.0008	0.0001	0.0001	0.0005	0.0013	0.0013	0.0000	0.0000	0.0000	0.0000	0.0000	0.0000	0.0000	0.0000	0.0000
Otara Hill	0.0055	0.0004	0.0006	0.0078	0.0049	0.0028	0.0020	0.0000	0.0000	0.0009	0.0069	0.0043	0.0130	0.2179	0.2639	0.1835	0.1266	0.0602	0.0659	0.0248	0.0081
Otuataua	0.6544	0.0065	0.0616	0.2280	0.0443	0.0039	0.0002	0.0011	0.0000	0.0000	0.0000	0.0000	0.0000	0.0000	0.0000	0.0000	0.0000	0.0000	0.0000	0.0000	0.0000
Panmure Basin	0.1249	0.0000	0.0001	0.0004	0.0004	0.7053	0.0842	0.0575	0.0000	0.0007	0.0226	0.0039	0.0000	0.0000	0.0000	0.0000	0.0000	0.0000	0.0000	0.0000	0.0000
Pigeon Mountain	0.7752	0.0272	0.0461	0.0351	0.0004	0.0052	0.0000	0.0000	0.0000	0.0000	0.0060	0.0000	0.0000	0.0228	0.0126	0.0151	0.0068	0.0293	0.0036	0.0032	0.0114
Pukaki	0.9155	0.0845	0.0000	0.0000	0.0000	0.0000	0.0000	0.0000	0.0000	0.0000	0.0000	0.0000	0.0000	0.0000	0.0000	0.0000	0.0000	0.0000	0.0000	0.0000	0.0000
Puketutu	0.0264	0.0000	0.0000	0.0000	0.0004	0.0035	0.0360	0.0467	0.1662	0.2285	0.4920	0.0003	0.0000	0.0000	0.0000	0.0000	0.0000	0.0000	0.0000	0.0000	0.0000
Robertson Hill	0.9993	0.0000	0.0000	0.0000	0.0000	0.0000	0.0007	0.0000	0.0000	0.0000	0.0000	0.0000	0.0000	0.0000	0.0000	0.0000	0.0000	0.0000	0.0000	0.0000	0.0000
Styaks Swamp	0.5198	0.0000	0.0000	0.0000	0.0000	0.0000	0.0000	0.0000	0.0000	0.0000	0.0000	0.0000	0.0000	0.0107	0.0161	0.0340	0.0346	0.0583	0.0509	0.0549	0.2207
Taylors Hill	0.5589	0.0000	0.0000	0.0001	0.0000	0.0207	0.2115	0.2080	0.0000	0.0000	0.0008	0.0000	0.0000	0.0000	0.0000	0.0000	0.0000	0.0000	0.0000	0.0000	0.0000
Te Pouhawaiki	0.7271	0.0961	0.0765	0.0716	0.0096	0.0055	0.0012	0.0003	0.0003	0.0005	0.0085	0.0028	0.0000	0.0000	0.0000	0.0000	0.0000	0.0000	0.0000	0.0000	0.0000
Three Kings	0.0000	0.0000	0.0000	0.0000	0.0000	0.0000	0.0000	0.0000	0.0000	0.0035	0.1012	0.5629	0.3324	0.0000	0.0000	0.0000	0.0000	0.0000	0.0000	0.0000	0.0000
Wiri Mountain	0.4147	0.0000	0.0000	0.0000	0.0000	0.0022	0.1571	0.2819	0.0216	0.0727	0.0498	0.0000	0.0000	0.0000	0.0000	0.0000	0.0000	0.0000	0.0000	0.0000	0.0000

Table A.3: Marginal posterior probabilities for a volcano to have produced a given tephra for the baseline scenario with D = $\{\alpha = 1.5, \beta U = 1.0\}$.

Volcano	AVF tephra (AVF 0 = 'unmatched')																				
	0	1	2	3	4	5	6	7	8	9	10	11	12	13	14	15	16	17	18	19	20
Ash Hill	0.6127	0.0000	0.0000	0.0000	0.0000	0.0009	0.2788	0.1076	0.0000	0.0000	0.0000	0.0000	0.0000	0.0000	0.0000	0.0000	0.0000	0.0000	0.0000	0.0000	0.0000
Cemetery Hill	0.0000	0.0000	0.0000	0.0000	0.0026	0.0107	0.0886	0.0417	0.6553	0.1954	0.0057	0.0000	0.0000	0.0000	0.0000	0.0000	0.0000	0.0000	0.0000	0.0000	0.0000
Crater Hill	0.0037	0.0000	0.0000	0.0000	0.0000	0.0004	0.0055	0.0032	0.1189	0.6354	0.2219	0.0110	0.0000	0.0000	0.0000	0.0000	0.0000	0.0000	0.0000	0.0000	0.0000
Domain	0.7767	0.1132	0.0887	0.0214	0.0000	0.0000	0.0000	0.0000	0.0000	0.0000	0.0000	0.0000	0.0000	0.0000	0.0000	0.0000	0.0000	0.0000	0.0000	0.0000	0.0000
Green Hill	0.0032	0.0012	0.0028	0.0133	0.0211	0.0180	0.0106	0.0007	0.0017	0.0014	0.0152	0.0378	0.0631	0.1910	0.1304	0.1076	0.0832	0.0962	0.1078	0.0754	0.0183
Hampton Park	0.5113	0.0000	0.0000	0.0000	0.0000	0.0002	0.0000	0.0002	0.0000	0.0000	0.0000	0.0000	0.0000	0.0483	0.1279	0.1491	0.0814	0.0599	0.0133	0.0048	0.0036
Hopua	0.5681	0.0000	0.0002	0.0009	0.0001	0.0386	0.1133	0.0511	0.0001	0.0008	0.0038	0.2230	0.0000	0.0000	0.0000	0.0000	0.0000	0.0000	0.0000	0.0000	0.0000
Kohuora	0.0000	0.0004	0.0026	0.0173	0.6289	0.2328	0.1102	0.0033	0.0043	0.0002	0.0000	0.0000	0.0000	0.0000	0.0000	0.0000	0.0000	0.0000	0.0000	0.0000	0.0000
Little Rangitoto	0.0178	0.2273	0.1650	0.1360	0.0214	0.0173	0.0026	0.0011	0.0012	0.0017	0.0061	0.0129	0.0202	0.0493	0.0405	0.0317	0.0213	0.0347	0.0510	0.0530	0.0879
Mangere Lagoon	0.7188	0.0442	0.0718	0.0537	0.0003	0.0140	0.0043	0.0003	0.0001	0.0004	0.0015	0.0089	0.0069	0.0272	0.0219	0.0169	0.0072	0.0016	0.0000	0.0000	0.0000
Matukutureia	0.0069	0.0000	0.0000	0.0000	0.0000	0.0000	0.0000	0.0000	0.0000	0.0004	0.0033	0.0069	0.0133	0.1386	0.1060	0.0922	0.0666	0.0732	0.1097	0.2250	0.1579
Maungataketake	0.9863	0.0009	0.0001	0.0097	0.0000	0.0003	0.0026	0.0001	0.0000	0.0000	0.0000	0.0000	0.0000	0.0000	0.0000	0.0000	0.0000	0.0000	0.0000	0.0000	0.0000
McLennan Hills	0.8697	0.0000	0.0292	0.0681	0.0000	0.0293	0.0026	0.0011	0.0000	0.0000	0.0000	0.0000	0.0000	0.0000	0.0000	0.0000	0.0000	0.0000	0.0000	0.0000	0.0000
Motukorea	0.9555	0.0019	0.0018	0.0008	0.0000	0.0018	0.0000	0.0000	0.0000	0.0000	0.0001	0.0000	0.0000	0.0025	0.0007	0.0009	0.0012	0.0281	0.0010	0.0016	0.0021
Mt Albert	0.8913	0.0529	0.0361	0.0177	0.0004	0.0014	0.0001	0.0000	0.0000	0.0000	0.0001	0.0000	0.0000	0.0000	0.0000	0.0000	0.0000	0.0000	0.0000	0.0000	0.0000
Mt Cambria	0.7788	0.0075	0.0190	0.0118	0.0045	0.0078	0.0000	0.0000	0.0000	0.0000	0.0060	0.0000	0.0000	0.0241	0.0074	0.0186	0.0073	0.1048	0.0012	0.0011	0.0001
Mt Eden	0.5331	0.0000	0.0000	0.0000	0.0000	0.0000	0.0000	0.0000	0.0000	0.0000	0.0088	0.3062	0.1519	0.0000	0.0000	0.0000	0.0000	0.0000	0.0000	0.0000	0.0000
Mt Hobson	0.0699	0.0000	0.0000	0.0000	0.0000	0.0000	0.0000	0.0000	0.0000	0.0000	0.0002	0.0036	0.0137	0.1246	0.0924	0.0782	0.0649	0.0913	0.1195	0.1307	0.2110
Mt Mangere	0.0288	0.0000	0.0000	0.0000	0.0000	0.0000	0.0000	0.0000	0.0000	0.0000	0.0000	0.0000	0.0000	0.0053	0.0464	0.1883	0.3868	0.2390	0.1018	0.0036	0.0000
Mt Richmond	0.8538	0.0000	0.0000	0.0000	0.0000	0.0003	0.0312	0.1147	0.0000	0.0000	0.0000	0.0000	0.0000	0.0000	0.0000	0.0000	0.0000	0.0000	0.0000	0.0000	0.0000
Mt Roskill	0.9726	0.0117	0.0054	0.0024	0.0001	0.0063	0.0004	0.0007	0.0000	0.0000	0.0004	0.0000	0.0000	0.0000	0.0000	0.0000	0.0000	0.0000	0.0000	0.0000	0.0000
Mt Smart	0.0032	0.0000	0.0000	0.0000	0.0000	0.0000	0.0000	0.0000	0.0000	0.0000	0.0000	0.0000	0.0000	0.0000	0.0005	0.0068	0.0437	0.1095	0.2907	0.3631	0.1825
Mt StJohn	0.7306	0.0396	0.1196	0.0817	0.0002	0.0169	0.0018	0.0006	0.0001	0.0000	0.0013	0.0076	0.0000	0.0000	0.0000	0.0000	0.0000	0.0000	0.0000	0.0000	0.0000
Mt Victoria	0.1583	0.0794	0.0734	0.0611	0.0117	0.0075	0.0048	0.0001	0.0007	0.0021	0.0012	0.0074	0.0096	0.1145	0.1246	0.0767	0.0825	0.0090	0.0766	0.0397	0.0591
North Head	0.7254	0.1101	0.0616	0.0441	0.0072	0.0049	0.0016	0.0003	0.0002	0.0002	0.0022	0.0043	0.0066	0.0107	0.0066	0.0043	0.0028	0.0024	0.0025	0.0015	0.0005
One Tree Hill	0.7029	0.0594	0.1265	0.0895	0.0006	0.0169	0.0013	0.0002	0.0001	0.0001	0.0003	0.0022	0.0000	0.0000	0.0000	0.0000	0.0000	0.0000	0.0000	0.0000	0.0000
Otara Hill	0.0010	0.0005	0.0011	0.0060	0.0065	0.0044	0.0022	0.0001	0.0005	0.0004	0.0030	0.0078	0.0176	0.2307	0.2703	0.1876	0.1130	0.0601	0.0575	0.0233	0.0064
Otuataua	0.3496	0.0090	0.0822	0.2670	0.2843	0.0059	0.0003	0.0017	0.0000	0.0000	0.0000	0.0000	0.0000	0.0000	0.0000	0.0000	0.0000	0.0000	0.0000	0.0000	0.0000
Panmure Basin	0.4022	0.0000	0.0001	0.0011	0.0004	0.5271	0.0187	0.0412	0.0000	0.0001	0.0034	0.0057	0.0000	0.0000	0.0000	0.0000	0.0000	0.0000	0.0000	0.0000	0.0000
Pigeon Mountain	0.8072	0.0260	0.0328	0.0303	0.0003	0.0085	0.0000	0.0000	0.0000	0.0000	0.0028	0.0000	0.0000	0.0206	0.0074	0.0111	0.0045	0.0317	0.0029	0.0021	0.0118
Pukaki	0.9037	0.0963	0.0000	0.0000	0.0000	0.0000	0.0000	0.0000	0.0000	0.0000	0.0000	0.0000	0.0000	0.0000	0.0000	0.0000	0.0000	0.0000	0.0000	0.0000	0.0000
Pukeiti	0.9997	0.0000	0.0003	0.0000	0.0000	0.0000	0.0000	0.0000	0.0000	0.0000	0.0000	0.0000	0.0000	0.0000	0.0000	0.0000	0.0000	0.0000	0.0000	0.0000	0.0000
Puketutu	0.0111	0.0000	0.0000	0.0000	0.0006	0.0087	0.0142	0.0205	0.1979	0.1118	0.6300	0.0052	0.0000	0.0000	0.0000	0.0000	0.0000	0.0000	0.0000	0.0000	0.0000
Robertson Hill	0.9996	0.0000	0.0000	0.0000	0.0000	0.0001	0.0003	0.0000	0.0000	0.0000	0.0000	0.0000	0.0000	0.0000	0.0000	0.0000	0.0000	0.0000	0.0000	0.0000	0.0000
Styaks Swamp	0.4497	0.0000	0.0000	0.0000	0.0000	0.0000	0.0000	0.0002	0.0000	0.0000	0.0000	0.0000	0.0000	0.0126	0.0170	0.0300	0.0336	0.0585	0.0645	0.0751	0.2588
Taylors Hill	0.4628	0.0000	0.0000	0.0001	0.0000	0.0073	0.2407	0.2891	0.0000	0.0000	0.0000	0.0000	0.0000	0.0000	0.0000	0.0000	0.0000	0.0000	0.0000	0.0000	0.0000
Te Pouhawaiki	0.7004	0.1185	0.0797	0.0660	0.0088	0.0108	0.0028	0.0006	0.0006	0.0004	0.0035	0.0067	0.0012	0.0000	0.0000	0.0000	0.0000	0.0000	0.0000	0.0000	0.0000
Three Kings	0.0000	0.0000	0.0000	0.0000	0.0000	0.0000	0.0000	0.0000	0.0000	0.0010	0.0530	0.2501	0.6959	0.0000	0.0000	0.0000	0.0000	0.0000	0.0000	0.0000	0.0000
Wiri Mountain	0.4336	0.0000	0.0000	0.0000	0.0000	0.0009	0.0605	0.3196	0.0183	0.0482	0.0262	0.0927	0.0000	0.0000	0.0000	0.0000	0.0000	0.0000	0.0000	0.0000	0.0000

Table A.4: Marginal posterior probabilities for a volcano to have produced a given tephra for the baseline scenario with E = $\{\alpha = 2.0, \beta U = 1.0\}$.

Volcano	AVF tephra (AVF 0 = 'unmatched')																				
	0	1	2	3	4	5	6	7	8	9	10	11	12	13	14	15	16	17	18	19	20
Ash Hill	0.5726	0.0000	0.0000	0.0000	0.0000	0.0010	0.3167	0.1097	0.0000	0.0000	0.0000	0.0000	0.0000	0.0000	0.0000	0.0000	0.0000	0.0000	0.0000	0.0000	0.0000
Cemetery Hill	0.0001	0.0000	0.0000	0.0000	0.0026	0.0113	0.0884	0.0389	0.6556	0.1977	0.0054	0.0000	0.0000	0.0000	0.0000	0.0000	0.0000	0.0000	0.0000	0.0000	0.0000
Crater Hill	0.0059	0.0000	0.0000	0.0000	0.0000	0.0004	0.0060	0.0035	0.1169	0.6321	0.2248	0.0104	0.0000	0.0000	0.0000	0.0000	0.0000	0.0000	0.0000	0.0000	0.0000
Domain	0.7764	0.1135	0.0893	0.0208	0.0000	0.0000	0.0000	0.0000	0.0000	0.0000	0.0000	0.0000	0.0000	0.0000	0.0000	0.0000	0.0000	0.0000	0.0000	0.0000	0.0000
Green Hill	0.0031	0.0012	0.0028	0.0131	0.0224	0.0198	0.0077	0.0007	0.0016	0.0015	0.0159	0.0372	0.0646	0.1900	0.1307	0.1074	0.0850	0.0963	0.1067	0.0747	0.0176
Hampton Park	0.5188	0.0000	0.0000	0.0000	0.0000	0.0002	0.0000	0.0003	0.0000	0.0000	0.0000	0.0000	0.0000	0.0480	0.1265	0.1459	0.0791	0.0597	0.0130	0.0050	0.0035
Hopua	0.5787	0.0000	0.0002	0.0010	0.0001	0.0599	0.0860	0.0479	0.0001	0.0013	0.0044	0.2204	0.0000	0.0000	0.0000	0.0000	0.0000	0.0000	0.0000	0.0000	0.0000
Kohuora	0.0000	0.0004	0.0029	0.0182	0.6640	0.1958	0.1107	0.0031	0.0047	0.0002	0.0000	0.0000	0.0000	0.0000	0.0000	0.0000	0.0000	0.0000	0.0000	0.0000	0.0000
Little Rangitoto	0.0132	0.2269	0.1693	0.1328	0.0232	0.0166	0.0024	0.0009	0.0013	0.0019	0.0066	0.0123	0.0206	0.0492	0.0406	0.0315	0.0214	0.0354	0.0511	0.0537	0.0891
Mangere Lagoon	0.7288	0.0398	0.0690	0.0519	0.0003	0.0138	0.0039	0.0003	0.0001	0.0004	0.0013	0.0094	0.0063	0.0275	0.0218	0.0169	0.0069	0.0016	0.0000	0.0000	0.0000
Matukutureia	0.0050	0.0000	0.0000	0.0000	0.0000	0.0000	0.0000	0.0000	0.0000	0.0004	0.0033	0.0070	0.0145	0.1379	0.1065	0.0918	0.0667	0.0731	0.1119	0.2245	0.1574
Maungataketake	0.9859	0.0009	0.0001	0.0095	0.0000	0.0006	0.0029	0.0001	0.0000	0.0000	0.0000	0.0000	0.0000	0.0000	0.0000	0.0000	0.0000	0.0000	0.0000	0.0000	0.0000
McLennan Hills	0.8629	0.0000	0.0297	0.0694	0.0000	0.0340	0.0026	0.0014	0.0000	0.0000	0.0000	0.0000	0.0000	0.0000	0.0000	0.0000	0.0000	0.0000	0.0000	0.0000	0.0000
Motukorea	0.9548	0.0019	0.0018	0.0009	0.0001	0.0019	0.0000	0.0000	0.0000	0.0000	0.0001	0.0000	0.0000	0.0026	0.0007	0.0009	0.0012	0.0283	0.0010	0.0016	0.0022
Mt Albert	0.8930	0.0521	0.0356	0.0174	0.0003	0.0014	0.0001	0.0000	0.0000	0.0000	0.0001	0.0000	0.0000	0.0000	0.0000	0.0000	0.0000	0.0000	0.0000	0.0000	0.0000
Mt Cambria	0.7674	0.0094	0.0199	0.0171	0.0048	0.0081	0.0000	0.0000	0.0000	0.0000	0.0069	0.0000	0.0000	0.0241	0.0076	0.0181	0.0076	0.1065	0.0012	0.0011	0.0002
Mt Eden	0.5289	0.0000	0.0000	0.0000	0.0000	0.0000	0.0000	0.0000	0.0000	0.0001	0.0093	0.3100	0.1517	0.0000	0.0000	0.0000	0.0000	0.0000	0.0000	0.0000	0.0000
Mt Hobson	0.0693	0.0000	0.0000	0.0000	0.0000	0.0000	0.0000	0.0000	0.0000	0.0000	0.0002	0.0034	0.0133	0.1262	0.0916	0.0783	0.0646	0.0929	0.1183	0.1299	0.2120
Mt Mangere	0.0293	0.0000	0.0000	0.0000	0.0000	0.0000	0.0000	0.0000	0.0000	0.0000	0.0000	0.0000	0.0000	0.0054	0.0473	0.1932	0.3853	0.2343	0.1017	0.0035	0.0000
Mt Richmond	0.8528	0.0000	0.0000	0.0000	0.0000	0.0003	0.0312	0.1157	0.0000	0.0000	0.0000	0.0000	0.0000	0.0000	0.0000	0.0000	0.0000	0.0000	0.0000	0.0000	0.0000
Mt Roskill	0.9724	0.0112	0.0061	0.0025	0.0001	0.0061	0.0005	0.0007	0.0000	0.0000	0.0004	0.0000	0.0000	0.0000	0.0000	0.0000	0.0000	0.0000	0.0000	0.0000	0.0000
Mt Smart	0.0024	0.0000	0.0000	0.0000	0.0000	0.0000	0.0000	0.0000	0.0000	0.0000	0.0000	0.0000	0.0000	0.0000	0.0005	0.0074	0.0453	0.1085	0.2933	0.3630	0.1796
Mt StJohn	0.7339	0.0410	0.1154	0.0817	0.0001	0.0167	0.0018	0.0004	0.0001	0.0000	0.0011	0.0078	0.0000	0.0000	0.0000	0.0000	0.0000	0.0000	0.0000	0.0000	0.0000
Mt Victoria	0.1544	0.0800	0.0749	0.0608	0.0126	0.0078	0.0042	0.0001	0.0007	0.0024	0.0009	0.0074	0.0100	0.1151	0.1247	0.0763	0.0829	0.0092	0.0759	0.0404	0.0593
North Head	0.7208	0.1129	0.0614	0.0459	0.0075	0.0052	0.0011	0.0003	0.0002	0.0002	0.0026	0.0039	0.0069	0.0105	0.0065	0.0044	0.0028	0.0023	0.0026	0.0015	0.0005
One Tree Hill	0.7036	0.0604	0.1247	0.0895	0.0008	0.0168	0.0013	0.0002	0.0001	0.0001	0.0003	0.0022	0.0000	0.0000	0.0000	0.0000	0.0000	0.0000	0.0000	0.0000	0.0000
Otara Hill	0.0008	0.0005	0.0011	0.0062	0.0069	0.0042	0.0018	0.0001	0.0005	0.0004	0.0032	0.0076	0.0191	0.2309	0.2704	0.1872	0.1129	0.0596	0.0568	0.0233	0.0065
Otuataua	0.3998	0.0089	0.0804	0.2607	0.2423	0.0055	0.0006	0.0018	0.0000	0.0000	0.0000	0.0000	0.0000	0.0000	0.0000	0.0000	0.0000	0.0000	0.0000	0.0000	0.0000
Panmure Basin	0.3895	0.0000	0.0001	0.0012	0.0004	0.5370	0.0196	0.0415	0.0000	0.0001	0.0050	0.0056	0.0000	0.0000	0.0000	0.0000	0.0000	0.0000	0.0000	0.0000	0.0000
Pigeon Mountain	0.8055	0.0253	0.0334	0.0324	0.0003	0.0088	0.0000	0.0000	0.0000	0.0000	0.0024	0.0000	0.0000	0.0201	0.0075	0.0111	0.0045	0.0319	0.0029	0.0021	0.0118
Pukaki	0.9060	0.0940	0.0000	0.0000	0.0000	0.0000	0.0000	0.0000	0.0000	0.0000	0.0000	0.0000	0.0000	0.0000	0.0000	0.0000	0.0000	0.0000	0.0000	0.0000	0.0000
Pukeiti	0.9998	0.0000	0.0002	0.0000	0.0000	0.0000	0.0000	0.0000	0.0000	0.0000	0.0000	0.0000	0.0000	0.0000	0.0000	0.0000	0.0000	0.0000	0.0000	0.0000	0.0000
Puketutu	0.0107	0.0000	0.0000	0.0000	0.0007	0.0086	0.0136	0.0192	0.2008	0.1148	0.6265	0.0051	0.0000	0.0000	0.0000	0.0000	0.0000	0.0000	0.0000	0.0000	0.0000
Robertson Hill	0.9994	0.0000	0.0000	0.0000	0.0000	0.0001	0.0005	0.0000	0.0000	0.0000	0.0000	0.0000	0.0000	0.0000	0.0000	0.0000	0.0000	0.0000	0.0000	0.0000	0.0000
Styaks Swamp	0.4468	0.0000	0.0000	0.0000	0.0000	0.0000	0.0000	0.0002	0.0000	0.0000	0.0000	0.0000	0.0000	0.0125	0.0171	0.0296	0.0338	0.0604	0.0636	0.0757	0.2603
Taylors Hill	0.4864	0.0000	0.0000	0.0001	0.0000	0.0073	0.2277	0.2785	0.0000	0.0000	0.0000	0.0000	0.0000	0.0000	0.0000	0.0000	0.0000	0.0000	0.0000	0.0000	0.0000
Te Pouhawaiki	0.6957	0.1197	0.0817	0.0669	0.0105	0.0098	0.0025	0.0006	0.0008	0.0004	0.0035	0.0067	0.0012	0.0000	0.0000	0.0000	0.0000	0.0000	0.0000	0.0000	0.0000
Three Kings	0.0000	0.0000	0.0000	0.0000	0.0000	0.0000	0.0000	0.0000	0.0000	0.0014	0.0552	0.2516	0.6918	0.0000	0.0000	0.0000	0.0000	0.0000	0.0000	0.0000	0.0000
Wiri Mountain	0.4252	0.0000	0.0000	0.0000	0.0000	0.0010	0.0662	0.3339	0.0165	0.0446	0.0206	0.0920	0.0000	0.0000	0.0000	0.0000	0.0000	0.0000	0.0000	0.0000	0.0000

Table A.5: Marginal posterior probabilities for a volcano to have produced a given tephra for the baseline scenario with F = $\{\alpha = 2.5, \beta U = 1.0\}$.

Volcano	AVF tephra (AVF 0 = 'unmatched')																				
	0	1	2	3	4	5	6	7	8	9	10	11	12	13	14	15	16	17	18	19	20
Ash Hill	0.5532	0.0000	0.0000	0.0000	0.0000	0.0012	0.3390	0.1066	0.0000	0.0000	0.0000	0.0000	0.0000	0.0000	0.0000	0.0000	0.0000	0.0000	0.0000	0.0000	0.0000
Cemetery Hill	0.0001	0.0000	0.0000	0.0000	0.0025	0.0146	0.0865	0.0379	0.6546	0.1995	0.0043	0.0000	0.0000	0.0000	0.0000	0.0000	0.0000	0.0000	0.0000	0.0000	0.0000
Crater Hill	0.0072	0.0000	0.0000	0.0000	0.0000	0.0004	0.0064	0.0036	0.1169	0.6305	0.2282	0.0068	0.0000	0.0000	0.0000	0.0000	0.0000	0.0000	0.0000	0.0000	0.0000
Domain	0.7774	0.1120	0.0901	0.0205	0.0000	0.0000	0.0000	0.0000	0.0000	0.0000	0.0000	0.0000	0.0000	0.0000	0.0000	0.0000	0.0000	0.0000	0.0000	0.0000	0.0000
Green Hill	0.0029	0.0012	0.0029	0.0133	0.0251	0.0175	0.0071	0.0006	0.0017	0.0017	0.0163	0.0367	0.0664	0.1898	0.1299	0.1085	0.0848	0.0962	0.1064	0.0739	0.0171
Hampton Park	0.5251	0.0000	0.0000	0.0000	0.0000	0.0002	0.0001	0.0003	0.0000	0.0000	0.0000	0.0000	0.0000	0.0481	0.1256	0.1417	0.0766	0.0607	0.0131	0.0049	0.0036
Hopua	0.5830	0.0000	0.0001	0.0009	0.0001	0.0650	0.0803	0.0472	0.0001	0.0014	0.0042	0.2177	0.0000	0.0000	0.0000	0.0000	0.0000	0.0000	0.0000	0.0000	0.0000
Kohuora	0.0000	0.0006	0.0028	0.0189	0.6797	0.1891	0.1003	0.0031	0.0053	0.0002	0.0000	0.0000	0.0000	0.0000	0.0000	0.0000	0.0000	0.0000	0.0000	0.0000	0.0000
Little Rangitoto	0.0104	0.2282	0.1721	0.1298	0.0270	0.0133	0.0020	0.0009	0.0012	0.0020	0.0069	0.0120	0.0215	0.0491	0.0406	0.0311	0.0220	0.0352	0.0507	0.0550	0.0890
Mangere Lagoon	0.7344	0.0381	0.0676	0.0513	0.0003	0.0126	0.0035	0.0003	0.0001	0.0004	0.0014	0.0093	0.0061	0.0278	0.0219	0.0165	0.0068	0.0016	0.0000	0.0000	0.0000
Matukutureia	0.0043	0.0000	0.0000	0.0000	0.0000	0.0000	0.0000	0.0000	0.0000	0.0004	0.0033	0.0070	0.0164	0.1369	0.1068	0.0918	0.0665	0.0731	0.1136	0.2246	0.1553
Maungataketake	0.9859	0.0009	0.0001	0.0089	0.0000	0.0011	0.0030	0.0001	0.0000	0.0000	0.0000	0.0000	0.0000	0.0000	0.0000	0.0000	0.0000	0.0000	0.0000	0.0000	0.0000
McLennan Hills	0.8589	0.0000	0.0305	0.0711	0.0000	0.0350	0.0026	0.0019	0.0000	0.0000	0.0000	0.0000	0.0000	0.0000	0.0000	0.0000	0.0000	0.0000	0.0000	0.0000	0.0000
Motukorea	0.9542	0.0021	0.0017	0.0009	0.0001	0.0021	0.0000	0.0000	0.0000	0.0000	0.0001	0.0000	0.0000	0.0028	0.0007	0.0009	0.0012	0.0284	0.0010	0.0016	0.0022
Mt Albert	0.8968	0.0522	0.0325	0.0167	0.0002	0.0014	0.0001	0.0000	0.0000	0.0000	0.0001	0.0000	0.0000	0.0000	0.0000	0.0000	0.0000	0.0000	0.0000	0.0000	0.0000
Mt Cambria	0.7506	0.0088	0.0301	0.0202	0.0041	0.0095	0.0000	0.0000	0.0000	0.0000	0.0072	0.0000	0.0000	0.0245	0.0084	0.0177	0.0077	0.1087	0.0012	0.0011	0.0002
Mt Eden	0.5227	0.0000	0.0000	0.0000	0.0000	0.0000	0.0000	0.0000	0.0000	0.0001	0.0100	0.3143	0.1529	0.0000	0.0000	0.0000	0.0000	0.0000	0.0000	0.0000	0.0000
Mt Hobson	0.0688	0.0000	0.0000	0.0000	0.0000	0.0000	0.0000	0.0000	0.0000	0.0000	0.0002	0.0034	0.0136	0.1284	0.0901	0.0779	0.0655	0.0947	0.1164	0.1298	0.2112
Mt Mangere	0.0296	0.0000	0.0000	0.0000	0.0000	0.0000	0.0000	0.0000	0.0000	0.0000	0.0000	0.0000	0.0000	0.0057	0.0483	0.1981	0.3845	0.2287	0.1017	0.0034	0.0000
Mt Richmond	0.8320	0.0000	0.0000	0.0000	0.0000	0.0004	0.0310	0.1366	0.0000	0.0000	0.0000	0.0000	0.0000	0.0000	0.0000	0.0000	0.0000	0.0000	0.0000	0.0000	0.0000
Mt Roskill	0.9712	0.0113	0.0054	0.0025	0.0001	0.0079	0.0006	0.0006	0.0000	0.0000	0.0004	0.0000	0.0000	0.0000	0.0000	0.0000	0.0000	0.0000	0.0000	0.0000	0.0000
Mt Smart	0.0014	0.0000	0.0000	0.0000	0.0000	0.0000	0.0000	0.0000	0.0000	0.0000	0.0000	0.0000	0.0000	0.0000	0.0007	0.0078	0.0471	0.1080	0.2947	0.3616	0.1787
Mt StJohn	0.7338	0.0422	0.1139	0.0825	0.0003	0.0162	0.0016	0.0004	0.0001	0.0000	0.0015	0.0075	0.0000	0.0000	0.0000	0.0000	0.0000	0.0000	0.0000	0.0000	0.0000
Mt Victoria	0.1518	0.0835	0.0681	0.0658	0.0135	0.0067	0.0041	0.0000	0.0007	0.0026	0.0008	0.0073	0.0117	0.1144	0.1246	0.0761	0.0836	0.0086	0.0754	0.0407	0.0600
North Head	0.7184	0.1158	0.0609	0.0458	0.0089	0.0045	0.0006	0.0002	0.0002	0.0002	0.0027	0.0038	0.0072	0.0104	0.0066	0.0043	0.0031	0.0020	0.0025	0.0015	0.0004
One Tree Hill	0.7011	0.0636	0.1246	0.0889	0.0009	0.0168	0.0012	0.0003	0.0000	0.0001	0.0004	0.0021	0.0000	0.0000	0.0000	0.0000	0.0000	0.0000	0.0000	0.0000	0.0000
Otara Hill	0.0008	0.0005	0.0008	0.0066	0.0067	0.0043	0.0018	0.0001	0.0004	0.0004	0.0033	0.0075	0.0211	0.2300	0.2712	0.1874	0.1123	0.0591	0.0560	0.0234	0.0063
Otuataua	0.4329	0.0080	0.0807	0.2527	0.2171	0.0056	0.0011	0.0019	0.0000	0.0000	0.0000	0.0000	0.0000	0.0000	0.0000	0.0000	0.0000	0.0000	0.0000	0.0000	0.0000
Panmure Basin	0.3753	0.0000	0.0004	0.0009	0.0003	0.5459	0.0213	0.0432	0.0000	0.0001	0.0072	0.0054	0.0000	0.0000	0.0000	0.0000	0.0000	0.0000	0.0000	0.0000	0.0000
Pigeon Mountain	0.8050	0.0241	0.0347	0.0336	0.0003	0.0084	0.0000	0.0000	0.0000	0.0000	0.0023	0.0000	0.0000	0.0199	0.0075	0.0107	0.0046	0.0322	0.0027	0.0021	0.0119
Pukaki	0.9175	0.0825	0.0000	0.0000	0.0000	0.0000	0.0000	0.0000	0.0000	0.0000	0.0000	0.0000	0.0000	0.0000	0.0000	0.0000	0.0000	0.0000	0.0000	0.0000	0.0000
Pukeiti	0.9997	0.0000	0.0002	0.0000	0.0000	0.0001	0.0000	0.0000	0.0000	0.0000	0.0000	0.0000	0.0000	0.0000	0.0000	0.0000	0.0000	0.0000	0.0000	0.0000	0.0000
Puketutu	0.0171	0.0000	0.0000	0.0000	0.0007	0.0024	0.0140	0.0173	0.2037	0.1208	0.6193	0.0047	0.0000	0.0000	0.0000	0.0000	0.0000	0.0000	0.0000	0.0000	0.0000
Robertson Hill	0.9994	0.0000	0.0000	0.0000	0.0000	0.0001	0.0005	0.0000	0.0000	0.0000	0.0000	0.0000	0.0000	0.0000	0.0000	0.0000	0.0000	0.0000	0.0000	0.0000	0.0000
Styaks Swamp	0.4394	0.0000	0.0000	0.0000	0.0000	0.0000	0.0000	0.0002	0.0000	0.0000	0.0000	0.0000	0.0000	0.0122	0.0171	0.0295	0.0337	0.0628	0.0646	0.0764	0.2641
Taylors Hill	0.5116	0.0000	0.0000	0.0002	0.0000	0.0074	0.2018	0.2790	0.0000	0.0000	0.0000	0.0000	0.0000	0.0000	0.0000	0.0000	0.0000	0.0000	0.0000	0.0000	0.0000
Te Pouhawaiki	0.6916	0.1244	0.0798	0.0678	0.0121	0.0093	0.0017	0.0007	0.0008	0.0004	0.0037	0.0065	0.0012	0.0000	0.0000	0.0000	0.0000	0.0000	0.0000	0.0000	0.0000
Three Kings	0.0000	0.0000	0.0000	0.0000	0.0000	0.0000	0.0000	0.0000	0.0000	0.0014	0.0598	0.2569	0.6819	0.0000	0.0000	0.0000	0.0000	0.0000	0.0000	0.0000	0.0000
Wiri Mountain	0.4345	0.0000	0.0000	0.0002	0.0000	0.0010	0.0878	0.3170	0.0142	0.0378	0.0164	0.0911	0.0000	0.0000	0.0000	0.0000	0.0000	0.0000	0.0000	0.0000	0.0000

Table A.6: Marginal posterior probabilities for a volcano to have produced a given tephra for the Maungataketake and North Head scenario with A = $\{\alpha = 1.5,\ \beta U = 0.5\}$.

Volcano	AVF tephra (AVF 0 = 'unmatched')																				
	0	1	2	3	4	5	6	7	8	9	10	11	12	13	14	15	16	17	18	19	20
Ash Hill	0.8134	0.0000	0.0000	0.0000	0.0000	0.0108	0.1467	0.0291	0.0000	0.0000	0.0000	0.0000	0.0000	0.0000	0.0000	0.0000	0.0000	0.0000	0.0000	0.0000	0.0000
Cemetery Hill	0.0363	0.0000	0.0000	0.0000	0.0003	0.0233	0.1401	0.1947	0.5053	0.0998	0.0002	0.0000	0.0000	0.0000	0.0000	0.0000	0.0000	0.0000	0.0000	0.0000	0.0000
Crater Hill	0.0000	0.0000	0.0000	0.0000	0.0000	0.0000	0.0162	0.0173	0.3005	0.5490	0.1168	0.0002	0.0000	0.0000	0.0000	0.0000	0.0000	0.0000	0.0000	0.0000	0.0000
Domain	0.7399	0.1251	0.1080	0.0270	0.0000	0.0000	0.0000	0.0000	0.0000	0.0000	0.0000	0.0000	0.0000	0.0000	0.0000	0.0000	0.0000	0.0000	0.0000	0.0000	0.0000
Green Hill	0.0111	0.0000	0.0025	0.0200	0.0199	0.0167	0.0040	0.0000	0.0001	0.0015	0.0311	0.0106	0.0453	0.1985	0.1292	0.1125	0.0879	0.0825	0.1117	0.0867	0.0282
Hampton Park	0.3292	0.0000	0.0000	0.0000	0.0000	0.0000	0.0000	0.0001	0.0000	0.0000	0.0000	0.0000	0.0000	0.0874	0.1695	0.2100	0.1133	0.0633	0.0163	0.0084	0.0025
Hopua	0.7691	0.0000	0.0000	0.0006	0.0004	0.0706	0.0457	0.0367	0.0018	0.0062	0.0655	0.0034	0.0000	0.0000	0.0000	0.0000	0.0000	0.0000	0.0000	0.0000	0.0000
Kohuora	0.0000	0.0000	0.0014	0.0121	0.9215	0.0444	0.0205	0.0001	0.0000	0.0000	0.0000	0.0000	0.0000	0.0000	0.0000	0.0000	0.0000	0.0000	0.0000	0.0000	0.0000
Little Rangitoto	0.0474	0.1736	0.1951	0.2009	0.0182	0.0097	0.0014	0.0001	0.0011	0.0029	0.0120	0.0044	0.0113	0.0446	0.0338	0.0305	0.0252	0.0310	0.0385	0.0506	0.0677
Mangere Lagoon	0.7187	0.0299	0.0726	0.0880	0.0012	0.0039	0.0013	0.0001	0.0000	0.0000	0.0068	0.0031	0.0033	0.0219	0.0212	0.0152	0.0098	0.0028	0.0002	0.0000	0.0000
Matukutureia	0.0187	0.0000	0.0000	0.0000	0.0000	0.0000	0.0000	0.0000	0.0000	0.0004	0.0055	0.0019	0.0031	0.1433	0.0986	0.0896	0.0795	0.0682	0.0995	0.1931	0.1986
McLennan Hills	0.9310	0.0000	0.0068	0.0604	0.0000	0.0018	0.0000	0.0000	0.0000	0.0000	0.0000	0.0000	0.0000	0.0000	0.0000	0.0000	0.0000	0.0000	0.0000	0.0000	0.0000
Motukorea	0.9366	0.0001	0.0022	0.0045	0.0002	0.0012	0.0000	0.0000	0.0000	0.0000	0.0005	0.0000	0.0000	0.0096	0.0018	0.0056	0.0045	0.0264	0.0016	0.0010	0.0042
Mt Albert	0.8592	0.0639	0.0502	0.0263	0.0003	0.0001	0.0000	0.0000	0.0000	0.0000	0.0000	0.0000	0.0000	0.0000	0.0000	0.0000	0.0000	0.0000	0.0000	0.0000	0.0000
Mt Cambria	0.7668	0.0129	0.0268	0.0232	0.0027	0.0071	0.0000	0.0000	0.0000	0.0000	0.0008	0.0000	0.0000	0.0253	0.0108	0.0452	0.0161	0.0600	0.0013	0.0009	0.0001
Mt Eden	0.0166	0.0000	0.0000	0.0000	0.0000	0.0000	0.0000	0.0000	0.0000	0.0004	0.0265	0.4001	0.5564	0.0000	0.0000	0.0000	0.0000	0.0000	0.0000	0.0000	0.0000
Mt Hobson	0.0979	0.0000	0.0000	0.0000	0.0000	0.0000	0.0000	0.0000	0.0000	0.0000	0.0000	0.0027	0.0156	0.1271	0.0866	0.0796	0.0732	0.0831	0.1200	0.1366	0.1776
Mt Mangere	0.0042	0.0000	0.0000	0.0000	0.0000	0.0000	0.0000	0.0000	0.0000	0.0000	0.0000	0.0000	0.0000	0.0053	0.0421	0.1252	0.3233	0.3609	0.1362	0.0028	0.0000
Mt Richmond	0.7734	0.0000	0.0000	0.0000	0.0001	0.0027	0.0717	0.1521	0.0000	0.0000	0.0000	0.0000	0.0000	0.0000	0.0000	0.0000	0.0000	0.0000	0.0000	0.0000	0.0000
Mt Roskill	0.9583	0.0028	0.0105	0.0209	0.0008	0.0037	0.0004	0.0002	0.0000	0.0000	0.0023	0.0001	0.0000	0.0000	0.0000	0.0000	0.0000	0.0000	0.0000	0.0000	0.0000
Mt Smart	0.0064	0.0000	0.0000	0.0000	0.0000	0.0000	0.0000	0.0000	0.0000	0.0000	0.0000	0.0000	0.0000	0.0000	0.0005	0.0050	0.0243	0.0699	0.2833	0.3744	0.2362
Mt StJohn	0.6796	0.0372	0.1305	0.1334	0.0009	0.0097	0.0006	0.0000	0.0000	0.0001	0.0064	0.0016	0.0000	0.0000	0.0000	0.0000	0.0000	0.0000	0.0000	0.0000	0.0000
Mt Victoria	0.2135	0.1033	0.1105	0.1174	0.0111	0.0052	0.0014	0.0001	0.0002	0.0003	0.0043	0.0030	0.0061	0.0818	0.1001	0.0461	0.0587	0.0143	0.0590	0.0295	0.0341
North Head	0.9179	0.0718	0.0100	0.0003	0.0000	0.0000	0.0000	0.0000	0.0000	0.0000	0.0000	0.0000	0.0000	0.0000	0.0000	0.0000	0.0000	0.0000	0.0000	0.0000	0.0000
One Tree Hill	0.6415	0.0687	0.1508	0.1251	0.0029	0.0083	0.0007	0.0001	0.0000	0.0002	0.0016	0.0001	0.0000	0.0000	0.0000	0.0000	0.0000	0.0000	0.0000	0.0000	0.0000
Otara Hill	0.0063	0.0001	0.0014	0.0072	0.0046	0.0027	0.0009	0.0000	0.0000	0.0007	0.0059	0.0020	0.0077	0.2233	0.2728	0.1838	0.1359	0.0533	0.0614	0.0239	0.0061
Otuataua	0.8713	0.1159	0.0114	0.0014	0.0000	0.0000	0.0000	0.0000	0.0000	0.0000	0.0000	0.0000	0.0000	0.0000	0.0000	0.0000	0.0000	0.0000	0.0000	0.0000	0.0000
Panmure Basin	0.0868	0.0000	0.0000	0.0005	0.0038	0.7401	0.0918	0.0393	0.0000	0.0024	0.0352	0.0001	0.0000	0.0000	0.0000	0.0000	0.0000	0.0000	0.0000	0.0000	0.0000
Pigeon Mountain	0.7810	0.0140	0.0395	0.0474	0.0017	0.0033	0.0000	0.0000	0.0000	0.0000	0.0039	0.0002	0.0000	0.0223	0.0109	0.0205	0.0073	0.0270	0.0044	0.0045	0.0121
Pukaki	0.8812	0.1188	0.0000	0.0000	0.0000	0.0000	0.0000	0.0000	0.0000	0.0000	0.0000	0.0000	0.0000	0.0000	0.0000	0.0000	0.0000	0.0000	0.0000	0.0000	0.0000
Puketutu	0.0356	0.0000	0.0000	0.0000	0.0003	0.0043	0.0314	0.0574	0.1547	0.2230	0.4933	0.0000	0.0000	0.0000	0.0000	0.0000	0.0000	0.0000	0.0000	0.0000	0.0000
Robertson Hill	0.9990	0.0000	0.0000	0.0000	0.0000	0.0001	0.0009	0.0000	0.0000	0.0000	0.0000	0.0000	0.0000	0.0000	0.0000	0.0000	0.0000	0.0000	0.0000	0.0000	0.0000
Styaks Swamp	0.4519	0.0000	0.0000	0.0000	0.0000	0.0001	0.0000	0.0000	0.0000	0.0000	0.0000	0.0000	0.0000	0.0096	0.0221	0.0312	0.0410	0.0573	0.0666	0.0876	0.2326
Taylors Hill	0.5122	0.0000	0.0000	0.0001	0.0000	0.0236	0.2599	0.2019	0.0000	0.0003	0.0020	0.0000	0.0000	0.0000	0.0000	0.0000	0.0000	0.0000	0.0000	0.0000	0.0000
Te Pouhawaiki	0.7615	0.0619	0.0698	0.0833	0.0089	0.0042	0.0012	0.0000	0.0000	0.0002	0.0067	0.0023	0.0000	0.0000	0.0000	0.0000	0.0000	0.0000	0.0000	0.0000	0.0000
Three Kings	0.0000	0.0000	0.0000	0.0000	0.0000	0.0000	0.0000	0.0000	0.0000	0.0028	0.0818	0.5642	0.3512	0.0000	0.0000	0.0000	0.0000	0.0000	0.0000	0.0000	0.0000
Wiri Mountain	0.3265	0.0000	0.0000	0.0000	0.0002	0.0024	0.1632	0.2707	0.0363	0.1098	0.0909	0.0000	0.0000	0.0000	0.0000	0.0000	0.0000	0.0000	0.0000	0.0000	0.0000

Table A.7: Marginal posterior probabilities for a volcano to have produced a given tephra for the Maungataketake and North Head scenario with B = $\{\alpha = 2.0,\ \beta U = 0.5\}$.

Volcano	AVF tephra (AVF 0 = ‘unmatched’)																				
	0	1	2	3	4	5	6	7	8	9	10	11	12	13	14	15	16	17	18	19	20
Ash Hill	0.7834	0.0000	0.0000	0.0000	0.0000	0.0112	0.1710	0.0344	0.0000	0.0000	0.0000	0.0000	0.0000	0.0000	0.0000	0.0000	0.0000	0.0000	0.0000	0.0000	0.0000
Cemetery Hill	0.0323	0.0000	0.0000	0.0000	0.0004	0.0230	0.1333	0.1788	0.5170	0.1150	0.0002	0.0000	0.0000	0.0000	0.0000	0.0000	0.0000	0.0000	0.0000	0.0000	0.0000
Crater Hill	0.0000	0.0000	0.0000	0.0000	0.0000	0.0001	0.0162	0.0170	0.2805	0.5533	0.1326	0.0003	0.0000	0.0000	0.0000	0.0000	0.0000	0.0000	0.0000	0.0000	0.0000
Domain	0.7373	0.1287	0.1055	0.0285	0.0000	0.0000	0.0000	0.0000	0.0000	0.0000	0.0000	0.0000	0.0000	0.0000	0.0000	0.0000	0.0000	0.0000	0.0000	0.0000	0.0000
Green Hill	0.0084	0.0000	0.0026	0.0187	0.0214	0.0163	0.0043	0.0001	0.0000	0.0015	0.0307	0.0100	0.0489	0.1980	0.1307	0.1147	0.0867	0.0849	0.1097	0.0860	0.0264
Hampton Park	0.3464	0.0000	0.0000	0.0000	0.0000	0.0000	0.0000	0.0001	0.0000	0.0000	0.0000	0.0000	0.0000	0.0850	0.1657	0.2026	0.1100	0.0630	0.0164	0.0083	0.0025
Hopua	0.7686	0.0000	0.0000	0.0006	0.0004	0.0718	0.0476	0.0366	0.0018	0.0061	0.0631	0.0034	0.0000	0.0000	0.0000	0.0000	0.0000	0.0000	0.0000	0.0000	0.0000
Kohuora	0.0002	0.0001	0.0015	0.0133	0.9118	0.0498	0.0232	0.0001	0.0000	0.0000	0.0000	0.0000	0.0000	0.0000	0.0000	0.0000	0.0000	0.0000	0.0000	0.0000	0.0000
Little Rangitoto	0.0359	0.1757	0.2006	0.1959	0.0216	0.0091	0.0014	0.0001	0.0011	0.0028	0.0112	0.0050	0.0129	0.0446	0.0344	0.0310	0.0247	0.0320	0.0394	0.0506	0.0700
Mangere Lagoon	0.7375	0.0266	0.0695	0.0762	0.0012	0.0040	0.0013	0.0001	0.0000	0.0001	0.0059	0.0036	0.0029	0.0222	0.0208	0.0159	0.0095	0.0025	0.0002	0.0000	0.0000
Matukutureia	0.0148	0.0000	0.0000	0.0000	0.0000	0.0000	0.0000	0.0000	0.0000	0.0004	0.0055	0.0023	0.0040	0.1429	0.1007	0.0901	0.0783	0.0688	0.1014	0.1991	0.1917
McLennan Hills	0.9224	0.0000	0.0069	0.0680	0.0000	0.0027	0.0000	0.0000	0.0000	0.0000	0.0000	0.0000	0.0000	0.0000	0.0000	0.0000	0.0000	0.0000	0.0000	0.0000	0.0000
Motukorea	0.9409	0.0001	0.0022	0.0020	0.0002	0.0015	0.0000	0.0000	0.0000	0.0000	0.0005	0.0000	0.0000	0.0091	0.0018	0.0042	0.0036	0.0271	0.0016	0.0011	0.0041
Mt Albert	0.8645	0.0614	0.0477	0.0260	0.0003	0.0001	0.0000	0.0000	0.0000	0.0000	0.0000	0.0000	0.0000	0.0000	0.0000	0.0000	0.0000	0.0000	0.0000	0.0000	0.0000
Mt Cambria	0.7593	0.0148	0.0327	0.0265	0.0028	0.0079	0.0000	0.0000	0.0000	0.0000	0.0024	0.0000	0.0000	0.0241	0.0099	0.0400	0.0140	0.0634	0.0012	0.0009	0.0001
Mt Eden	0.0285	0.0000	0.0000	0.0000	0.0000	0.0000	0.0000	0.0000	0.0000	0.0003	0.0272	0.3954	0.5486	0.0000	0.0000	0.0000	0.0000	0.0000	0.0000	0.0000	0.0000
Mt Hobson	0.0918	0.0000	0.0000	0.0000	0.0000	0.0000	0.0000	0.0000	0.0000	0.0000	0.0000	0.0027	0.0157	0.1290	0.0860	0.0809	0.0715	0.0870	0.1196	0.1361	0.1797
Mt Mangere	0.0051	0.0000	0.0000	0.0000	0.0000	0.0000	0.0000	0.0000	0.0000	0.0000	0.0000	0.0000	0.0000	0.0054	0.0428	0.1322	0.3367	0.3426	0.1326	0.0026	0.0000
Mt Richmond	0.7718	0.0000	0.0000	0.0001	0.0000	0.0025	0.0727	0.1529	0.0000	0.0000	0.0000	0.0000	0.0000	0.0000	0.0000	0.0000	0.0000	0.0000	0.0000	0.0000	0.0000
Mt Roskill	0.9542	0.0023	0.0105	0.0225	0.0009	0.0049	0.0004	0.0002	0.0000	0.0000	0.0041	0.0000	0.0000	0.0000	0.0000	0.0000	0.0000	0.0000	0.0000	0.0000	0.0000
Mt Smart	0.0047	0.0000	0.0000	0.0000	0.0000	0.0000	0.0000	0.0000	0.0000	0.0000	0.0000	0.0000	0.0000	0.0000	0.0005	0.0050	0.0271	0.0740	0.2866	0.3702	0.2319
Mt StJohn	0.6827	0.0408	0.1225	0.1343	0.0010	0.0098	0.0006	0.0001	0.0000	0.0001	0.0054	0.0027	0.0000	0.0000	0.0000	0.0000	0.0000	0.0000	0.0000	0.0000	0.0000
Mt Victoria	0.2066	0.1069	0.1118	0.1148	0.0128	0.0048	0.0015	0.0000	0.0002	0.0007	0.0028	0.0040	0.0070	0.0827	0.0982	0.0485	0.0593	0.0133	0.0588	0.0292	0.0361
North Head	0.9110	0.0782	0.0105	0.0003	0.0000	0.0000	0.0000	0.0000	0.0000	0.0000	0.0000	0.0000	0.0000	0.0000	0.0000	0.0000	0.0000	0.0000	0.0000	0.0000	0.0000
One Tree Hill	0.6397	0.0715	0.1474	0.1269	0.0034	0.0082	0.0009	0.0001	0.0000	0.0001	0.0016	0.0002	0.0000	0.0000	0.0000	0.0000	0.0000	0.0000	0.0000	0.0000	0.0000
Otara Hill	0.0054	0.0002	0.0012	0.0069	0.0056	0.0025	0.0009	0.0000	0.0000	0.0007	0.0056	0.0023	0.0089	0.2253	0.2756	0.1839	0.1321	0.0532	0.0602	0.0235	0.0060
Otuataua	0.8925	0.0974	0.0091	0.0010	0.0000	0.0000	0.0000	0.0000	0.0000	0.0000	0.0000	0.0000	0.0000	0.0000	0.0000	0.0000	0.0000	0.0000	0.0000	0.0000	0.0000
Panmure Basin	0.0917	0.0000	0.0000	0.0005	0.0038	0.7306	0.0930	0.0481	0.0000	0.0025	0.0296	0.0002	0.0000	0.0000	0.0000	0.0000	0.0000	0.0000	0.0000	0.0000	0.0000
Pigeon Mountain	0.7768	0.0182	0.0407	0.0465	0.0014	0.0034	0.0000	0.0000	0.0000	0.0000	0.0039	0.0002	0.0000	0.0222	0.0110	0.0202	0.0068	0.0279	0.0043	0.0042	0.0123
Pukaki	0.9077	0.0923	0.0000	0.0000	0.0000	0.0000	0.0000	0.0000	0.0000	0.0000	0.0000	0.0000	0.0000	0.0000	0.0000	0.0000	0.0000	0.0000	0.0000	0.0000	0.0000
Puketutu	0.0252	0.0000	0.0000	0.0000	0.0003	0.0044	0.0399	0.0470	0.1662	0.2138	0.5030	0.0002	0.0000	0.0000	0.0000	0.0000	0.0000	0.0000	0.0000	0.0000	0.0000
Robertson Hill	0.9990	0.0000	0.0000	0.0000	0.0000	0.0001	0.0009	0.0000	0.0000	0.0000	0.0000	0.0000	0.0000	0.0000	0.0000	0.0000	0.0000	0.0000	0.0000	0.0000	0.0000
Styaks Swamp	0.4423	0.0000	0.0000	0.0000	0.0000	0.0001	0.0000	0.0000	0.0000	0.0000	0.0000	0.0000	0.0000	0.0095	0.0219	0.0308	0.0397	0.0603	0.0680	0.0882	0.2392
Taylors Hill	0.5330	0.0000	0.0000	0.0001	0.0000	0.0241	0.2291	0.2113	0.0000	0.0003	0.0021	0.0000	0.0000	0.0000	0.0000	0.0000	0.0000	0.0000	0.0000	0.0000	0.0000
Te Pouhawaiki	0.7215	0.0848	0.0771	0.0904	0.0105	0.0048	0.0010	0.0000	0.0001	0.0003	0.0069	0.0026	0.0000	0.0000	0.0000	0.0000	0.0000	0.0000	0.0000	0.0000	0.0000
Three Kings	0.0000	0.0000	0.0000	0.0000	0.0000	0.0000	0.0000	0.0000	0.0000	0.0023	0.0817	0.5649	0.3511	0.0000	0.0000	0.0000	0.0000	0.0000	0.0000	0.0000	0.0000
Wiri Mountain	0.3569	0.0000	0.0000	0.0000	0.0002	0.0023	0.1608	0.2730	0.0331	0.0997	0.0740	0.0000	0.0000	0.0000	0.0000	0.0000	0.0000	0.0000	0.0000	0.0000	0.0000

Table A.8: Marginal posterior probabilities for a volcano to have produced a given tephra for the Maungataketake and North Head scenario with C = $\{\alpha = 2.5,\ \beta U = 0.5\}$.

Volcano	AVF tephra (AVF 0 = 'unmatched')																				
	0	1	2	3	4	5	6	7	8	9	10	11	12	13	14	15	16	17	18	19	20
Ash Hill	0.7714	0.0000	0.0000	0.0000	0.0000	0.0116	0.1819	0.0351	0.0000	0.0000	0.0000	0.0000	0.0000	0.0000	0.0000	0.0000	0.0000	0.0000	0.0000	0.0000	0.0000
Cemetery Hill	0.0283	0.0000	0.0000	0.0000	0.0004	0.0225	0.1322	0.1706	0.5223	0.1233	0.0004	0.0000	0.0000	0.0000	0.0000	0.0000	0.0000	0.0000	0.0000	0.0000	0.0000
Crater Hill	0.0001	0.0000	0.0000	0.0000	0.0000	0.0001	0.0160	0.0176	0.2764	0.5444	0.1449	0.0005	0.0000	0.0000	0.0000	0.0000	0.0000	0.0000	0.0000	0.0000	0.0000
Domain	0.7334	0.1331	0.1042	0.0293	0.0000	0.0000	0.0000	0.0000	0.0000	0.0000	0.0000	0.0000	0.0000	0.0000	0.0000	0.0000	0.0000	0.0000	0.0000	0.0000	0.0000
Green Hill	0.0058	0.0003	0.0026	0.0171	0.0228	0.0158	0.0043	0.0001	0.0002	0.0014	0.0300	0.0107	0.0513	0.1972	0.1316	0.1155	0.0880	0.0873	0.1092	0.0828	0.0260
Hampton Park	0.3612	0.0000	0.0000	0.0000	0.0000	0.0000	0.0000	0.0001	0.0000	0.0000	0.0000	0.0000	0.0000	0.0827	0.1701	0.1925	0.1023	0.0645	0.0158	0.0083	0.0025
Hopua	0.7634	0.0000	0.0000	0.0006	0.0004	0.0770	0.0469	0.0374	0.0016	0.0065	0.0624	0.0038	0.0000	0.0000	0.0000	0.0000	0.0000	0.0000	0.0000	0.0000	0.0000
Kohuora	0.0010	0.0001	0.0013	0.0147	0.9066	0.0512	0.0250	0.0001	0.0000	0.0000	0.0000	0.0000	0.0000	0.0000	0.0000	0.0000	0.0000	0.0000	0.0000	0.0000	0.0000
Little Rangitoto	0.0275	0.1794	0.2040	0.1890	0.0241	0.0085	0.0014	0.0001	0.0011	0.0028	0.0112	0.0050	0.0135	0.0445	0.0344	0.0319	0.0240	0.0337	0.0397	0.0507	0.0735
Mangere Lagoon	0.7429	0.0263	0.0691	0.0723	0.0009	0.0038	0.0012	0.0003	0.0000	0.0001	0.0046	0.0046	0.0028	0.0224	0.0211	0.0161	0.0088	0.0025	0.0002	0.0000	0.0000
Matukutureia	0.0110	0.0000	0.0000	0.0000	0.0000	0.0000	0.0000	0.0000	0.0000	0.0007	0.0047	0.0029	0.0051	0.1433	0.1012	0.0915	0.0775	0.0688	0.1043	0.2042	0.1848
McLennan Hills	0.9061	0.0000	0.0072	0.0831	0.0000	0.0036	0.0000	0.0000	0.0000	0.0000	0.0000	0.0000	0.0000	0.0000	0.0000	0.0000	0.0000	0.0000	0.0000	0.0000	0.0000
Motukorea	0.9417	0.0000	0.0021	0.0008	0.0002	0.0016	0.0000	0.0000	0.0000	0.0000	0.0021	0.0000	0.0000	0.0085	0.0018	0.0035	0.0034	0.0274	0.0016	0.0011	0.0042
Mt Albert	0.8718	0.0610	0.0426	0.0240	0.0005	0.0001	0.0000	0.0000	0.0000	0.0000	0.0000	0.0000	0.0000	0.0000	0.0000	0.0000	0.0000	0.0000	0.0000	0.0000	0.0000
Mt Cambria	0.7648	0.0163	0.0355	0.0253	0.0029	0.0082	0.0000	0.0000	0.0000	0.0000	0.0031	0.0000	0.0000	0.0230	0.0099	0.0300	0.0125	0.0664	0.0012	0.0009	0.0000
Mt Eden	0.0361	0.0000	0.0000	0.0000	0.0000	0.0000	0.0000	0.0000	0.0000	0.0003	0.0285	0.3956	0.5395	0.0000	0.0000	0.0000	0.0000	0.0000	0.0000	0.0000	0.0000
Mt Hobson	0.0817	0.0000	0.0000	0.0000	0.0000	0.0000	0.0000	0.0000	0.0000	0.0000	0.0000	0.0028	0.0171	0.1305	0.0854	0.0822	0.0701	0.0924	0.1171	0.1371	0.1836
Mt Mangere	0.0068	0.0000	0.0000	0.0000	0.0000	0.0000	0.0000	0.0000	0.0000	0.0000	0.0000	0.0000	0.0000	0.0055	0.0441	0.1392	0.3496	0.3219	0.1305	0.0024	0.0000
Mt Richmond	0.7733	0.0000	0.0000	0.0001	0.0000	0.0025	0.0710	0.1531	0.0000	0.0000	0.0000	0.0000	0.0000	0.0000	0.0000	0.0000	0.0000	0.0000	0.0000	0.0000	0.0000
Mt Roskill	0.9518	0.0020	0.0106	0.0260	0.0006	0.0047	0.0004	0.0002	0.0000	0.0000	0.0037	0.0000	0.0000	0.0000	0.0000	0.0000	0.0000	0.0000	0.0000	0.0000	0.0000
Mt Smart	0.0035	0.0000	0.0000	0.0000	0.0000	0.0000	0.0000	0.0000	0.0000	0.0000	0.0000	0.0000	0.0000	0.0000	0.0005	0.0055	0.0292	0.0775	0.2917	0.3679	0.2242
Mt StJohn	0.6844	0.0423	0.1235	0.1300	0.0010	0.0097	0.0006	0.0001	0.0000	0.0001	0.0050	0.0033	0.0000	0.0000	0.0000	0.0000	0.0000	0.0000	0.0000	0.0000	0.0000
Mt Victoria	0.2024	0.1086	0.1115	0.1144	0.0142	0.0043	0.0014	0.0000	0.0002	0.0011	0.0024	0.0040	0.0085	0.0833	0.0927	0.0549	0.0595	0.0130	0.0577	0.0288	0.0371
North Head	0.9071	0.0822	0.0103	0.0004	0.0000	0.0000	0.0000	0.0000	0.0000	0.0000	0.0000	0.0000	0.0000	0.0000	0.0000	0.0000	0.0000	0.0000	0.0000	0.0000	0.0000
One Tree Hill	0.6412	0.0715	0.1457	0.1274	0.0030	0.0082	0.0010	0.0001	0.0000	0.0001	0.0016	0.0002	0.0000	0.0000	0.0000	0.0000	0.0000	0.0000	0.0000	0.0000	0.0000
Otara Hill	0.0056	0.0003	0.0011	0.0067	0.0054	0.0024	0.0009	0.0000	0.0000	0.0007	0.0054	0.0025	0.0097	0.2281	0.2748	0.1867	0.1306	0.0506	0.0597	0.0230	0.0058
Otuataua	0.9130	0.0793	0.0071	0.0006	0.0000	0.0000	0.0000	0.0000	0.0000	0.0000	0.0000	0.0000	0.0000	0.0000	0.0000	0.0000	0.0000	0.0000	0.0000	0.0000	0.0000
Panmure Basin	0.0898	0.0000	0.0000	0.0004	0.0039	0.7246	0.0976	0.0503	0.0000	0.0026	0.0289	0.0019	0.0000	0.0000	0.0000	0.0000	0.0000	0.0000	0.0000	0.0000	0.0000
Pigeon Mountain	0.7766	0.0177	0.0430	0.0455	0.0012	0.0035	0.0000	0.0000	0.0000	0.0000	0.0037	0.0002	0.0000	0.0221	0.0113	0.0198	0.0059	0.0289	0.0040	0.0036	0.0130
Pukaki	0.9123	0.0877	0.0000	0.0000	0.0000	0.0000	0.0000	0.0000	0.0000	0.0000	0.0000	0.0000	0.0000	0.0000	0.0000	0.0000	0.0000	0.0000	0.0000	0.0000	0.0000
Puketutu	0.0249	0.0000	0.0000	0.0000	0.0003	0.0043	0.0384	0.0443	0.1670	0.2175	0.5031	0.0002	0.0000	0.0000	0.0000	0.0000	0.0000	0.0000	0.0000	0.0000	0.0000
Robertson Hill	0.9990	0.0000	0.0000	0.0000	0.0000	0.0001	0.0009	0.0000	0.0000	0.0000	0.0000	0.0000	0.0000	0.0000	0.0000	0.0000	0.0000	0.0000	0.0000	0.0000	0.0000
Styaks Swamp	0.4337	0.0000	0.0000	0.0000	0.0000	0.0001	0.0000	0.0000	0.0000	0.0000	0.0000	0.0000	0.0000	0.0089	0.0211	0.0307	0.0386	0.0651	0.0673	0.0892	0.2453
Taylors Hill	0.5406	0.0000	0.0000	0.0001	0.0000	0.0239	0.2162	0.2169	0.0000	0.0003	0.0020	0.0000	0.0000	0.0000	0.0000	0.0000	0.0000	0.0000	0.0000	0.0000	0.0000
Te Pouhawaiki	0.7092	0.0919	0.0786	0.0922	0.0115	0.0054	0.0013	0.0000	0.0001	0.0003	0.0069	0.0026	0.0000	0.0000	0.0000	0.0000	0.0000	0.0000	0.0000	0.0000	0.0000
Three Kings	0.0000	0.0000	0.0000	0.0000	0.0000	0.0000	0.0000	0.0000	0.0000	0.0025	0.0858	0.5592	0.3525	0.0000	0.0000	0.0000	0.0000	0.0000	0.0000	0.0000	0.0000
Wiri Mountain	0.3766	0.0000	0.0000	0.0000	0.0001	0.0023	0.1614	0.2736	0.0311	0.0953	0.0596	0.0000	0.0000	0.0000	0.0000	0.0000	0.0000	0.0000	0.0000	0.0000	0.0000

Table A.9: Marginal posterior probabilities for a volcano to have produced a given tephra for the Maungataketake and North Head scenario with D = $\{\alpha = 1.5, \beta U = 1.0\}$.

Volcano	AVF tephra (AVF 0 = ‘unmatched’)																				
	0	1	2	3	4	5	6	7	8	9	10	11	12	13	14	15	16	17	18	19	20
Ash Hill	0.6102	0.0000	0.0000	0.0000	0.0000	0.0278	0.3070	0.0550	0.0000	0.0000	0.0000	0.0000	0.0000	0.0000	0.0000	0.0000	0.0000	0.0000	0.0000	0.0000	0.0000
Cemetery Hill	0.0002	0.0000	0.0000	0.0000	0.0026	0.0360	0.1129	0.1101	0.5692	0.1651	0.0039	0.0000	0.0000	0.0000	0.0000	0.0000	0.0000	0.0000	0.0000	0.0000	0.0000
Crater Hill	0.0010	0.0000	0.0000	0.0000	0.0000	0.0004	0.0116	0.0170	0.2033	0.5692	0.1893	0.0082	0.0000	0.0000	0.0000	0.0000	0.0000	0.0000	0.0000	0.0000	0.0000
Domain	0.7573	0.0994	0.1128	0.0305	0.0000	0.0000	0.0000	0.0000	0.0000	0.0000	0.0000	0.0000	0.0000	0.0000	0.0000	0.0000	0.0000	0.0000	0.0000	0.0000	0.0000
Green Hill	0.0024	0.0001	0.0024	0.0150	0.0269	0.0155	0.0045	0.0003	0.0003	0.0007	0.0153	0.0241	0.0569	0.1971	0.1383	0.1174	0.0909	0.0938	0.1059	0.0770	0.0152
Hampton Park	0.4410	0.0000	0.0000	0.0000	0.0000	0.0000	0.0000	0.0000	0.0000	0.0000	0.0000	0.0000	0.0000	0.0711	0.1530	0.1672	0.0873	0.0566	0.0146	0.0068	0.0024
Hopua	0.5304	0.0000	0.0000	0.0003	0.0006	0.0909	0.0532	0.0457	0.0026	0.0065	0.0320	0.2378	0.0000	0.0000	0.0000	0.0000	0.0000	0.0000	0.0000	0.0000	0.0000
Kohuora	0.0000	0.0000	0.0018	0.0144	0.8873	0.0741	0.0217	0.0004	0.0003	0.0000	0.0000	0.0000	0.0000	0.0000	0.0000	0.0000	0.0000	0.0000	0.0000	0.0000	0.0000
Little Rangitoto	0.0150	0.1904	0.1708	0.2039	0.0286	0.0090	0.0016	0.0003	0.0011	0.0018	0.0056	0.0113	0.0152	0.0437	0.0358	0.0327	0.0258	0.0348	0.0432	0.0498	0.0796
Mangere Lagoon	0.7377	0.0083	0.0749	0.0809	0.0029	0.0070	0.0012	0.0002	0.0000	0.0001	0.0015	0.0090	0.0056	0.0225	0.0218	0.0165	0.0075	0.0022	0.0002	0.0000	0.0000
Matukutureia	0.0041	0.0000	0.0000	0.0000	0.0000	0.0000	0.0000	0.0000	0.0000	0.0001	0.0021	0.0054	0.0092	0.1443	0.1054	0.0955	0.0758	0.0725	0.1154	0.2110	0.1592
McLennan Hills	0.9067	0.0000	0.0095	0.0804	0.0000	0.0032	0.0002	0.0000	0.0000	0.0000	0.0000	0.0000	0.0000	0.0000	0.0000	0.0000	0.0000	0.0000	0.0000	0.0000	0.0000
Motukorea	0.9519	0.0000	0.0018	0.0004	0.0000	0.0015	0.0000	0.0000	0.0000	0.0000	0.0001	0.0000	0.0000	0.0045	0.0017	0.0019	0.0019	0.0282	0.0016	0.0010	0.0035
Mt Albert	0.8732	0.0469	0.0514	0.0278	0.0006	0.0001	0.0000	0.0000	0.0000	0.0000	0.0000	0.0000	0.0000	0.0000	0.0000	0.0000	0.0000	0.0000	0.0000	0.0000	0.0000
Mt Cambria	0.8150	0.0038	0.0159	0.0241	0.0037	0.0073	0.0000	0.0000	0.0000	0.0000	0.0031	0.0000	0.0000	0.0191	0.0074	0.0169	0.0066	0.0749	0.0013	0.0009	0.0000
Mt Eden	0.4424	0.0000	0.0000	0.0000	0.0000	0.0000	0.0000	0.0000	0.0000	0.0002	0.0123	0.3529	0.1922	0.0000	0.0000	0.0000	0.0000	0.0000	0.0000	0.0000	0.0000
Mt Hobson	0.0516	0.0000	0.0000	0.0000	0.0000	0.0000	0.0000	0.0000	0.0000	0.0000	0.0000	0.0032	0.0132	0.1314	0.0904	0.0830	0.0752	0.0926	0.1228	0.1372	0.1994
Mt Mangere	0.0165	0.0000	0.0000	0.0000	0.0000	0.0000	0.0000	0.0000	0.0000	0.0000	0.0000	0.0000	0.0000	0.0060	0.0457	0.1707	0.3690	0.2827	0.1074	0.0020	0.0000
Mt Richmond	0.8428	0.0000	0.0000	0.0001	0.0000	0.0014	0.0395	0.1162	0.0000	0.0000	0.0000	0.0000	0.0000	0.0000	0.0000	0.0000	0.0000	0.0000	0.0000	0.0000	0.0000
Mt Roskill	0.9821	0.0014	0.0082	0.0016	0.0012	0.0042	0.0004	0.0001	0.0000	0.0000	0.0008	0.0000	0.0000	0.0000	0.0000	0.0000	0.0000	0.0000	0.0000	0.0000	0.0000
Mt Smart	0.0012	0.0000	0.0000	0.0000	0.0000	0.0000	0.0000	0.0000	0.0000	0.0000	0.0000	0.0000	0.0000	0.0000	0.0007	0.0065	0.0412	0.1036	0.2927	0.3537	0.2004
Mt StJohn	0.7015	0.0077	0.1349	0.1344	0.0019	0.0085	0.0016	0.0001	0.0000	0.0001	0.0012	0.0081	0.0000	0.0000	0.0000	0.0000	0.0000	0.0000	0.0000	0.0000	0.0000
Mt Victoria	0.1985	0.0982	0.1133	0.1186	0.0121	0.0060	0.0020	0.0002	0.0002	0.0006	0.0009	0.0050	0.0116	0.0878	0.0951	0.0583	0.0572	0.0078	0.0581	0.0286	0.0399
North Head	0.9071	0.0828	0.0095	0.0006	0.0000	0.0000	0.0000	0.0000	0.0000	0.0000	0.0000	0.0000	0.0000	0.0000	0.0000	0.0000	0.0000	0.0000	0.0000	0.0000	0.0000
One Tree Hill	0.6680	0.0305	0.1571	0.1306	0.0028	0.0083	0.0009	0.0002	0.0000	0.0000	0.0006	0.0010	0.0000	0.0000	0.0000	0.0000	0.0000	0.0000	0.0000	0.0000	0.0000
Otara Hill	0.0015	0.0001	0.0015	0.0060	0.0079	0.0031	0.0008	0.0001	0.0001	0.0003	0.0027	0.0052	0.0139	0.2408	0.2761	0.1883	0.1197	0.0521	0.0527	0.0224	0.0047
Otuataua	0.7538	0.2257	0.0190	0.0015	0.0000	0.0000	0.0000	0.0000	0.0000	0.0000	0.0000	0.0000	0.0000	0.0000	0.0000	0.0000	0.0000	0.0000	0.0000	0.0000	0.0000
Panmure Basin	0.2308	0.0000	0.0000	0.0011	0.0029	0.6584	0.0464	0.0419	0.0000	0.0003	0.0141	0.0041	0.0000	0.0000	0.0000	0.0000	0.0000	0.0000	0.0000	0.0000	0.0000
Pigeon Mountain	0.8179	0.0062	0.0310	0.0372	0.0025	0.0038	0.0000	0.0000	0.0000	0.0000	0.0030	0.0000	0.0000	0.0213	0.0076	0.0155	0.0033	0.0315	0.0031	0.0031	0.0130
Pukaki	0.9029	0.0971	0.0000	0.0000	0.0000	0.0000	0.0000	0.0000	0.0000	0.0000	0.0000	0.0000	0.0000	0.0000	0.0000	0.0000	0.0000	0.0000	0.0000	0.0000	0.0000
Puketutu	0.0115	0.0000	0.0000	0.0000	0.0005	0.0106	0.0231	0.0419	0.1783	0.1488	0.5835	0.0018	0.0000	0.0000	0.0000	0.0000	0.0000	0.0000	0.0000	0.0000	0.0000
Robertson Hill	0.9993	0.0000	0.0000	0.0000	0.0000	0.0001	0.0005	0.0001	0.0000	0.0000	0.0000	0.0000	0.0000	0.0000	0.0000	0.0000	0.0000	0.0000	0.0000	0.0000	0.0000
Styaks Swamp	0.3634	0.0000	0.0000	0.0000	0.0000	0.0001	0.0000	0.0000	0.0000	0.0000	0.0000	0.0000	0.0000	0.0104	0.0210	0.0296	0.0386	0.0667	0.0810	0.1065	0.2827
Taylors Hill	0.4355	0.0000	0.0000	0.0001	0.0000	0.0134	0.2881	0.2623	0.0001	0.0004	0.0000	0.0001	0.0000	0.0000	0.0000	0.0000	0.0000	0.0000	0.0000	0.0000	0.0000
Te Pouhawaiki	0.6901	0.1014	0.0842	0.0905	0.0146	0.0076	0.0015	0.0003	0.0002	0.0004	0.0035	0.0048	0.0009	0.0000	0.0000	0.0000	0.0000	0.0000	0.0000	0.0000	0.0000
Three Kings	0.0000	0.0000	0.0000	0.0000	0.0000	0.0000	0.0000	0.0000	0.0000	0.0013	0.0577	0.2597	0.6813	0.0000	0.0000	0.0000	0.0000	0.0000	0.0000	0.0000	0.0000
Wiri Mountain	0.3355	0.0000	0.0000	0.0000	0.0004	0.0017	0.0813	0.3076	0.0443	0.1041	0.0668	0.0583	0.0000	0.0000	0.0000	0.0000	0.0000	0.0000	0.0000	0.0000	0.0000

Table A.10: Marginal posterior probabilities for a volcano to have produced a given tephra for the Maungataketake and North Head scenario with E = $\{\alpha = 2.0, \beta U = 1.0\}$.

Volcano	AVF tephra (AVF 0 = 'unmatched')																				
	0	1	2	3	4	5	6	7	8	9	10	11	12	13	14	15	16	17	18	19	20
Ash Hill	0.6077	0.0000	0.0000	0.0000	0.0000	0.0278	0.3091	0.0554	0.0000	0.0000	0.0000	0.0000	0.0000	0.0000	0.0000	0.0000	0.0000	0.0000	0.0000	0.0000	0.0000
Cemetery Hill	0.0002	0.0000	0.0000	0.0000	0.0029	0.0357	0.1126	0.1085	0.5694	0.1677	0.0030	0.0000	0.0000	0.0000	0.0000	0.0000	0.0000	0.0000	0.0000	0.0000	0.0000
Crater Hill	0.0019	0.0000	0.0000	0.0000	0.0000	0.0004	0.0120	0.0174	0.2021	0.5672	0.1918	0.0072	0.0000	0.0000	0.0000	0.0000	0.0000	0.0000	0.0000	0.0000	0.0000
Domain	0.7547	0.1000	0.1149	0.0304	0.0000	0.0000	0.0000	0.0000	0.0000	0.0000	0.0000	0.0000	0.0000	0.0000	0.0000	0.0000	0.0000	0.0000	0.0000	0.0000	0.0000
Green Hill	0.0023	0.0001	0.0025	0.0148	0.0271	0.0154	0.0045	0.0003	0.0003	0.0007	0.0172	0.0225	0.0581	0.1966	0.1384	0.1177	0.0909	0.0936	0.1061	0.0770	0.0139
Hampton Park	0.4461	0.0000	0.0000	0.0000	0.0000	0.0000	0.0000	0.0000	0.0000	0.0000	0.0000	0.0000	0.0000	0.0709	0.1518	0.1655	0.0849	0.0573	0.0145	0.0066	0.0024
Hopua	0.5261	0.0000	0.0000	0.0003	0.0006	0.0907	0.0591	0.0449	0.0027	0.0078	0.0332	0.2346	0.0000	0.0000	0.0000	0.0000	0.0000	0.0000	0.0000	0.0000	0.0000
Kohuora	0.0000	0.0001	0.0016	0.0158	0.8816	0.0776	0.0224	0.0005	0.0004	0.0000	0.0000	0.0000	0.0000	0.0000	0.0000	0.0000	0.0000	0.0000	0.0000	0.0000	0.0000
Little Rangitoto	0.0125	0.1896	0.1761	0.2001	0.0295	0.0090	0.0014	0.0003	0.0011	0.0018	0.0066	0.0103	0.0157	0.0438	0.0362	0.0320	0.0260	0.0354	0.0426	0.0500	0.0800
Mangere Lagoon	0.7421	0.0077	0.0745	0.0772	0.0033	0.0069	0.0012	0.0002	0.0000	0.0003	0.0013	0.0090	0.0056	0.0228	0.0217	0.0164	0.0074	0.0022	0.0002	0.0000	0.0000
Matukutureia	0.0036	0.0000	0.0000	0.0000	0.0000	0.0000	0.0000	0.0000	0.0000	0.0001	0.0028	0.0049	0.0109	0.1429	0.1058	0.0958	0.0758	0.0723	0.1174	0.2093	0.1584
McLennan Hills	0.9052	0.0000	0.0096	0.0814	0.0000	0.0035	0.0003	0.0000	0.0000	0.0000	0.0000	0.0000	0.0000	0.0000	0.0000	0.0000	0.0000	0.0000	0.0000	0.0000	0.0000
Motukorea	0.9512	0.0000	0.0018	0.0003	0.0003	0.0019	0.0000	0.0000	0.0000	0.0000	0.0001	0.0000	0.0000	0.0046	0.0017	0.0019	0.0019	0.0282	0.0016	0.0010	0.0035
Mt Albert	0.8780	0.0456	0.0483	0.0275	0.0005	0.0001	0.0000	0.0000	0.0000	0.0000	0.0000	0.0000	0.0000	0.0000	0.0000	0.0000	0.0000	0.0000	0.0000	0.0000	0.0000
Mt Cambria	0.7945	0.0043	0.0317	0.0265	0.0036	0.0078	0.0000	0.0000	0.0000	0.0000	0.0035	0.0001	0.0000	0.0194	0.0076	0.0167	0.0065	0.0756	0.0013	0.0009	0.0000
Mt Eden	0.4387	0.0000	0.0000	0.0000	0.0000	0.0000	0.0000	0.0000	0.0000	0.0002	0.0129	0.3576	0.1906	0.0000	0.0000	0.0000	0.0000	0.0000	0.0000	0.0000	0.0000
Mt Hobson	0.0483	0.0000	0.0000	0.0000	0.0000	0.0000	0.0000	0.0000	0.0000	0.0000	0.0000	0.0030	0.0132	0.1340	0.0884	0.0828	0.0756	0.0932	0.1223	0.1374	0.2018
Mt Mangere	0.0166	0.0000	0.0000	0.0000	0.0000	0.0000	0.0000	0.0000	0.0000	0.0000	0.0000	0.0000	0.0000	0.0062	0.0464	0.1740	0.3696	0.2781	0.1071	0.0020	0.0000
Mt Richmond	0.8438	0.0000	0.0000	0.0001	0.0000	0.0014	0.0394	0.1153	0.0000	0.0000	0.0000	0.0000	0.0000	0.0000	0.0000	0.0000	0.0000	0.0000	0.0000	0.0000	0.0000
Mt Roskill	0.9825	0.0013	0.0081	0.0011	0.0012	0.0045	0.0004	0.0001	0.0000	0.0000	0.0008	0.0000	0.0000	0.0000	0.0000	0.0000	0.0000	0.0000	0.0000	0.0000	0.0000
Mt Smart	0.0013	0.0000	0.0000	0.0000	0.0000	0.0000	0.0000	0.0000	0.0000	0.0000	0.0000	0.0000	0.0000	0.0000	0.0008	0.0071	0.0416	0.1041	0.2934	0.3539	0.1978
Mt StJohn	0.7075	0.0079	0.1298	0.1331	0.0020	0.0087	0.0015	0.0001	0.0000	0.0001	0.0013	0.0080	0.0000	0.0000	0.0000	0.0000	0.0000	0.0000	0.0000	0.0000	0.0000
Mt Victoria	0.1895	0.1124	0.1054	0.1201	0.0125	0.0058	0.0020	0.0002	0.0002	0.0010	0.0005	0.0050	0.0132	0.0869	0.0955	0.0576	0.0582	0.0073	0.0573	0.0292	0.0402
North Head	0.9043	0.0856	0.0095	0.0006	0.0000	0.0000	0.0000	0.0000	0.0000	0.0000	0.0000	0.0000	0.0000	0.0000	0.0000	0.0000	0.0000	0.0000	0.0000	0.0000	0.0000
One Tree Hill	0.6699	0.0349	0.1506	0.1307	0.0029	0.0082	0.0010	0.0002	0.0000	0.0000	0.0007	0.0009	0.0000	0.0000	0.0000	0.0000	0.0000	0.0000	0.0000	0.0000	0.0000
Otara Hill	0.0015	0.0001	0.0014	0.0058	0.0084	0.0029	0.0008	0.0001	0.0001	0.0003	0.0029	0.0050	0.0158	0.2400	0.2770	0.1879	0.1195	0.0512	0.0523	0.0224	0.0046
Otuataua	0.7817	0.1996	0.0172	0.0015	0.0000	0.0000	0.0000	0.0000	0.0000	0.0000	0.0000	0.0000	0.0000	0.0000	0.0000	0.0000	0.0000	0.0000	0.0000	0.0000	0.0000
Panmure Basin	0.2328	0.0000	0.0001	0.0010	0.0029	0.6548	0.0457	0.0426	0.0000	0.0003	0.0158	0.0040	0.0000	0.0000	0.0000	0.0000	0.0000	0.0000	0.0000	0.0000	0.0000
Pigeon Mountain	0.8117	0.0061	0.0352	0.0384	0.0025	0.0039	0.0000	0.0000	0.0000	0.0000	0.0028	0.0000	0.0000	0.0215	0.0076	0.0151	0.0035	0.0319	0.0031	0.0030	0.0137
Pukaki	0.9045	0.0955	0.0000	0.0000	0.0000	0.0000	0.0000	0.0000	0.0000	0.0000	0.0000	0.0000	0.0000	0.0000	0.0000	0.0000	0.0000	0.0000	0.0000	0.0000	0.0000
Puketutu	0.0116	0.0000	0.0000	0.0000	0.0005	0.0104	0.0223	0.0409	0.1816	0.1524	0.5784	0.0019	0.0000	0.0000	0.0000	0.0000	0.0000	0.0000	0.0000	0.0000	0.0000
Robertson Hill	0.9990	0.0000	0.0000	0.0000	0.0000	0.0001	0.0008	0.0001	0.0000	0.0000	0.0000	0.0000	0.0000	0.0000	0.0000	0.0000	0.0000	0.0000	0.0000	0.0000	0.0000
Styaks Swamp	0.3588	0.0000	0.0000	0.0000	0.0000	0.0001	0.0000	0.0001	0.0000	0.0000	0.0000	0.0000	0.0000	0.0104	0.0211	0.0295	0.0386	0.0696	0.0808	0.1073	0.2837
Taylors Hill	0.4609	0.0000	0.0000	0.0002	0.0000	0.0135	0.2732	0.2518	0.0001	0.0003	0.0000	0.0000	0.0000	0.0000	0.0000	0.0000	0.0000	0.0000	0.0000	0.0000	0.0000
Te Pouhawaiki	0.6798	0.1092	0.0817	0.0931	0.0173	0.0073	0.0013	0.0003	0.0002	0.0004	0.0037	0.0048	0.0009	0.0000	0.0000	0.0000	0.0000	0.0000	0.0000	0.0000	0.0000
Three Kings	0.0000	0.0000	0.0000	0.0000	0.0000	0.0000	0.0000	0.0000	0.0000	0.0015	0.0618	0.2607	0.6760	0.0000	0.0000	0.0000	0.0000	0.0000	0.0000	0.0000	0.0000
Wiri Mountain	0.3292	0.0000	0.0000	0.0000	0.0004	0.0016	0.0890	0.3207	0.0418	0.0979	0.0589	0.0605	0.0000	0.0000	0.0000	0.0000	0.0000	0.0000	0.0000	0.0000	0.0000

Table A.11: Marginal posterior probabilities for a volcano to have produced a given tephra for the Maungataketake and North Head scenario with F = $\{\alpha = 2.5,\ \beta U = 1.0\}$.

Volcano	AVF tephra (AVF 0 = 'unmatched')																				
	0	1	2	3	4	5	6	7	8	9	10	11	12	13	14	15	16	17	18	19	20
Ash Hill	0.6037	0.0000	0.0000	0.0000	0.0000	0.0282	0.3123	0.0558	0.0000	0.0000	0.0000	0.0000	0.0000	0.0000	0.0000	0.0000	0.0000	0.0000	0.0000	0.0000	0.0000
Cemetery Hill	0.0001	0.0000	0.0000	0.0000	0.0030	0.0331	0.1153	0.1084	0.5669	0.1725	0.0007	0.0000	0.0000	0.0000	0.0000	0.0000	0.0000	0.0000	0.0000	0.0000	0.0000
Crater Hill	0.0027	0.0000	0.0000	0.0000	0.0000	0.0004	0.0096	0.0200	0.2022	0.5645	0.1982	0.0024	0.0000	0.0000	0.0000	0.0000	0.0000	0.0000	0.0000	0.0000	0.0000
Domain	0.7553	0.1018	0.1120	0.0309	0.0000	0.0000	0.0000	0.0000	0.0000	0.0000	0.0000	0.0000	0.0000	0.0000	0.0000	0.0000	0.0000	0.0000	0.0000	0.0000	0.0000
Green Hill	0.0023	0.0001	0.0026	0.0152	0.0267	0.0154	0.0044	0.0003	0.0003	0.0008	0.0164	0.0233	0.0603	0.1958	0.1373	0.1181	0.0920	0.0933	0.1058	0.0764	0.0132
Hampton Park	0.4505	0.0000	0.0000	0.0000	0.0000	0.0000	0.0000	0.0000	0.0000	0.0000	0.0000	0.0000	0.0000	0.0706	0.1512	0.1631	0.0831	0.0577	0.0148	0.0066	0.0024
Hopua	0.5278	0.0000	0.0000	0.0004	0.0007	0.0907	0.0590	0.0457	0.0027	0.0081	0.0333	0.2316	0.0000	0.0000	0.0000	0.0000	0.0000	0.0000	0.0000	0.0000	0.0000
Kohuora	0.0000	0.0002	0.0017	0.0164	0.8803	0.0778	0.0227	0.0005	0.0004	0.0000	0.0000	0.0000	0.0000	0.0000	0.0000	0.0000	0.0000	0.0000	0.0000	0.0000	0.0000
Little Rangitoto	0.0093	0.1967	0.1738	0.1976	0.0298	0.0084	0.0013	0.0003	0.0012	0.0018	0.0065	0.0104	0.0167	0.0432	0.0364	0.0320	0.0257	0.0360	0.0427	0.0502	0.0800
Mangere Lagoon	0.7450	0.0074	0.0743	0.0753	0.0032	0.0068	0.0012	0.0002	0.0000	0.0003	0.0013	0.0089	0.0054	0.0232	0.0217	0.0162	0.0073	0.0021	0.0002	0.0000	0.0000
Matukutureia	0.0027	0.0000	0.0000	0.0000	0.0000	0.0000	0.0000	0.0000	0.0000	0.0001	0.0028	0.0048	0.0126	0.1421	0.1068	0.0949	0.0752	0.0731	0.1187	0.2084	0.1578
McLennan Hills	0.9040	0.0000	0.0097	0.0826	0.0000	0.0034	0.0003	0.0000	0.0000	0.0000	0.0000	0.0000	0.0000	0.0000	0.0000	0.0000	0.0000	0.0000	0.0000	0.0000	0.0000
Motukorea	0.9516	0.0000	0.0019	0.0002	0.0003	0.0018	0.0000	0.0000	0.0000	0.0000	0.0001	0.0000	0.0000	0.0046	0.0017	0.0019	0.0019	0.0279	0.0016	0.0010	0.0035
Mt Albert	0.8845	0.0455	0.0436	0.0259	0.0004	0.0001	0.0000	0.0000	0.0000	0.0000	0.0000	0.0000	0.0000	0.0000	0.0000	0.0000	0.0000	0.0000	0.0000	0.0000	0.0000
Mt Cambria	0.7657	0.0150	0.0441	0.0298	0.0035	0.0084	0.0000	0.0000	0.0000	0.0000	0.0040	0.0001	0.0000	0.0204	0.0079	0.0159	0.0064	0.0766	0.0013	0.0009	0.0000
Mt Eden	0.4332	0.0000	0.0000	0.0000	0.0000	0.0000	0.0000	0.0000	0.0000	0.0002	0.0137	0.3609	0.1920	0.0000	0.0000	0.0000	0.0000	0.0000	0.0000	0.0000	0.0000
Mt Hobson	0.0466	0.0000	0.0000	0.0000	0.0000	0.0000	0.0000	0.0000	0.0000	0.0000	0.0000	0.0033	0.0128	0.1355	0.0875	0.0826	0.0760	0.0953	0.1202	0.1371	0.2031
Mt Mangere	0.0169	0.0000	0.0000	0.0000	0.0000	0.0000	0.0000	0.0000	0.0000	0.0000	0.0000	0.0000	0.0000	0.0063	0.0480	0.1776	0.3698	0.2721	0.1074	0.0019	0.0000
Mt Richmond	0.8251	0.0000	0.0000	0.0001	0.0000	0.0014	0.0386	0.1348	0.0000	0.0000	0.0000	0.0000	0.0000	0.0000	0.0000	0.0000	0.0000	0.0000	0.0000	0.0000	0.0000
Mt Roskill	0.9829	0.0012	0.0079	0.0011	0.0012	0.0044	0.0003	0.0001	0.0000	0.0000	0.0009	0.0000	0.0000	0.0000	0.0000	0.0000	0.0000	0.0000	0.0000	0.0000	0.0000
Mt Smart	0.0008	0.0000	0.0000	0.0000	0.0000	0.0000	0.0000	0.0000	0.0000	0.0000	0.0000	0.0000	0.0000	0.0000	0.0009	0.0075	0.0433	0.1036	0.2945	0.3540	0.1954
Mt StJohn	0.7046	0.0118	0.1310	0.1309	0.0020	0.0090	0.0013	0.0001	0.0000	0.0001	0.0014	0.0078	0.0000	0.0000	0.0000	0.0000	0.0000	0.0000	0.0000	0.0000	0.0000
Mt Victoria	0.1869	0.1162	0.1048	0.1191	0.0128	0.0056	0.0020	0.0001	0.0002	0.0015	0.0001	0.0048	0.0150	0.0860	0.0951	0.0578	0.0584	0.0074	0.0567	0.0293	0.0402
North Head	0.9030	0.0866	0.0097	0.0007	0.0000	0.0000	0.0000	0.0000	0.0000	0.0000	0.0000	0.0000	0.0000	0.0000	0.0000	0.0000	0.0000	0.0000	0.0000	0.0000	0.0000
One Tree Hill	0.6679	0.0402	0.1474	0.1303	0.0032	0.0082	0.0010	0.0002	0.0000	0.0000	0.0009	0.0007	0.0000	0.0000	0.0000	0.0000	0.0000	0.0000	0.0000	0.0000	0.0000
Otara Hill	0.0014	0.0002	0.0015	0.0057	0.0083	0.0029	0.0008	0.0001	0.0001	0.0003	0.0029	0.0050	0.0175	0.2404	0.2766	0.1886	0.1188	0.0508	0.0513	0.0222	0.0046
Otuataua	0.8077	0.1738	0.0170	0.0015	0.0000	0.0000	0.0000	0.0000	0.0000	0.0000	0.0000	0.0000	0.0000	0.0000	0.0000	0.0000	0.0000	0.0000	0.0000	0.0000	0.0000
Panmure Basin	0.2218	0.0000	0.0001	0.0009	0.0029	0.6656	0.0453	0.0417	0.0000	0.0003	0.0174	0.0040	0.0000	0.0000	0.0000	0.0000	0.0000	0.0000	0.0000	0.0000	0.0000
Pigeon Mountain	0.8122	0.0054	0.0332	0.0404	0.0028	0.0039	0.0000	0.0000	0.0000	0.0000	0.0025	0.0000	0.0000	0.0213	0.0077	0.0145	0.0035	0.0324	0.0030	0.0030	0.0142
Pukaki	0.9154	0.0846	0.0000	0.0000	0.0000	0.0000	0.0000	0.0000	0.0000	0.0000	0.0000	0.0000	0.0000	0.0000	0.0000	0.0000	0.0000	0.0000	0.0000	0.0000	0.0000
Puketutu	0.0189	0.0000	0.0000	0.0000	0.0004	0.0032	0.0225	0.0372	0.1879	0.1551	0.5731	0.0017	0.0000	0.0000	0.0000	0.0000	0.0000	0.0000	0.0000	0.0000	0.0000
Robertson Hill	0.9990	0.0000	0.0000	0.0000	0.0000	0.0001	0.0007	0.0002	0.0000	0.0000	0.0000	0.0000	0.0000	0.0000	0.0000	0.0000	0.0000	0.0000	0.0000	0.0000	0.0000
Styaks Swamp	0.3520	0.0000	0.0000	0.0000	0.0000	0.0001	0.0000	0.0001	0.0000	0.0000	0.0000	0.0000	0.0000	0.0106	0.0212	0.0293	0.0386	0.0717	0.0818	0.1090	0.2856
Taylors Hill	0.4871	0.0000	0.0000	0.0002	0.0000	0.0130	0.2479	0.2514	0.0001	0.0003	0.0000	0.0000	0.0000	0.0000	0.0000	0.0000	0.0000	0.0000	0.0000	0.0000	0.0000
Te Pouhawaiki	0.6714	0.1133	0.0837	0.0948	0.0182	0.0069	0.0014	0.0003	0.0002	0.0005	0.0036	0.0047	0.0010	0.0000	0.0000	0.0000	0.0000	0.0000	0.0000	0.0000	0.0000
Three Kings	0.0000	0.0000	0.0000	0.0000	0.0000	0.0000	0.0000	0.0000	0.0000	0.0014	0.0669	0.2650	0.6667	0.0000	0.0000	0.0000	0.0000	0.0000	0.0000	0.0000	0.0000
Wiri Mountain	0.3400	0.0000	0.0000	0.0000	0.0003	0.0012	0.1121	0.3025	0.0378	0.0922	0.0533	0.0606	0.0000	0.0000	0.0000	0.0000	0.0000	0.0000	0.0000	0.0000	0.0000

Table A.12: Marginal posterior probabilities for a volcano to have produced a given tephra for the Three Kings=AVF 9 scenario with A = $\{\alpha = 1.5,\ \beta U = 0.5\}$.

Volcano	AVF tephra (AVF 0 = 'unmatched')																				
	0	1	2	3	4	5	6	7	8	9	10	11	12	13	14	15	16	17	18	19	20
Ash Hill	0.9762	0.0000	0.0000	0.0001	0.0020	0.0044	0.0105	0.0065	0.0003	0.0000	0.0000	0.0000	0.0000	0.0000	0.0000	0.0000	0.0000	0.0000	0.0000	0.0000	0.0000
Cemetery Hill	0.3497	0.0000	0.0000	0.0002	0.0027	0.0143	0.1287	0.4887	0.0062	0.0000	0.0095	0.0000	0.0000	0.0000	0.0000	0.0000	0.0000	0.0000	0.0000	0.0000	0.0000
Crater Hill	0.0039	0.0000	0.0000	0.0000	0.0002	0.0002	0.3312	0.0254	0.6062	0.0000	0.0189	0.0140	0.0000	0.0000	0.0000	0.0000	0.0000	0.0000	0.0000	0.0000	0.0000
Domain	0.7610	0.1302	0.0891	0.0197	0.0000	0.0000	0.0000	0.0000	0.0000	0.0000	0.0000	0.0000	0.0000	0.0000	0.0000	0.0000	0.0000	0.0000	0.0000	0.0000	0.0000
Green Hill	0.0104	0.0009	0.0041	0.0231	0.0198	0.0155	0.0026	0.0003	0.0065	0.0000	0.0194	0.0415	0.1312	0.1456	0.1102	0.0895	0.0798	0.0863	0.1064	0.0838	0.0231
Hampton Park	0.2693	0.0000	0.0000	0.0000	0.0001	0.0002	0.0000	0.0001	0.0000	0.0000	0.0001	0.0040	0.0218	0.1293	0.1812	0.1970	0.0986	0.0653	0.0208	0.0080	0.0042
Hopua	0.5126	0.0000	0.0000	0.0022	0.0013	0.0168	0.0197	0.0179	0.0008	0.0000	0.2546	0.1741	0.0000	0.0000	0.0000	0.0000	0.0000	0.0000	0.0000	0.0000	0.0000
Kohuora	0.0031	0.0014	0.0077	0.0373	0.8918	0.0363	0.0167	0.0047	0.0010	0.0000	0.0000	0.0000	0.0000	0.0000	0.0000	0.0000	0.0000	0.0000	0.0000	0.0000	0.0000
Little Rangitoto	0.0510	0.2019	0.1856	0.1502	0.0140	0.0107	0.0006	0.0011	0.0030	0.0000	0.0080	0.0122	0.0379	0.0406	0.0305	0.0275	0.0201	0.0324	0.0493	0.0502	0.0732
Mangere Lagoon	0.7303	0.0472	0.0619	0.0613	0.0004	0.0014	0.0012	0.0005	0.0003	0.0000	0.0049	0.0081	0.0190	0.0233	0.0169	0.0129	0.0088	0.0016	0.0000	0.0000	0.0000
Matukutureia	0.0190	0.0000	0.0000	0.0000	0.0000	0.0000	0.0000	0.0001	0.0007	0.0000	0.0048	0.0117	0.0591	0.1175	0.0858	0.0780	0.0647	0.0682	0.0998	0.2073	0.1833
Maungataketake	0.9876	0.0000	0.0023	0.0022	0.0068	0.0007	0.0004	0.0000	0.0000	0.0000	0.0000	0.0000	0.0000	0.0000	0.0000	0.0000	0.0000	0.0000	0.0000	0.0000	0.0000
McLennan Hills	0.9436	0.0000	0.0112	0.0351	0.0014	0.0043	0.0042	0.0002	0.0000	0.0000	0.0000	0.0000	0.0000	0.0000	0.0000	0.0000	0.0000	0.0000	0.0000	0.0000	0.0000
Motukorea	0.9112	0.0027	0.0028	0.0002	0.0002	0.0002	0.0000	0.0000	0.0000	0.0000	0.0063	0.0038	0.0055	0.0110	0.0045	0.0077	0.0045	0.0267	0.0035	0.0040	0.0052
Mt Albert	0.8836	0.0621	0.0364	0.0170	0.0005	0.0002	0.0001	0.0000	0.0001	0.0000	0.0000	0.0000	0.0000	0.0000	0.0000	0.0000	0.0000	0.0000	0.0000	0.0000	0.0000
Mt Cambria	0.6573	0.0063	0.0115	0.0159	0.0004	0.0018	0.0000	0.0000	0.0000	0.0000	0.0041	0.0119	0.0090	0.0823	0.0213	0.0629	0.0238	0.0851	0.0033	0.0027	0.0004
Mt Eden	0.0015	0.0000	0.0000	0.0000	0.0000	0.0000	0.0000	0.0000	0.0000	0.0000	0.0820	0.4365	0.4800	0.0000	0.0000	0.0000	0.0000	0.0000	0.0000	0.0000	0.0000
Mt Hobson	0.0931	0.0000	0.0000	0.0000	0.0000	0.0000	0.0000	0.0000	0.0000	0.0000	0.0000	0.0137	0.0640	0.1133	0.0718	0.0705	0.0590	0.0860	0.1132	0.1331	0.1823
Mt Mangere	0.0017	0.0000	0.0000	0.0000	0.0000	0.0000	0.0000	0.0000	0.0000	0.0000	0.0000	0.0001	0.0008	0.0150	0.0688	0.1690	0.3543	0.2837	0.1033	0.0033	0.0000
Mt Richmond	0.7916	0.0000	0.0000	0.0000	0.0000	0.0036	0.0430	0.1193	0.0007	0.0000	0.0361	0.0057	0.0000	0.0000	0.0000	0.0000	0.0000	0.0000	0.0000	0.0000	0.0000
Mt Roskill	0.9396	0.0175	0.0217	0.0022	0.0007	0.0012	0.0000	0.0002	0.0000	0.0000	0.0103	0.0061	0.0005	0.0000	0.0000	0.0000	0.0000	0.0000	0.0000	0.0000	0.0000
Mt Smart	0.0092	0.0000	0.0000	0.0000	0.0000	0.0000	0.0000	0.0000	0.0000	0.0000	0.0000	0.0000	0.0001	0.0001	0.0012	0.0086	0.0363	0.0968	0.2828	0.3579	0.2070
Mt StJohn	0.7186	0.0523	0.1209	0.0892	0.0005	0.0095	0.0000	0.0002	0.0001	0.0000	0.0047	0.0036	0.0004	0.0000	0.0000	0.0000	0.0000	0.0000	0.0000	0.0000	0.0000
Mt Victoria	0.1799	0.0710	0.0792	0.0653	0.0098	0.0054	0.0010	0.0000	0.0014	0.0000	0.0031	0.0097	0.0619	0.0745	0.1215	0.0559	0.0803	0.0194	0.0724	0.0361	0.0522
North Head	0.7426	0.0961	0.0605	0.0485	0.0043	0.0035	0.0006	0.0000	0.0009	0.0000	0.0034	0.0040	0.0095	0.0086	0.0047	0.0032	0.0025	0.0024	0.0019	0.0016	0.0012
One Tree Hill	0.6826	0.0816	0.1300	0.0924	0.0018	0.0092	0.0000	0.0001	0.0005	0.0000	0.0014	0.0004	0.0000	0.0000	0.0000	0.0000	0.0000	0.0000	0.0000	0.0000	0.0000
Otara Hill	0.0070	0.0004	0.0010	0.0092	0.0037	0.0009	0.0009	0.0001	0.0014	0.0000	0.0038	0.0129	0.0886	0.1940	0.2498	0.1625	0.1186	0.0558	0.0590	0.0228	0.0076
Otuataua	0.6760	0.0081	0.0637	0.2276	0.0160	0.0077	0.0007	0.0002	0.0000	0.0000	0.0000	0.0000	0.0000	0.0000	0.0000	0.0000	0.0000	0.0000	0.0000	0.0000	0.0000
Panmure Basin	0.1556	0.0000	0.0009	0.0032	0.0143	0.7964	0.0139	0.0056	0.0043	0.0000	0.0047	0.0011	0.0000	0.0000	0.0000	0.0000	0.0000	0.0000	0.0000	0.0000	0.0000
Pigeon Mountain	0.7562	0.0292	0.0420	0.0356	0.0004	0.0012	0.0000	0.0001	0.0000	0.0000	0.0047	0.0064	0.0061	0.0268	0.0087	0.0158	0.0100	0.0263	0.0092	0.0071	0.0142
Pukaki	0.8867	0.1133	0.0000	0.0000	0.0000	0.0000	0.0000	0.0000	0.0000	0.0000	0.0000	0.0000	0.0000	0.0000	0.0000	0.0000	0.0000	0.0000	0.0000	0.0000	0.0000
Pukeiti	0.9970	0.0012	0.0017	0.0001	0.0000	0.0000	0.0000	0.0000	0.0000	0.0000	0.0000	0.0000	0.0000	0.0000	0.0000	0.0000	0.0000	0.0000	0.0000	0.0000	0.0000
Puketutu	0.4736	0.0000	0.0000	0.0000	0.0039	0.0103	0.0259	0.0203	0.3479	0.0000	0.0984	0.0197	0.0000	0.0000	0.0000	0.0000	0.0000	0.0000	0.0000	0.0000	0.0000
Robertson Hill	0.5226	0.0000	0.0000	0.0000	0.0000	0.0000	0.0003	0.0002	0.0000	0.0000	0.3126	0.1627	0.0016	0.0000	0.0000	0.0000	0.0000	0.0000	0.0000	0.0000	0.0000
Styaks Swamp	0.4099	0.0000	0.0000	0.0000	0.0000	0.0001	0.0000	0.0000	0.0000	0.0000	0.0001	0.0007	0.0030	0.0181	0.0231	0.0390	0.0387	0.0640	0.0751	0.0821	0.2461
Taylors Hill	0.7194	0.0000	0.0002	0.0010	0.0006	0.0355	0.0993	0.0363	0.0012	0.0000	0.0809	0.0256	0.0000	0.0000	0.0000	0.0000	0.0000	0.0000	0.0000	0.0000	0.0000
Te Pouhawaiki	0.7834	0.0759	0.0655	0.0610	0.0019	0.0013	0.0004	0.0000	0.0003	0.0000	0.0049	0.0054	0.0000	0.0000	0.0000	0.0000	0.0000	0.0000	0.0000	0.0000	0.0000
Three Kings	0.0000	0.0000	0.0000	0.0000	0.0000	0.0000	0.0000	0.0000	0.0000	1.0000	0.0000	0.0000	0.0000	0.0000	0.0000	0.0000	0.0000	0.0000	0.0000	0.0000	0.0000
Waitomokia	0.9992	0.0007	0.0001	0.0000	0.0000	0.0000	0.0000	0.0000	0.0000	0.0000	0.0000	0.0000	0.0000	0.0000	0.0000	0.0000	0.0000	0.0000	0.0000	0.0000	0.0000
Wiri Mountain	0.3832	0.0000	0.0000	0.0002	0.0005	0.0072	0.2981	0.2719	0.0162	0.0000	0.0183	0.0044	0.0000	0.0000	0.0000	0.0000	0.0000	0.0000	0.0000	0.0000	0.0000

Table A.13: Marginal posterior probabilities for a volcano to have produced a given tephra for the Three Kings=AVF 9 scenario with B = $\{\alpha = 2.0,\ \beta U = 0.5\}$.

Volcano	AVF tephra (AVF 0 = 'unmatched')																				
	0	1	2	3	4	5	6	7	8	9	10	11	12	13	14	15	16	17	18	19	20
Ash Hill	0.9823	0.0000	0.0000	0.0000	0.0000	0.0001	0.0104	0.0069	0.0003	0.0000	0.0000	0.0000	0.0000	0.0000	0.0000	0.0000	0.0000	0.0000	0.0000	0.0000	0.0000
Cemetery Hill	0.3662	0.0000	0.0000	0.0001	0.0027	0.0132	0.2056	0.3929	0.0064	0.0000	0.0126	0.0003	0.0000	0.0000	0.0000	0.0000	0.0000	0.0000	0.0000	0.0000	0.0000
Crater Hill	0.0063	0.0000	0.0000	0.0000	0.0001	0.0004	0.3546	0.0722	0.5359	0.0000	0.0159	0.0143	0.0003	0.0000	0.0000	0.0000	0.0000	0.0000	0.0000	0.0000	0.0000
Domain	0.7605	0.1332	0.0859	0.0204	0.0000	0.0000	0.0000	0.0000	0.0000	0.0000	0.0000	0.0000	0.0000	0.0000	0.0000	0.0000	0.0000	0.0000	0.0000	0.0000	0.0000
Green Hill	0.0090	0.0009	0.0040	0.0238	0.0197	0.0145	0.0024	0.0001	0.0073	0.0000	0.0207	0.0410	0.1375	0.1428	0.1084	0.0896	0.0811	0.0887	0.1053	0.0807	0.0225
Hampton Park	0.2805	0.0000	0.0000	0.0000	0.0000	0.0001	0.0000	0.0001	0.0000	0.0000	0.0001	0.0038	0.0212	0.1292	0.1811	0.1886	0.0965	0.0651	0.0210	0.0081	0.0046
Hopua	0.5239	0.0000	0.0002	0.0013	0.0000	0.0124	0.0103	0.0237	0.0007	0.0000	0.2600	0.1675	0.0000	0.0000	0.0000	0.0000	0.0000	0.0000	0.0000	0.0000	0.0000
Kohuora	0.0006	0.0021	0.0071	0.0296	0.9226	0.0250	0.0117	0.0003	0.0010	0.0000	0.0000	0.0000	0.0000	0.0000	0.0000	0.0000	0.0000	0.0000	0.0000	0.0000	0.0000
Little Rangitoto	0.0364	0.2002	0.1970	0.1507	0.0133	0.0092	0.0005	0.0012	0.0035	0.0000	0.0079	0.0130	0.0385	0.0408	0.0302	0.0272	0.0200	0.0333	0.0495	0.0509	0.0767
Mangere Lagoon	0.7466	0.0430	0.0578	0.0545	0.0002	0.0014	0.0009	0.0002	0.0002	0.0000	0.0050	0.0084	0.0186	0.0236	0.0167	0.0131	0.0082	0.0016	0.0000	0.0000	0.0000
Matukutureia	0.0155	0.0000	0.0000	0.0000	0.0000	0.0000	0.0000	0.0001	0.0007	0.0000	0.0049	0.0117	0.0617	0.1167	0.0870	0.0785	0.0638	0.0687	0.1021	0.2134	0.1752
Maungataketake	0.9970	0.0000	0.0001	0.0014	0.0009	0.0004	0.0002	0.0000	0.0000	0.0000	0.0000	0.0000	0.0000	0.0000	0.0000	0.0000	0.0000	0.0000	0.0000	0.0000	0.0000
McLennan Hills	0.9464	0.0000	0.0147	0.0347	0.0003	0.0034	0.0003	0.0002	0.0000	0.0000	0.0000	0.0000	0.0000	0.0000	0.0000	0.0000	0.0000	0.0000	0.0000	0.0000	0.0000
Motukorea	0.9159	0.0017	0.0004	0.0002	0.0000	0.0001	0.0000	0.0000	0.0000	0.0000	0.0063	0.0041	0.0052	0.0101	0.0042	0.0071	0.0042	0.0280	0.0035	0.0039	0.0051
Mt Albert	0.8870	0.0592	0.0353	0.0181	0.0000	0.0003	0.0000	0.0000	0.0001	0.0000	0.0000	0.0000	0.0000	0.0000	0.0000	0.0000	0.0000	0.0000	0.0000	0.0000	0.0000
Mt Cambria	0.6392	0.0100	0.0234	0.0157	0.0004	0.0023	0.0000	0.0000	0.0000	0.0000	0.0041	0.0130	0.0077	0.0852	0.0233	0.0593	0.0208	0.0891	0.0032	0.0027	0.0006
Mt Eden	0.0030	0.0000	0.0000	0.0000	0.0000	0.0000	0.0000	0.0000	0.0000	0.0000	0.0907	0.4436	0.4627	0.0000	0.0000	0.0000	0.0000	0.0000	0.0000	0.0000	0.0000
Mt Hobson	0.0849	0.0000	0.0000	0.0000	0.0000	0.0000	0.0000	0.0000	0.0000	0.0000	0.0000	0.0170	0.0629	0.1141	0.0703	0.0711	0.0593	0.0876	0.1139	0.1316	0.1873
Mt Mangere	0.0016	0.0000	0.0000	0.0000	0.0000	0.0000	0.0000	0.0000	0.0000	0.0000	0.0000	0.0001	0.0009	0.0161	0.0721	0.1781	0.3596	0.2692	0.0992	0.0031	0.0000
Mt Richmond	0.7876	0.0000	0.0000	0.0001	0.0000	0.0031	0.0305	0.1374	0.0012	0.0000	0.0344	0.0057	0.0000	0.0000	0.0000	0.0000	0.0000	0.0000	0.0000	0.0000	0.0000
Mt Roskill	0.9411	0.0170	0.0231	0.0011	0.0002	0.0004	0.0000	0.0002	0.0000	0.0000	0.0103	0.0060	0.0006	0.0000	0.0000	0.0000	0.0000	0.0000	0.0000	0.0000	0.0000
Mt Smart	0.0067	0.0000	0.0000	0.0000	0.0000	0.0000	0.0000	0.0000	0.0000	0.0000	0.0000	0.0000	0.0001	0.0001	0.0013	0.0094	0.0384	0.1005	0.2864	0.3550	0.2021
Mt StJohn	0.7213	0.0570	0.1131	0.0897	0.0002	0.0098	0.0000	0.0002	0.0001	0.0000	0.0048	0.0034	0.0004	0.0000	0.0000	0.0000	0.0000	0.0000	0.0000	0.0000	0.0000
Mt Victoria	0.1705	0.0720	0.0741	0.0755	0.0119	0.0045	0.0004	0.0000	0.0016	0.0000	0.0032	0.0099	0.0681	0.0729	0.1197	0.0558	0.0813	0.0174	0.0720	0.0365	0.0527
North Head	0.7318	0.1034	0.0620	0.0502	0.0049	0.0030	0.0001	0.0000	0.0013	0.0000	0.0034	0.0045	0.0099	0.0086	0.0041	0.0034	0.0025	0.0024	0.0019	0.0014	0.0012
One Tree Hill	0.6783	0.0840	0.1288	0.0979	0.0003	0.0085	0.0000	0.0001	0.0003	0.0000	0.0014	0.0004	0.0000	0.0000	0.0000	0.0000	0.0000	0.0000	0.0000	0.0000	0.0000
Otara Hill	0.0065	0.0004	0.0008	0.0099	0.0031	0.0010	0.0009	0.0000	0.0016	0.0000	0.0038	0.0139	0.0935	0.1942	0.2491	0.1638	0.1160	0.0551	0.0564	0.0229	0.0071
Otuataua	0.7073	0.0070	0.0557	0.2181	0.0101	0.0012	0.0004	0.0002	0.0000	0.0000	0.0000	0.0000	0.0000	0.0000	0.0000	0.0000	0.0000	0.0000	0.0000	0.0000	0.0000
Panmure Basin	0.1265	0.0000	0.0014	0.0044	0.0006	0.8404	0.0104	0.0065	0.0040	0.0000	0.0047	0.0011	0.0000	0.0000	0.0000	0.0000	0.0000	0.0000	0.0000	0.0000	0.0000
Pigeon Mountain	0.7590	0.0289	0.0427	0.0320	0.0000	0.0010	0.0000	0.0001	0.0000	0.0000	0.0047	0.0062	0.0055	0.0268	0.0096	0.0162	0.0089	0.0266	0.0094	0.0073	0.0151
Pukaki	0.9138	0.0862	0.0000	0.0000	0.0000	0.0000	0.0000	0.0000	0.0000	0.0000	0.0000	0.0000	0.0000	0.0000	0.0000	0.0000	0.0000	0.0000	0.0000	0.0000	0.0000
Pukeiti	0.9998	0.0001	0.0001	0.0000	0.0000	0.0000	0.0000	0.0000	0.0000	0.0000	0.0000	0.0000	0.0000	0.0000	0.0000	0.0000	0.0000	0.0000	0.0000	0.0000	0.0000
Puketutu	0.3721	0.0000	0.0000	0.0000	0.0045	0.0093	0.0408	0.0391	0.4161	0.0000	0.0999	0.0181	0.0001	0.0000	0.0000	0.0000	0.0000	0.0000	0.0000	0.0000	0.0000
Robertson Hill	0.5435	0.0000	0.0000	0.0000	0.0000	0.0000	0.0003	0.0003	0.0000	0.0000	0.2987	0.1556	0.0016	0.0000	0.0000	0.0000	0.0000	0.0000	0.0000	0.0000	0.0000
Styaks Swamp	0.4011	0.0000	0.0000	0.0000	0.0000	0.0000	0.0000	0.0000	0.0000	0.0000	0.0001	0.0007	0.0030	0.0188	0.0229	0.0388	0.0394	0.0667	0.0762	0.0825	0.2498
Taylors Hill	0.7977	0.0000	0.0002	0.0014	0.0000	0.0299	0.0288	0.0334	0.0015	0.0000	0.0801	0.0270	0.0000	0.0000	0.0000	0.0000	0.0000	0.0000	0.0000	0.0000	0.0000
Te Pouhawaiki	0.7494	0.0936	0.0721	0.0690	0.0035	0.0010	0.0001	0.0000	0.0008	0.0000	0.0052	0.0053	0.0000	0.0000	0.0000	0.0000	0.0000	0.0000	0.0000	0.0000	0.0000
Three Kings	0.0000	0.0000	0.0000	0.0000	0.0000	0.0000	0.0000	0.0000	0.0000	1.0000	0.0000	0.0000	0.0000	0.0000	0.0000	0.0000	0.0000	0.0000	0.0000	0.0000	0.0000
Waitomokia	0.9999	0.0001	0.0000	0.0000	0.0000	0.0000	0.0000	0.0000	0.0000	0.0000	0.0000	0.0000	0.0000	0.0000	0.0000	0.0000	0.0000	0.0000	0.0000	0.0000	0.0000
Wiri Mountain	0.3833	0.0000	0.0000	0.0002	0.0005	0.0041	0.2904	0.2846	0.0154	0.0000	0.0171	0.0044	0.0000	0.0000	0.0000	0.0000	0.0000	0.0000	0.0000	0.0000	0.0000

Table A.14: Marginal posterior probabilities for a volcano to have produced a given tephra for the Three Kings=AVF 9 scenario with C = $\{\alpha = 2.5,\ \beta U = 0.5\}$.

Volcano	AVF tephra (AVF 0 = 'unmatched')																				
	0	1	2	3	4	5	6	7	8	9	10	11	12	13	14	15	16	17	18	19	20
Ash Hill	0.9758	0.0000	0.0000	0.0002	0.0006	0.0031	0.0125	0.0076	0.0002	0.0000	0.0000	0.0000	0.0000	0.0000	0.0000	0.0000	0.0000	0.0000	0.0000	0.0000	0.0000
Cemetery Hill	0.3369	0.0000	0.0000	0.0001	0.0058	0.0173	0.3129	0.2957	0.0065	0.0000	0.0208	0.0040	0.0000	0.0000	0.0000	0.0000	0.0000	0.0000	0.0000	0.0000	0.0000
Crater Hill	0.0175	0.0000	0.0000	0.0000	0.0001	0.0005	0.3379	0.2385	0.3857	0.0000	0.0076	0.0108	0.0014	0.0000	0.0000	0.0000	0.0000	0.0000	0.0000	0.0000	0.0000
Domain	0.7574	0.1388	0.0814	0.0224	0.0000	0.0000	0.0000	0.0000	0.0000	0.0000	0.0000	0.0000	0.0000	0.0000	0.0000	0.0000	0.0000	0.0000	0.0000	0.0000	0.0000
Green Hill	0.0087	0.0011	0.0040	0.0228	0.0202	0.0136	0.0024	0.0005	0.0073	0.0000	0.0218	0.0424	0.1408	0.1393	0.1091	0.0909	0.0810	0.0906	0.1048	0.0783	0.0204
Hampton Park	0.2891	0.0000	0.0000	0.0000	0.0000	0.0002	0.0003	0.0001	0.0000	0.0000	0.0001	0.0039	0.0211	0.1331	0.1793	0.1814	0.0916	0.0675	0.0207	0.0075	0.0041
Hopua	0.5190	0.0000	0.0002	0.0025	0.0010	0.0150	0.0141	0.0212	0.0007	0.0000	0.2654	0.1609	0.0000	0.0000	0.0000	0.0000	0.0000	0.0000	0.0000	0.0000	0.0000
Kohuora	0.0055	0.0022	0.0103	0.0394	0.8899	0.0337	0.0152	0.0028	0.0010	0.0000	0.0000	0.0000	0.0000	0.0000	0.0000	0.0000	0.0000	0.0000	0.0000	0.0000	0.0000
Little Rangitoto	0.0302	0.2077	0.1908	0.1455	0.0169	0.0090	0.0005	0.0012	0.0034	0.0000	0.0083	0.0128	0.0403	0.0401	0.0295	0.0283	0.0198	0.0338	0.0504	0.0506	0.0809
Mangere Lagoon	0.7534	0.0390	0.0583	0.0504	0.0003	0.0019	0.0010	0.0002	0.0003	0.0000	0.0051	0.0085	0.0189	0.0236	0.0164	0.0131	0.0082	0.0014	0.0000	0.0000	0.0000
Matukutureia	0.0114	0.0000	0.0000	0.0000	0.0000	0.0000	0.0000	0.0001	0.0007	0.0000	0.0053	0.0132	0.0655	0.1136	0.0865	0.0801	0.0638	0.0678	0.1058	0.2156	0.1706
Maungataketake	0.9932	0.0000	0.0005	0.0012	0.0041	0.0007	0.0003	0.0000	0.0000	0.0000	0.0000	0.0000	0.0000	0.0000	0.0000	0.0000	0.0000	0.0000	0.0000	0.0000	0.0000
McLennan Hills	0.9351	0.0000	0.0170	0.0402	0.0009	0.0038	0.0027	0.0003	0.0000	0.0000	0.0000	0.0000	0.0000	0.0000	0.0000	0.0000	0.0000	0.0000	0.0000	0.0000	0.0000
Motukorea	0.9127	0.0017	0.0020	0.0007	0.0000	0.0001	0.0000	0.0000	0.0000	0.0000	0.0064	0.0045	0.0050	0.0095	0.0041	0.0072	0.0044	0.0286	0.0036	0.0039	0.0056
Mt Albert	0.8919	0.0579	0.0328	0.0170	0.0001	0.0002	0.0000	0.0000	0.0001	0.0000	0.0000	0.0000	0.0000	0.0000	0.0000	0.0000	0.0000	0.0000	0.0000	0.0000	0.0000
Mt Cambria	0.6377	0.0101	0.0267	0.0165	0.0004	0.0014	0.0000	0.0000	0.0000	0.0000	0.0045	0.0133	0.0079	0.0878	0.0235	0.0516	0.0192	0.0928	0.0034	0.0027	0.0005
Mt Eden	0.0053	0.0000	0.0000	0.0000	0.0000	0.0000	0.0000	0.0000	0.0000	0.0000	0.1005	0.4523	0.4419	0.0000	0.0000	0.0000	0.0000	0.0000	0.0000	0.0000	0.0000
Mt Hobson	0.0765	0.0000	0.0000	0.0000	0.0000	0.0000	0.0000	0.0000	0.0000	0.0000	0.0000	0.0190	0.0623	0.1158	0.0701	0.0722	0.0580	0.0903	0.1146	0.1311	0.1901
Mt Mangere	0.0017	0.0000	0.0000	0.0000	0.0000	0.0000	0.0000	0.0000	0.0000	0.0000	0.0000	0.0001	0.0008	0.0176	0.0753	0.1892	0.3678	0.2488	0.0956	0.0031	0.0000
Mt Richmond	0.8045	0.0000	0.0000	0.0001	0.0000	0.0043	0.0308	0.1200	0.0011	0.0000	0.0336	0.0056	0.0000	0.0000	0.0000	0.0000	0.0000	0.0000	0.0000	0.0000	0.0000
Mt Roskill	0.9435	0.0132	0.0223	0.0027	0.0003	0.0007	0.0000	0.0002	0.0000	0.0000	0.0106	0.0060	0.0005	0.0000	0.0000	0.0000	0.0000	0.0000	0.0000	0.0000	0.0000
Mt Smart	0.0051	0.0000	0.0000	0.0000	0.0000	0.0000	0.0000	0.0000	0.0000	0.0000	0.0000	0.0000	0.0001	0.0001	0.0014	0.0097	0.0431	0.1050	0.2866	0.3561	0.1928
Mt StJohn	0.7227	0.0557	0.1130	0.0894	0.0004	0.0099	0.0000	0.0001	0.0001	0.0000	0.0048	0.0036	0.0003	0.0000	0.0000	0.0000	0.0000	0.0000	0.0000	0.0000	0.0000
Mt Victoria	0.1681	0.0715	0.0719	0.0769	0.0155	0.0014	0.0006	0.0000	0.0016	0.0000	0.0030	0.0104	0.0726	0.0723	0.1180	0.0573	0.0804	0.0173	0.0709	0.0362	0.0541
North Head	0.7286	0.1054	0.0634	0.0498	0.0055	0.0023	0.0003	0.0000	0.0015	0.0000	0.0034	0.0046	0.0105	0.0084	0.0040	0.0033	0.0026	0.0021	0.0020	0.0014	0.0009
One Tree Hill	0.6810	0.0830	0.1243	0.0993	0.0008	0.0093	0.0000	0.0002	0.0003	0.0000	0.0014	0.0004	0.0000	0.0000	0.0000	0.0000	0.0000	0.0000	0.0000	0.0000	0.0000
Otara Hill	0.0059	0.0004	0.0011	0.0099	0.0033	0.0010	0.0005	0.0000	0.0016	0.0000	0.0039	0.0151	0.1003	0.1936	0.2498	0.1621	0.1125	0.0555	0.0548	0.0215	0.0072
Otuataua	0.7120	0.0074	0.0575	0.2028	0.0148	0.0047	0.0006	0.0002	0.0000	0.0000	0.0000	0.0000	0.0000	0.0000	0.0000	0.0000	0.0000	0.0000	0.0000	0.0000	0.0000
Panmure Basin	0.1415	0.0000	0.0014	0.0067	0.0086	0.8113	0.0151	0.0055	0.0041	0.0000	0.0047	0.0011	0.0000	0.0000	0.0000	0.0000	0.0000	0.0000	0.0000	0.0000	0.0000
Pigeon Mountain	0.7614	0.0253	0.0443	0.0318	0.0001	0.0011	0.0000	0.0001	0.0000	0.0000	0.0047	0.0064	0.0053	0.0271	0.0096	0.0155	0.0089	0.0274	0.0091	0.0072	0.0147
Pukaki	0.9183	0.0817	0.0000	0.0000	0.0000	0.0000	0.0000	0.0000	0.0000	0.0000	0.0000	0.0000	0.0000	0.0000	0.0000	0.0000	0.0000	0.0000	0.0000	0.0000	0.0000
Pukeiti	0.9981	0.0008	0.0008	0.0002	0.0001	0.0000	0.0000	0.0000	0.0000	0.0000	0.0000	0.0000	0.0000	0.0000	0.0000	0.0000	0.0000	0.0000	0.0000	0.0000	0.0000
Puketutu	0.2241	0.0000	0.0000	0.0000	0.0044	0.0095	0.0400	0.0344	0.5694	0.0000	0.1000	0.0180	0.0002	0.0000	0.0000	0.0000	0.0000	0.0000	0.0000	0.0000	0.0000
Robertson Hill	0.5695	0.0000	0.0000	0.0000	0.0000	0.0001	0.0002	0.0003	0.0000	0.0000	0.2831	0.1455	0.0013	0.0000	0.0000	0.0000	0.0000	0.0000	0.0000	0.0000	0.0000
Styaks Swamp	0.3861	0.0000	0.0000	0.0000	0.0000	0.0001	0.0000	0.0000	0.0000	0.0000	0.0001	0.0007	0.0030	0.0181	0.0234	0.0381	0.0387	0.0711	0.0777	0.0848	0.2581
Taylors Hill	0.8007	0.0000	0.0002	0.0013	0.0004	0.0366	0.0347	0.0184	0.0016	0.0000	0.0790	0.0271	0.0000	0.0000	0.0000	0.0000	0.0000	0.0000	0.0000	0.0000	0.0000
Te Pouhawaiki	0.7391	0.0966	0.0758	0.0700	0.0051	0.0018	0.0004	0.0000	0.0007	0.0000	0.0052	0.0053	0.0000	0.0000	0.0000	0.0000	0.0000	0.0000	0.0000	0.0000	0.0000
Three Kings	0.0000	0.0000	0.0000	0.0000	0.0000	0.0000	0.0000	0.0000	0.0000	1.0000	0.0000	0.0000	0.0000	0.0000	0.0000	0.0000	0.0000	0.0000	0.0000	0.0000	0.0000
Waitomokia	0.9995	0.0005	0.0000	0.0000	0.0000	0.0000	0.0000	0.0000	0.0000	0.0000	0.0000	0.0000	0.0000	0.0000	0.0000	0.0000	0.0000	0.0000	0.0000	0.0000	0.0000
Wiri Mountain	0.5313	0.0000	0.0000	0.0002	0.0004	0.0054	0.1770	0.2524	0.0121	0.0000	0.0167	0.0045	0.0000	0.0000	0.0000	0.0000	0.0000	0.0000	0.0000	0.0000	0.0000

Table A.15: Marginal posterior probabilities for a volcano to have produced a given tephra for the Three Kings=AVF 9 scenario with D = $\{\alpha = 1.5, \beta U = 1.0\}$.

Volcano	AVF tephra (AVF 0 = 'unmatched')																				
	0	1	2	3	4	5	6	7	8	9	10	11	12	13	14	15	16	17	18	19	20
Ash Hill	0.9737	0.0000	0.0000	0.0002	0.0004	0.0006	0.0150	0.0093	0.0008	0.0000	0.0000	0.0000	0.0000	0.0000	0.0000	0.0000	0.0000	0.0000	0.0000	0.0000	0.0000
Boggust	1.0000	0.0000	0.0000	0.0000	0.0000	0.0000	0.0000	0.0000	0.0000	0.0000	0.0000	0.0000	0.0000	0.0000	0.0000	0.0000	0.0000	0.0000	0.0000	0.0000	0.0000
Cemetery Hill	0.0526	0.0000	0.0000	0.0002	0.0255	0.2775	0.3060	0.1884	0.1219	0.0000	0.0239	0.0040	0.0000	0.0000	0.0000	0.0000	0.0000	0.0000	0.0000	0.0000	0.0000
Crater Hill	0.1252	0.0000	0.0000	0.0000	0.0001	0.0077	0.3358	0.2503	0.2547	0.0000	0.0078	0.0163	0.0021	0.0000	0.0000	0.0000	0.0000	0.0000	0.0000	0.0000	0.0000
Domain	0.7804	0.1134	0.0877	0.0185	0.0000	0.0000	0.0000	0.0000	0.0000	0.0000	0.0000	0.0000	0.0000	0.0000	0.0000	0.0000	0.0000	0.0000	0.0000	0.0000	0.0000
Grafton	1.0000	0.0000	0.0000	0.0000	0.0000	0.0000	0.0000	0.0000	0.0000	0.0000	0.0000	0.0000	0.0000	0.0000	0.0000	0.0000	0.0000	0.0000	0.0000	0.0000	0.0000
Green Hill	0.0028	0.0017	0.0046	0.0216	0.0241	0.0135	0.0022	0.0001	0.0073	0.0000	0.0246	0.0498	0.1653	0.1269	0.1051	0.0924	0.0838	0.0983	0.1000	0.0628	0.0131
Hampton Park	0.3005	0.0000	0.0000	0.0000	0.0000	0.0000	0.0000	0.0002	0.0000	0.0000	0.0001	0.0153	0.0201	0.1534	0.1758	0.1558	0.0835	0.0630	0.0205	0.0076	0.0042
Hopua	0.4530	0.0000	0.0014	0.0043	0.0014	0.0198	0.0244	0.0726	0.0007	0.0000	0.3014	0.1210	0.0000	0.0000	0.0000	0.0000	0.0000	0.0000	0.0000	0.0000	0.0000
Kohuora	0.0004	0.0054	0.0256	0.0411	0.8670	0.0462	0.0123	0.0009	0.0011	0.0000	0.0000	0.0000	0.0000	0.0000	0.0000	0.0000	0.0000	0.0000	0.0000	0.0000	0.0000
LakePupuke	1.0000	0.0000	0.0000	0.0000	0.0000	0.0000	0.0000	0.0000	0.0000	0.0000	0.0000	0.0000	0.0000	0.0000	0.0000	0.0000	0.0000	0.0000	0.0000	0.0000	0.0000
Little Rangitoto	0.0141	0.2409	0.1668	0.1362	0.0177	0.0074	0.0010	0.0005	0.0044	0.0000	0.0094	0.0149	0.0479	0.0350	0.0298	0.0273	0.0230	0.0356	0.0516	0.0510	0.0855
Mangere Lagoon	0.7353	0.0358	0.0714	0.0510	0.0003	0.0080	0.0006	0.0002	0.0004	0.0000	0.0055	0.0109	0.0250	0.0220	0.0152	0.0118	0.0056	0.0010	0.0000	0.0000	0.0000
Matukutureia	0.0039	0.0000	0.0000	0.0000	0.0000	0.0000	0.0000	0.0001	0.0007	0.0000	0.0062	0.0175	0.0886	0.1033	0.0839	0.0800	0.0628	0.0720	0.1219	0.2175	0.1416
Maungataketake	0.9960	0.0000	0.0003	0.0015	0.0016	0.0004	0.0002	0.0000	0.0000	0.0000	0.0000	0.0000	0.0000	0.0000	0.0000	0.0000	0.0000	0.0000	0.0000	0.0000	0.0000
McLennan Hills	0.9356	0.0000	0.0220	0.0383	0.0003	0.0030	0.0006	0.0002	0.0000	0.0000	0.0000	0.0000	0.0000	0.0000	0.0000	0.0000	0.0000	0.0000	0.0000	0.0000	0.0000
Motukorea	0.9179	0.0013	0.0005	0.0001	0.0001	0.0001	0.0000	0.0000	0.0000	0.0000	0.0068	0.0045	0.0050	0.0078	0.0034	0.0048	0.0038	0.0302	0.0036	0.0041	0.0060
Mt Albert	0.8938	0.0522	0.0367	0.0166	0.0001	0.0005	0.0000	0.0000	0.0001	0.0000	0.0000	0.0000	0.0000	0.0000	0.0000	0.0000	0.0000	0.0000	0.0000	0.0000	0.0000
Mt Cambria	0.6665	0.0044	0.0109	0.0082	0.0002	0.0005	0.0000	0.0000	0.0000	0.0000	0.0064	0.0146	0.0084	0.0932	0.0258	0.0415	0.0171	0.0931	0.0047	0.0031	0.0014
Mt Eden	0.0283	0.0000	0.0000	0.0000	0.0000	0.0000	0.0000	0.0000	0.0000	0.0000	0.1510	0.5291	0.2916	0.0000	0.0000	0.0000	0.0000	0.0000	0.0000	0.0000	0.0000
Mt Hobson	0.0297	0.0000	0.0000	0.0000	0.0000	0.0000	0.0000	0.0000	0.0000	0.0000	0.0000	0.0275	0.0781	0.1032	0.0716	0.0710	0.0651	0.0949	0.1183	0.1301	0.2105
Mt Mangere	0.0053	0.0000	0.0000	0.0000	0.0000	0.0000	0.0000	0.0000	0.0000	0.0000	0.0000	0.0001	0.0008	0.0286	0.0911	0.2361	0.3698	0.2020	0.0636	0.0026	0.0000
Mt Richmond	0.8389	0.0000	0.0000	0.0001	0.0000	0.0030	0.0182	0.1119	0.0006	0.0000	0.0233	0.0040	0.0000	0.0000	0.0000	0.0000	0.0000	0.0000	0.0000	0.0000	0.0000
Mt Roskill	0.9729	0.0073	0.0018	0.0009	0.0003	0.0001	0.0001	0.0001	0.0000	0.0000	0.0121	0.0039	0.0005	0.0000	0.0000	0.0000	0.0000	0.0000	0.0000	0.0000	0.0000
Mt Smart	0.0011	0.0000	0.0000	0.0000	0.0000	0.0000	0.0000	0.0000	0.0000	0.0000	0.0000	0.0000	0.0001	0.0001	0.0025	0.0154	0.0606	0.1355	0.2870	0.3348	0.1629
Mt StJohn	0.7442	0.0316	0.1227	0.0820	0.0003	0.0097	0.0002	0.0002	0.0001	0.0000	0.0054	0.0033	0.0003	0.0000	0.0000	0.0000	0.0000	0.0000	0.0000	0.0000	0.0000
Mt Victoria	0.1565	0.0890	0.0758	0.0574	0.0105	0.0054	0.0008	0.0000	0.0016	0.0000	0.0028	0.0129	0.0940	0.0735	0.1158	0.0560	0.0722	0.0145	0.0671	0.0394	0.0548
Mt Wellington	1.0000	0.0000	0.0000	0.0000	0.0000	0.0000	0.0000	0.0000	0.0000	0.0000	0.0000	0.0000	0.0000	0.0000	0.0000	0.0000	0.0000	0.0000	0.0000	0.0000	0.0000
North Head	0.7294	0.1161	0.0596	0.0416	0.0049	0.0031	0.0004	0.0000	0.0015	0.0000	0.0033	0.0057	0.0111	0.0080	0.0042	0.0029	0.0026	0.0018	0.0020	0.0013	0.0005
One Tree Hill	0.7114	0.0553	0.1314	0.0910	0.0002	0.0088	0.0000	0.0000	0.0001	0.0000	0.0014	0.0004	0.0000	0.0000	0.0000	0.0000	0.0000	0.0000	0.0000	0.0000	0.0000
OnepotoBasin	1.0000	0.0000	0.0000	0.0000	0.0000	0.0000	0.0000	0.0000	0.0000	0.0000	0.0000	0.0000	0.0000	0.0000	0.0000	0.0000	0.0000	0.0000	0.0000	0.0000	0.0000
OrakeiBasin	1.0000	0.0000	0.0000	0.0000	0.0000	0.0000	0.0000	0.0000	0.0000	0.0000	0.0000	0.0000	0.0000	0.0000	0.0000	0.0000	0.0000	0.0000	0.0000	0.0000	0.0000
Otara Hill	0.0009	0.0005	0.0016	0.0099	0.0052	0.0025	0.0011	0.0001	0.0016	0.0000	0.0043	0.0160	0.1456	0.1946	0.2408	0.1537	0.0990	0.0528	0.0461	0.0187	0.0050
Otuataua	0.6188	0.0125	0.0755	0.2682	0.0222	0.0022	0.0004	0.0002	0.0000	0.0000	0.0000	0.0000	0.0000	0.0000	0.0000	0.0000	0.0000	0.0000	0.0000	0.0000	0.0000
Panmure Basin	0.4626	0.0000	0.0027	0.0191	0.0044	0.4941	0.0035	0.0048	0.0036	0.0000	0.0045	0.0007	0.0000	0.0000	0.0000	0.0000	0.0000	0.0000	0.0000	0.0000	0.0000
Pigeon Mountain	0.7922	0.0182	0.0248	0.0233	0.0000	0.0010	0.0000	0.0000	0.0000	0.0000	0.0061	0.0059	0.0061	0.0267	0.0081	0.0147	0.0085	0.0280	0.0104	0.0086	0.0174
Pukaki	0.9116	0.0884	0.0000	0.0000	0.0000	0.0000	0.0000	0.0000	0.0000	0.0000	0.0000	0.0000	0.0000	0.0000	0.0000	0.0000	0.0000	0.0000	0.0000	0.0000	0.0000
Pukeiti	0.9994	0.0003	0.0003	0.0000	0.0000	0.0000	0.0000	0.0000	0.0000	0.0000	0.0000	0.0000	0.0000	0.0000	0.0000	0.0000	0.0000	0.0000	0.0000	0.0000	0.0000
Puketutu	0.2071	0.0000	0.0000	0.0000	0.0076	0.0511	0.0229	0.0093	0.5839	0.0000	0.0963	0.0167	0.0051	0.0000	0.0000	0.0000	0.0000	0.0000	0.0000	0.0000	0.0000
Pukewairiki	1.0000	0.0000	0.0000	0.0000	0.0000	0.0000	0.0000	0.0000	0.0000	0.0000	0.0000	0.0000	0.0000	0.0000	0.0000	0.0000	0.0000	0.0000	0.0000	0.0000	0.0000
PurchasHill	1.0000	0.0000	0.0000	0.0000	0.0000	0.0000	0.0000	0.0000	0.0000	0.0000	0.0000	0.0000	0.0000	0.0000	0.0000	0.0000	0.0000	0.0000	0.0000	0.0000	0.0000
Rangitoto	1.0000	0.0000	0.0000	0.0000	0.0000	0.0000	0.0000	0.0000	0.0000	0.0000	0.0000	0.0000	0.0000	0.0000	0.0000	0.0000	0.0000	0.0000	0.0000	0.0000	0.0000
Robertson Hill	0.7148	0.0000	0.0000	0.0000	0.0000	0.0000	0.0002	0.0001	0.0000	0.0000	0.2084	0.0754	0.0011	0.0000	0.0000	0.0000	0.0000	0.0000	0.0000	0.0000	0.0000
StHeliers	1.0000	0.0000	0.0000	0.0000	0.0000	0.0000	0.0000	0.0000	0.0000	0.0000	0.0000	0.0000	0.0000	0.0000	0.0000	0.0000	0.0000	0.0000	0.0000	0.0000	0.0000
Styaks Swamp	0.2706	0.0000	0.0000	0.0000	0.0000	0.0000	0.0000	0.0000	0.0000	0.0000	0.0001	0.0007	0.0028	0.0237	0.0269	0.0366	0.0426	0.0773	0.1032	0.1184	0.2971
TankFarm	1.0000	0.0000	0.0000	0.0000	0.0000	0.0000	0.0000	0.0000	0.0000	0.0000	0.0000	0.0000	0.0000	0.0000	0.0000	0.0000	0.0000	0.0000	0.0000	0.0000	0.0000
Taylors Hill	0.7003	0.0000	0.0001	0.0036	0.0001	0.0197	0.1510	0.0398	0.0014	0.0000	0.0648	0.0192	0.0000	0.0000	0.0000	0.0000	0.0000	0.0000	0.0000	0.0000	0.0000
Te Pouhawaiki	0.7101	0.1255	0.0758	0.0649	0.0049	0.0062	0.0004	0.0001	0.0016	0.0000	0.0060	0.0041	0.0004	0.0000	0.0000	0.0000	0.0000	0.0000	0.0000	0.0000	0.0000
Three Kings	0.0000	0.0000	0.0000	0.0000	0.0000	0.0000	0.0000	0.0000	0.0000	1.0000	0.0000	0.0000	0.0000	0.0000	0.0000	0.0000	0.0000	0.0000	0.0000	0.0000	0.0000
Waitomokia	0.9998	0.0002	0.0000	0.0000	0.0000	0.0000	0.0000	0.0000	0.0000	0.0000	0.0000	0.0000	0.0000	0.0000	0.0000	0.0000	0.0000	0.0000	0.0000	0.0000	0.0000
Wiri Mountain	0.5424	0.0000	0.0000	0.0002	0.0006	0.0079	0.1027	0.3106	0.0119	0.0000	0.0181	0.0056	0.0000	0.0000	0.0000	0.0000	0.0000	0.0000	0.0000	0.0000	0.0000

Table A.16: Marginal posterior probabilities for a volcano to have produced a given tephra for the Three Kings=AVF 9 scenario with $E = \{\alpha = 2.0, \beta U = 1.0\}$.

Volcano	AVF tephra (AVF 0 = 'unmatched')																				
	0	1	2	3	4	5	6	7	8	9	10	11	12	13	14	15	16	17	18	19	20
Ash Hill	0.9734	0.0000	0.0000	0.0000	0.0000	0.0002	0.0163	0.0093	0.0008	0.0000	0.0000	0.0000	0.0000	0.0000	0.0000	0.0000	0.0000	0.0000	0.0000	0.0000	0.0000
Cemetery Hill	0.0460	0.0000	0.0000	0.0002	0.0256	0.2891	0.3112	0.1136	0.1864	0.0000	0.0239	0.0040	0.0000	0.0000	0.0000	0.0000	0.0000	0.0000	0.0000	0.0000	0.0000
Crater Hill	0.1897	0.0000	0.0000	0.0000	0.0001	0.0074	0.3415	0.2558	0.1793	0.0000	0.0078	0.0163	0.0021	0.0000	0.0000	0.0000	0.0000	0.0000	0.0000	0.0000	0.0000
Domain	0.7795	0.1144	0.0878	0.0183	0.0000	0.0000	0.0000	0.0000	0.0000	0.0000	0.0000	0.0000	0.0000	0.0000	0.0000	0.0000	0.0000	0.0000	0.0000	0.0000	0.0000
Green Hill	0.0027	0.0018	0.0042	0.0213	0.0244	0.0137	0.0023	0.0001	0.0073	0.0000	0.0249	0.0500	0.1672	0.1251	0.1054	0.0930	0.0840	0.0983	0.0995	0.0623	0.0125
Hampton Park	0.3027	0.0000	0.0000	0.0000	0.0000	0.0000	0.0000	0.0002	0.0000	0.0000	0.0001	0.0149	0.0201	0.1548	0.1760	0.1522	0.0832	0.0631	0.0208	0.0077	0.0042
Hopua	0.4739	0.0000	0.0022	0.0038	0.0000	0.0190	0.0256	0.0548	0.0007	0.0000	0.3012	0.1188	0.0000	0.0000	0.0000	0.0000	0.0000	0.0000	0.0000	0.0000	0.0000
Kohuora	0.0001	0.0069	0.0238	0.0375	0.8708	0.0481	0.0110	0.0006	0.0012	0.0000	0.0000	0.0000	0.0000	0.0000	0.0000	0.0000	0.0000	0.0000	0.0000	0.0000	0.0000
Little Rangitoto	0.0101	0.2381	0.1741	0.1334	0.0191	0.0069	0.0008	0.0007	0.0045	0.0000	0.0096	0.0147	0.0495	0.0340	0.0292	0.0276	0.0228	0.0365	0.0515	0.0508	0.0861
Mangere Lagoon	0.7433	0.0320	0.0678	0.0505	0.0003	0.0080	0.0006	0.0001	0.0004	0.0000	0.0055	0.0116	0.0245	0.0219	0.0151	0.0120	0.0055	0.0009	0.0000	0.0000	0.0000
Matukutureia	0.0031	0.0000	0.0000	0.0000	0.0000	0.0000	0.0000	0.0001	0.0007	0.0000	0.0062	0.0179	0.0898	0.1024	0.0840	0.0804	0.0627	0.0716	0.1237	0.2162	0.1412
Maungataketake	0.9972	0.0000	0.0002	0.0014	0.0005	0.0004	0.0003	0.0000	0.0000	0.0000	0.0000	0.0000	0.0000	0.0000	0.0000	0.0000	0.0000	0.0000	0.0000	0.0000	0.0000
McLennan Hills	0.9336	0.0000	0.0224	0.0400	0.0002	0.0031	0.0004	0.0003	0.0000	0.0000	0.0000	0.0000	0.0000	0.0000	0.0000	0.0000	0.0000	0.0000	0.0000	0.0000	0.0000
Motukorea	0.9178	0.0011	0.0005	0.0001	0.0000	0.0001	0.0000	0.0000	0.0000	0.0000	0.0067	0.0045	0.0049	0.0079	0.0034	0.0050	0.0038	0.0301	0.0036	0.0041	0.0064
Mt Albert	0.8960	0.0513	0.0354	0.0168	0.0000	0.0004	0.0000	0.0000	0.0001	0.0000	0.0000	0.0000	0.0000	0.0000	0.0000	0.0000	0.0000	0.0000	0.0000	0.0000	0.0000
Mt Cambria	0.6533	0.0057	0.0131	0.0146	0.0003	0.0008	0.0000	0.0000	0.0000	0.0000	0.0066	0.0144	0.0086	0.0946	0.0269	0.0409	0.0174	0.0931	0.0047	0.0033	0.0017
Mt Eden	0.0282	0.0000	0.0000	0.0000	0.0000	0.0000	0.0000	0.0000	0.0000	0.0000	0.1538	0.5340	0.2840	0.0000	0.0000	0.0000	0.0000	0.0000	0.0000	0.0000	0.0000
Mt Hobson	0.0288	0.0000	0.0000	0.0000	0.0000	0.0000	0.0000	0.0000	0.0000	0.0000	0.0000	0.0291	0.0774	0.1033	0.0713	0.0716	0.0645	0.0957	0.1176	0.1298	0.2109
Mt Mangere	0.0055	0.0000	0.0000	0.0000	0.0000	0.0000	0.0000	0.0000	0.0000	0.0000	0.0000	0.0001	0.0008	0.0295	0.0921	0.2376	0.3711	0.1976	0.0631	0.0026	0.0000
Mt Richmond	0.8025	0.0000	0.0000	0.0000	0.0000	0.0029	0.0313	0.1361	0.0006	0.0000	0.0229	0.0037	0.0000	0.0000	0.0000	0.0000	0.0000	0.0000	0.0000	0.0000	0.0000
Mt Roskill	0.9739	0.0071	0.0016	0.0004	0.0002	0.0002	0.0001	0.0001	0.0000	0.0000	0.0121	0.0039	0.0004	0.0000	0.0000	0.0000	0.0000	0.0000	0.0000	0.0000	0.0000
Mt Smart	0.0005	0.0000	0.0000	0.0000	0.0000	0.0000	0.0000	0.0000	0.0000	0.0000	0.0000	0.0000	0.0001	0.0001	0.0025	0.0161	0.0614	0.1369	0.2874	0.3335	0.1615
Mt StJohn	0.7470	0.0341	0.1173	0.0826	0.0002	0.0092	0.0002	0.0003	0.0001	0.0000	0.0055	0.0032	0.0003	0.0000	0.0000	0.0000	0.0000	0.0000	0.0000	0.0000	0.0000
Mt Victoria	0.1522	0.0900	0.0763	0.0580	0.0123	0.0047	0.0009	0.0000	0.0016	0.0000	0.0028	0.0131	0.0958	0.0725	0.1149	0.0566	0.0722	0.0145	0.0667	0.0397	0.0552
North Head	0.7225	0.1190	0.0612	0.0437	0.0055	0.0030	0.0002	0.0000	0.0015	0.0000	0.0033	0.0058	0.0112	0.0079	0.0041	0.0031	0.0024	0.0019	0.0019	0.0013	0.0005
One Tree Hill	0.7130	0.0559	0.1288	0.0915	0.0000	0.0089	0.0000	0.0000	0.0001	0.0000	0.0014	0.0004	0.0000	0.0000	0.0000	0.0000	0.0000	0.0000	0.0000	0.0000	0.0000
Otara Hill	0.0009	0.0005	0.0017	0.0096	0.0057	0.0023	0.0009	0.0001	0.0016	0.0000	0.0045	0.0160	0.1479	0.1953	0.2398	0.1532	0.0982	0.0525	0.0456	0.0186	0.0051
Otuataua	0.6331	0.0121	0.0745	0.2599	0.0188	0.0010	0.0004	0.0002	0.0000	0.0000	0.0000	0.0000	0.0000	0.0000	0.0000	0.0000	0.0000	0.0000	0.0000	0.0000	0.0000
Panmure Basin	0.4658	0.0000	0.0032	0.0195	0.0006	0.4943	0.0032	0.0048	0.0034	0.0000	0.0045	0.0007	0.0000	0.0000	0.0000	0.0000	0.0000	0.0000	0.0000	0.0000	0.0000
Pigeon Mountain	0.7882	0.0181	0.0253	0.0267	0.0000	0.0009	0.0000	0.0000	0.0000	0.0000	0.0061	0.0058	0.0061	0.0269	0.0082	0.0144	0.0082	0.0281	0.0104	0.0088	0.0178
Pukaki	0.9150	0.0850	0.0000	0.0000	0.0000	0.0000	0.0000	0.0000	0.0000	0.0000	0.0000	0.0000	0.0000	0.0000	0.0000	0.0000	0.0000	0.0000	0.0000	0.0000	0.0000
Pukeiti	0.9997	0.0001	0.0002	0.0000	0.0000	0.0000	0.0000	0.0000	0.0000	0.0000	0.0000	0.0000	0.0000	0.0000	0.0000	0.0000	0.0000	0.0000	0.0000	0.0000	0.0000
Puketutu	0.1836	0.0000	0.0000	0.0000	0.0069	0.0442	0.0227	0.0298	0.5945	0.0000	0.0968	0.0164	0.0051	0.0000	0.0000	0.0000	0.0000	0.0000	0.0000	0.0000	0.0000
Robertson Hill	0.7211	0.0000	0.0000	0.0000	0.0000	0.0000	0.0002	0.0002	0.0000	0.0000	0.2058	0.0716	0.0011	0.0000	0.0000	0.0000	0.0000	0.0000	0.0000	0.0000	0.0000
Styaks Swamp	0.2657	0.0000	0.0000	0.0000	0.0000	0.0000	0.0000	0.0000	0.0000	0.0000	0.0001	0.0007	0.0028	0.0238	0.0271	0.0363	0.0426	0.0792	0.1035	0.1213	0.2969
Taylors Hill	0.7206	0.0000	0.0001	0.0040	0.0000	0.0187	0.1406	0.0315	0.0015	0.0000	0.0641	0.0189	0.0000	0.0000	0.0000	0.0000	0.0000	0.0000	0.0000	0.0000	0.0000
Te Pouhawaiki	0.7026	0.1267	0.0783	0.0661	0.0080	0.0056	0.0005	0.0001	0.0016	0.0000	0.0060	0.0042	0.0003	0.0000	0.0000	0.0000	0.0000	0.0000	0.0000	0.0000	0.0000
Three Kings	0.0000	0.0000	0.0000	0.0000	0.0000	0.0000	0.0000	0.0000	0.0000	1.0000	0.0000	0.0000	0.0000	0.0000	0.0000	0.0000	0.0000	0.0000	0.0000	0.0000	0.0000
Waitomokia	0.9999	0.0001	0.0000	0.0000	0.0000	0.0000	0.0000	0.0000	0.0000	0.0000	0.0000	0.0000	0.0000	0.0000	0.0000	0.0000	0.0000	0.0000	0.0000	0.0000	0.0000
Wiri Mountain	0.5073	0.0000	0.0000	0.0001	0.0005	0.0069	0.0888	0.3612	0.0121	0.0000	0.0178	0.0053	0.0000	0.0000	0.0000	0.0000	0.0000	0.0000	0.0000	0.0000	0.0000

Table A.17: Marginal posterior probabilities for a volcano to have produced a given tephra for the Three Kings=AVF 9 scenario with F = $\{\alpha = 2.5, \beta U = 1.0\}$.

Volcano	AVF tephra (AVF 0 = 'unmatched')																				
	0	1	2	3	4	5	6	7	8	9	10	11	12	13	14	15	16	17	18	19	20
Ash Hill	0.9715	0.0000	0.0000	0.0000	0.0000	0.0002	0.0182	0.0093	0.0008	0.0000	0.0000	0.0000	0.0000	0.0000	0.0000	0.0000	0.0000	0.0000	0.0000	0.0000	0.0000
Cemetery Hill	0.0250	0.0000	0.0000	0.0002	0.0261	0.2345	0.3732	0.0916	0.2215	0.0000	0.0239	0.0040	0.0000	0.0000	0.0000	0.0000	0.0000	0.0000	0.0000	0.0000	0.0000
Crater Hill	0.2459	0.0000	0.0000	0.0000	0.0001	0.0071	0.2652	0.3318	0.1240	0.0000	0.0075	0.0163	0.0021	0.0000	0.0000	0.0000	0.0000	0.0000	0.0000	0.0000	0.0000
Domain	0.7808	0.1127	0.0887	0.0178	0.0000	0.0000	0.0000	0.0000	0.0000	0.0000	0.0000	0.0000	0.0000	0.0000	0.0000	0.0000	0.0000	0.0000	0.0000	0.0000	0.0000
Green Hill	0.0022	0.0017	0.0045	0.0215	0.0250	0.0133	0.0021	0.0001	0.0073	0.0000	0.0253	0.0498	0.1682	0.1248	0.1043	0.0936	0.0853	0.0976	0.0991	0.0623	0.0120
Hampton Park	0.3073	0.0000	0.0000	0.0000	0.0000	0.0000	0.0000	0.0002	0.0000	0.0000	0.0001	0.0150	0.0201	0.1547	0.1764	0.1497	0.0816	0.0629	0.0202	0.0077	0.0041
Hopua	0.4756	0.0000	0.0019	0.0039	0.0004	0.0192	0.0267	0.0534	0.0007	0.0000	0.3000	0.1182	0.0000	0.0000	0.0000	0.0000	0.0000	0.0000	0.0000	0.0000	0.0000
Kohuora	0.0002	0.0073	0.0244	0.0376	0.8673	0.0504	0.0104	0.0010	0.0014	0.0000	0.0000	0.0000	0.0000	0.0000	0.0000	0.0000	0.0000	0.0000	0.0000	0.0000	0.0000
Little Rangitoto	0.0077	0.2386	0.1780	0.1291	0.0203	0.0067	0.0006	0.0008	0.0045	0.0000	0.0095	0.0149	0.0501	0.0334	0.0298	0.0270	0.0231	0.0365	0.0511	0.0514	0.0869
Mangere Lagoon	0.7477	0.0304	0.0665	0.0496	0.0002	0.0076	0.0006	0.0001	0.0004	0.0000	0.0056	0.0117	0.0242	0.0220	0.0150	0.0120	0.0055	0.0009	0.0000	0.0000	0.0000
Matukutureia	0.0030	0.0000	0.0000	0.0000	0.0000	0.0000	0.0000	0.0001	0.0007	0.0000	0.0063	0.0179	0.0896	0.1020	0.0847	0.0807	0.0618	0.0727	0.1249	0.2156	0.1400
Maungataketake	0.9966	0.0000	0.0002	0.0014	0.0008	0.0005	0.0005	0.0000	0.0000	0.0000	0.0000	0.0000	0.0000	0.0000	0.0000	0.0000	0.0000	0.0000	0.0000	0.0000	0.0000
McLennan Hills	0.9325	0.0000	0.0228	0.0403	0.0002	0.0031	0.0007	0.0004	0.0000	0.0000	0.0000	0.0000	0.0000	0.0000	0.0000	0.0000	0.0000	0.0000	0.0000	0.0000	0.0000
Motukorea	0.9174	0.0012	0.0006	0.0001	0.0000	0.0002	0.0000	0.0000	0.0000	0.0000	0.0068	0.0045	0.0049	0.0078	0.0035	0.0050	0.0038	0.0298	0.0037	0.0041	0.0066
Mt Albert	0.9000	0.0508	0.0324	0.0163	0.0000	0.0004	0.0000	0.0000	0.0001	0.0000	0.0000	0.0000	0.0000	0.0000	0.0000	0.0000	0.0000	0.0000	0.0000	0.0000	0.0000
Mt Cambria	0.6373	0.0061	0.0231	0.0171	0.0003	0.0013	0.0000	0.0000	0.0000	0.0000	0.0069	0.0142	0.0086	0.0954	0.0276	0.0409	0.0177	0.0929	0.0049	0.0038	0.0019
Mt Eden	0.0290	0.0000	0.0000	0.0000	0.0000	0.0000	0.0000	0.0000	0.0000	0.0000	0.1548	0.5355	0.2807	0.0000	0.0000	0.0000	0.0000	0.0000	0.0000	0.0000	0.0000
Mt Hobson	0.0287	0.0000	0.0000	0.0000	0.0000	0.0000	0.0000	0.0000	0.0000	0.0000	0.0001	0.0296	0.0760	0.1052	0.0708	0.0710	0.0649	0.0970	0.1163	0.1303	0.2101
Mt Mangere	0.0051	0.0000	0.0000	0.0000	0.0000	0.0000	0.0000	0.0000	0.0000	0.0000	0.0000	0.0003	0.0008	0.0305	0.0917	0.2408	0.3695	0.1956	0.0631	0.0026	0.0000
Mt Richmond	0.8676	0.0000	0.0000	0.0000	0.0000	0.0031	0.0305	0.0725	0.0006	0.0000	0.0221	0.0036	0.0000	0.0000	0.0000	0.0000	0.0000	0.0000	0.0000	0.0000	0.0000
Mt Roskill	0.9739	0.0072	0.0017	0.0005	0.0002	0.0002	0.0001	0.0001	0.0000	0.0000	0.0119	0.0038	0.0004	0.0000	0.0000	0.0000	0.0000	0.0000	0.0000	0.0000	0.0000
Mt Smart	0.0003	0.0000	0.0000	0.0000	0.0000	0.0000	0.0000	0.0000	0.0000	0.0000	0.0000	0.0000	0.0001	0.0001	0.0026	0.0166	0.0623	0.1367	0.2886	0.3322	0.1605
Mt StJohn	0.7443	0.0375	0.1163	0.0830	0.0002	0.0092	0.0001	0.0003	0.0001	0.0000	0.0055	0.0032	0.0003	0.0000	0.0000	0.0000	0.0000	0.0000	0.0000	0.0000	0.0000
Mt Victoria	0.1512	0.0928	0.0682	0.0636	0.0123	0.0048	0.0009	0.0000	0.0016	0.0000	0.0028	0.0134	0.0971	0.0713	0.1153	0.0563	0.0724	0.0144	0.0668	0.0395	0.0553
North Head	0.7198	0.1234	0.0585	0.0441	0.0061	0.0031	0.0002	0.0000	0.0015	0.0000	0.0034	0.0058	0.0110	0.0081	0.0040	0.0032	0.0024	0.0020	0.0017	0.0013	0.0004
One Tree Hill	0.7106	0.0592	0.1278	0.0915	0.0002	0.0088	0.0000	0.0000	0.0001	0.0000	0.0014	0.0004	0.0000	0.0000	0.0000	0.0000	0.0000	0.0000	0.0000	0.0000	0.0000
Otara Hill	0.0011	0.0005	0.0014	0.0097	0.0054	0.0025	0.0010	0.0001	0.0016	0.0000	0.0046	0.0162	0.1502	0.1944	0.2387	0.1531	0.0981	0.0523	0.0457	0.0183	0.0051
Otuataua	0.6447	0.0098	0.0740	0.2519	0.0174	0.0015	0.0005	0.0002	0.0000	0.0000	0.0000	0.0000	0.0000	0.0000	0.0000	0.0000	0.0000	0.0000	0.0000	0.0000	0.0000
Panmure Basin	0.3772	0.0000	0.0039	0.0196	0.0008	0.5814	0.0037	0.0049	0.0033	0.0000	0.0045	0.0007	0.0000	0.0000	0.0000	0.0000	0.0000	0.0000	0.0000	0.0000	0.0000
Pigeon Mountain	0.7839	0.0175	0.0286	0.0283	0.0000	0.0009	0.0000	0.0000	0.0000	0.0000	0.0060	0.0057	0.0062	0.0268	0.0083	0.0141	0.0087	0.0279	0.0103	0.0087	0.0181
Pukaki	0.9279	0.0721	0.0000	0.0000	0.0000	0.0000	0.0000	0.0000	0.0000	0.0000	0.0000	0.0000	0.0000	0.0000	0.0000	0.0000	0.0000	0.0000	0.0000	0.0000	0.0000
Pukeiti	0.9996	0.0002	0.0002	0.0000	0.0000	0.0000	0.0000	0.0000	0.0000	0.0000	0.0000	0.0000	0.0000	0.0000	0.0000	0.0000	0.0000	0.0000	0.0000	0.0000	0.0000
Puketutu	0.1765	0.0000	0.0000	0.0000	0.0065	0.0076	0.0265	0.0495	0.6151	0.0000	0.0975	0.0157	0.0051	0.0000	0.0000	0.0000	0.0000	0.0000	0.0000	0.0000	0.0000
Robertson Hill	0.7214	0.0000	0.0000	0.0000	0.0000	0.0000	0.0002	0.0003	0.0000	0.0000	0.2056	0.0714	0.0011	0.0000	0.0000	0.0000	0.0000	0.0000	0.0000	0.0000	0.0000
Styaks Swamp	0.2611	0.0000	0.0000	0.0000	0.0000	0.0000	0.0000	0.0000	0.0000	0.0000	0.0001	0.0007	0.0028	0.0235	0.0273	0.0360	0.0429	0.0808	0.1036	0.1222	0.2990
Taylors Hill	0.7228	0.0000	0.0002	0.0041	0.0001	0.0205	0.1373	0.0310	0.0016	0.0000	0.0642	0.0182	0.0000	0.0000	0.0000	0.0000	0.0000	0.0000	0.0000	0.0000	0.0000
Te Pouhawaiki	0.6972	0.1309	0.0761	0.0683	0.0095	0.0052	0.0006	0.0001	0.0016	0.0000	0.0061	0.0040	0.0004	0.0000	0.0000	0.0000	0.0000	0.0000	0.0000	0.0000	0.0000
Three Kings	0.0000	0.0000	0.0000	0.0000	0.0000	0.0000	0.0000	0.0000	0.0000	1.0000	0.0000	0.0000	0.0000	0.0000	0.0000	0.0000	0.0000	0.0000	0.0000	0.0000	0.0000
Waitomokia	0.9999	0.0001	0.0000	0.0000	0.0000	0.0000	0.0000	0.0000	0.0000	0.0000	0.0000	0.0000	0.0000	0.0000	0.0000	0.0000	0.0000	0.0000	0.0000	0.0000	0.0000
Wiri Mountain	0.5055	0.0000	0.0000	0.0005	0.0006	0.0067	0.1002	0.3522	0.0115	0.0000	0.0175	0.0053	0.0000	0.0000	0.0000	0.0000	0.0000	0.0000	0.0000	0.0000	0.0000

Table A.18: Marginal posterior probabilities for a volcano to have produced a given tephra for the Three Kings=AVF 10 scenario with $A = \{\alpha = 1.5, \beta U = 0.5\}$.

Volcano	AVF tephra (AVF 0 = 'unmatched')																				
	0	1	2	3	4	5	6	7	8	9	10	11	12	13	14	15	16	17	18	19	20
Ash Hill	0.9447	0.0000	0.0000	0.0001	0.0000	0.0031	0.0346	0.0175	0.0000	0.0000	0.0000	0.0000	0.0000	0.0000	0.0000	0.0000	0.0000	0.0000	0.0000	0.0000	0.0000
Cemetery Hill	0.1164	0.0000	0.0000	0.0000	0.0001	0.0186	0.1918	0.5034	0.1681	0.0014	0.0000	0.0002	0.0000	0.0000	0.0000	0.0000	0.0000	0.0000	0.0000	0.0000	0.0000
Crater Hill	0.0022	0.0000	0.0000	0.0000	0.0000	0.0000	0.0263	0.0171	0.6640	0.2883	0.0000	0.0019	0.0002	0.0000	0.0000	0.0000	0.0000	0.0000	0.0000	0.0000	0.0000
Domain	0.7610	0.1284	0.0909	0.0197	0.0000	0.0000	0.0000	0.0000	0.0000	0.0000	0.0000	0.0000	0.0000	0.0000	0.0000	0.0000	0.0000	0.0000	0.0000	0.0000	0.0000
Green Hill	0.0106	0.0007	0.0040	0.0219	0.0200	0.0153	0.0054	0.0001	0.0000	0.0130	0.0000	0.0397	0.0897	0.1777	0.1140	0.0957	0.0785	0.0840	0.1116	0.0889	0.0292
Hampton Park	0.3252	0.0000	0.0000	0.0000	0.0000	0.0002	0.0000	0.0001	0.0000	0.0000	0.0000	0.0000	0.0050	0.0874	0.1699	0.2084	0.1069	0.0701	0.0158	0.0072	0.0038
Hopua	0.6272	0.0000	0.0000	0.0006	0.0011	0.0347	0.0317	0.0163	0.0005	0.0003	0.0000	0.2876	0.0000	0.0000	0.0000	0.0000	0.0000	0.0000	0.0000	0.0000	0.0000
Kohuora	0.0026	0.0000	0.0021	0.0229	0.8943	0.0503	0.0233	0.0039	0.0005	0.0001	0.0000	0.0000	0.0000	0.0000	0.0000	0.0000	0.0000	0.0000	0.0000	0.0000	0.0000
Little Rangitoto	0.0548	0.1983	0.1884	0.1502	0.0148	0.0121	0.0011	0.0006	0.0013	0.0057	0.0000	0.0134	0.0277	0.0460	0.0346	0.0281	0.0217	0.0295	0.0493	0.0511	0.0713
Mangere Lagoon	0.7291	0.0485	0.0630	0.0614	0.0007	0.0034	0.0020	0.0000	0.0000	0.0006	0.0000	0.0072	0.0120	0.0267	0.0181	0.0156	0.0094	0.0023	0.0000	0.0000	0.0000
Matukutureia	0.0239	0.0000	0.0000	0.0000	0.0000	0.0000	0.0000	0.0000	0.0001	0.0020	0.0000	0.0077	0.0286	0.1288	0.0956	0.0812	0.0678	0.0649	0.0953	0.2043	0.1998
Maungataketake	0.9869	0.0008	0.0011	0.0022	0.0076	0.0003	0.0011	0.0000	0.0000	0.0000	0.0000	0.0000	0.0000	0.0000	0.0000	0.0000	0.0000	0.0000	0.0000	0.0000	0.0000
McLennan Hills	0.9372	0.0000	0.0142	0.0404	0.0020	0.0030	0.0031	0.0001	0.0000	0.0000	0.0000	0.0000	0.0000	0.0000	0.0000	0.0000	0.0000	0.0000	0.0000	0.0000	0.0000
Motukorea	0.9385	0.0031	0.0025	0.0003	0.0000	0.0007	0.0000	0.0000	0.0000	0.0000	0.0000	0.0004	0.0012	0.0100	0.0019	0.0049	0.0032	0.0270	0.0015	0.0019	0.0029
Mt Albert	0.8829	0.0617	0.0371	0.0169	0.0009	0.0003	0.0001	0.0000	0.0000	0.0001	0.0000	0.0000	0.0000	0.0000	0.0000	0.0000	0.0000	0.0000	0.0000	0.0000	0.0000
Mt Cambria	0.7287	0.0072	0.0111	0.0160	0.0007	0.0030	0.0000	0.0000	0.0000	0.0000	0.0000	0.0001	0.0020	0.0535	0.0151	0.0531	0.0213	0.0850	0.0014	0.0014	0.0004
Mt Eden	0.0114	0.0000	0.0000	0.0000	0.0000	0.0000	0.0000	0.0000	0.0000	0.0000	0.0000	0.2782	0.7104	0.0000	0.0000	0.0000	0.0000	0.0000	0.0000	0.0000	0.0000
Mt Hobson	0.1163	0.0000	0.0000	0.0000	0.0000	0.0000	0.0000	0.0000	0.0000	0.0000	0.0000	0.0013	0.0436	0.1206	0.0801	0.0716	0.0615	0.0795	0.1124	0.1337	0.1794
Mt Mangere	0.0043	0.0000	0.0000	0.0000	0.0000	0.0000	0.0000	0.0000	0.0000	0.0000	0.0000	0.0000	0.0002	0.0079	0.0505	0.1460	0.3350	0.3178	0.1341	0.0042	0.0000
Mt Richmond	0.8256	0.0000	0.0000	0.0000	0.0000	0.0024	0.0709	0.0963	0.0001	0.0002	0.0000	0.0045	0.0000	0.0000	0.0000	0.0000	0.0000	0.0000	0.0000	0.0000	0.0000
Mt Roskill	0.9451	0.0183	0.0242	0.0029	0.0004	0.0021	0.0001	0.0000	0.0000	0.0000	0.0000	0.0067	0.0002	0.0000	0.0000	0.0000	0.0000	0.0000	0.0000	0.0000	0.0000
Mt Smart	0.0120	0.0000	0.0000	0.0000	0.0000	0.0000	0.0000	0.0000	0.0000	0.0000	0.0000	0.0000	0.0000	0.0001	0.0008	0.0056	0.0256	0.0793	0.2762	0.3765	0.2239
Mt StJohn	0.7194	0.0544	0.1196	0.0898	0.0002	0.0103	0.0000	0.0003	0.0000	0.0002	0.0000	0.0054	0.0004	0.0000	0.0000	0.0000	0.0000	0.0000	0.0000	0.0000	0.0000
Mt Victoria	0.1829	0.0702	0.0804	0.0651	0.0112	0.0064	0.0005	0.0001	0.0000	0.0026	0.0000	0.0080	0.0282	0.0925	0.1210	0.0619	0.0858	0.0196	0.0751	0.0380	0.0505
North Head	0.7416	0.0963	0.0601	0.0493	0.0055	0.0037	0.0003	0.0001	0.0000	0.0021	0.0000	0.0044	0.0080	0.0092	0.0056	0.0035	0.0030	0.0022	0.0019	0.0018	0.0014
One Tree Hill	0.6805	0.0822	0.1298	0.0929	0.0024	0.0093	0.0003	0.0002	0.0000	0.0010	0.0000	0.0014	0.0000	0.0000	0.0000	0.0000	0.0000	0.0000	0.0000	0.0000	0.0000
Otara Hill	0.0066	0.0004	0.0007	0.0088	0.0042	0.0017	0.0014	0.0000	0.0001	0.0025	0.0000	0.0084	0.0392	0.2001	0.2625	0.1725	0.1338	0.0573	0.0669	0.0248	0.0081
Otuataua	0.6566	0.0073	0.0609	0.2408	0.0253	0.0088	0.0002	0.0001	0.0000	0.0000	0.0000	0.0000	0.0000	0.0000	0.0000	0.0000	0.0000	0.0000	0.0000	0.0000	0.0000
Panmure Basin	0.1641	0.0000	0.0000	0.0003	0.0030	0.7748	0.0359	0.0182	0.0008	0.0023	0.0000	0.0006	0.0000	0.0000	0.0000	0.0000	0.0000	0.0000	0.0000	0.0000	0.0000
Pigeon Mountain	0.7715	0.0310	0.0424	0.0363	0.0002	0.0026	0.0000	0.0000	0.0000	0.0000	0.0000	0.0040	0.0019	0.0249	0.0112	0.0151	0.0095	0.0271	0.0055	0.0047	0.0121
Pukaki	0.8863	0.1137	0.0000	0.0000	0.0000	0.0000	0.0000	0.0000	0.0000	0.0000	0.0000	0.0000	0.0000	0.0000	0.0000	0.0000	0.0000	0.0000	0.0000	0.0000	0.0000
Pukeiti	0.9979	0.0010	0.0009	0.0000	0.0001	0.0001	0.0000	0.0000	0.0000	0.0000	0.0000	0.0000	0.0000	0.0000	0.0000	0.0000	0.0000	0.0000	0.0000	0.0000	0.0000
Puketutu	0.0626	0.0000	0.0000	0.0000	0.0006	0.0043	0.0324	0.0775	0.1378	0.6588	0.0000	0.0260	0.0000	0.0000	0.0000	0.0000	0.0000	0.0000	0.0000	0.0000	0.0000
Robertson Hill	0.7339	0.0000	0.0000	0.0000	0.0000	0.0000	0.0004	0.0000	0.0000	0.0000	0.0000	0.2644	0.0013	0.0000	0.0000	0.0000	0.0000	0.0000	0.0000	0.0000	0.0000
Styaks Swamp	0.5060	0.0000	0.0000	0.0000	0.0000	0.0000	0.0000	0.0000	0.0000	0.0000	0.0000	0.0002	0.0002	0.0146	0.0191	0.0368	0.0370	0.0544	0.0530	0.0615	0.2172
Taylors Hill	0.6369	0.0000	0.0000	0.0000	0.0002	0.0228	0.2212	0.1017	0.0002	0.0000	0.0000	0.0170	0.0000	0.0000	0.0000	0.0000	0.0000	0.0000	0.0000	0.0000	0.0000
Te Pouhawaiki	0.7794	0.0759	0.0665	0.0612	0.0045	0.0028	0.0003	0.0002	0.0001	0.0009	0.0000	0.0082	0.0000	0.0000	0.0000	0.0000	0.0000	0.0000	0.0000	0.0000	0.0000
Three Kings	0.0000	0.0000	0.0000	0.0000	0.0000	0.0000	0.0000	0.0000	0.0000	0.0000	1.0000	0.0000	0.0000	0.0000	0.0000	0.0000	0.0000	0.0000	0.0000	0.0000	0.0000
Waitomokia	0.9993	0.0006	0.0001	0.0000	0.0000	0.0000	0.0000	0.0000	0.0000	0.0000	0.0000	0.0000	0.0000	0.0000	0.0000	0.0000	0.0000	0.0000	0.0000	0.0000	0.0000
Wiri Mountain	0.4879	0.0000	0.0000	0.0000	0.0000	0.0029	0.3156	0.1462	0.0264	0.0179	0.0000	0.0031	0.0000	0.0000	0.0000	0.0000	0.0000	0.0000	0.0000	0.0000	0.0000

Table A.19: Marginal posterior probabilities for a volcano to have produced a given tephra for the Three Kings=AVF 10 scenario with B = $\{\alpha = 2.0,\ \beta U = 0.5\}$.

Volcano	AVF tephra (AVF 0 = 'unmatched')																				
	0	1	2	3	4	5	6	7	8	9	10	11	12	13	14	15	16	17	18	19	20
Ash Hill	0.9446	0.0000	0.0000	0.0000	0.0000	0.0004	0.0379	0.0171	0.0000	0.0000	0.0000	0.0000	0.0000	0.0000	0.0000	0.0000	0.0000	0.0000	0.0000	0.0000	0.0000
Cemetery Hill	0.0885	0.0000	0.0000	0.0000	0.0004	0.0190	0.1999	0.5089	0.1815	0.0014	0.0000	0.0004	0.0000	0.0000	0.0000	0.0000	0.0000	0.0000	0.0000	0.0000	0.0000
Crater Hill	0.0020	0.0000	0.0000	0.0000	0.0000	0.0002	0.0246	0.0165	0.6668	0.2876	0.0000	0.0018	0.0005	0.0000	0.0000	0.0000	0.0000	0.0000	0.0000	0.0000	0.0000
Domain	0.7600	0.1327	0.0866	0.0207	0.0000	0.0000	0.0000	0.0000	0.0000	0.0000	0.0000	0.0000	0.0000	0.0000	0.0000	0.0000	0.0000	0.0000	0.0000	0.0000	0.0000
Green Hill	0.0108	0.0007	0.0037	0.0222	0.0211	0.0135	0.0046	0.0002	0.0000	0.0130	0.0000	0.0398	0.0952	0.1741	0.1143	0.0965	0.0798	0.0859	0.1107	0.0856	0.0283
Hampton Park	0.3444	0.0000	0.0000	0.0000	0.0000	0.0000	0.0000	0.0001	0.0000	0.0000	0.0000	0.0000	0.0048	0.0852	0.1662	0.1999	0.1032	0.0686	0.0170	0.0066	0.0040
Hopua	0.6334	0.0000	0.0000	0.0006	0.0000	0.0288	0.0302	0.0195	0.0004	0.0005	0.0000	0.2866	0.0000	0.0000	0.0000	0.0000	0.0000	0.0000	0.0000	0.0000	0.0000
Kohuora	0.0007	0.0003	0.0026	0.0254	0.9115	0.0422	0.0168	0.0000	0.0004	0.0001	0.0000	0.0000	0.0000	0.0000	0.0000	0.0000	0.0000	0.0000	0.0000	0.0000	0.0000
Little Rangitoto	0.0422	0.2004	0.1948	0.1491	0.0148	0.0106	0.0010	0.0004	0.0013	0.0057	0.0000	0.0130	0.0292	0.0466	0.0342	0.0276	0.0215	0.0309	0.0502	0.0510	0.0755
Mangere Lagoon	0.7456	0.0440	0.0591	0.0549	0.0004	0.0029	0.0018	0.0000	0.0000	0.0005	0.0000	0.0071	0.0118	0.0269	0.0188	0.0153	0.0088	0.0021	0.0000	0.0000	0.0000
Matukutureia	0.0194	0.0000	0.0000	0.0000	0.0000	0.0000	0.0000	0.0000	0.0001	0.0023	0.0000	0.0079	0.0310	0.1281	0.0972	0.0810	0.0683	0.0642	0.0975	0.2130	0.1900
Maungataketake	0.9977	0.0006	0.0000	0.0013	0.0000	0.0001	0.0003	0.0000	0.0000	0.0000	0.0000	0.0000	0.0000	0.0000	0.0000	0.0000	0.0000	0.0000	0.0000	0.0000	0.0000
McLennan Hills	0.9421	0.0000	0.0162	0.0393	0.0001	0.0021	0.0000	0.0002	0.0000	0.0000	0.0000	0.0000	0.0000	0.0000	0.0000	0.0000	0.0000	0.0000	0.0000	0.0000	0.0000
Motukorea	0.9432	0.0023	0.0008	0.0001	0.0000	0.0006	0.0000	0.0000	0.0000	0.0000	0.0000	0.0006	0.0012	0.0089	0.0017	0.0038	0.0028	0.0278	0.0013	0.0018	0.0031
Mt Albert	0.8868	0.0590	0.0354	0.0177	0.0006	0.0004	0.0000	0.0000	0.0000	0.0001	0.0000	0.0000	0.0000	0.0000	0.0000	0.0000	0.0000	0.0000	0.0000	0.0000	0.0000
Mt Cambria	0.7123	0.0101	0.0233	0.0167	0.0005	0.0035	0.0000	0.0000	0.0000	0.0000	0.0000	0.0001	0.0017	0.0550	0.0156	0.0493	0.0184	0.0903	0.0014	0.0014	0.0004
Mt Eden	0.0157	0.0000	0.0000	0.0000	0.0000	0.0000	0.0000	0.0000	0.0000	0.0000	0.0000	0.2944	0.6899	0.0000	0.0000	0.0000	0.0000	0.0000	0.0000	0.0000	0.0000
Mt Hobson	0.1062	0.0000	0.0000	0.0000	0.0000	0.0000	0.0000	0.0000	0.0000	0.0000	0.0000	0.0015	0.0453	0.1221	0.0791	0.0728	0.0620	0.0818	0.1136	0.1328	0.1828
Mt Mangere	0.0040	0.0000	0.0000	0.0000	0.0000	0.0000	0.0000	0.0000	0.0000	0.0000	0.0000	0.0000	0.0002	0.0086	0.0537	0.1556	0.3443	0.3017	0.1280	0.0039	0.0000
Mt Richmond	0.8135	0.0000	0.0000	0.0000	0.0000	0.0022	0.0768	0.1025	0.0003	0.0002	0.0000	0.0045	0.0000	0.0000	0.0000	0.0000	0.0000	0.0000	0.0000	0.0000	0.0000
Mt Roskill	0.9481	0.0171	0.0250	0.0014	0.0000	0.0015	0.0000	0.0000	0.0000	0.0000	0.0000	0.0067	0.0002	0.0000	0.0000	0.0000	0.0000	0.0000	0.0000	0.0000	0.0000
Mt Smart	0.0090	0.0000	0.0000	0.0000	0.0000	0.0000	0.0000	0.0000	0.0000	0.0000	0.0000	0.0000	0.0000	0.0001	0.0009	0.0064	0.0283	0.0830	0.2797	0.3755	0.2171
Mt StJohn	0.7231	0.0569	0.1120	0.0908	0.0002	0.0106	0.0000	0.0002	0.0000	0.0003	0.0000	0.0055	0.0004	0.0000	0.0000	0.0000	0.0000	0.0000	0.0000	0.0000	0.0000
Mt Victoria	0.1733	0.0717	0.0750	0.0739	0.0128	0.0053	0.0003	0.0000	0.0000	0.0026	0.0000	0.0078	0.0316	0.0935	0.1188	0.0637	0.0850	0.0186	0.0761	0.0365	0.0535
North Head	0.7314	0.1027	0.0616	0.0503	0.0064	0.0032	0.0001	0.0000	0.0000	0.0021	0.0000	0.0046	0.0094	0.0089	0.0052	0.0041	0.0030	0.0022	0.0018	0.0016	0.0014
One Tree Hill	0.6772	0.0842	0.1281	0.0977	0.0007	0.0094	0.0001	0.0002	0.0000	0.0010	0.0000	0.0014	0.0000	0.0000	0.0000	0.0000	0.0000	0.0000	0.0000	0.0000	0.0000
Otara Hill	0.0060	0.0004	0.0007	0.0095	0.0037	0.0012	0.0014	0.0000	0.0001	0.0025	0.0000	0.0083	0.0438	0.2022	0.2647	0.1723	0.1285	0.0577	0.0642	0.0250	0.0078
Otuataua	0.6868	0.0071	0.0591	0.2256	0.0205	0.0007	0.0001	0.0001	0.0000	0.0000	0.0000	0.0000	0.0000	0.0000	0.0000	0.0000	0.0000	0.0000	0.0000	0.0000	0.0000
Panmure Basin	0.1387	0.0000	0.0003	0.0006	0.0009	0.8069	0.0311	0.0180	0.0007	0.0022	0.0000	0.0006	0.0000	0.0000	0.0000	0.0000	0.0000	0.0000	0.0000	0.0000	0.0000
Pigeon Mountain	0.7762	0.0301	0.0428	0.0332	0.0003	0.0020	0.0000	0.0000	0.0000	0.0000	0.0000	0.0036	0.0018	0.0251	0.0110	0.0151	0.0089	0.0274	0.0053	0.0044	0.0128
Pukaki	0.9137	0.0863	0.0000	0.0000	0.0000	0.0000	0.0000	0.0000	0.0000	0.0000	0.0000	0.0000	0.0000	0.0000	0.0000	0.0000	0.0000	0.0000	0.0000	0.0000	0.0000
Puketutu	0.0592	0.0000	0.0000	0.0000	0.0006	0.0041	0.0514	0.0737	0.1274	0.6571	0.0000	0.0265	0.0000	0.0000	0.0000	0.0000	0.0000	0.0000	0.0000	0.0000	0.0000
Robertson Hill	0.7503	0.0000	0.0000	0.0000	0.0000	0.0000	0.0004	0.0000	0.0000	0.0000	0.0000	0.2476	0.0017	0.0000	0.0000	0.0000	0.0000	0.0000	0.0000	0.0000	0.0000
Styaks Swamp	0.4972	0.0000	0.0000	0.0000	0.0000	0.0000	0.0000	0.0000	0.0000	0.0000	0.0000	0.0002	0.0003	0.0147	0.0186	0.0366	0.0372	0.0578	0.0532	0.0609	0.2233
Taylors Hill	0.6672	0.0000	0.0000	0.0003	0.0000	0.0236	0.1965	0.0949	0.0003	0.0000	0.0000	0.0172	0.0000	0.0000	0.0000	0.0000	0.0000	0.0000	0.0000	0.0000	0.0000
Te Pouhawaiki	0.7461	0.0934	0.0729	0.0686	0.0045	0.0028	0.0003	0.0002	0.0001	0.0018	0.0000	0.0093	0.0000	0.0000	0.0000	0.0000	0.0000	0.0000	0.0000	0.0000	0.0000
Three Kings	0.0000	0.0000	0.0000	0.0000	0.0000	0.0000	0.0000	0.0000	0.0000	0.0000	1.0000	0.0000	0.0000	0.0000	0.0000	0.0000	0.0000	0.0000	0.0000	0.0000	0.0000
Wiri Mountain	0.4834	0.0000	0.0000	0.0001	0.0000	0.0022	0.3244	0.1473	0.0206	0.0190	0.0000	0.0030	0.0000	0.0000	0.0000	0.0000	0.0000	0.0000	0.0000	0.0000	0.0000

Table A.20: Marginal posterior probabilities for a volcano to have produced a given tephra for the Three Kings=AVF 10 scenario with $C = \{\alpha = 2.5, \beta U = 0.5\}$.

Volcano	AVF tephra (AVF 0 = 'unmatched')																				
	0	1	2	3	4	5	6	7	8	9	10	11	12	13	14	15	16	17	18	19	20
Ash Hill	0.9395	0.0000	0.0000	0.0000	0.0000	0.0016	0.0416	0.0173	0.0000	0.0000	0.0000	0.0000	0.0000	0.0000	0.0000	0.0000	0.0000	0.0000	0.0000	0.0000	0.0000
Cemetery Hill	0.0763	0.0000	0.0000	0.0000	0.0005	0.0187	0.2037	0.5033	0.1945	0.0014	0.0000	0.0016	0.0000	0.0000	0.0000	0.0000	0.0000	0.0000	0.0000	0.0000	0.0000
Crater Hill	0.0030	0.0000	0.0000	0.0000	0.0000	0.0002	0.0242	0.0238	0.6603	0.2869	0.0000	0.0007	0.0009	0.0000	0.0000	0.0000	0.0000	0.0000	0.0000	0.0000	0.0000
Domain	0.7569	0.1386	0.0820	0.0225	0.0000	0.0000	0.0000	0.0000	0.0000	0.0000	0.0000	0.0000	0.0000	0.0000	0.0000	0.0000	0.0000	0.0000	0.0000	0.0000	0.0000
Green Hill	0.0100	0.0008	0.0038	0.0212	0.0219	0.0128	0.0047	0.0002	0.0000	0.0130	0.0000	0.0400	0.1033	0.1682	0.1161	0.0977	0.0790	0.0874	0.1107	0.0833	0.0259
Hampton Park	0.3585	0.0000	0.0000	0.0000	0.0000	0.0000	0.0001	0.0001	0.0000	0.0000	0.0000	0.0000	0.0045	0.0863	0.1666	0.1897	0.0954	0.0725	0.0163	0.0063	0.0037
Hopua	0.6315	0.0000	0.0000	0.0010	0.0001	0.0312	0.0311	0.0191	0.0007	0.0007	0.0000	0.2846	0.0000	0.0000	0.0000	0.0000	0.0000	0.0000	0.0000	0.0000	0.0000
Kohuora	0.0039	0.0005	0.0027	0.0270	0.9018	0.0444	0.0189	0.0002	0.0005	0.0001	0.0000	0.0000	0.0000	0.0000	0.0000	0.0000	0.0000	0.0000	0.0000	0.0000	0.0000
Little Rangitoto	0.0341	0.2057	0.1906	0.1478	0.0166	0.0097	0.0009	0.0006	0.0014	0.0057	0.0000	0.0131	0.0314	0.0459	0.0331	0.0286	0.0206	0.0322	0.0510	0.0507	0.0803
Mangere Lagoon	0.7526	0.0409	0.0597	0.0505	0.0004	0.0030	0.0018	0.0000	0.0000	0.0005	0.0000	0.0070	0.0117	0.0275	0.0183	0.0157	0.0085	0.0019	0.0000	0.0000	0.0000
Matukutureia	0.0144	0.0000	0.0000	0.0000	0.0000	0.0000	0.0000	0.0000	0.0001	0.0023	0.0000	0.0081	0.0347	0.1273	0.0972	0.0838	0.0669	0.0649	0.1005	0.2150	0.1848
Maungataketake	0.9964	0.0006	0.0001	0.0007	0.0018	0.0001	0.0003	0.0000	0.0000	0.0000	0.0000	0.0000	0.0000	0.0000	0.0000	0.0000	0.0000	0.0000	0.0000	0.0000	0.0000
McLennan Hills	0.9336	0.0000	0.0183	0.0450	0.0005	0.0022	0.0002	0.0002	0.0000	0.0000	0.0000	0.0000	0.0000	0.0000	0.0000	0.0000	0.0000	0.0000	0.0000	0.0000	0.0000
Motukorea	0.9418	0.0022	0.0011	0.0001	0.0000	0.0005	0.0000	0.0000	0.0000	0.0000	0.0000	0.0006	0.0011	0.0081	0.0017	0.0037	0.0029	0.0298	0.0013	0.0019	0.0032
Mt Albert	0.8915	0.0577	0.0329	0.0168	0.0006	0.0003	0.0000	0.0001	0.0000	0.0001	0.0000	0.0000	0.0000	0.0000	0.0000	0.0000	0.0000	0.0000	0.0000	0.0000	0.0000
Mt Cambria	0.7110	0.0108	0.0280	0.0166	0.0007	0.0036	0.0000	0.0000	0.0000	0.0000	0.0000	0.0001	0.0014	0.0571	0.0157	0.0392	0.0167	0.0959	0.0014	0.0014	0.0004
Mt Eden	0.0181	0.0000	0.0000	0.0000	0.0000	0.0000	0.0000	0.0000	0.0000	0.0000	0.0000	0.3166	0.6653	0.0000	0.0000	0.0000	0.0000	0.0000	0.0000	0.0000	0.0000
Mt Hobson	0.0970	0.0000	0.0000	0.0000	0.0000	0.0000	0.0000	0.0000	0.0000	0.0000	0.0000	0.0016	0.0451	0.1259	0.0785	0.0736	0.0604	0.0863	0.1119	0.1319	0.1878
Mt Mangere	0.0049	0.0000	0.0000	0.0000	0.0000	0.0000	0.0000	0.0000	0.0000	0.0000	0.0000	0.0000	0.0002	0.0093	0.0576	0.1656	0.3591	0.2749	0.1245	0.0039	0.0000
Mt Richmond	0.8141	0.0000	0.0000	0.0000	0.0000	0.0025	0.0781	0.1002	0.0003	0.0003	0.0000	0.0045	0.0000	0.0000	0.0000	0.0000	0.0000	0.0000	0.0000	0.0000	0.0000
Mt Roskill	0.9508	0.0141	0.0248	0.0022	0.0000	0.0012	0.0002	0.0000	0.0000	0.0000	0.0000	0.0065	0.0002	0.0000	0.0000	0.0000	0.0000	0.0000	0.0000	0.0000	0.0000
Mt Smart	0.0077	0.0000	0.0000	0.0000	0.0000	0.0000	0.0000	0.0000	0.0000	0.0000	0.0000	0.0000	0.0000	0.0001	0.0010	0.0066	0.0337	0.0863	0.2822	0.3768	0.2056
Mt StJohn	0.7234	0.0565	0.1130	0.0901	0.0002	0.0102	0.0000	0.0003	0.0000	0.0003	0.0000	0.0056	0.0004	0.0000	0.0000	0.0000	0.0000	0.0000	0.0000	0.0000	0.0000
Mt Victoria	0.1701	0.0713	0.0721	0.0761	0.0163	0.0024	0.0005	0.0000	0.0000	0.0026	0.0000	0.0078	0.0369	0.0922	0.1146	0.0683	0.0853	0.0181	0.0746	0.0357	0.0551
North Head	0.7273	0.1049	0.0634	0.0498	0.0072	0.0028	0.0001	0.0000	0.0000	0.0021	0.0000	0.0046	0.0100	0.0089	0.0057	0.0034	0.0032	0.0020	0.0021	0.0015	0.0010
One Tree Hill	0.6792	0.0830	0.1244	0.1001	0.0011	0.0094	0.0001	0.0002	0.0000	0.0011	0.0000	0.0014	0.0000	0.0000	0.0000	0.0000	0.0000	0.0000	0.0000	0.0000	0.0000
Otara Hill	0.0052	0.0004	0.0009	0.0095	0.0039	0.0013	0.0011	0.0000	0.0001	0.0025	0.0000	0.0083	0.0498	0.2038	0.2642	0.1738	0.1244	0.0567	0.0624	0.0238	0.0079
Otuataua	0.6921	0.0069	0.0611	0.2183	0.0184	0.0030	0.0001	0.0001	0.0000	0.0000	0.0000	0.0000	0.0000	0.0000	0.0000	0.0000	0.0000	0.0000	0.0000	0.0000	0.0000
Panmure Basin	0.1417	0.0000	0.0003	0.0007	0.0015	0.8024	0.0317	0.0174	0.0008	0.0029	0.0000	0.0006	0.0000	0.0000	0.0000	0.0000	0.0000	0.0000	0.0000	0.0000	0.0000
Pigeon Mountain	0.7792	0.0270	0.0445	0.0327	0.0002	0.0023	0.0000	0.0000	0.0000	0.0000	0.0000	0.0034	0.0016	0.0254	0.0112	0.0144	0.0084	0.0290	0.0052	0.0036	0.0119
Pukaki	0.9185	0.0815	0.0000	0.0000	0.0000	0.0000	0.0000	0.0000	0.0000	0.0000	0.0000	0.0000	0.0000	0.0000	0.0000	0.0000	0.0000	0.0000	0.0000	0.0000	0.0000
Pukeiti	0.9994	0.0003	0.0003	0.0000	0.0000	0.0000	0.0000	0.0000	0.0000	0.0000	0.0000	0.0000	0.0000	0.0000	0.0000	0.0000	0.0000	0.0000	0.0000	0.0000	0.0000
Puketutu	0.0537	0.0000	0.0000	0.0000	0.0005	0.0045	0.0514	0.0868	0.1206	0.6564	0.0000	0.0261	0.0000	0.0000	0.0000	0.0000	0.0000	0.0000	0.0000	0.0000	0.0000
Robertson Hill	0.7711	0.0000	0.0000	0.0000	0.0000	0.0000	0.0004	0.0000	0.0000	0.0000	0.0000	0.2274	0.0011	0.0000	0.0000	0.0000	0.0000	0.0000	0.0000	0.0000	0.0000
Styaks Swamp	0.4810	0.0000	0.0000	0.0000	0.0000	0.0001	0.0000	0.0000	0.0000	0.0000	0.0000	0.0002	0.0002	0.0140	0.0185	0.0359	0.0355	0.0621	0.0559	0.0642	0.2324
Taylors Hill	0.6848	0.0000	0.0000	0.0003	0.0000	0.0244	0.1769	0.0964	0.0003	0.0000	0.0000	0.0169	0.0000	0.0000	0.0000	0.0000	0.0000	0.0000	0.0000	0.0000	0.0000
Te Pouhawaiki	0.7351	0.0963	0.0760	0.0709	0.0058	0.0032	0.0006	0.0002	0.0001	0.0019	0.0000	0.0097	0.0002	0.0000	0.0000	0.0000	0.0000	0.0000	0.0000	0.0000	0.0000
Three Kings	0.0000	0.0000	0.0000	0.0000	0.0000	0.0000	0.0000	0.0000	0.0000	0.0000	1.0000	0.0000	0.0000	0.0000	0.0000	0.0000	0.0000	0.0000	0.0000	0.0000	0.0000
Wiri Mountain	0.4906	0.0000	0.0000	0.0001	0.0000	0.0020	0.3313	0.1335	0.0203	0.0192	0.0000	0.0030	0.0000	0.0000	0.0000	0.0000	0.0000	0.0000	0.0000	0.0000	0.0000

Table A.21: Marginal posterior probabilities for a volcano to have produced a given tephra for the Three Kings=AVF 10 scenario with D = $\{\alpha = 1.5,\ \beta U = 1.0\}$.

Volcano	AVF tephra (AVF 0 = 'unmatched')																				
	0	1	2	3	4	5	6	7	8	9	10	11	12	13	14	15	16	17	18	19	20
Ash Hill	0.9256	0.0000	0.0000	0.0000	0.0001	0.0008	0.0511	0.0224	0.0000	0.0000	0.0000	0.0000	0.0000	0.0000	0.0000	0.0000	0.0000	0.0000	0.0000	0.0000	0.0000
Cemetery Hill	0.0010	0.0000	0.0000	0.0000	0.0029	0.0246	0.2078	0.3431	0.3492	0.0685	0.0000	0.0029	0.0000	0.0000	0.0000	0.0000	0.0000	0.0000	0.0000	0.0000	0.0000
Crater Hill	0.2340	0.0000	0.0000	0.0000	0.0000	0.0006	0.0188	0.0193	0.5136	0.2119	0.0000	0.0010	0.0008	0.0000	0.0000	0.0000	0.0000	0.0000	0.0000	0.0000	0.0000
Domain	0.7795	0.1136	0.0879	0.0190	0.0000	0.0000	0.0000	0.0000	0.0000	0.0000	0.0000	0.0000	0.0000	0.0000	0.0000	0.0000	0.0000	0.0000	0.0000	0.0000	0.0000
Green Hill	0.0026	0.0013	0.0040	0.0200	0.0247	0.0129	0.0055	0.0002	0.0002	0.0129	0.0000	0.0305	0.1461	0.1570	0.1130	0.0992	0.0831	0.0963	0.1049	0.0697	0.0159
Hampton Park	0.4046	0.0000	0.0000	0.0000	0.0000	0.0000	0.0000	0.0001	0.0000	0.0000	0.0000	0.0000	0.0045	0.1006	0.1588	0.1576	0.0845	0.0631	0.0167	0.0057	0.0038
Hopua	0.5829	0.0000	0.0001	0.0015	0.0003	0.0291	0.0524	0.0449	0.0003	0.0004	0.0000	0.2881	0.0000	0.0000	0.0000	0.0000	0.0000	0.0000	0.0000	0.0000	0.0000
Kohuora	0.0003	0.0004	0.0043	0.0291	0.8520	0.0912	0.0214	0.0006	0.0006	0.0001	0.0000	0.0000	0.0000	0.0000	0.0000	0.0000	0.0000	0.0000	0.0000	0.0000	0.0000
Little Rangitoto	0.0154	0.2358	0.1675	0.1366	0.0181	0.0102	0.0018	0.0003	0.0016	0.0059	0.0000	0.0103	0.0441	0.0412	0.0345	0.0287	0.0220	0.0342	0.0526	0.0523	0.0869
Mangere Lagoon	0.7290	0.0399	0.0722	0.0514	0.0005	0.0096	0.0020	0.0000	0.0000	0.0006	0.0000	0.0091	0.0199	0.0260	0.0177	0.0143	0.0065	0.0013	0.0000	0.0000	0.0000
Matukutureia	0.0057	0.0000	0.0000	0.0000	0.0000	0.0000	0.0000	0.0000	0.0001	0.0023	0.0000	0.0064	0.0631	0.1181	0.0950	0.0842	0.0654	0.0732	0.1152	0.2214	0.1499
Maungataketake	0.9968	0.0003	0.0001	0.0018	0.0004	0.0001	0.0005	0.0000	0.0000	0.0000	0.0000	0.0000	0.0000	0.0000	0.0000	0.0000	0.0000	0.0000	0.0000	0.0000	0.0000
McLennan Hills	0.9134	0.0000	0.0291	0.0539	0.0003	0.0024	0.0006	0.0003	0.0000	0.0000	0.0000	0.0000	0.0000	0.0000	0.0000	0.0000	0.0000	0.0000	0.0000	0.0000	0.0000
Motukorea	0.9501	0.0017	0.0005	0.0001	0.0000	0.0002	0.0000	0.0000	0.0000	0.0000	0.0000	0.0004	0.0011	0.0047	0.0011	0.0015	0.0017	0.0306	0.0013	0.0019	0.0031
Mt Albert	0.8927	0.0530	0.0365	0.0167	0.0005	0.0004	0.0001	0.0000	0.0000	0.0001	0.0000	0.0000	0.0000	0.0000	0.0000	0.0000	0.0000	0.0000	0.0000	0.0000	0.0000
Mt Cambria	0.7548	0.0053	0.0118	0.0092	0.0004	0.0010	0.0000	0.0000	0.0000	0.0000	0.0000	0.0000	0.0009	0.0588	0.0138	0.0277	0.0089	0.1041	0.0014	0.0015	0.0004
Mt Eden	0.0510	0.0000	0.0000	0.0000	0.0000	0.0000	0.0000	0.0000	0.0000	0.0000	0.0000	0.4587	0.4903	0.0000	0.0000	0.0000	0.0000	0.0000	0.0000	0.0000	0.0000
Mt Hobson	0.0419	0.0000	0.0000	0.0000	0.0000	0.0000	0.0000	0.0000	0.0000	0.0000	0.0000	0.0033	0.0616	0.1234	0.0791	0.0728	0.0663	0.0917	0.1190	0.1308	0.2101
Mt Mangere	0.0106	0.0000	0.0000	0.0000	0.0000	0.0000	0.0000	0.0000	0.0000	0.0000	0.0000	0.0000	0.0001	0.0153	0.0704	0.2183	0.3775	0.2203	0.0841	0.0034	0.0000
Mt Richmond	0.8673	0.0000	0.0000	0.0000	0.0000	0.0013	0.0446	0.0828	0.0001	0.0002	0.0000	0.0037	0.0000	0.0000	0.0000	0.0000	0.0000	0.0000	0.0000	0.0000	0.0000
Mt Roskill	0.9806	0.0095	0.0028	0.0011	0.0001	0.0007	0.0001	0.0000	0.0000	0.0000	0.0000	0.0050	0.0001	0.0000	0.0000	0.0000	0.0000	0.0000	0.0000	0.0000	0.0000
Mt Smart	0.0022	0.0000	0.0000	0.0000	0.0000	0.0000	0.0000	0.0000	0.0000	0.0000	0.0000	0.0000	0.0001	0.0000	0.0018	0.0092	0.0518	0.1200	0.2905	0.3528	0.1716
Mt StJohn	0.7414	0.0355	0.1207	0.0836	0.0002	0.0110	0.0002	0.0002	0.0000	0.0004	0.0000	0.0064	0.0004	0.0000	0.0000	0.0000	0.0000	0.0000	0.0000	0.0000	0.0000
Mt Victoria	0.1574	0.0863	0.0769	0.0576	0.0117	0.0056	0.0011	0.0000	0.0000	0.0026	0.0000	0.0062	0.0577	0.0931	0.1184	0.0669	0.0793	0.0087	0.0744	0.0395	0.0566
North Head	0.7277	0.1133	0.0614	0.0426	0.0061	0.0035	0.0005	0.0000	0.0000	0.0021	0.0000	0.0042	0.0128	0.0078	0.0061	0.0031	0.0024	0.0022	0.0022	0.0015	0.0005
One Tree Hill	0.7085	0.0573	0.1303	0.0910	0.0003	0.0105	0.0000	0.0003	0.0000	0.0004	0.0000	0.0014	0.0000	0.0000	0.0000	0.0000	0.0000	0.0000	0.0000	0.0000	0.0000
Otara Hill	0.0006	0.0005	0.0012	0.0091	0.0060	0.0028	0.0014	0.0000	0.0001	0.0025	0.0000	0.0061	0.0920	0.2095	0.2588	0.1700	0.1046	0.0554	0.0522	0.0213	0.0059
Otuataua	0.5506	0.0100	0.0877	0.2838	0.0657	0.0019	0.0001	0.0002	0.0000	0.0000	0.0000	0.0000	0.0000	0.0000	0.0000	0.0000	0.0000	0.0000	0.0000	0.0000	0.0000
Panmure Basin	0.2423	0.0000	0.0002	0.0016	0.0016	0.7365	0.0038	0.0125	0.0008	0.0003	0.0000	0.0004	0.0000	0.0000	0.0000	0.0000	0.0000	0.0000	0.0000	0.0000	0.0000
Pigeon Mountain	0.8135	0.0213	0.0279	0.0245	0.0000	0.0020	0.0000	0.0000	0.0000	0.0000	0.0000	0.0028	0.0012	0.0262	0.0090	0.0123	0.0066	0.0300	0.0053	0.0038	0.0136
Pukaki	0.9079	0.0921	0.0000	0.0000	0.0000	0.0000	0.0000	0.0000	0.0000	0.0000	0.0000	0.0000	0.0000	0.0000	0.0000	0.0000	0.0000	0.0000	0.0000	0.0000	0.0000
Pukeiti	0.9999	0.0001	0.0000	0.0000	0.0000	0.0000	0.0000	0.0000	0.0000	0.0000	0.0000	0.0000	0.0000	0.0000	0.0000	0.0000	0.0000	0.0000	0.0000	0.0000	0.0000
Puketutu	0.0593	0.0000	0.0000	0.0000	0.0012	0.0165	0.0241	0.0775	0.1176	0.6784	0.0000	0.0236	0.0018	0.0000	0.0000	0.0000	0.0000	0.0000	0.0000	0.0000	0.0000
Robertson Hill	0.8972	0.0000	0.0000	0.0000	0.0000	0.0000	0.0003	0.0000	0.0000	0.0000	0.0000	0.1019	0.0006	0.0000	0.0000	0.0000	0.0000	0.0000	0.0000	0.0000	0.0000
Styaks Swamp	0.3601	0.0000	0.0000	0.0000	0.0000	0.0000	0.0000	0.0000	0.0000	0.0000	0.0000	0.0002	0.0001	0.0183	0.0225	0.0342	0.0394	0.0689	0.0802	0.0944	0.2817
Taylors Hill	0.4585	0.0000	0.0000	0.0004	0.0000	0.0151	0.3819	0.1301	0.0003	0.0001	0.0000	0.0136	0.0000	0.0000	0.0000	0.0000	0.0000	0.0000	0.0000	0.0000	0.0000
Te Pouhawaiki	0.7082	0.1225	0.0769	0.0653	0.0069	0.0069	0.0009	0.0004	0.0001	0.0021	0.0000	0.0091	0.0007	0.0000	0.0000	0.0000	0.0000	0.0000	0.0000	0.0000	0.0000
Three Kings	0.0000	0.0000	0.0000	0.0000	0.0000	0.0000	0.0000	0.0000	0.0000	0.0000	1.0000	0.0000	0.0000	0.0000	0.0000	0.0000	0.0000	0.0000	0.0000	0.0000	0.0000
Waitomokia	0.9997	0.0003	0.0000	0.0000	0.0000	0.0000	0.0000	0.0000	0.0000	0.0000	0.0000	0.0000	0.0000	0.0000	0.0000	0.0000	0.0000	0.0000	0.0000	0.0000	0.0000
Wiri Mountain	0.5252	0.0000	0.0000	0.0001	0.0000	0.0026	0.1790	0.2648	0.0154	0.0082	0.0000	0.0047	0.0000	0.0000	0.0000	0.0000	0.0000	0.0000	0.0000	0.0000	0.0000

Table A.22: Marginal posterior probabilities for a volcano to have produced a given tephra for the Three Kings=AVF 10 scenario with $E = \{\alpha = 2.0, \beta U = 1.0\}$.

Volcano	AVF tephra (AVF 0 = 'unmatched')																				
	0	1	2	3	4	5	6	7	8	9	10	11	12	13	14	15	16	17	18	19	20
Ash Hill	0.9166	0.0000	0.0000	0.0000	0.0000	0.0011	0.0596	0.0227	0.0000	0.0000	0.0000	0.0000	0.0000	0.0000	0.0000	0.0000	0.0000	0.0000	0.0000	0.0000	0.0000
Cemetery Hill	0.0009	0.0000	0.0000	0.0000	0.0028	0.0254	0.2014	0.2923	0.3989	0.0754	0.0000	0.0029	0.0000	0.0000	0.0000	0.0000	0.0000	0.0000	0.0000	0.0000	0.0000
Crater Hill	0.2966	0.0000	0.0000	0.0000	0.0000	0.0006	0.0190	0.0201	0.4563	0.2056	0.0000	0.0010	0.0008	0.0000	0.0000	0.0000	0.0000	0.0000	0.0000	0.0000	0.0000
Domain	0.7781	0.1143	0.0885	0.0191	0.0000	0.0000	0.0000	0.0000	0.0000	0.0000	0.0000	0.0000	0.0000	0.0000	0.0000	0.0000	0.0000	0.0000	0.0000	0.0000	0.0000
Green Hill	0.0025	0.0013	0.0040	0.0197	0.0246	0.0134	0.0054	0.0003	0.0002	0.0129	0.0000	0.0305	0.1500	0.1545	0.1138	0.0991	0.0841	0.0958	0.1042	0.0684	0.0153
Hampton Park	0.4089	0.0000	0.0000	0.0000	0.0000	0.0000	0.0000	0.0001	0.0000	0.0000	0.0000	0.0000	0.0044	0.1028	0.1562	0.1552	0.0825	0.0640	0.0164	0.0057	0.0038
Hopua	0.5842	0.0000	0.0001	0.0013	0.0001	0.0343	0.0504	0.0448	0.0003	0.0004	0.0000	0.2841	0.0000	0.0000	0.0000	0.0000	0.0000	0.0000	0.0000	0.0000	0.0000
Kohuora	0.0000	0.0004	0.0045	0.0288	0.8539	0.0872	0.0236	0.0008	0.0007	0.0001	0.0000	0.0000	0.0000	0.0000	0.0000	0.0000	0.0000	0.0000	0.0000	0.0000	0.0000
Little Rangitoto	0.0116	0.2338	0.1739	0.1322	0.0204	0.0097	0.0014	0.0008	0.0020	0.0055	0.0000	0.0103	0.0458	0.0404	0.0348	0.0280	0.0224	0.0350	0.0522	0.0524	0.0874
Mangere Lagoon	0.7369	0.0361	0.0692	0.0508	0.0003	0.0093	0.0019	0.0001	0.0000	0.0006	0.0000	0.0093	0.0199	0.0261	0.0177	0.0141	0.0064	0.0013	0.0000	0.0000	0.0000
Matukutureia	0.0043	0.0000	0.0000	0.0000	0.0000	0.0000	0.0000	0.0000	0.0001	0.0023	0.0000	0.0062	0.0666	0.1163	0.0951	0.0848	0.0644	0.0727	0.1179	0.2204	0.1489
Maungataketake	0.9973	0.0003	0.0000	0.0017	0.0000	0.0001	0.0006	0.0000	0.0000	0.0000	0.0000	0.0000	0.0000	0.0000	0.0000	0.0000	0.0000	0.0000	0.0000	0.0000	0.0000
McLennan Hills	0.9121	0.0000	0.0293	0.0545	0.0001	0.0029	0.0008	0.0003	0.0000	0.0000	0.0000	0.0000	0.0000	0.0000	0.0000	0.0000	0.0000	0.0000	0.0000	0.0000	0.0000
Motukorea	0.9492	0.0018	0.0005	0.0000	0.0000	0.0002	0.0000	0.0000	0.0000	0.0000	0.0000	0.0004	0.0011	0.0047	0.0011	0.0017	0.0017	0.0308	0.0014	0.0019	0.0035
Mt Albert	0.8948	0.0520	0.0352	0.0169	0.0005	0.0004	0.0001	0.0000	0.0000	0.0001	0.0000	0.0000	0.0000	0.0000	0.0000	0.0000	0.0000	0.0000	0.0000	0.0000	0.0000
Mt Cambria	0.7405	0.0070	0.0144	0.0155	0.0006	0.0026	0.0000	0.0000	0.0000	0.0000	0.0000	0.0000	0.0009	0.0591	0.0147	0.0273	0.0091	0.1050	0.0014	0.0015	0.0004
Mt Eden	0.0528	0.0000	0.0000	0.0000	0.0000	0.0000	0.0000	0.0000	0.0000	0.0000	0.0000	0.4724	0.4748	0.0000	0.0000	0.0000	0.0000	0.0000	0.0000	0.0000	0.0000
Mt Hobson	0.0407	0.0000	0.0000	0.0000	0.0000	0.0000	0.0000	0.0000	0.0000	0.0000	0.0000	0.0038	0.0614	0.1251	0.0778	0.0727	0.0658	0.0939	0.1180	0.1302	0.2106
Mt Mangere	0.0106	0.0000	0.0000	0.0000	0.0000	0.0000	0.0000	0.0000	0.0000	0.0000	0.0000	0.0000	0.0001	0.0162	0.0724	0.2228	0.3773	0.2136	0.0837	0.0033	0.0000
Mt Richmond	0.8289	0.0000	0.0000	0.0000	0.0000	0.0014	0.0593	0.1067	0.0001	0.0002	0.0000	0.0034	0.0000	0.0000	0.0000	0.0000	0.0000	0.0000	0.0000	0.0000	0.0000
Mt Roskill	0.9816	0.0095	0.0026	0.0006	0.0001	0.0007	0.0001	0.0000	0.0000	0.0000	0.0000	0.0047	0.0001	0.0000	0.0000	0.0000	0.0000	0.0000	0.0000	0.0000	0.0000
Mt Smart	0.0015	0.0000	0.0000	0.0000	0.0000	0.0000	0.0000	0.0000	0.0000	0.0000	0.0000	0.0000	0.0001	0.0000	0.0018	0.0103	0.0540	0.1208	0.2905	0.3515	0.1695
Mt StJohn	0.7445	0.0377	0.1161	0.0832	0.0001	0.0109	0.0001	0.0002	0.0000	0.0004	0.0000	0.0064	0.0004	0.0000	0.0000	0.0000	0.0000	0.0000	0.0000	0.0000	0.0000
Mt Victoria	0.1533	0.0874	0.0766	0.0584	0.0132	0.0052	0.0013	0.0000	0.0000	0.0026	0.0000	0.0061	0.0595	0.0934	0.1178	0.0660	0.0795	0.0087	0.0740	0.0397	0.0573
North Head	0.7218	0.1164	0.0616	0.0443	0.0074	0.0033	0.0003	0.0000	0.0000	0.0021	0.0000	0.0042	0.0130	0.0076	0.0061	0.0034	0.0021	0.0022	0.0023	0.0014	0.0005
One Tree Hill	0.7088	0.0584	0.1282	0.0915	0.0002	0.0105	0.0003	0.0003	0.0000	0.0004	0.0000	0.0014	0.0000	0.0000	0.0000	0.0000	0.0000	0.0000	0.0000	0.0000	0.0000
Otara Hill	0.0004	0.0005	0.0014	0.0084	0.0065	0.0029	0.0014	0.0000	0.0001	0.0025	0.0000	0.0061	0.0966	0.2084	0.2593	0.1681	0.1048	0.0539	0.0516	0.0211	0.0060
Otuataua	0.5701	0.0098	0.0853	0.2757	0.0565	0.0022	0.0001	0.0003	0.0000	0.0000	0.0000	0.0000	0.0000	0.0000	0.0000	0.0000	0.0000	0.0000	0.0000	0.0000	0.0000
Panmure Basin	0.2451	0.0000	0.0002	0.0017	0.0011	0.7339	0.0036	0.0129	0.0008	0.0003	0.0000	0.0004	0.0000	0.0000	0.0000	0.0000	0.0000	0.0000	0.0000	0.0000	0.0000
Pigeon Mountain	0.8067	0.0205	0.0289	0.0283	0.0000	0.0026	0.0000	0.0000	0.0000	0.0000	0.0000	0.0027	0.0012	0.0270	0.0091	0.0121	0.0066	0.0304	0.0054	0.0043	0.0142
Pukaki	0.9109	0.0891	0.0000	0.0000	0.0000	0.0000	0.0000	0.0000	0.0000	0.0000	0.0000	0.0000	0.0000	0.0000	0.0000	0.0000	0.0000	0.0000	0.0000	0.0000	0.0000
Puketutu	0.0542	0.0000	0.0000	0.0000	0.0012	0.0153	0.0233	0.0773	0.1243	0.6790	0.0000	0.0236	0.0018	0.0000	0.0000	0.0000	0.0000	0.0000	0.0000	0.0000	0.0000
Robertson Hill	0.9062	0.0000	0.0000	0.0000	0.0000	0.0000	0.0003	0.0000	0.0000	0.0000	0.0000	0.0929	0.0006	0.0000	0.0000	0.0000	0.0000	0.0000	0.0000	0.0000	0.0000
Styaks Swamp	0.3516	0.0000	0.0000	0.0000	0.0000	0.0000	0.0000	0.0000	0.0000	0.0000	0.0000	0.0002	0.0001	0.0184	0.0223	0.0344	0.0393	0.0719	0.0810	0.0982	0.2826
Taylors Hill	0.4778	0.0000	0.0000	0.0004	0.0000	0.0148	0.3766	0.1166	0.0003	0.0001	0.0000	0.0134	0.0000	0.0000	0.0000	0.0000	0.0000	0.0000	0.0000	0.0000	0.0000
Te Pouhawaiki	0.6996	0.1237	0.0795	0.0669	0.0104	0.0066	0.0008	0.0004	0.0001	0.0021	0.0000	0.0091	0.0008	0.0000	0.0000	0.0000	0.0000	0.0000	0.0000	0.0000	0.0000
Three Kings	0.0000	0.0000	0.0000	0.0000	0.0000	0.0000	0.0000	0.0000	0.0000	0.0000	1.0000	0.0000	0.0000	0.0000	0.0000	0.0000	0.0000	0.0000	0.0000	0.0000	0.0000
Wiri Mountain	0.4984	0.0000	0.0000	0.0001	0.0000	0.0025	0.1683	0.3030	0.0158	0.0074	0.0000	0.0045	0.0000	0.0000	0.0000	0.0000	0.0000	0.0000	0.0000	0.0000	0.0000

Table A.23: Marginal posterior probabilities for a volcano to have produced a given tephra for the Three Kings=AVF 10 scenario with F $= \{\alpha = 2.5,\ \beta U = 1.0\}$.

Volcano	AVF tephra (AVF 0 = 'unmatched')																				
	0	1	2	3	4	5	6	7	8	9	10	11	12	13	14	15	16	17	18	19	20
Ash Hill	0.9108	0.0000	0.0000	0.0000	0.0000	0.0013	0.0652	0.0227	0.0000	0.0000	0.0000	0.0000	0.0000	0.0000	0.0000	0.0000	0.0000	0.0000	0.0000	0.0000	0.0000
Cemetery Hill	0.0004	0.0000	0.0000	0.0000	0.0028	0.0255	0.1975	0.2876	0.4057	0.0776	0.0000	0.0029	0.0000	0.0000	0.0000	0.0000	0.0000	0.0000	0.0000	0.0000	0.0000
Crater Hill	0.3076	0.0000	0.0000	0.0000	0.0000	0.0006	0.0154	0.0240	0.4465	0.2041	0.0000	0.0010	0.0008	0.0000	0.0000	0.0000	0.0000	0.0000	0.0000	0.0000	0.0000
Domain	0.7789	0.1128	0.0895	0.0188	0.0000	0.0000	0.0000	0.0000	0.0000	0.0000	0.0000	0.0000	0.0000	0.0000	0.0000	0.0000	0.0000	0.0000	0.0000	0.0000	0.0000
Green Hill	0.0025	0.0014	0.0038	0.0187	0.0261	0.0127	0.0054	0.0004	0.0002	0.0129	0.0000	0.0305	0.1511	0.1537	0.1134	0.1002	0.0848	0.0953	0.1041	0.0683	0.0145
Hampton Park	0.4134	0.0000	0.0000	0.0000	0.0000	0.0000	0.0000	0.0001	0.0000	0.0000	0.0000	0.0000	0.0044	0.1028	0.1560	0.1519	0.0807	0.0645	0.0165	0.0059	0.0038
Hopua	0.5883	0.0000	0.0001	0.0013	0.0001	0.0323	0.0512	0.0443	0.0003	0.0005	0.0000	0.2816	0.0000	0.0000	0.0000	0.0000	0.0000	0.0000	0.0000	0.0000	0.0000
Kohuora	0.0000	0.0005	0.0045	0.0292	0.8531	0.0868	0.0232	0.0012	0.0014	0.0001	0.0000	0.0000	0.0000	0.0000	0.0000	0.0000	0.0000	0.0000	0.0000	0.0000	0.0000
Little Rangitoto	0.0089	0.2339	0.1762	0.1292	0.0233	0.0085	0.0014	0.0009	0.0021	0.0054	0.0000	0.0103	0.0465	0.0396	0.0351	0.0275	0.0230	0.0354	0.0516	0.0531	0.0881
Mangere Lagoon	0.7403	0.0345	0.0677	0.0505	0.0002	0.0093	0.0020	0.0001	0.0000	0.0006	0.0000	0.0094	0.0196	0.0266	0.0175	0.0140	0.0064	0.0013	0.0000	0.0000	0.0000
Matukutureia	0.0041	0.0000	0.0000	0.0000	0.0000	0.0000	0.0000	0.0000	0.0001	0.0023	0.0000	0.0062	0.0670	0.1160	0.0953	0.0854	0.0637	0.0733	0.1193	0.2196	0.1477
Maungataketake	0.9964	0.0001	0.0001	0.0019	0.0002	0.0001	0.0012	0.0000	0.0000	0.0000	0.0000	0.0000	0.0000	0.0000	0.0000	0.0000	0.0000	0.0000	0.0000	0.0000	0.0000
McLennan Hills	0.9098	0.0000	0.0301	0.0551	0.0001	0.0029	0.0013	0.0007	0.0000	0.0000	0.0000	0.0000	0.0000	0.0000	0.0000	0.0000	0.0000	0.0000	0.0000	0.0000	0.0000
Motukorea	0.9490	0.0019	0.0004	0.0001	0.0000	0.0002	0.0000	0.0000	0.0000	0.0000	0.0000	0.0004	0.0011	0.0049	0.0011	0.0016	0.0017	0.0305	0.0014	0.0020	0.0037
Mt Albert	0.8984	0.0519	0.0323	0.0164	0.0004	0.0004	0.0001	0.0000	0.0000	0.0001	0.0000	0.0000	0.0000	0.0000	0.0000	0.0000	0.0000	0.0000	0.0000	0.0000	0.0000
Mt Cambria	0.7207	0.0073	0.0266	0.0186	0.0006	0.0044	0.0000	0.0000	0.0000	0.0000	0.0000	0.0000	0.0010	0.0595	0.0159	0.0269	0.0094	0.1057	0.0013	0.0016	0.0005
Mt Eden	0.0540	0.0000	0.0000	0.0000	0.0000	0.0000	0.0000	0.0000	0.0000	0.0000	0.0000	0.4758	0.4702	0.0000	0.0000	0.0000	0.0000	0.0000	0.0000	0.0000	0.0000
Mt Hobson	0.0406	0.0000	0.0000	0.0000	0.0000	0.0000	0.0000	0.0000	0.0000	0.0000	0.0000	0.0038	0.0604	0.1273	0.0764	0.0725	0.0665	0.0949	0.1168	0.1304	0.2104
Mt Mangere	0.0111	0.0000	0.0000	0.0000	0.0000	0.0000	0.0000	0.0000	0.0000	0.0000	0.0000	0.0000	0.0001	0.0162	0.0730	0.2266	0.3757	0.2095	0.0845	0.0033	0.0000
Mt Richmond	0.8212	0.0000	0.0000	0.0000	0.0000	0.0013	0.0600	0.1139	0.0001	0.0002	0.0000	0.0033	0.0000	0.0000	0.0000	0.0000	0.0000	0.0000	0.0000	0.0000	0.0000
Mt Roskill	0.9821	0.0095	0.0021	0.0007	0.0001	0.0010	0.0001	0.0000	0.0000	0.0000	0.0000	0.0043	0.0001	0.0000	0.0000	0.0000	0.0000	0.0000	0.0000	0.0000	0.0000
Mt Smart	0.0011	0.0000	0.0000	0.0000	0.0000	0.0000	0.0000	0.0000	0.0000	0.0000	0.0000	0.0000	0.0001	0.0000	0.0019	0.0106	0.0551	0.1210	0.2913	0.3504	0.1685
Mt StJohn	0.7429	0.0394	0.1148	0.0843	0.0002	0.0109	0.0001	0.0002	0.0000	0.0004	0.0000	0.0064	0.0004	0.0000	0.0000	0.0000	0.0000	0.0000	0.0000	0.0000	0.0000
Mt Victoria	0.1514	0.0896	0.0688	0.0644	0.0143	0.0047	0.0013	0.0001	0.0000	0.0026	0.0000	0.0061	0.0604	0.0927	0.1175	0.0670	0.0795	0.0083	0.0737	0.0402	0.0574
North Head	0.7197	0.1194	0.0604	0.0442	0.0082	0.0031	0.0002	0.0000	0.0000	0.0021	0.0000	0.0042	0.0129	0.0081	0.0057	0.0037	0.0021	0.0020	0.0022	0.0014	0.0004
One Tree Hill	0.7061	0.0618	0.1268	0.0921	0.0001	0.0107	0.0004	0.0002	0.0000	0.0004	0.0000	0.0014	0.0000	0.0000	0.0000	0.0000	0.0000	0.0000	0.0000	0.0000	0.0000
Otara Hill	0.0006	0.0005	0.0010	0.0085	0.0065	0.0030	0.0014	0.0000	0.0001	0.0025	0.0000	0.0060	0.0988	0.2073	0.2597	0.1669	0.1048	0.0542	0.0512	0.0211	0.0059
Otuataua	0.5863	0.0095	0.0852	0.2648	0.0505	0.0031	0.0001	0.0005	0.0000	0.0000	0.0000	0.0000	0.0000	0.0000	0.0000	0.0000	0.0000	0.0000	0.0000	0.0000	0.0000
Panmure Basin	0.2297	0.0000	0.0003	0.0016	0.0010	0.7484	0.0045	0.0130	0.0008	0.0003	0.0000	0.0004	0.0000	0.0000	0.0000	0.0000	0.0000	0.0000	0.0000	0.0000	0.0000
Pigeon Mountain	0.8029	0.0203	0.0315	0.0306	0.0000	0.0025	0.0000	0.0000	0.0000	0.0000	0.0000	0.0026	0.0013	0.0270	0.0091	0.0116	0.0070	0.0300	0.0051	0.0041	0.0144
Pukaki	0.9221	0.0779	0.0000	0.0000	0.0000	0.0000	0.0000	0.0000	0.0000	0.0000	0.0000	0.0000	0.0000	0.0000	0.0000	0.0000	0.0000	0.0000	0.0000	0.0000	0.0000
Puketutu	0.0645	0.0000	0.0000	0.0000	0.0010	0.0030	0.0231	0.0781	0.1264	0.6785	0.0000	0.0236	0.0018	0.0000	0.0000	0.0000	0.0000	0.0000	0.0000	0.0000	0.0000
Robertson Hill	0.9058	0.0000	0.0000	0.0000	0.0000	0.0000	0.0004	0.0000	0.0000	0.0000	0.0000	0.0932	0.0006	0.0000	0.0000	0.0000	0.0000	0.0000	0.0000	0.0000	0.0000
Styaks Swamp	0.3474	0.0000	0.0000	0.0000	0.0000	0.0000	0.0000	0.0000	0.0000	0.0000	0.0000	0.0002	0.0001	0.0183	0.0224	0.0336	0.0396	0.0741	0.0810	0.0986	0.2847
Taylors Hill	0.4880	0.0000	0.0000	0.0003	0.0000	0.0150	0.3653	0.1177	0.0003	0.0002	0.0000	0.0132	0.0000	0.0000	0.0000	0.0000	0.0000	0.0000	0.0000	0.0000	0.0000
Te Pouhawaiki	0.6950	0.1278	0.0778	0.0685	0.0112	0.0060	0.0012	0.0004	0.0001	0.0021	0.0000	0.0086	0.0013	0.0000	0.0000	0.0000	0.0000	0.0000	0.0000	0.0000	0.0000
Three Kings	0.0000	0.0000	0.0000	0.0000	0.0000	0.0000	0.0000	0.0000	0.0000	0.0000	1.0000	0.0000	0.0000	0.0000	0.0000	0.0000	0.0000	0.0000	0.0000	0.0000	0.0000
Wiri Mountain	0.4980	0.0000	0.0000	0.0002	0.0000	0.0023	0.1780	0.2939	0.0159	0.0071	0.0000	0.0046	0.0000	0.0000	0.0000	0.0000	0.0000	0.0000	0.0000	0.0000	0.0000

Table A.24: Marginal posterior probabilities for a volcano to have produced a given tephra for the AVF 9A/9B scenario with A $= \{\alpha = 1.5, \beta U = 0.5\}$.

Volcano	AVF tephra (AVF 0 = 'unmatched')																					
	0	1	2	3	4	5	6	7	8	9A	9B	10	11	12	13	14	15	16	17	18	19	20
Ash Hill	0.8921	0.0000	0.0000	0.0000	0.0000	0.0001	0.0813	0.0265	0.0000	0.0000	0.0000	0.0000	0.0000	0.0000	0.0000	0.0000	0.0000	0.0000	0.0000	0.0000	0.0000	0.0000
Cemetery Hill	0.0205	0.0000	0.0000	0.0000	0.0001	0.0191	0.1685	0.2842	0.3214	0.1465	0.0397	0.0000	0.0000	0.0000	0.0000	0.0000	0.0000	0.0000	0.0000	0.0000	0.0000	0.0000
Crater Hill	0.0000	0.0000	0.0000	0.0000	0.0000	0.0001	0.0171	0.0124	0.4475	0.2829	0.1869	0.0529	0.0002	0.0000	0.0000	0.0000	0.0000	0.0000	0.0000	0.0000	0.0000	0.0000
Domain	0.7613	0.1285	0.0912	0.0190	0.0000	0.0000	0.0000	0.0000	0.0000	0.0000	0.0000	0.0000	0.0000	0.0000	0.0000	0.0000	0.0000	0.0000	0.0000	0.0000	0.0000	0.0000
Green Hill	0.0409	0.0007	0.0035	0.0199	0.0214	0.0157	0.0052	0.0002	0.0011	0.0006	0.0034	0.0439	0.0106	0.0542	0.1914	0.1237	0.1002	0.0770	0.0843	0.1104	0.0917	0.0311
Hampton Park	0.3761	0.0000	0.0000	0.0000	0.0000	0.0000	0.0000	0.0003	0.0000	0.0000	0.0000	0.0000	0.0000	0.0000	0.0654	0.1527	0.2031	0.1096	0.0694	0.0161	0.0073	0.0038
Hopua	0.4632	0.0000	0.0000	0.0005	0.0000	0.0648	0.0491	0.0391	0.0014	0.0291	0.0516	0.2970	0.0042	0.0000	0.0000	0.0000	0.0000	0.0000	0.0000	0.0000	0.0000	0.0000
Kohuora	0.0000	0.0001	0.0017	0.0174	0.8995	0.0498	0.0289	0.0003	0.0023	0.0000	0.0000	0.0000	0.0000	0.0000	0.0000	0.0000	0.0000	0.0000	0.0000	0.0000	0.0000	0.0000
Little Rangitoto	0.1262	0.1975	0.1909	0.1472	0.0167	0.0113	0.0010	0.0006	0.0018	0.0011	0.0020	0.0154	0.0026	0.0178	0.0491	0.0381	0.0290	0.0210	0.0302	0.0484	0.0521	0.0705
Mangere Lagoon	0.7192	0.0495	0.0636	0.0627	0.0006	0.0057	0.0021	0.0002	0.0000	0.0000	0.0023	0.0083	0.0019	0.0087	0.0252	0.0211	0.0158	0.0103	0.0028	0.0000	0.0000	0.0000
Matukutureia	0.2270	0.0000	0.0000	0.0000	0.0000	0.0000	0.0000	0.0000	0.0000	0.0000	0.0008	0.0088	0.0020	0.0086	0.1384	0.0989	0.0849	0.0686	0.0648	0.0930	0.2042	0.2046
Maungataketake	0.9958	0.0010	0.0000	0.0013	0.0000	0.0000	0.0019	0.0000	0.0000	0.0000	0.0000	0.0000	0.0000	0.0000	0.0000	0.0000	0.0000	0.0000	0.0000	0.0000	0.0000	0.0000
McLennan Hills	0.9428	0.0000	0.0139	0.0390	0.0000	0.0030	0.0006	0.0007	0.0000	0.0000	0.0000	0.0000	0.0000	0.0000	0.0000	0.0000	0.0000	0.0000	0.0000	0.0000	0.0000	0.0000
Motukorea	0.9478	0.0026	0.0014	0.0000	0.0000	0.0009	0.0000	0.0000	0.0000	0.0000	0.0008	0.0017	0.0001	0.0000	0.0075	0.0010	0.0045	0.0023	0.0269	0.0009	0.0016	0.0023
Mt Albert	0.8827	0.0610	0.0374	0.0174	0.0008	0.0005	0.0001	0.0000	0.0000	0.0000	0.0000	0.0001	0.0000	0.0000	0.0000	0.0000	0.0000	0.0000	0.0000	0.0000	0.0000	0.0000
Mt Cambria	0.7480	0.0075	0.0109	0.0153	0.0022	0.0064	0.0000	0.0000	0.0000	0.0003	0.0025	0.0020	0.0013	0.0000	0.0344	0.0102	0.0552	0.0168	0.0846	0.0012	0.0012	0.0001
Mt Eden	0.0054	0.0000	0.0000	0.0000	0.0000	0.0000	0.0000	0.0000	0.0000	0.0001	0.0041	0.0584	0.3695	0.5625	0.0000	0.0000	0.0000	0.0000	0.0000	0.0000	0.0000	0.0000
Mt Hobson	0.2979	0.0000	0.0000	0.0000	0.0000	0.0000	0.0000	0.0000	0.0000	0.0000	0.0000	0.0005	0.0034	0.0301	0.1204	0.0875	0.0730	0.0603	0.0819	0.1123	0.1327	0.1776
Mt Mangere	0.0083	0.0000	0.0000	0.0000	0.0000	0.0000	0.0000	0.0000	0.0000	0.0000	0.0000	0.0000	0.0000	0.0000	0.0047	0.0417	0.1355	0.3433	0.3226	0.1396	0.0043	0.0000
Mt Richmond	0.6252	0.0000	0.0000	0.0000	0.0000	0.0018	0.0658	0.1516	0.0000	0.0516	0.0891	0.0149	0.0000	0.0000	0.0000	0.0000	0.0000	0.0000	0.0000	0.0000	0.0000	0.0000
Mt Roskill	0.9425	0.0198	0.0265	0.0011	0.0000	0.0030	0.0000	0.0003	0.0000	0.0001	0.0017	0.0046	0.0004	0.0000	0.0000	0.0000	0.0000	0.0000	0.0000	0.0000	0.0000	0.0000
Mt Smart	0.2413	0.0000	0.0000	0.0000	0.0000	0.0000	0.0000	0.0000	0.0000	0.0000	0.0000	0.0000	0.0000	0.0000	0.0000	0.0003	0.0047	0.0232	0.0748	0.2735	0.3822	0.2284
Mt StJohn	0.7122	0.0563	0.1180	0.0907	0.0001	0.0120	0.0004	0.0003	0.0000	0.0001	0.0006	0.0088	0.0005	0.0000	0.0000	0.0000	0.0000	0.0000	0.0000	0.0000	0.0000	0.0000
Mt Victoria	0.2335	0.0705	0.0817	0.0626	0.0125	0.0070	0.0015	0.0000	0.0005	0.0001	0.0019	0.0076	0.0017	0.0075	0.1051	0.1272	0.0618	0.0844	0.0175	0.0775	0.0379	0.0515
North Head	0.7410	0.0960	0.0611	0.0491	0.0059	0.0042	0.0003	0.0000	0.0001	0.0002	0.0005	0.0054	0.0009	0.0054	0.0111	0.0057	0.0043	0.0029	0.0023	0.0019	0.0017	0.0015
One Tree Hill	0.6784	0.0830	0.1279	0.0950	0.0012	0.0105	0.0007	0.0002	0.0000	0.0002	0.0003	0.0023	0.0003	0.0000	0.0000	0.0000	0.0000	0.0000	0.0000	0.0000	0.0000	0.0000
Otara Hill	0.0139	0.0003	0.0007	0.0084	0.0046	0.0022	0.0014	0.0000	0.0004	0.0000	0.0012	0.0081	0.0030	0.0123	0.2127	0.2634	0.1766	0.1350	0.0606	0.0700	0.0252	0.0084
Otuataua	0.6500	0.0060	0.0598	0.2543	0.0272	0.0016	0.0000	0.0011	0.0000	0.0000	0.0000	0.0000	0.0000	0.0000	0.0000	0.0000	0.0000	0.0000	0.0000	0.0000	0.0000	0.0000
Panmure Basin	0.1036	0.0000	0.0001	0.0004	0.0006	0.7449	0.0679	0.0377	0.0000	0.0021	0.0067	0.0360	0.0000	0.0000	0.0000	0.0000	0.0000	0.0000	0.0000	0.0000	0.0000	0.0000
Pigeon Mountain	0.7796	0.0319	0.0422	0.0365	0.0005	0.0047	0.0000	0.0000	0.0000	0.0000	0.0009	0.0078	0.0010	0.0000	0.0227	0.0120	0.0164	0.0081	0.0276	0.0043	0.0038	0.0114
Pukaki	0.8874	0.1126	0.0000	0.0000	0.0000	0.0000	0.0000	0.0000	0.0000	0.0000	0.0000	0.0000	0.0000	0.0000	0.0000	0.0000	0.0000	0.0000	0.0000	0.0000	0.0000	0.0000
Puketutu	0.0229	0.0000	0.0000	0.0000	0.0006	0.0051	0.0310	0.0221	0.1797	0.2638	0.3152	0.1596	0.0000	0.0000	0.0000	0.0000	0.0000	0.0000	0.0000	0.0000	0.0000	0.0000
Robertson Hill	0.9989	0.0000	0.0000	0.0000	0.0000	0.0000	0.0006	0.0000	0.0000	0.0001	0.0004	0.0000	0.0000	0.0000	0.0000	0.0000	0.0000	0.0000	0.0000	0.0000	0.0000	0.0000
Styaks Swamp	0.7447	0.0000	0.0000	0.0000	0.0000	0.0000	0.0000	0.0000	0.0000	0.0000	0.0000	0.0000	0.0000	0.0000	0.0119	0.0165	0.0350	0.0372	0.0497	0.0509	0.0541	0.2088
Taylors Hill	0.2811	0.0000	0.0000	0.0001	0.0000	0.0188	0.3036	0.1758	0.0000	0.0099	0.1635	0.0472	0.0000	0.0000	0.0000	0.0000	0.0000	0.0000	0.0000	0.0000	0.0000	0.0000
Te Pouhawaiki	0.7721	0.0752	0.0675	0.0621	0.0055	0.0046	0.0013	0.0003	0.0000	0.0003	0.0005	0.0091	0.0015	0.0000	0.0000	0.0000	0.0000	0.0000	0.0000	0.0000	0.0000	0.0000
Three Kings	0.0000	0.0000	0.0000	0.0000	0.0000	0.0000	0.0000	0.0000	0.0000	0.0002	0.0023	0.1097	0.5949	0.2929	0.0000	0.0000	0.0000	0.0000	0.0000	0.0000	0.0000	0.0000
Wiri Mountain	0.1165	0.0000	0.0000	0.0000	0.0000	0.0022	0.1697	0.2461	0.0438	0.2107	0.1211	0.0899	0.0000	0.0000	0.0000	0.0000	0.0000	0.0000	0.0000	0.0000	0.0000	0.0000

Table A.25: Marginal posterior probabilities for a volcano to have produced a given tephra for the AVF 9A/9B scenario with $B = \{\alpha = 2.0, \beta U = 0.5\}$.

Volcano	AVF tephra (AVF 0 = 'unmatched')																					
	0	1	2	3	4	5	6	7	8	9A	9B	10	11	12	13	14	15	16	17	18	19	20
Ash Hill	0.8814	0.0000	0.0000	0.0000	0.0000	0.0001	0.0892	0.0293	0.0000	0.0000	0.0000	0.0000	0.0000	0.0000	0.0000	0.0000	0.0000	0.0000	0.0000	0.0000	0.0000	0.0000
Cemetery Hill	0.0174	0.0000	0.0000	0.0000	0.0002	0.0203	0.1690	0.2712	0.3383	0.1435	0.0400	0.0001	0.0000	0.0000	0.0000	0.0000	0.0000	0.0000	0.0000	0.0000	0.0000	0.0000
Crater Hill	0.0000	0.0000	0.0000	0.0000	0.0000	0.0002	0.0163	0.0135	0.4347	0.2976	0.1838	0.0534	0.0005	0.0000	0.0000	0.0000	0.0000	0.0000	0.0000	0.0000	0.0000	0.0000
Domain	0.7603	0.1322	0.0865	0.0210	0.0000	0.0000	0.0000	0.0000	0.0000	0.0000	0.0000	0.0000	0.0000	0.0000	0.0000	0.0000	0.0000	0.0000	0.0000	0.0000	0.0000	0.0000
Green Hill	0.0395	0.0007	0.0034	0.0189	0.0226	0.0147	0.0052	0.0003	0.0012	0.0007	0.0030	0.0443	0.0105	0.0561	0.1910	0.1234	0.1019	0.0773	0.0874	0.1098	0.0881	0.0303
Hampton Park	0.3960	0.0000	0.0000	0.0000	0.0000	0.0000	0.0000	0.0002	0.0000	0.0000	0.0000	0.0000	0.0000	0.0000	0.0639	0.1492	0.1917	0.1061	0.0697	0.0162	0.0070	0.0039
Hopua	0.3846	0.0000	0.0000	0.0005	0.0000	0.0639	0.0502	0.0403	0.0013	0.0493	0.1097	0.2960	0.0042	0.0000	0.0000	0.0000	0.0000	0.0000	0.0000	0.0000	0.0000	0.0000
Kohuora	0.0002	0.0002	0.0018	0.0198	0.8924	0.0509	0.0315	0.0003	0.0029	0.0000	0.0000	0.0000	0.0000	0.0000	0.0000	0.0000	0.0000	0.0000	0.0000	0.0000	0.0000	0.0000
Little Rangitoto	0.1184	0.1995	0.1936	0.1446	0.0196	0.0106	0.0011	0.0006	0.0018	0.0011	0.0020	0.0151	0.0029	0.0185	0.0498	0.0379	0.0288	0.0209	0.0312	0.0495	0.0525	0.0738
Mangere Lagoon	0.7340	0.0444	0.0613	0.0560	0.0005	0.0056	0.0021	0.0003	0.0000	0.0001	0.0021	0.0083	0.0019	0.0082	0.0255	0.0214	0.0163	0.0094	0.0026	0.0000	0.0000	0.0000
Matukutureia	0.2151	0.0000	0.0000	0.0000	0.0000	0.0000	0.0000	0.0000	0.0000	0.0000	0.0008	0.0088	0.0020	0.0091	0.1382	0.1015	0.0847	0.0685	0.0646	0.0947	0.2120	0.1962
Maungataketake	0.9954	0.0009	0.0000	0.0012	0.0000	0.0002	0.0023	0.0000	0.0000	0.0000	0.0000	0.0000	0.0000	0.0000	0.0000	0.0000	0.0000	0.0000	0.0000	0.0000	0.0000	0.0000
McLennan Hills	0.9366	0.0000	0.0165	0.0410	0.0000	0.0042	0.0006	0.0011	0.0000	0.0000	0.0000	0.0000	0.0000	0.0000	0.0000	0.0000	0.0000	0.0000	0.0000	0.0000	0.0000	0.0000
Motukorea	0.9506	0.0024	0.0009	0.0000	0.0000	0.0010	0.0000	0.0000	0.0000	0.0000	0.0008	0.0011	0.0001	0.0000	0.0067	0.0009	0.0031	0.0021	0.0278	0.0009	0.0016	0.0024
Mt Albert	0.8864	0.0582	0.0362	0.0177	0.0008	0.0005	0.0001	0.0000	0.0000	0.0000	0.0000	0.0001	0.0000	0.0000	0.0000	0.0000	0.0000	0.0000	0.0000	0.0000	0.0000	0.0000
Mt Cambria	0.7297	0.0105	0.0235	0.0172	0.0027	0.0077	0.0000	0.0000	0.0000	0.0003	0.0023	0.0038	0.0030	0.0000	0.0328	0.0101	0.0490	0.0153	0.0897	0.0012	0.0012	0.0001
Mt Eden	0.0117	0.0000	0.0000	0.0000	0.0000	0.0000	0.0000	0.0000	0.0000	0.0001	0.0040	0.0593	0.3708	0.5541	0.0000	0.0000	0.0000	0.0000	0.0000	0.0000	0.0000	0.0000
Mt Hobson	0.2935	0.0000	0.0000	0.0000	0.0000	0.0000	0.0000	0.0000	0.0000	0.0000	0.0000	0.0004	0.0037	0.0305	0.1218	0.0872	0.0743	0.0609	0.0831	0.1134	0.1312	0.1822
Mt Mangere	0.0088	0.0000	0.0000	0.0000	0.0000	0.0000	0.0000	0.0000	0.0000	0.0000	0.0000	0.0000	0.0000	0.0000	0.0048	0.0432	0.1461	0.3523	0.3042	0.1365	0.0041	0.0000
Mt Richmond	0.6282	0.0000	0.0000	0.0000	0.0000	0.0017	0.0666	0.1494	0.0000	0.0514	0.0881	0.0146	0.0000	0.0000	0.0000	0.0000	0.0000	0.0000	0.0000	0.0000	0.0000	0.0000
Mt Roskill	0.9442	0.0178	0.0263	0.0009	0.0000	0.0034	0.0000	0.0003	0.0000	0.0002	0.0017	0.0048	0.0004	0.0000	0.0000	0.0000	0.0000	0.0000	0.0000	0.0000	0.0000	0.0000
Mt Smart	0.2329	0.0000	0.0000	0.0000	0.0000	0.0000	0.0000	0.0000	0.0000	0.0000	0.0000	0.0000	0.0000	0.0000	0.0000	0.0003	0.0053	0.0263	0.0781	0.2764	0.3807	0.2231
Mt StJohn	0.7172	0.0573	0.1123	0.0906	0.0001	0.0118	0.0005	0.0003	0.0000	0.0001	0.0007	0.0086	0.0005	0.0000	0.0000	0.0000	0.0000	0.0000	0.0000	0.0000	0.0000	0.0000
Mt Victoria	0.2281	0.0711	0.0737	0.0713	0.0152	0.0064	0.0016	0.0000	0.0005	0.0001	0.0018	0.0060	0.0034	0.0082	0.1066	0.1246	0.0648	0.0854	0.0167	0.0769	0.0376	0.0532
North Head	0.7324	0.1016	0.0619	0.0500	0.0076	0.0036	0.0003	0.0000	0.0001	0.0002	0.0004	0.0055	0.0009	0.0058	0.0111	0.0057	0.0044	0.0026	0.0026	0.0018	0.0015	0.0016
One Tree Hill	0.6769	0.0841	0.1253	0.0980	0.0012	0.0104	0.0008	0.0002	0.0000	0.0003	0.0003	0.0022	0.0003	0.0000	0.0000	0.0000	0.0000	0.0000	0.0000	0.0000	0.0000	0.0000
Otara Hill	0.0131	0.0004	0.0006	0.0086	0.0046	0.0022	0.0015	0.0000	0.0003	0.0000	0.0010	0.0081	0.0032	0.0140	0.2136	0.2663	0.1798	0.1286	0.0609	0.0680	0.0252	0.0081
Otuataua	0.6688	0.0068	0.0593	0.2380	0.0236	0.0020	0.0002	0.0013	0.0000	0.0000	0.0000	0.0000	0.0000	0.0000	0.0000	0.0000	0.0000	0.0000	0.0000	0.0000	0.0000	0.0000
Panmure Basin	0.1050	0.0000	0.0002	0.0003	0.0006	0.7425	0.0653	0.0403	0.0000	0.0039	0.0059	0.0360	0.0000	0.0000	0.0000	0.0000	0.0000	0.0000	0.0000	0.0000	0.0000	0.0000
Pigeon Mountain	0.7828	0.0305	0.0432	0.0350	0.0005	0.0045	0.0000	0.0000	0.0000	0.0001	0.0008	0.0077	0.0010	0.0000	0.0226	0.0118	0.0158	0.0078	0.0284	0.0039	0.0036	0.0118
Pukaki	0.9122	0.0878	0.0000	0.0000	0.0000	0.0000	0.0000	0.0000	0.0000	0.0000	0.0000	0.0000	0.0000	0.0000	0.0000	0.0000	0.0000	0.0000	0.0000	0.0000	0.0000	0.0000
Puketutu	0.0165	0.0000	0.0000	0.0000	0.0005	0.0046	0.0376	0.0213	0.1827	0.2692	0.3093	0.1583	0.0000	0.0000	0.0000	0.0000	0.0000	0.0000	0.0000	0.0000	0.0000	0.0000
Robertson Hill	0.9985	0.0000	0.0000	0.0000	0.0000	0.0000	0.0005	0.0000	0.0000	0.0001	0.0009	0.0000	0.0000	0.0000	0.0000	0.0000	0.0000	0.0000	0.0000	0.0000	0.0000	0.0000
Styaks Swamp	0.7439	0.0000	0.0000	0.0000	0.0000	0.0000	0.0000	0.0000	0.0000	0.0000	0.0000	0.0000	0.0000	0.0000	0.0116	0.0165	0.0340	0.0365	0.0530	0.0508	0.0537	0.2133
Taylors Hill	0.3258	0.0000	0.0000	0.0001	0.0000	0.0200	0.2886	0.1755	0.0000	0.0086	0.1345	0.0469	0.0000	0.0000	0.0000	0.0000	0.0000	0.0000	0.0000	0.0000	0.0000	0.0000
Te Pouhawaiki	0.7375	0.0936	0.0735	0.0692	0.0073	0.0051	0.0012	0.0003	0.0003	0.0003	0.0005	0.0095	0.0017	0.0000	0.0000	0.0000	0.0000	0.0000	0.0000	0.0000	0.0000	0.0000
Three Kings	0.0000	0.0000	0.0000	0.0000	0.0000	0.0000	0.0000	0.0000	0.0000	0.0003	0.0020	0.1132	0.5890	0.2955	0.0000	0.0000	0.0000	0.0000	0.0000	0.0000	0.0000	0.0000
Wiri Mountain	0.1764	0.0000	0.0000	0.0001	0.0000	0.0019	0.1677	0.2540	0.0359	0.1725	0.1036	0.0879	0.0000	0.0000	0.0000	0.0000	0.0000	0.0000	0.0000	0.0000	0.0000	0.0000

Table A.26: Marginal posterior probabilities for a volcano to have produced a given tephra for the AVF 9A/9B scenario with $C = \{\alpha = 2.5, \beta U = 0.5\}$.

Volcano	AVF tephra (AVF 0 = 'unmatched')																					
	0	1	2	3	4	5	6	7	8	9A	9B	10	11	12	13	14	15	16	17	18	19	20
Ash Hill	0.8623	0.0000	0.0000	0.0000	0.0000	0.0005	0.1067	0.0305	0.0000	0.0000	0.0000	0.0000	0.0000	0.0000	0.0000	0.0000	0.0000	0.0000	0.0000	0.0000	0.0000	0.0000
Cemetery Hill	0.0185	0.0000	0.0000	0.0000	0.0002	0.0200	0.1684	0.2486	0.3648	0.1357	0.0432	0.0006	0.0000	0.0000	0.0000	0.0000	0.0000	0.0000	0.0000	0.0000	0.0000	0.0000
Crater Hill	0.0001	0.0000	0.0000	0.0000	0.0000	0.0002	0.0177	0.0152	0.4091	0.3229	0.1767	0.0571	0.0010	0.0000	0.0000	0.0000	0.0000	0.0000	0.0000	0.0000	0.0000	0.0000
Domain	0.7577	0.1370	0.0830	0.0223	0.0000	0.0000	0.0000	0.0000	0.0000	0.0000	0.0000	0.0000	0.0000	0.0000	0.0000	0.0000	0.0000	0.0000	0.0000	0.0000	0.0000	0.0000
Green Hill	0.0364	0.0007	0.0032	0.0185	0.0236	0.0139	0.0049	0.0003	0.0016	0.0010	0.0026	0.0444	0.0106	0.0585	0.1897	0.1255	0.1021	0.0782	0.0883	0.1102	0.0858	0.0283
Hampton Park	0.4162	0.0000	0.0000	0.0000	0.0000	0.0001	0.0000	0.0002	0.0000	0.0000	0.0000	0.0000	0.0000	0.0000	0.0596	0.1524	0.1809	0.0978	0.0703	0.0159	0.0066	0.0039
Hopua	0.3621	0.0000	0.0000	0.0005	0.0000	0.0632	0.0504	0.0387	0.0016	0.0542	0.1306	0.2943	0.0044	0.0000	0.0000	0.0000	0.0000	0.0000	0.0000	0.0000	0.0000	0.0000
Kohuora	0.0019	0.0002	0.0018	0.0216	0.8895	0.0489	0.0316	0.0006	0.0039	0.0000	0.0000	0.0000	0.0000	0.0000	0.0000	0.0000	0.0000	0.0000	0.0000	0.0000	0.0000	0.0000
Little Rangitoto	0.1139	0.2051	0.1892	0.1433	0.0223	0.0099	0.0010	0.0004	0.0018	0.0013	0.0021	0.0151	0.0029	0.0191	0.0495	0.0386	0.0289	0.0206	0.0328	0.0503	0.0519	0.0785
Mangere Lagoon	0.7395	0.0424	0.0618	0.0530	0.0003	0.0052	0.0022	0.0004	0.0000	0.0001	0.0019	0.0083	0.0017	0.0081	0.0257	0.0217	0.0169	0.0084	0.0024	0.0000	0.0000	0.0000
Matukutureia	0.2042	0.0000	0.0000	0.0000	0.0000	0.0000	0.0000	0.0000	0.0000	0.0000	0.0008	0.0088	0.0019	0.0100	0.1388	0.1022	0.0866	0.0678	0.0655	0.0972	0.2162	0.1894
Maungataketake	0.9950	0.0009	0.0000	0.0007	0.0000	0.0005	0.0029	0.0000	0.0000	0.0000	0.0000	0.0000	0.0000	0.0000	0.0000	0.0000	0.0000	0.0000	0.0000	0.0000	0.0000	0.0000
McLennan Hills	0.9288	0.0000	0.0191	0.0445	0.0000	0.0052	0.0010	0.0014	0.0000	0.0000	0.0000	0.0000	0.0000	0.0000	0.0000	0.0000	0.0000	0.0000	0.0000	0.0000	0.0000	0.0000
Motukorea	0.9518	0.0020	0.0006	0.0000	0.0000	0.0013	0.0000	0.0000	0.0000	0.0000	0.0010	0.0008	0.0001	0.0000	0.0063	0.0009	0.0025	0.0020	0.0282	0.0009	0.0016	0.0023
Mt Albert	0.8906	0.0573	0.0340	0.0166	0.0007	0.0006	0.0001	0.0000	0.0000	0.0000	0.0000	0.0001	0.0000	0.0000	0.0000	0.0000	0.0000	0.0000	0.0000	0.0000	0.0000	0.0000
Mt Cambria	0.7366	0.0112	0.0282	0.0167	0.0031	0.0080	0.0000	0.0000	0.0000	0.0003	0.0025	0.0039	0.0032	0.0000	0.0309	0.0114	0.0349	0.0134	0.0933	0.0012	0.0012	0.0001
Mt Eden	0.0135	0.0000	0.0000	0.0000	0.0000	0.0000	0.0000	0.0000	0.0000	0.0001	0.0040	0.0610	0.3726	0.5488	0.0000	0.0000	0.0000	0.0000	0.0000	0.0000	0.0000	0.0000
Mt Hobson	0.2883	0.0000	0.0000	0.0000	0.0000	0.0000	0.0000	0.0000	0.0000	0.0000	0.0000	0.0003	0.0041	0.0306	0.1237	0.0864	0.0768	0.0593	0.0877	0.1127	0.1301	0.1876
Mt Mangere	0.0091	0.0000	0.0000	0.0000	0.0000	0.0000	0.0000	0.0000	0.0000	0.0000	0.0000	0.0000	0.0000	0.0000	0.0049	0.0456	0.1546	0.3691	0.2803	0.1323	0.0041	0.0000
Mt Richmond	0.6363	0.0000	0.0000	0.0000	0.0000	0.0019	0.0665	0.1498	0.0000	0.0485	0.0804	0.0166	0.0000	0.0000	0.0000	0.0000	0.0000	0.0000	0.0000	0.0000	0.0000	0.0000
Mt Roskill	0.9476	0.0141	0.0261	0.0008	0.0000	0.0033	0.0001	0.0004	0.0000	0.0003	0.0018	0.0051	0.0004	0.0000	0.0000	0.0000	0.0000	0.0000	0.0000	0.0000	0.0000	0.0000
Mt Smart	0.2202	0.0000	0.0000	0.0000	0.0000	0.0000	0.0000	0.0000	0.0000	0.0000	0.0000	0.0000	0.0000	0.0000	0.0000	0.0003	0.0056	0.0290	0.0824	0.2814	0.3811	0.2128
Mt StJohn	0.7169	0.0579	0.1122	0.0906	0.0001	0.0114	0.0005	0.0003	0.0000	0.0001	0.0008	0.0087	0.0005	0.0000	0.0000	0.0000	0.0000	0.0000	0.0000	0.0000	0.0000	0.0000
Mt Victoria	0.2262	0.0710	0.0712	0.0734	0.0171	0.0052	0.0016	0.0000	0.0005	0.0002	0.0019	0.0058	0.0034	0.0088	0.1093	0.1180	0.0723	0.0848	0.0173	0.0748	0.0372	0.0554
North Head	0.7274	0.1043	0.0639	0.0492	0.0089	0.0031	0.0002	0.0000	0.0001	0.0003	0.0003	0.0055	0.0009	0.0064	0.0108	0.0058	0.0043	0.0028	0.0023	0.0021	0.0014	0.0012
One Tree Hill	0.6792	0.0822	0.1218	0.1016	0.0011	0.0099	0.0009	0.0002	0.0000	0.0005	0.0000	0.0023	0.0003	0.0000	0.0000	0.0000	0.0000	0.0000	0.0000	0.0000	0.0000	0.0000
Otara Hill	0.0125	0.0004	0.0006	0.0086	0.0046	0.0023	0.0013	0.0000	0.0004	0.0000	0.0012	0.0080	0.0031	0.0154	0.2179	0.2629	0.1848	0.1251	0.0607	0.0657	0.0245	0.0079
Otuataua	0.6758	0.0068	0.0617	0.2322	0.0183	0.0028	0.0005	0.0019	0.0000	0.0000	0.0000	0.0000	0.0000	0.0000	0.0000	0.0000	0.0000	0.0000	0.0000	0.0000	0.0000	0.0000
Panmure Basin	0.1038	0.0000	0.0002	0.0002	0.0006	0.7460	0.0647	0.0405	0.0000	0.0037	0.0055	0.0348	0.0000	0.0000	0.0000	0.0000	0.0000	0.0000	0.0000	0.0000	0.0000	0.0000
Pigeon Mountain	0.7870	0.0271	0.0445	0.0346	0.0005	0.0043	0.0000	0.0000	0.0000	0.0001	0.0009	0.0073	0.0010	0.0000	0.0223	0.0122	0.0150	0.0070	0.0296	0.0036	0.0030	0.0113
Pukaki	0.9164	0.0836	0.0000	0.0000	0.0000	0.0000	0.0000	0.0000	0.0000	0.0000	0.0000	0.0000	0.0000	0.0000	0.0000	0.0000	0.0000	0.0000	0.0000	0.0000	0.0000	0.0000
Puketutu	0.0175	0.0000	0.0000	0.0000	0.0003	0.0047	0.0370	0.0214	0.1870	0.2721	0.3155	0.1445	0.0000	0.0000	0.0000	0.0000	0.0000	0.0000	0.0000	0.0000	0.0000	0.0000
Robertson Hill	0.9980	0.0000	0.0000	0.0000	0.0000	0.0000	0.0007	0.0000	0.0000	0.0001	0.0012	0.0000	0.0000	0.0000	0.0000	0.0000	0.0000	0.0000	0.0000	0.0000	0.0000	0.0000
Styaks Swamp	0.7389	0.0000	0.0000	0.0000	0.0000	0.0000	0.0000	0.0000	0.0000	0.0000	0.0000	0.0000	0.0000	0.0000	0.0106	0.0161	0.0338	0.0347	0.0589	0.0517	0.0553	0.2213
Taylors Hill	0.3367	0.0000	0.0000	0.0001	0.0000	0.0210	0.2711	0.1860	0.0000	0.0109	0.1209	0.0533	0.0000	0.0000	0.0000	0.0000	0.0000	0.0000	0.0000	0.0000	0.0000	0.0000
Te Pouhawaiki	0.7292	0.0958	0.0769	0.0709	0.0088	0.0046	0.0011	0.0003	0.0004	0.0003	0.0004	0.0095	0.0018	0.0000	0.0000	0.0000	0.0000	0.0000	0.0000	0.0000	0.0000	0.0000
Three Kings	0.0000	0.0000	0.0000	0.0000	0.0000	0.0000	0.0000	0.0000	0.0000	0.0003	0.0020	0.1173	0.5861	0.2943	0.0000	0.0000	0.0000	0.0000	0.0000	0.0000	0.0000	0.0000
Wiri Mountain	0.2039	0.0000	0.0000	0.0001	0.0000	0.0020	0.1669	0.2629	0.0288	0.1470	0.1018	0.0866	0.0000	0.0000	0.0000	0.0000	0.0000	0.0000	0.0000	0.0000	0.0000	0.0000

Table A.27: Marginal posterior probabilities for a volcano to have produced a given tephra for the AVF 9A/9B scenario with D $= \{\alpha = 1.5, \beta U = 1.0\}$.

Volcano	AVF tephra (AVF 0 = 'unmatched')																					
	0	1	2	3	4	5	6	7	8	9A	9B	10	11	12	13	14	15	16	17	18	19	20
Ash Hill	0.6925	0.0000	0.0000	0.0000	0.0000	0.0006	0.2077	0.0992	0.0000	0.0000	0.0000	0.0000	0.0000	0.0000	0.0000	0.0000	0.0000	0.0000	0.0000	0.0000	0.0000	0.0000
Cemetery Hill	0.0000	0.0000	0.0000	0.0000	0.0020	0.0114	0.1184	0.1370	0.5052	0.1360	0.0766	0.0133	0.0001	0.0000	0.0000	0.0000	0.0000	0.0000	0.0000	0.0000	0.0000	0.0000
Crater Hill	0.0019	0.0000	0.0000	0.0000	0.0000	0.0003	0.0044	0.0054	0.2512	0.4094	0.2123	0.0994	0.0157	0.0000	0.0000	0.0000	0.0000	0.0000	0.0000	0.0000	0.0000	0.0000
Domain	0.7775	0.1135	0.0881	0.0209	0.0000	0.0000	0.0000	0.0000	0.0000	0.0000	0.0000	0.0000	0.0000	0.0000	0.0000	0.0000	0.0000	0.0000	0.0000	0.0000	0.0000	0.0000
Green Hill	0.0211	0.0012	0.0027	0.0139	0.0207	0.0174	0.0087	0.0009	0.0036	0.0005	0.0007	0.0260	0.0267	0.0698	0.1887	0.1313	0.1051	0.0830	0.0953	0.1078	0.0749	0.0182
Hampton Park	0.5081	0.0000	0.0000	0.0000	0.0000	0.0001	0.0001	0.0009	0.0000	0.0000	0.0000	0.0000	0.0000	0.0000	0.0474	0.1291	0.1510	0.0822	0.0629	0.0132	0.0050	0.0036
Hopua	0.3261	0.0000	0.0000	0.0008	0.0002	0.0415	0.1164	0.0480	0.0008	0.0461	0.1363	0.2025	0.0813	0.0000	0.0000	0.0000	0.0000	0.0000	0.0000	0.0000	0.0000	0.0000
Kohuora	0.0000	0.0002	0.0024	0.0187	0.7010	0.1770	0.0872	0.0037	0.0097	0.0001	0.0000	0.0000	0.0000	0.0000	0.0000	0.0000	0.0000	0.0000	0.0000	0.0000	0.0000	0.0000
Little Rangitoto	0.1056	0.2285	0.1663	0.1334	0.0212	0.0168	0.0017	0.0013	0.0022	0.0011	0.0013	0.0107	0.0077	0.0227	0.0484	0.0413	0.0303	0.0209	0.0344	0.0516	0.0526	0.0880
Mangere Lagoon	0.7148	0.0428	0.0722	0.0540	0.0004	0.0134	0.0041	0.0006	0.0001	0.0000	0.0004	0.0063	0.0064	0.0098	0.0279	0.0219	0.0165	0.0069	0.0015	0.0000	0.0000	0.0000
Matukutureia	0.1631	0.0000	0.0000	0.0000	0.0000	0.0000	0.0000	0.0000	0.0000	0.0000	0.0002	0.0054	0.0049	0.0178	0.1390	0.1058	0.0883	0.0668	0.0729	0.1102	0.2256	0.1563
Maungataketake	0.9905	0.0003	0.0000	0.0041	0.0000	0.0018	0.0032	0.0001	0.0000	0.0000	0.0000	0.0000	0.0000	0.0000	0.0000	0.0000	0.0000	0.0000	0.0000	0.0000	0.0000	0.0000
McLennan Hills	0.8844	0.0000	0.0309	0.0614	0.0000	0.0172	0.0032	0.0029	0.0000	0.0000	0.0000	0.0000	0.0000	0.0000	0.0000	0.0000	0.0000	0.0000	0.0000	0.0000	0.0000	0.0000
Motukorea	0.9582	0.0021	0.0011	0.0003	0.0000	0.0012	0.0000	0.0000	0.0000	0.0000	0.0001	0.0000	0.0000	0.0000	0.0025	0.0008	0.0009	0.0012	0.0291	0.0009	0.0016	0.0021
Mt Albert	0.8915	0.0525	0.0366	0.0174	0.0006	0.0011	0.0001	0.0001	0.0000	0.0000	0.0000	0.0001	0.0000	0.0000	0.0000	0.0000	0.0000	0.0000	0.0000	0.0000	0.0000	0.0000
Mt Cambria	0.7679	0.0067	0.0185	0.0112	0.0040	0.0084	0.0000	0.0000	0.0000	0.0006	0.0008	0.0042	0.0112	0.0000	0.0250	0.0074	0.0184	0.0071	0.1062	0.0012	0.0012	0.0001
Mt Eden	0.2675	0.0000	0.0000	0.0000	0.0000	0.0000	0.0000	0.0000	0.0000	0.0001	0.0073	0.0569	0.3621	0.3061	0.0000	0.0000	0.0000	0.0000	0.0000	0.0000	0.0000	0.0000
Mt Hobson	0.2676	0.0000	0.0000	0.0000	0.0000	0.0000	0.0000	0.0000	0.0000	0.0000	0.0000	0.0006	0.0043	0.0255	0.1293	0.0890	0.0769	0.0647	0.0916	0.1192	0.1313	0.2106
Mt Mangere	0.0189	0.0000	0.0000	0.0000	0.0000	0.0000	0.0000	0.0000	0.0000	0.0000	0.0000	0.0000	0.0000	0.0000	0.0058	0.0495	0.1992	0.3864	0.2359	0.1007	0.0036	0.0000
Mt Richmond	0.7125	0.0000	0.0000	0.0000	0.0000	0.0006	0.0381	0.1133	0.0000	0.0441	0.0909	0.0005	0.0000	0.0000	0.0000	0.0000	0.0000	0.0000	0.0000	0.0000	0.0000	0.0000
Mt Roskill	0.9791	0.0109	0.0024	0.0016	0.0001	0.0042	0.0002	0.0009	0.0000	0.0001	0.0000	0.0005	0.0000	0.0000	0.0000	0.0000	0.0000	0.0000	0.0000	0.0000	0.0000	0.0000
Mt Smart	0.1843	0.0000	0.0000	0.0000	0.0000	0.0000	0.0000	0.0000	0.0000	0.0000	0.0000	0.0000	0.0000	0.0000	0.0000	0.0004	0.0076	0.0440	0.1091	0.2916	0.3630	0.1812
Mt StJohn	0.7308	0.0383	0.1190	0.0814	0.0003	0.0162	0.0021	0.0006	0.0002	0.0000	0.0000	0.0069	0.0042	0.0000	0.0000	0.0000	0.0000	0.0000	0.0000	0.0000	0.0000	0.0000
Mt Victoria	0.2172	0.0820	0.0730	0.0594	0.0120	0.0069	0.0048	0.0002	0.0012	0.0002	0.0002	0.0054	0.0047	0.0142	0.1138	0.1218	0.0765	0.0824	0.0090	0.0762	0.0389	0.0590
North Head	0.7262	0.1111	0.0615	0.0431	0.0070	0.0046	0.0014	0.0004	0.0005	0.0001	0.0001	0.0038	0.0029	0.0085	0.0094	0.0068	0.0038	0.0027	0.0022	0.0024	0.0015	0.0005
One Tree Hill	0.7031	0.0592	0.1274	0.0877	0.0006	0.0171	0.0013	0.0004	0.0001	0.0002	0.0000	0.0019	0.0010	0.0000	0.0000	0.0000	0.0000	0.0000	0.0000	0.0000	0.0000	0.0000
Otara Hill	0.0070	0.0005	0.0010	0.0065	0.0059	0.0041	0.0020	0.0001	0.0011	0.0000	0.0002	0.0050	0.0063	0.0251	0.2281	0.2706	0.1842	0.1131	0.0586	0.0577	0.0229	0.0062
Otuataua	0.3943	0.0093	0.0864	0.2870	0.2138	0.0055	0.0018	0.0019	0.0000	0.0000	0.0000	0.0000	0.0000	0.0000	0.0000	0.0000	0.0000	0.0000	0.0000	0.0000	0.0000	0.0000
Panmure Basin	0.3457	0.0000	0.0001	0.0009	0.0006	0.5942	0.0115	0.0338	0.0009	0.0002	0.0010	0.0076	0.0035	0.0000	0.0000	0.0000	0.0000	0.0000	0.0000	0.0000	0.0000	0.0000
Pigeon Mountain	0.8137	0.0248	0.0311	0.0304	0.0003	0.0079	0.0000	0.0000	0.0000	0.0001	0.0003	0.0051	0.0040	0.0000	0.0221	0.0074	0.0114	0.0045	0.0318	0.0029	0.0022	0.0116
Pukaki	0.9034	0.0966	0.0000	0.0000	0.0000	0.0000	0.0000	0.0000	0.0000	0.0000	0.0000	0.0000	0.0000	0.0000	0.0000	0.0000	0.0000	0.0000	0.0000	0.0000	0.0000	0.0000
Puketutu	0.0094	0.0000	0.0000	0.0000	0.0007	0.0105	0.0172	0.0225	0.1760	0.2010	0.2414	0.2672	0.0541	0.0000	0.0000	0.0000	0.0000	0.0000	0.0000	0.0000	0.0000	0.0000
Robertson Hill	0.9994	0.0000	0.0000	0.0000	0.0000	0.0000	0.0003	0.0000	0.0000	0.0001	0.0002	0.0000	0.0000	0.0000	0.0000	0.0000	0.0000	0.0000	0.0000	0.0000	0.0000	0.0000
Styaks Swamp	0.7064	0.0000	0.0000	0.0000	0.0000	0.0000	0.0001	0.0004	0.0000	0.0000	0.0000	0.0000	0.0000	0.0000	0.0126	0.0169	0.0299	0.0341	0.0595	0.0644	0.0757	0.2626
Taylors Hill	0.3218	0.0000	0.0000	0.0001	0.0000	0.0084	0.2618	0.2662	0.0001	0.0390	0.0953	0.0073	0.0000	0.0000	0.0000	0.0000	0.0000	0.0000	0.0000	0.0000	0.0000	0.0000
Te Pouhawaiki	0.6998	0.1195	0.0793	0.0657	0.0086	0.0105	0.0030	0.0008	0.0008	0.0001	0.0001	0.0066	0.0045	0.0007	0.0000	0.0000	0.0000	0.0000	0.0000	0.0000	0.0000	0.0000
Three Kings	0.0000	0.0000	0.0000	0.0000	0.0000	0.0000	0.0000	0.0000	0.0000	0.0003	0.0006	0.1241	0.3752	0.4998	0.0000	0.0000	0.0000	0.0000	0.0000	0.0000	0.0000	0.0000
Wiri Mountain	0.1887	0.0000	0.0000	0.0001	0.0000	0.0011	0.0992	0.2584	0.0463	0.1206	0.1337	0.1327	0.0192	0.0000	0.0000	0.0000	0.0000	0.0000	0.0000	0.0000	0.0000	0.0000

Table A.28: Marginal posterior probabilities for a volcano to have produced a given tephra for the AVF 9A/9B scenario with $E = \{\alpha = 2.0, \beta U = 1.0\}$.

Volcano	AVF tephra (AVF 0 = 'unmatched')																					
	0	1	2	3	4	5	6	7	8	9A	9B	10	11	12	13	14	15	16	17	18	19	20
Ash Hill	0.6493	0.0000	0.0000	0.0000	0.0000	0.0008	0.2528	0.0971	0.0000	0.0000	0.0000	0.0000	0.0000	0.0000	0.0000	0.0000	0.0000	0.0000	0.0000	0.0000	0.0000	0.0000
Cemetery Hill	0.0001	0.0000	0.0000	0.0000	0.0021	0.0119	0.1180	0.1290	0.5172	0.1357	0.0743	0.0116	0.0001	0.0000	0.0000	0.0000	0.0000	0.0000	0.0000	0.0000	0.0000	0.0000
Crater Hill	0.0027	0.0000	0.0000	0.0000	0.0000	0.0003	0.0049	0.0056	0.2430	0.4208	0.2129	0.0962	0.0136	0.0000	0.0000	0.0000	0.0000	0.0000	0.0000	0.0000	0.0000	0.0000
Domain	0.7770	0.1133	0.0890	0.0207	0.0000	0.0000	0.0000	0.0000	0.0000	0.0000	0.0000	0.0000	0.0000	0.0000	0.0000	0.0000	0.0000	0.0000	0.0000	0.0000	0.0000	0.0000
Green Hill	0.0206	0.0012	0.0028	0.0137	0.0217	0.0187	0.0059	0.0010	0.0037	0.0005	0.0007	0.0263	0.0265	0.0730	0.1872	0.1308	0.1048	0.0849	0.0954	0.1065	0.0741	0.0174
Hampton Park	0.5140	0.0000	0.0000	0.0000	0.0000	0.0001	0.0001	0.0010	0.0000	0.0000	0.0000	0.0000	0.0000	0.0000	0.0471	0.1281	0.1484	0.0804	0.0628	0.0131	0.0049	0.0037
Hopua	0.3378	0.0000	0.0000	0.0008	0.0002	0.0643	0.0830	0.0465	0.0007	0.0473	0.1380	0.2016	0.0798	0.0000	0.0000	0.0000	0.0000	0.0000	0.0000	0.0000	0.0000	0.0000
Kohuora	0.0000	0.0002	0.0027	0.0199	0.7422	0.1353	0.0855	0.0032	0.0108	0.0002	0.0000	0.0000	0.0000	0.0000	0.0000	0.0000	0.0000	0.0000	0.0000	0.0000	0.0000	0.0000
Little Rangitoto	0.1020	0.2280	0.1715	0.1297	0.0228	0.0158	0.0016	0.0012	0.0022	0.0009	0.0015	0.0108	0.0077	0.0234	0.0484	0.0412	0.0298	0.0216	0.0348	0.0512	0.0539	0.0890
Mangere Lagoon	0.7241	0.0384	0.0693	0.0529	0.0003	0.0131	0.0040	0.0006	0.0001	0.0000	0.0004	0.0065	0.0066	0.0092	0.0280	0.0221	0.0161	0.0068	0.0015	0.0000	0.0000	0.0000
Matukutureia	0.1604	0.0000	0.0000	0.0000	0.0000	0.0000	0.0000	0.0000	0.0000	0.0000	0.0002	0.0055	0.0048	0.0202	0.1380	0.1052	0.0883	0.0670	0.0727	0.1125	0.2252	0.1556
Maungataketake	0.9891	0.0003	0.0000	0.0042	0.0000	0.0027	0.0036	0.0001	0.0000	0.0000	0.0000	0.0000	0.0000	0.0000	0.0000	0.0000	0.0000	0.0000	0.0000	0.0000	0.0000	0.0000
McLennan Hills	0.8809	0.0000	0.0310	0.0617	0.0000	0.0198	0.0031	0.0035	0.0000	0.0000	0.0000	0.0000	0.0000	0.0000	0.0000	0.0000	0.0000	0.0000	0.0000	0.0000	0.0000	0.0000
Motukorea	0.9576	0.0022	0.0011	0.0004	0.0000	0.0015	0.0000	0.0000	0.0000	0.0000	0.0001	0.0000	0.0000	0.0000	0.0026	0.0008	0.0009	0.0012	0.0291	0.0009	0.0016	0.0022
Mt Albert	0.8932	0.0519	0.0357	0.0173	0.0005	0.0011	0.0001	0.0001	0.0000	0.0000	0.0000	0.0001	0.0000	0.0000	0.0000	0.0000	0.0000	0.0000	0.0000	0.0000	0.0000	0.0000
Mt Cambria	0.7560	0.0081	0.0189	0.0170	0.0046	0.0087	0.0000	0.0000	0.0000	0.0006	0.0008	0.0042	0.0125	0.0000	0.0255	0.0075	0.0180	0.0071	0.1081	0.0012	0.0012	0.0002
Mt Eden	0.2604	0.0000	0.0000	0.0000	0.0000	0.0000	0.0000	0.0000	0.0000	0.0001	0.0081	0.0605	0.3688	0.3021	0.0000	0.0000	0.0000	0.0000	0.0000	0.0000	0.0000	0.0000
Mt Hobson	0.2671	0.0000	0.0000	0.0000	0.0000	0.0000	0.0000	0.0000	0.0000	0.0000	0.0000	0.0007	0.0044	0.0254	0.1324	0.0872	0.0765	0.0645	0.0932	0.1181	0.1305	0.2109
Mt Mangere	0.0183	0.0000	0.0000	0.0000	0.0000	0.0000	0.0000	0.0000	0.0000	0.0000	0.0000	0.0000	0.0000	0.0000	0.0060	0.0516	0.2062	0.3831	0.2311	0.1002	0.0035	0.0000
Mt Richmond	0.7145	0.0000	0.0000	0.0000	0.0000	0.0006	0.0389	0.1150	0.0000	0.0419	0.0885	0.0006	0.0000	0.0000	0.0000	0.0000	0.0000	0.0000	0.0000	0.0000	0.0000	0.0000
Mt Roskill	0.9787	0.0109	0.0028	0.0013	0.0001	0.0042	0.0002	0.0012	0.0000	0.0001	0.0000	0.0005	0.0000	0.0000	0.0000	0.0000	0.0000	0.0000	0.0000	0.0000	0.0000	0.0000
Mt Smart	0.1808	0.0000	0.0000	0.0000	0.0000	0.0000	0.0000	0.0000	0.0000	0.0000	0.0000	0.0000	0.0000	0.0000	0.0000	0.0005	0.0078	0.0464	0.1087	0.2941	0.3617	0.1783
Mt StJohn	0.7345	0.0397	0.1143	0.0813	0.0003	0.0163	0.0018	0.0005	0.0002	0.0000	0.0000	0.0069	0.0042	0.0000	0.0000	0.0000	0.0000	0.0000	0.0000	0.0000	0.0000	0.0000
Mt Victoria	0.2130	0.0833	0.0749	0.0586	0.0125	0.0071	0.0044	0.0001	0.0013	0.0002	0.0002	0.0054	0.0047	0.0164	0.1131	0.1224	0.0750	0.0833	0.0085	0.0759	0.0397	0.0592
North Head	0.7220	0.1143	0.0612	0.0444	0.0071	0.0048	0.0010	0.0004	0.0005	0.0001	0.0001	0.0038	0.0029	0.0091	0.0091	0.0065	0.0039	0.0027	0.0021	0.0025	0.0015	0.0005
One Tree Hill	0.7048	0.0596	0.1258	0.0876	0.0005	0.0168	0.0013	0.0004	0.0001	0.0002	0.0000	0.0018	0.0011	0.0000	0.0000	0.0000	0.0000	0.0000	0.0000	0.0000	0.0000	0.0000
Otara Hill	0.0068	0.0005	0.0011	0.0065	0.0063	0.0040	0.0016	0.0001	0.0011	0.0000	0.0002	0.0049	0.0064	0.0279	0.2273	0.2719	0.1834	0.1121	0.0581	0.0569	0.0229	0.0061
Otuataua	0.4476	0.0092	0.0847	0.2822	0.1664	0.0048	0.0027	0.0024	0.0000	0.0000	0.0000	0.0000	0.0000	0.0000	0.0000	0.0000	0.0000	0.0000	0.0000	0.0000	0.0000	0.0000
Panmure Basin	0.3303	0.0000	0.0001	0.0010	0.0006	0.6104	0.0116	0.0333	0.0005	0.0004	0.0009	0.0075	0.0034	0.0000	0.0000	0.0000	0.0000	0.0000	0.0000	0.0000	0.0000	0.0000
Pigeon Mountain	0.8107	0.0236	0.0321	0.0323	0.0004	0.0080	0.0000	0.0000	0.0000	0.0001	0.0003	0.0048	0.0040	0.0000	0.0228	0.0073	0.0114	0.0045	0.0326	0.0029	0.0022	0.0117
Pukaki	0.9060	0.0940	0.0000	0.0000	0.0000	0.0000	0.0000	0.0000	0.0000	0.0000	0.0000	0.0000	0.0000	0.0000	0.0000	0.0000	0.0000	0.0000	0.0000	0.0000	0.0000	0.0000
Puketutu	0.0089	0.0000	0.0000	0.0000	0.0007	0.0100	0.0171	0.0230	0.1787	0.1997	0.2504	0.2585	0.0530	0.0000	0.0000	0.0000	0.0000	0.0000	0.0000	0.0000	0.0000	0.0000
Robertson Hill	0.9993	0.0000	0.0000	0.0000	0.0000	0.0000	0.0004	0.0000	0.0000	0.0001	0.0002	0.0000	0.0000	0.0000	0.0000	0.0000	0.0000	0.0000	0.0000	0.0000	0.0000	0.0000
Styaks Swamp	0.7039	0.0000	0.0000	0.0000	0.0000	0.0000	0.0001	0.0003	0.0000	0.0000	0.0000	0.0000	0.0000	0.0000	0.0125	0.0169	0.0295	0.0344	0.0613	0.0640	0.0771	0.2652
Taylors Hill	0.3407	0.0000	0.0000	0.0001	0.0000	0.0086	0.2499	0.2587	0.0001	0.0384	0.0913	0.0122	0.0000	0.0000	0.0000	0.0000	0.0000	0.0000	0.0000	0.0000	0.0000	0.0000
Te Pouhawaiki	0.6952	0.1213	0.0810	0.0663	0.0107	0.0092	0.0026	0.0008	0.0009	0.0002	0.0001	0.0065	0.0044	0.0008	0.0000	0.0000	0.0000	0.0000	0.0000	0.0000	0.0000	0.0000
Three Kings	0.0000	0.0000	0.0000	0.0000	0.0000	0.0000	0.0000	0.0000	0.0000	0.0005	0.0007	0.1344	0.3719	0.4925	0.0000	0.0000	0.0000	0.0000	0.0000	0.0000	0.0000	0.0000
Wiri Mountain	0.1917	0.0000	0.0000	0.0001	0.0000	0.0011	0.1038	0.2749	0.0389	0.1120	0.1301	0.1282	0.0192	0.0000	0.0000	0.0000	0.0000	0.0000	0.0000	0.0000	0.0000	0.0000

Table A.29: Marginal posterior probabilities for a volcano to have produced a given tephra for the AVF 9A/9B scenario with $F = \{\alpha = 2.5, \beta U = 1.0\}$.

Volcano	AVF tephra (AVF 0 = 'unmatched')																					
	0	1	2	3	4	5	6	7	8	9A	9B	10	11	12	13	14	15	16	17	18	19	20
Ash Hill	0.6221	0.0000	0.0000	0.0000	0.0000	0.0010	0.2874	0.0895	0.0000	0.0000	0.0000	0.0000	0.0000	0.0000	0.0000	0.0000	0.0000	0.0000	0.0000	0.0000	0.0000	0.0000
Cemetery Hill	0.0001	0.0000	0.0000	0.0000	0.0018	0.0156	0.1182	0.1101	0.5388	0.1371	0.0680	0.0102	0.0001	0.0000	0.0000	0.0000	0.0000	0.0000	0.0000	0.0000	0.0000	0.0000
Crater Hill	0.0037	0.0000	0.0000	0.0000	0.0000	0.0003	0.0051	0.0069	0.2261	0.4442	0.2147	0.0875	0.0115	0.0000	0.0000	0.0000	0.0000	0.0000	0.0000	0.0000	0.0000	0.0000
Domain	0.7778	0.1122	0.0901	0.0199	0.0000	0.0000	0.0000	0.0000	0.0000	0.0000	0.0000	0.0000	0.0000	0.0000	0.0000	0.0000	0.0000	0.0000	0.0000	0.0000	0.0000	0.0000
Green Hill	0.0193	0.0012	0.0029	0.0141	0.0243	0.0163	0.0057	0.0010	0.0034	0.0005	0.0009	0.0261	0.0268	0.0768	0.1855	0.1298	0.1057	0.0845	0.0953	0.1059	0.0740	0.0165
Hampton Park	0.5170	0.0000	0.0000	0.0000	0.0000	0.0002	0.0001	0.0011	0.0000	0.0000	0.0000	0.0000	0.0000	0.0000	0.0473	0.1273	0.1455	0.0779	0.0654	0.0131	0.0051	0.0038
Hopua	0.3412	0.0000	0.0000	0.0008	0.0002	0.0707	0.0754	0.0467	0.0009	0.0474	0.1367	0.2034	0.0766	0.0000	0.0000	0.0000	0.0000	0.0000	0.0000	0.0000	0.0000	0.0000
Kohuora	0.0000	0.0004	0.0027	0.0200	0.7667	0.1219	0.0741	0.0032	0.0107	0.0002	0.0001	0.0000	0.0000	0.0000	0.0000	0.0000	0.0000	0.0000	0.0000	0.0000	0.0000	0.0000
Little Rangitoto	0.0991	0.2296	0.1746	0.1266	0.0257	0.0129	0.0014	0.0010	0.0021	0.0010	0.0014	0.0111	0.0074	0.0246	0.0480	0.0409	0.0295	0.0219	0.0355	0.0509	0.0548	0.0888
Mangere Lagoon	0.7302	0.0361	0.0687	0.0515	0.0003	0.0118	0.0036	0.0005	0.0001	0.0000	0.0004	0.0068	0.0065	0.0090	0.0286	0.0223	0.0156	0.0065	0.0015	0.0000	0.0000	0.0000
Matukutureia	0.1576	0.0000	0.0000	0.0000	0.0000	0.0000	0.0000	0.0000	0.0000	0.0000	0.0003	0.0055	0.0047	0.0231	0.1367	0.1050	0.0883	0.0670	0.0723	0.1143	0.2252	0.1533
Maungataketake	0.9889	0.0003	0.0000	0.0040	0.0000	0.0031	0.0036	0.0001	0.0000	0.0000	0.0000	0.0000	0.0000	0.0000	0.0000	0.0000	0.0000	0.0000	0.0000	0.0000	0.0000	0.0000
McLennan Hills	0.8803	0.0000	0.0317	0.0614	0.0000	0.0196	0.0032	0.0038	0.0000	0.0000	0.0000	0.0000	0.0000	0.0000	0.0000	0.0000	0.0000	0.0000	0.0000	0.0000	0.0000	0.0000
Motukorea	0.9574	0.0020	0.0009	0.0004	0.0000	0.0015	0.0000	0.0000	0.0000	0.0000	0.0001	0.0000	0.0000	0.0000	0.0028	0.0008	0.0009	0.0012	0.0295	0.0009	0.0016	0.0022
Mt Albert	0.8972	0.0516	0.0328	0.0166	0.0005	0.0011	0.0001	0.0000	0.0000	0.0000	0.0000	0.0001	0.0000	0.0000	0.0000	0.0000	0.0000	0.0000	0.0000	0.0000	0.0000	0.0000
Mt Cambria	0.7350	0.0076	0.0308	0.0200	0.0038	0.0099	0.0000	0.0000	0.0000	0.0008	0.0009	0.0045	0.0145	0.0000	0.0269	0.0084	0.0176	0.0073	0.1096	0.0012	0.0012	0.0002
Mt Eden	0.2475	0.0000	0.0000	0.0000	0.0000	0.0000	0.0000	0.0000	0.0000	0.0003	0.0091	0.0637	0.3770	0.3024	0.0000	0.0000	0.0000	0.0000	0.0000	0.0000	0.0000	0.0000
Mt Hobson	0.2657	0.0000	0.0000	0.0000	0.0000	0.0000	0.0000	0.0000	0.0000	0.0000	0.0000	0.0007	0.0049	0.0255	0.1349	0.0860	0.0756	0.0653	0.0949	0.1165	0.1300	0.2108
Mt Mangere	0.0178	0.0000	0.0000	0.0000	0.0000	0.0000	0.0000	0.0000	0.0000	0.0000	0.0000	0.0000	0.0000	0.0000	0.0067	0.0537	0.2120	0.3810	0.2253	0.1001	0.0034	0.0000
Mt Richmond	0.6973	0.0000	0.0000	0.0000	0.0000	0.0005	0.0379	0.1371	0.0000	0.0404	0.0862	0.0006	0.0000	0.0000	0.0000	0.0000	0.0000	0.0000	0.0000	0.0000	0.0000	0.0000
Mt Roskill	0.9782	0.0105	0.0027	0.0010	0.0001	0.0053	0.0002	0.0013	0.0000	0.0001	0.0000	0.0005	0.0001	0.0000	0.0000	0.0000	0.0000	0.0000	0.0000	0.0000	0.0000	0.0000
Mt Smart	0.1782	0.0000	0.0000	0.0000	0.0000	0.0000	0.0000	0.0000	0.0000	0.0000	0.0000	0.0000	0.0000	0.0000	0.0000	0.0007	0.0083	0.0485	0.1079	0.2953	0.3611	0.1768
Mt StJohn	0.7340	0.0413	0.1136	0.0819	0.0003	0.0154	0.0017	0.0005	0.0002	0.0000	0.0000	0.0074	0.0037	0.0000	0.0000	0.0000	0.0000	0.0000	0.0000	0.0000	0.0000	0.0000
Mt Victoria	0.2119	0.0867	0.0655	0.0657	0.0135	0.0062	0.0039	0.0001	0.0013	0.0001	0.0007	0.0051	0.0046	0.0204	0.1106	0.1225	0.0743	0.0835	0.0083	0.0754	0.0397	0.0599
North Head	0.7195	0.1175	0.0601	0.0444	0.0086	0.0042	0.0005	0.0004	0.0005	0.0001	0.0001	0.0039	0.0030	0.0095	0.0087	0.0066	0.0040	0.0026	0.0019	0.0024	0.0015	0.0004
One Tree Hill	0.7025	0.0627	0.1250	0.0881	0.0006	0.0163	0.0012	0.0004	0.0001	0.0003	0.0000	0.0017	0.0011	0.0000	0.0000	0.0000	0.0000	0.0000	0.0000	0.0000	0.0000	0.0000
Otara Hill	0.0066	0.0005	0.0008	0.0069	0.0062	0.0039	0.0016	0.0001	0.0011	0.0000	0.0004	0.0047	0.0064	0.0299	0.2280	0.2716	0.1823	0.1140	0.0562	0.0561	0.0227	0.0059
Otuataua	0.4885	0.0086	0.0845	0.2741	0.1342	0.0046	0.0031	0.0024	0.0000	0.0000	0.0000	0.0000	0.0000	0.0000	0.0000	0.0000	0.0000	0.0000	0.0000	0.0000	0.0000	0.0000
Panmure Basin	0.3117	0.0000	0.0003	0.0008	0.0006	0.6274	0.0126	0.0340	0.0002	0.0005	0.0010	0.0075	0.0034	0.0000	0.0000	0.0000	0.0000	0.0000	0.0000	0.0000	0.0000	0.0000
Pigeon Mountain	0.8091	0.0227	0.0338	0.0337	0.0004	0.0074	0.0000	0.0000	0.0000	0.0000	0.0005	0.0048	0.0040	0.0000	0.0231	0.0074	0.0109	0.0047	0.0327	0.0027	0.0021	0.0119
Pukaki	0.9174	0.0826	0.0000	0.0000	0.0000	0.0000	0.0000	0.0000	0.0000	0.0000	0.0000	0.0000	0.0000	0.0000	0.0000	0.0000	0.0000	0.0000	0.0000	0.0000	0.0000	0.0000
Puketutu	0.0179	0.0000	0.0000	0.0000	0.0007	0.0030	0.0175	0.0238	0.1801	0.1832	0.2734	0.2523	0.0481	0.0000	0.0000	0.0000	0.0000	0.0000	0.0000	0.0000	0.0000	0.0000
Robertson Hill	0.9992	0.0000	0.0000	0.0000	0.0000	0.0000	0.0004	0.0000	0.0000	0.0001	0.0003	0.0000	0.0000	0.0000	0.0000	0.0000	0.0000	0.0000	0.0000	0.0000	0.0000	0.0000
Styaks Swamp	0.7002	0.0000	0.0000	0.0000	0.0000	0.0000	0.0001	0.0004	0.0000	0.0000	0.0000	0.0000	0.0000	0.0000	0.0122	0.0170	0.0295	0.0341	0.0637	0.0652	0.0776	0.2695
Taylors Hill	0.3766	0.0000	0.0000	0.0001	0.0000	0.0094	0.2258	0.2607	0.0001	0.0356	0.0772	0.0145	0.0000	0.0000	0.0000	0.0000	0.0000	0.0000	0.0000	0.0000	0.0000	0.0000
Te Pouhawaiki	0.6915	0.1259	0.0785	0.0677	0.0115	0.0095	0.0016	0.0008	0.0010	0.0002	0.0002	0.0065	0.0044	0.0007	0.0000	0.0000	0.0000	0.0000	0.0000	0.0000	0.0000	0.0000
Three Kings	0.0000	0.0000	0.0000	0.0000	0.0000	0.0000	0.0000	0.0000	0.0000	0.0005	0.0012	0.1466	0.3736	0.4781	0.0000	0.0000	0.0000	0.0000	0.0000	0.0000	0.0000	0.0000
Wiri Mountain	0.2018	0.0000	0.0000	0.0003	0.0000	0.0010	0.1140	0.2741	0.0333	0.1074	0.1262	0.1243	0.0176	0.0000	0.0000	0.0000	0.0000	0.0000	0.0000	0.0000	0.0000	0.0000